

**SYNTHESIS, CHARACTERIZATION AND BIOLOGICAL ACTIVITY OF
d¹⁰ METAL ION COMPLEXES OF THIO- AND
SELENOSEMICARBAZONES**

Thesis Submitted to
LOVELY PROFESSIONAL UNIVERSITY
For the award of
DOCTOR OF PHILOSOPHY
IN
CHEMISTRY

By
ASHIQ KHAN
(Reg. No. 11209265)
Supervised By
DR. REKHA SHARMA

FACULTY OF TECHNOLOGY AND SCIENCES
LOVELY PROFESSIONAL UNIVERSITY
PUNJAB
2017

**SYNTHESIS, CHARACTERIZATION AND BIOLOGICAL ACTIVITY
OF d^{10} METAL ION COMPLEXES OF THIO- AND
SELENOSEMICARBAZONES**

Thesis Submitted to
LOVELY PROFESSIONAL UNIVERSITY
For the award of
DOCTOR OF PHILOSOPHY
IN
CHEMISTRY

By
ASHIQ KHAN
(Reg. No. 11209265)
Supervised By
DR. REKHA SHARMA

**FACULTY OF TECHNOLOGY AND SCIENCES
LOVELY PROFESSIONAL UNIVERSITY
PUNJAB-144411
2017**

DECLARATION

I hereby declare that the thesis entitled, “**Synthesis, characterization and biological activity of d¹⁰ metal ion complexes of thio- and selenosemicarbazones**” has been prepared by me under the guidance of Dr. Rekha Associate Professor of Chemistry, Lovely Professional University. This work is entirely my original work and all ideas and references have been duly acknowledged. It does not contain any work for the award of any other degree or fellowship previously at any University.

Ashiq Khan

Regd. No. 11209265

Department of Chemistry,

Lovely Professional University,

Phagwara, Punjab

Date:

CERTIFICATE

This is to certify that **Ashiq khan** has completed his Ph.D. thesis entitled, “**Synthesis, characterization and biological activity of d^{10} metal ion complexes of thio- and selenosemicarbazones**” for the award of Ph.D. of the Lovely Professional University under my guidance and supervision. To the best of my knowledge, the present work is the result of his original investigation and study. No part of the dissertation has ever been submitted for any other degree or fellowship previously at any university.

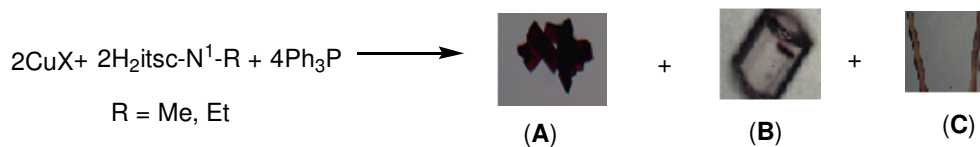
The thesis is fit for the submission and the partial fulfillment of the conditions for the award of Ph.D. Chemistry.

Dr. Rekha
Associate Professor,
Department of Chemistry,
Lovely Professional University,
Phagwara-144402

Date:

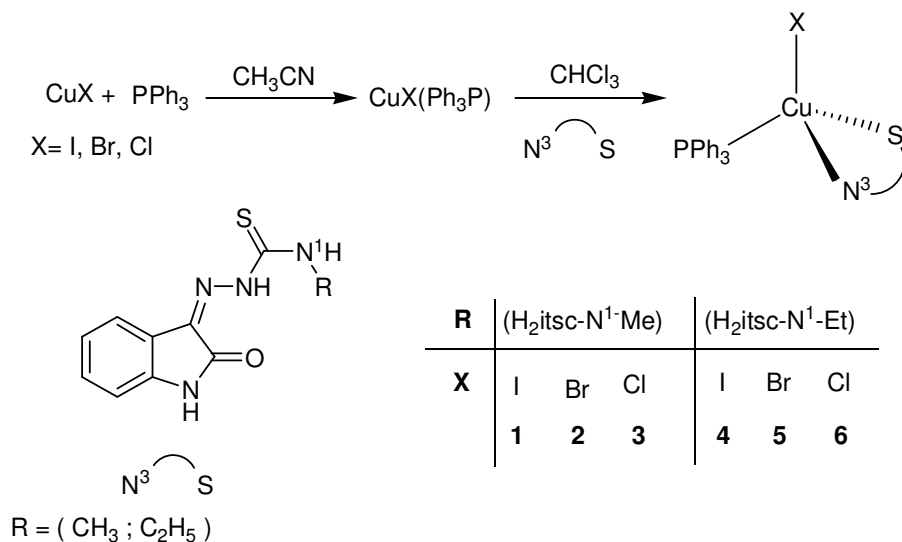
ABSTRACT

Chapter 1 and 2 covers the introduction and literature review in detail while chapter 3 discusses the experimental part. In chapter 4, reaction of un-substituted isatin-3-thiosemicarbazone (H_2itsc) with copper(I) halides and Ph_3P in 1 : 1 : 1 (M : L : PPh_3) molar ratio were carried out, which formed insoluble orange colored compounds. To solubilize them and to get crystalline product, one mole of Ph_3P had been further added, which formed tetrahedral monomeric complexes, $[CuX(\eta^1-S-H_2itsc)(Ph_3P)_2]$ ($X = I, Cl, Br$). However, with substituted isatin-3-thiosemicarbazone ($H_2itsc-N^1-R$) ($R=Me, Et$), the similar reaction in 1 : 1 : 2 molar ratio formed three types of crystals (i) Red crystals of stoichiometry, $[CuX(H_2itsc-N^1-R)(Ph_3P)]$ (**A**), (ii) white crystals of formula, $[CuX(Ph_3P)_3]$ (**B**) and (iii) yellow needles of free ligand (**C**). (Scheme 1)



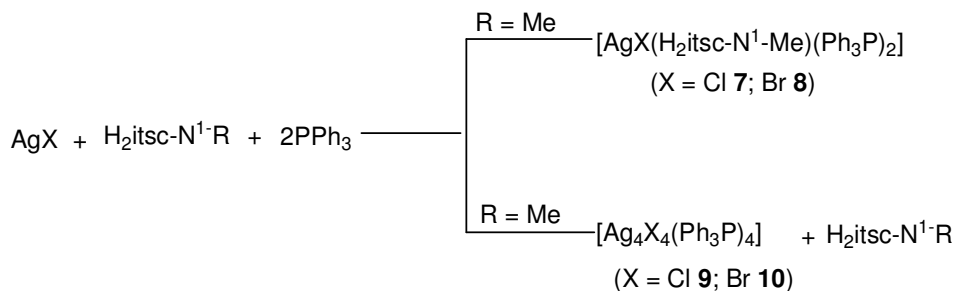
(Scheme 1)

Compounds of stoichiometry, $[CuX(H_2itsc-N^1-R)(Ph_3P)]$ were of our interest and were obtained by another route. Copper(I) halides ($X = I, Br, Cl$) were reacted with Ph_3P in 1 : 1 molar ratio to form white solid of composition, $CuX(Ph_3P)$ in acetonitrile. Acetonitrile was then removed and precipitates were dissolved in chloroform and one mole of ($H_2itsc-N^1-Me$) and ($H_2itsc-N^1-Et$) was added to get complexes of stoichiometry, $[Cu(\eta^2-N^3, S-H_2itsc-N^1-Me)(Ph_3P)]$ ($X = I, 1; Br, 2; Cl, 3$) and $[CuX(\eta^2-N^3, S-H_2itsc-N^1-Et)(Ph_3P)]$ ($X = I, 4; Br, 5; Cl, 6$) respectively. (Scheme 2)



(Scheme 2)

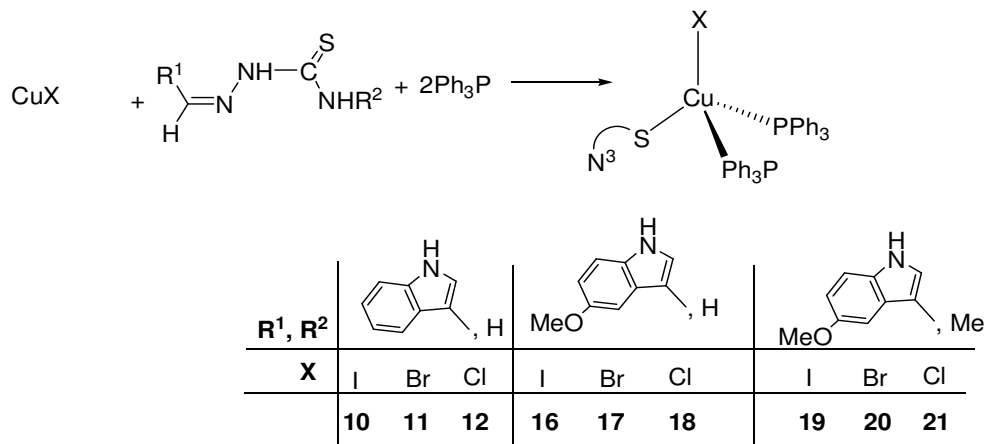
Silver(I) halides (X = Cl, Br) also reacted with H₂itsc-N¹-Me in 1 : 1 : 2 (M : HL : Ph₃P) molar ratio to form tetrahedral monomers, [AgX(η¹-S-H₂itsc-N¹-Me)(Ph₃P)₂] (X = Cl, **7**; Br, **8**). When an attempt was made to get the similar product with H₂itsc-N¹-Et, transparent crystals of [Ag₄X₄(Ph₃P)₄] (X = Cl, **9**; Br, **10**) were obtained. No coordination of silver(I) halides with H₂itsc-N¹-Et has been observed. (Scheme 3)



(Scheme 3)

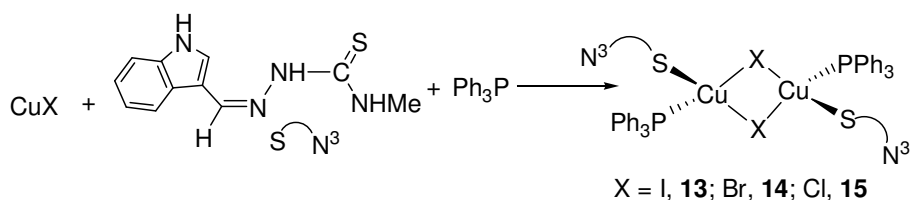
In chapter 5, reaction of indole-3-thiosemicarbazone (HIntsc, H¹L), 5-methoxy indole-3-thiosemicarbazone (5-MeOHIntsc, H²L) and 5-methoxy indole-N¹-methyl-3-thiosemicarbazone (5-MeOHIntsc-N¹-Me, H³L) with copper(I) halides and triphenylphosphine in 1 : 1 : 1 (M : HL : Ph₃P) ratio were carried out, which yielded insoluble product similar to the reaction of copper(I) iodide and bromide with isatin-3-

thiosemicarbazone. Addition of one extra mole of triphenylphosphine formed clear solution which on evaporation give crystalline products of stoichiometry, $[\text{CuX}(\text{HL})(\text{Ph}_3\text{P})_2]$ (H^1L , $\text{X} = \text{I}$, **10**; Br , **11**; Cl , **12**; H^2L , $\text{X} = \text{I}$, **16**; Br , **17**; Cl , **18**; H^3L , $\text{X} = \text{I}$, **19**; Br , **20**; Cl , **21**) (Scheme 4).



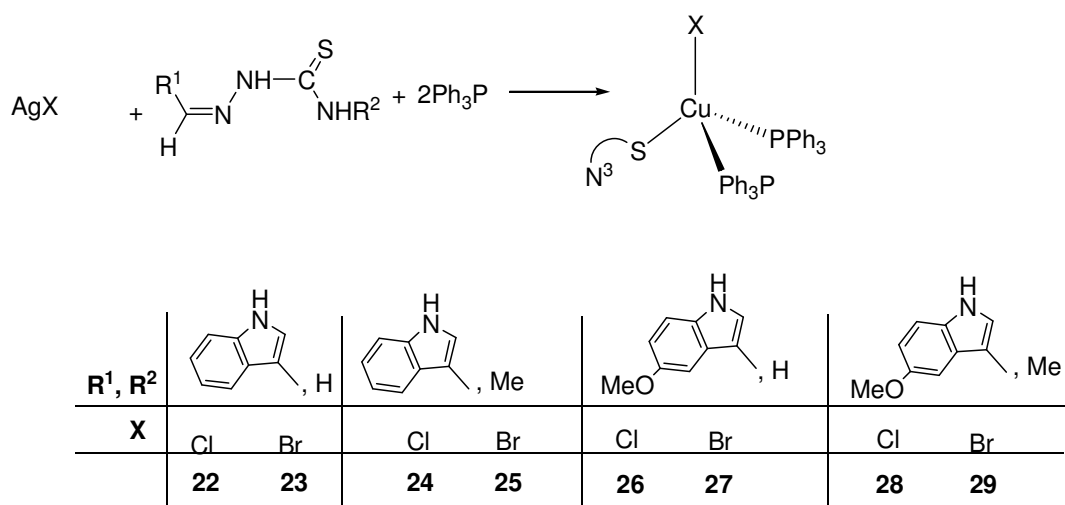
(Scheme 4)

In contrast to above, reaction of indole- N^1 -methyl-3-thiosemicarbazone ($\text{HIntsc-N}^1\text{-Me}$, H^4L) with copper(I) halides and triphenylphosphine in 1 : 1 : 1 ($\text{HL} : \text{M} : \text{Ph}_3\text{P}$) molar ratio yielded halogen bridged dimers of formula, $[\text{Cu}_2(\mu\text{-X})_2(\eta^1\text{-S-HIntsc-N}^1\text{-Me})_2(\text{Ph}_3\text{P})_2]$ ($\text{X} = \text{I}$, **13**; Br , **14**; Cl , **15**) (Scheme 5). Substitution of methyl group at N^1 atom of indole-3-thiosemicarbazones has changed the nuclearity of its copper(I) complexes. This behaviour is similar to the complexes of N^1 -substituted furane-2-carbaldehyde and thiophene-2-carbaldehyde thiosemicarbazones. X-ray quality crystals were obtained for H^2L , **12**, **13**, **14**, **19** and **20**.



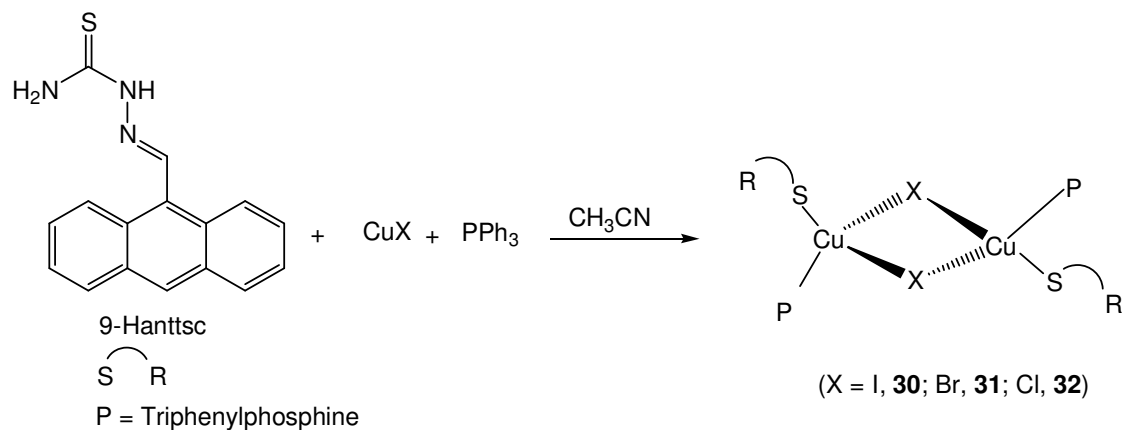
(Scheme 5)

Reaction of silver(I) halides (X= Cl, Br) with indole-3-thiosemicarbazone (HIntsc, H¹L), -N¹-methyl-3-thiosemicarbazone (HIntsc-N¹-Me, H⁴L), 5-methoxy indole-3-thiosemicarbazone (5-MeOHIntsc, H²L) and 5-methoxy indole-N¹-methyl-3-thiosemicarbazone (5-MeOHIntsc-N¹-Me, H³L) and triphenylphosphine in 1 : 1 : 1 (M : HL : Ph₃P) molar ratio in acetonitrile formed yellow coloured highly insoluble compound. To solubilize it, one mole of triphenylphosphine has been added. The clear solution thus formed gave complexes of stoichiometry [AgX(HL)(Ph₃P)₂] (H¹L, X = Cl(**22**), Br(**23**), H²L, X = Cl(**24**), Br(**25**), H³L, X = Cl(**26**), Br(**27**), H⁴L, X = Cl(**28**), Br(**29**) (Scheme 6). X-ray quality crystals were obtained for **22**.



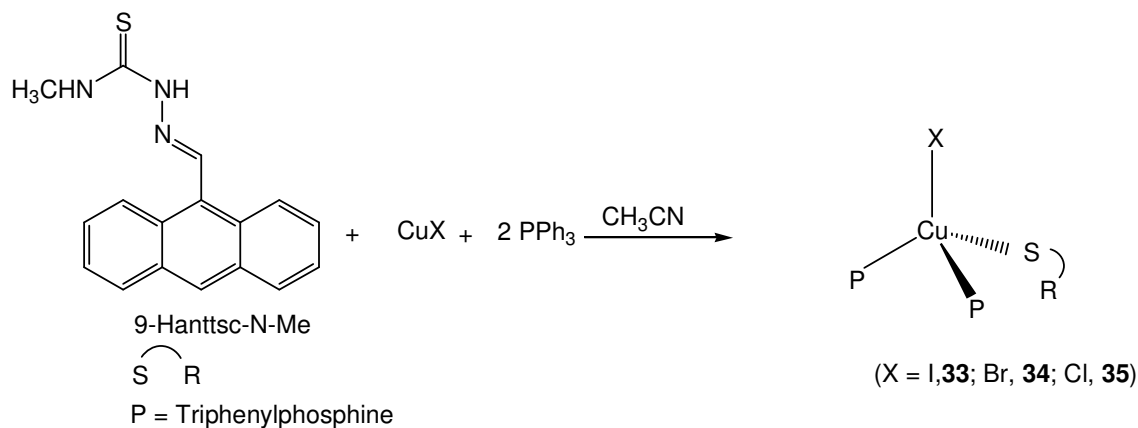
(Scheme 6)

Chapter 6 described the reaction of copper(I) halides (X= I, Br, Cl) with 9-anthraldehyde thiosemicarbazone (9-Hantsc, H⁵L) and triphenylphosphine in 1 : 1 : 1 (M : L : Ph₃P) molar ratio in acetonitrile, which formed orange coloured clear solution. On evaporation crystalline products of stoichiometry [Cu₂(μ₂-X)₂(η¹-S-9-Hanttsc)(Ph₃P)₂] (X = I, **30**; Br, **31**; Cl, **32**) (Scheme 7) was obtained.



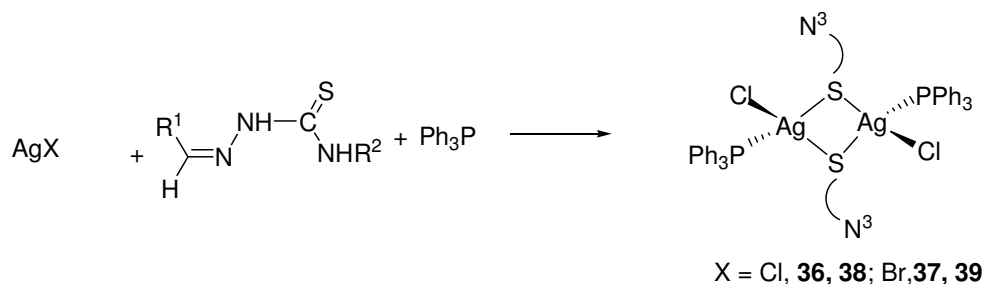
(Scheme 7)

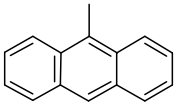
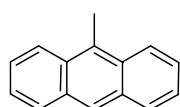
The reaction of copper(I) halides with 9-anthraldehyde- N^1 -methyl thiosemicarbazone (9-Hanttsc- N^1 -Me, H^6L) and triphenylphosphine in 1 : 1 : 1 molar ratio formed insoluble product. To solubilize it, an additional mole of triphenylphosphine was added, which resulted into formed complexes of stoichiometry, $[\text{CuCl}(\eta^1\text{-S-9-Hanttsc-}\text{N}^1\text{-Me})(\text{Ph}_3\text{P})_2]$ ($\text{X} = \text{I}$, **33**; Br, **34**; Cl, **35**) (Scheme-8). The behaviour of 9-Hanttsc- N^1 -Me ligand towards their copper(I) halide complexes is similar to that of isatin-3-thiosemicarbazone, indole-3-thiosemicarbazone (**10-12**), 5-methoxy indole-3-thiosemicarbazone (**16-18**) and 5-methoxy indole- N^1 -methyl-3-thiosemicarbazone (**19-21**).



(Scheme 8)

Silver (I) halides ($\text{X} = \text{Cl}, \text{Br}$) when reacted with 9-anthraldehyde-3-thiosemicarbazones (9-Hanttsc, H^5L) or 9-anthraldehyde- N^1 -methyl-3-thiosemicarbazone (9-Hanttsc- N^1 -Me, H^6L) in the presence of triphenylphosphine in 1 : 1 : 1 ($\text{M} : \text{HL} : \text{Ph}_3\text{P}$) molar ratio formed sulphur bridged dimers of formula, $[\text{Ag}_2\text{X}_2(\mu_2\text{-S-9-Hanttsc-}\text{N}^1\text{-Me})_2(\text{Ph}_3\text{P})_2]$ ($\text{X} = \text{Cl}$, **36**, **38**; Br, **37**, **39**) (Scheme 9).



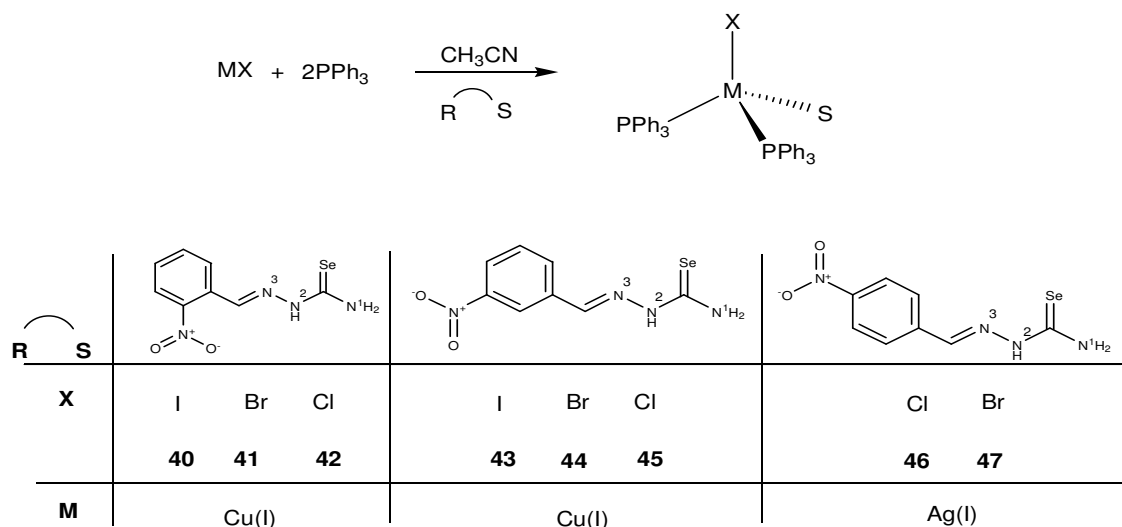
R ¹ , R ²	 ,H	 ,Me
X	Cl Br	Cl Br
	36 37	38 39

(Scheme 9)

In chapter 7, biological activities (antifungal, antibacterial and anti-tubercular) of all the ligands and their metal complexes mentioned in chapter 5 and 6 were carried out. It has been observed that all these ligands and complexes either showed low to moderate anti fungal and anti bacterial activities. However, all these ligands (H¹L-H⁶L) exhibit significant anti-tubercular activities. A very interesting result has been obtained in case of their complexes. The ant-TB activities of ligands got enhanced on complexation. Most of the complexes have shown anti-TB activities even more than the standard drugs.

In chapter 8, synthesis of selenosemicarbazones and their metal complexes has been described. Attempt to prepare m-hydroxy benzaldehyde selenosemicarbazone, o-nitro benzaldehyde selenosemicarbazone, m-nitrobenzaldehyde selenosemicarbazone and anisaldehyde selenosemicarbazone was successful, but instead of o-, m- and p- chloro benzaldehyde selenosemicarbazones, {1,2-bis(2-chlorobenzylidene)hydrazine}, {1,2-bis(3-chlorobenzylidene)hydrazine} and {1,2-bis(4-chlorobenzylidene)hydrazine} were obtained respectively. Reaction of copper(I) halides (X= I, Br, Cl) with 2-nitrobenzaldehyde selenosemicarbazones (2-NO₂-Hbsesc, H⁸L) or 3-nitrobenzaldehyde selenosemicarbazones (3-NO₂-Hbsesc, H⁹L) and triphenylphosphine in 1 : 1 : 1 (M : L : Ph₃P) molar ratio in acetonitrile formed highly insoluble compounds. To solubilise it, one mole of triphenylphosphine has been added. The clear solution thus formed gave complexes of stoichiometry [CuX(HL)(Ph₃P)₂] (H⁸L, X = I (**40**), Br (**41**), Cl (**42**), H⁹L, X = I (**43**), Br (**44**),

Cl (**45**). The similar reaction of silver(I) halides (X= Br, Cl) with 4-nitrobenzaldehyde selenosemicarbazones (4-NO₂-Hbsesc, H¹⁰L) and triphenylphosphine in 1 : 1 : 2 molar ratio yielded complexes having formula, [AgX(HL)(Ph₃P)₂] (H¹⁰L, X = Cl (**46**), Br (**47**) (Scheme 10).



(Scheme 10)

Keywords: *isatin-N¹-methyl-thiosemicarbazone; isatin-N¹-ethyl-thiosemicarbazone; indole-3-thiosemicarbazone; indole-N¹-methyl-3-thiosemicarbazone; indole-N¹-methyl-3-thiosemicarbazone; 5-methoxy indole-3-thiosemicarbazone; 5-methoxy indole-N¹-methyl-3-thiosemicarbazone; 9-anthraldehyde-3-thiosemicarbazone; 9-anthraldehyde-N¹-methyl-3-thiosemicarbazones; selenosemicarbazone; 1,2-bis(3-chlorobenzylidene)hydrazine; 1,2-bis(3-chlorobenzylidene)hydrazine; copper(I) halide; silver(I) halide X-ray crystallography; cytotoxicity; docking; anti-bacterial, anti-fungal, anti-Tuberculosis.*

PREFACE

Synthesis of various fused ring thiosemicarbazones were carried out. Prepared thiosemicarbazones were reacted with copper(I) halides and silver(I) halides to yield complexes of various nuclearity and bonding modes. Characterization of synthesized ligands and their complexes were done using various techniques viz. M.P, IR, NMR (^1H , ^{13}C), single crystal x-ray. Further, MTT assay, docking studies, anti-fungal, anti-bacterial and anti-Tuberculosis activities were carried out. Main challenge in this research work was stabilization of selenosemicarbazone ligands and preparation of their metal complexes. Although an attempt to prepare some of selenosemicarbazones and their copper(I) and silver(I) complexes was successful.

ACKNOWLEDGEMENT

"O my Lord! Open my chest for me and make my task easy for me and make loose the knot from my tongue so that they understand my speech,' "RABBI ZIDNEE ILMA" (Verse 25-28 Surah TA-HA Quran).

All praise of Almighty Allah, the most merciful, and compassionate, the creator of the universe, who enables me to complete research work successfully. I offer my humblest and sincerest words of thanks to His Prophet Muhammad (Peace be upon him) who is forever a torch of guidance and knowledge for the humanity.

It gives me immense pleasure in expressing my sincere gratitude and reverence towards my supervisor, Dr. Rekha, Associate Professor, Dep't. of Chemistry, Lovely Professional University, Her plain and smiling way of talking, sincerity towards work, attitude of research, timely encouragement, art of management, unending zeal, enthusiastic approach, untiring efforts and feeling of being there always, whenever I need her or approached her during the course of work in time. She not only provides dextrous guidance balanced by the freedom to express myself thoroughly but also shares her experiences and gives valuable criticism which helped me out to overcome each and every obstacle during the course of this work.

Thanks to Dr. Khursheed Bhat and Dr. Shoaib Rasool, IIIM Srinagar for helping me to carry out NMR analysis.

Many people in the faculty of this University encouraged me in various ways during my stay over here which include Dr. Ramesh Thakur, Dr. Gupinder Singh, who besides motivating also gave suggestions during my course work.

I owe my cordial thanks to Lab. Assistants' especially Mr. Manoj, Mr. Varun, Madam Rinki, for their help whenever needed or called.

I am tempted to thank all my friends since childhood who joined me through this walk of life and my discovery of what life is. I wish to take the names of my friends who I met during my research which include Manzoor Ahmed, Abdul Basit, Dharmender, Simranjeet, with whom I have shared many

refreshing tea and lunch sessions and whose company during our stay made life enjoyable, fun and humorous.

Where would I be without my family? My parents indeed deserve a special mention for their inseparable support and prayers. My father in the first place is the person who put the fundament of my learning character, showing me the joy of intellectual pursuit and being an inspiration ever since I was a child. Its because of him that I have been able to inculcate endurance, consistency, dedication, management and sincerity in my life. My mother especially is the one who sincerely raised me with caring, her gentle love, unending prayers, affection and being an essential corner stone of our sweet home. I cannot forget her long and hourly calls during my stay in the hostel with all the daily doses of advice and tips of health care. Special mention of my nephews Tahir, Burhan and niece Pariza, the little stars of our family.

I cannot finish without mentioning my lovable thanks to my wife "Shugufta" for taking care of me and my family. May Almighty fulfil her wishes?

Finally, I would like to thank everybody who was important in the successful realisation of this research and thesis.

Ashiq Khan

TABLE OF CONTENTS

S. No	Title	Page No.
01.	Declaration	[II]
02.	Certificate	[III]
03.	Abstract	[IV-X]
04.	Preface	[XI]
05	Acknowledgement	[XII-XIII]
06.	Table of contents	[XIV-XVI]
07.	List of Figures	[X11-XIV]
08.	List of Tables	[XXI-XXIII]
09.	Glossary of Abbreviations	[XXIV]
10.	Chapter – 1 Introduction	[1-3]
11.	Chapter – 2 Review of literature and Scope 2.1 Literature Survey 2.1.1 Metal-complexes of thiosemicarbazones containing fused rings 2.1.2 Silver complexes of thiosemicarbazones 2.1.3 Metal-complexes of selenosemicarbazones 2.2 Significance 2.4 Objectives	[4-26]
12.	Chapter – 3 General Experimental 3.1 Instrumentation 3.2 Experimental 3.2.1 Synthesis of Copper(I) and Silver(I) halides 3.2.2 Synthesis of Ligands (Thio- and Selenosemicarbazones) 3.2.3 Synthesis of metal complexes	[27-56]
13.	Chapter – 4 Complexes of Isatin-3-thiosemicarbazones 4.1 Complexes of Isatin-3-thiosemicarbazones	[57-78]

	4.2 Synthesis 4.3 ¹ H NMR Studies 4.4 Structure of N ¹ -methyl-isatin-3-thiosemicarbazone (H ₂ itsc-N ¹ -Me) and Complex 2 4.4.1 Structure of (H ₂ itsc-N ¹ -Me) 4.4.2 Structure of [CuBr(η ² -N ³ , S-H ₂ itsc-N ¹ -Me)(Ph ₃ P)] 4.4.3 Structure of [Ag ₄ Cl ₄ (Ph ₃ P) ₄] 4.5 Cytotoxicity studies 4.5.1 Molecular modeling studies 4.5.2 Docking studies	
14.	Chapter – 5 Complexes of Copper(I) halides with indole based thiosemicarbazones 5.1 Complexes of Copper(I) and Silver(I) halides halides with indole based thiosemicarbazones 5.1.1 Synthesis 5.1.2 Discussion on IR spectroscopy 5.1.3 Discussion on NMR spectroscopy 5.1.4 Structure of HIntsc-N ¹ -Me 5.1.5 Structure of monomers 5.1.6 Structure of dimers 5.1.7 Structure of silver(I) complex	[79-124]
15.	Chapter – 6 Complexes of Copper(I) halides with 9-anthraldehyde based thiosemicarbazones 6.1 Complexes of Copper(I) halides with 9-anthraldehyde based thiosemicarbazones 6.1.1 Synthesis 6.1.2 Discussion on IR spectroscopy 6.1.3 Discussion on NMR spectroscopy 6.1.4 Structure of dimer 6.1.5 Structure of monomer 6.1.6 Structure of silver(I) complex	[125-148]
16.	Chapter – 7 Biological Activity 7.1 Biological activity	[149-167]

	7.2 Antimicrobial activities 7.2.1 Discussion on <i>Antifungal</i> activity 7.2.2 Discussion on <i>Antibacterial</i> activity 7.3 <i>Anti-Tuberculosis</i> Activity	
17.	Chapter – 8 Selenosemicarbazones 8.1 Selenosemicarbazones 8.2 Result and discussion 8.3 Discussion on IR spectroscopy 8.4 Discussion on NMR spectroscopy	[168-193]
	8.5 Structure of 1,2-bis(3-chlorobenzylidene)hydrazine	
	8.6 Structure of 1,2-bis(4-chlorobenzylidene)hydrazine	
18.	Chapter – 9 Summary and Conclusion	[194-195]
19.	Chapter – 10 References	[196-202]
20.	List of Publications	[203]
21.	Annexure	[204-229]

LIST OF FIGURES

Figures	TITLE	Page No.
Figure-1	ORTEP view of H ₂ Intsc-N ¹ -Me with numbering scheme	[62]
Figure-2	ORTEP view of complex 2 with numbering scheme	[64]
Figure-3	Packing diagram of 2 showing H-bonding and various interactions	[65]
Figure-4	ORTEP view of [Ag ₄ Cl ₄ (Ph ₃ P) ₄] 9 with numbering scheme	[70]
Figure-5	Docking of cisplatin (A) and complex 2 (B) in the active site of Hodgkin lymphoma (PDB ID 1QOK)	[76]
Figure-5a	Docking of cisplatin (A) and complex 2 (B) in the active site of DNA (PDB ID: 1BNA)	[77]
Figure-6	Structure of HIntsc-N ¹ -Me with numbering scheme	[92]
Figure-7	Structure [CuCl(η ¹ -S-Hintsc)(Ph ₃ P) ₂] 12 with numbering scheme	[93]
Figure-7a	Packing Diagram of [CuCl(η ¹ -S-Hintsc)(Ph ₃ P) ₂] 12 .	[94]
Figure-8	Structure of [CuI(η ¹ -S-5-MeOHIntsc-N-Me)(Ph ₃ P) ₂] 19 with numbering scheme	[94]
Figure-8a	Packing Diagram of [CuI(η ¹ -S-5-MeOHIntsc-N-Me)(Ph ₃ P) ₂] 19 .	[95]
Figure-9	ORTEP view of [CuBr(η ¹ -S-5-MeOHIntsc-N-Me)(Ph ₃ P) ₂].CH ₃ CN 20 with numbering scheme	[95]
Figure-9a	Packing Diagram of [CuBr(η ¹ -S-5-MeOHIntsc-N-Me)(Ph ₃ P) ₂].CH ₃ CN 20 .	[96]
Figure 10	ORTEP view of [Cu ₂ (μ ₂ -I) ₂ (HIntsc-N-Me) ₂ (Ph ₃ P) ₂] 13	[98]
Figure-10a	Packing Diagram of [Cu ₂ (μ ₂ -I) ₂ (HIntsc-N-Me) ₂ (Ph ₃ P) ₂] 13 .	[98]
Figure-11	ORTEP view of [Cu ₂ (μ ₂ -Br) ₂ (HIntsc-N-Me) ₂ (Ph ₃ P) ₂] 14 with numbering scheme	[99]
Figure-11a	Packing Diagram of [Cu ₂ (μ ₂ -Br) ₂ (HIntsc-N-Me) ₂ (Ph ₃ P) ₂] 14 .	[99]
Figure-12	ORTEP view of [AgCl(η ¹ -S-HIntsc)(Ph ₃ P) ₂] 22 with numbering scheme.	[118]

Figure-12a	Packing Diagram of $[\text{AgCl}(\eta^1\text{-S-HIntsc})(\text{Ph}_3\text{P})_2]$	[119]
Figure-13	ORTEP view of $\text{Cu}_2(\mu_2\text{-Br})_2[(\eta^1\text{-S-9-Hanttsc})(\text{Ph}_3\text{P})_2]$ 31 with numbering scheme	[133]
Figure-13a	Packing Diagram of $\text{Cu}_2(\mu_2\text{-Br})_2[(\eta^1\text{-S-9-Hanttsc})(\text{Ph}_3\text{P})_2]$ 31 .	[133]
Figure-14	ORTEP view of $[\text{CuCl}(\eta^1\text{-S-9-Hanttsc-N}^1\text{-Me})(\text{Ph}_3\text{P})_2]$ 35 with numbering scheme.	[134]
Figure-14a	Packing Diagram of $[\text{CuCl}(\eta^1\text{-S-9-Hanttsc-N}^1\text{-Me})(\text{Ph}_3\text{P})_2]$ 35 .	[135]
Figure-15	ORTEP view of $[\text{Ag}_2\text{Cl}_2(\mu_2\text{-S-9-Hanttsc-N}^1\text{-Me})(\text{Ph}_3\text{P})_2]$ 38 with numbering scheme.	[143]
Figure-15a	Packing Diagram of $[\text{Ag}_2\text{Cl}_2(\mu_2\text{-S-9-Hanttsc-N}^1\text{-Me})(\text{Ph}_3\text{P})_2]$ 38 .	[144]
Figure-16	A comparative presentation of antifungal activity against <i>Aspergillus fumigates</i> (a) and <i>Pencillium chrysogenum</i> (b) of ligand B and complex B1-B5 with numbering scheme.	[154]
Figure-17	A comparative presentation of antibacterial activity against <i>Salmonella typhimurium</i> (c) and <i>E.coli</i> (d) of ligand B and complex B1-B5 with numbering scheme.	[154]
Figure-18	A comparative presentation of antifungal activity against <i>Aspergillus fumigates</i> (a) and <i>Pencillium chrysogenum</i> (b) of ligand C and complex C1-C5 with numbering scheme.	[155]
Figure-19	A comparative presentation of antibacterial activity against <i>Salmonella typhimurium</i> (c) and <i>E.coli</i> (d) of ligand C and complex C1-C5 with numbering scheme.	[155]
Figure-20	A comparative presentation of antifungal activity against <i>Aspergillus fumigates</i> (a) and <i>Pencillium chrysogenum</i> (b) of ligand D and complex D1-D5 with numbering scheme.	[156]
Figure-21	A comparative presentation of antibacterial activity against <i>Salmonella typhimurium</i> (c) and <i>E.coli</i> (d) of ligand D and complex D1-D5 with numbering scheme.	[156]
Figure-22	A comparative presentation of antifungal activity against <i>Aspergillus fumigates</i> (a) and <i>Pencillium chrysogenum</i> (b) of ligand A and complex A1-A5 with numbering scheme.	[157]
Figure-23	A comparative presentation of antibacterial activity against	[157]

- Salmonella typhimurium* (c) and *E.Coli* (d) of ligand A and complex A1-A5 with numbering scheme.
- Figure-24 A comparative presentation of antifungal activity against [158]
Aspergillus fumigates (a) and *Pencillium chrysogenum* (b) of ligand E and complex E1-E5 with numbering scheme.
- Figure-25 A comparative presentation of antibacterial activity against [158]
Salmonella typhimurium (c) and *E.coli* (d) of ligand E and complex E1-E5 with numbering scheme.
- Figure-26 A comparative presentation of antifungal activity against [159]
Aspergillus fumigates (a) and *Pencillium chrysogenum* (b) of ligand F and complex F1-F5 with numbering scheme.
- Figure-27 A comparative presentation of antibacterial activity against [159]
Salmonella typhimurium (c) and *E.coli* (d) of ligand F and complex F1-F5 with numbering scheme.
- Figure-28 MIC inhibition zones ($\mu\text{g/ml}$) of standard drugs namely [161]
Streptomycin, Ciprofloxacin and Pyrazinamide.
- Figure-29 Anti-Tuberculosis MIC inhibition zones ($\mu\text{g/ml}$) of complex B, [161]
B1-B5 with numbering scheme.
- Figure-30 Anti-Tuberculosis MIC inhibition zones ($\mu\text{g/ml}$) of complex C, [162]
C1-C5 with numbering scheme.
- Figure-31 Anti-Tuberculosis MIC inhibition zones ($\mu\text{g/ml}$) of complex D, [163]
D1-D5 with numbering scheme.
- Figure-32 Anti-Tuberculosis MIC inhibition zones ($\mu\text{g/ml}$) of complex A, [164]
A1-A5 with numbering scheme.
- Figure-33 Anti-Tuberculosis MIC inhibition zones ($\mu\text{g/ml}$) of complex E, [165]
E1-E5 with numbering scheme.
- Figure-34 Anti-Tuberculosis MIC inhibition zones ($\mu\text{g/ml}$) of complex F, [166]
F1-F5 with numbering scheme.
- Figure-35(a) ^1H NMR signals for 3-hydroxybenzaldehyde H^7L (δ , ppm). [173]
- Figure-35(b) ^1H NMR signals for (3-nitrobenzaldehyde) H^9L (δ , ppm). [174]
- Figure-35(c) ^1H NMR signals for (3-methoxybenzaldehyde) H^{11}L (δ , ppm). [174]
- Figure-35(d) ^{13}C NMR signals for 3-hydroxybenzaldehyde H^7L (δ , ppm). [175]

Figure-35(e)	^{13}C NMR signals for (2-nitrobenzaldehyde) H^8L (δ , ppm).	[175]
Figure-35(f)	^{13}C NMR signals for (3-nitrobenzaldehyde) H^9L (δ , ppm)	[176]
Figure-35(g)	^{13}C NMR signals for (3-methoxybenzaldehyde) H^{11}L (δ , ppm).	[176]
Figure-35(h)	^1H NMR signals for {1,2-bis(2-chlorobenzylidene)hydrazine} H^{12}L (δ , ppm).	[179]
Figure-35(i)	^1H NMR signals for {1,2-bis(3-chlorobenzylidene)hydrazine} H^{13}L (δ , ppm).	[179]
Figure-35(j)	^1H NMR signals for {1,2-bis(4-chlorobenzylidene)hydrazine} H^{12}L (δ , ppm).	[180]
Figure-35(k)	^{13}C NMR signals for {1,2-bis(2-chlorobenzylidene)hydrazine} H^{12}L (δ , ppm).	[180]
Figure-35(l)	^{13}C NMR signals for {1,2-bis(3-chlorobenzylidene)hydrazine} H^{13}L	[181]
Figure-35(m)	^{13}C NMR signals for {1,2-bis(4-chlorobenzylidene)hydrazine} H^{14}L (δ , ppm).	[181]
Figure-36	ORTEP view of 1,2-bis(3-chlorobenzylidene)hydrazine H^{13}L .	[183]
Figure-36a	Packing Diagram of 1,2-bis(3-chlorobenzyl)hydrazine H^{13}L .	[183]
Figure-37	ORTEP view of 1,2-bis(4-chlorobenzylidene)hydrazine H^{14}L .	[184]
Figure-37a	Packing Diagram of 1,2-bis(4-chlorobenzyl)hydrazine H^{14}L .	[184]
Figure 38-64	Annexure	[204-229]

LIST OF TABLES

TABLE	TITLE	Page No.
Table-1	List of complexes of isatin-3-thiosemicarbazones 1-8 with copper(I) and silver(I) halides:	[57]
Table-2	Crystallographic data for H ₂ itsc-N ¹ -Me and [CuBr(η ² -N ³ , S-H ₂ itsc-N ¹ -Me)(Ph ₃ P)] 2 .	[65]
Table-3	Selected bond distance (Å) and bond angles (°) for H ₂ itsc-N ¹ -Me and [CuBr(η ² -N ³ , S-H ₂ itsc-N ¹ -Me)(Ph ₃ P)] 2	[67]
Table-4	Crystallographic data for [Ag ₄ Cl ₄ (Ph ₃ P) ₄] 9 .	[71]
Table-5	Bond distance (Å) and bond angles (°) for [Ag ₄ Cl ₄ (Ph ₃ P) ₄] 9 .	[72]
Table-6	Cytotoxicity profile of synthesized compounds and reference drug Cisplatin.	[75]
Table-7	List of copper(I) and silver(I) halide complexes of indole based thiosemicarbazones.	[79]
Table-8	Important peaks in IR spectrum of Ligands (H ¹ L-H ⁴ L) and their copper(I) complexes 10-21 .	[86]
Table-9	Important peaks in IR spectrum of silver(I) complexes 22-29 .	[87]
Table-10	¹ H NMR signals for HL ¹ -HL ⁵ (δ, ppm) and their copper(I) complexes 10-21 .	[89]
Table-11	¹ H NMR signals for silver(I) and their complexes 22-27 .	[90]
Table-12	Crystallographic data for HIntsc-N ¹ -Me (H ² L).	[100]
Table-13	Bond distance (Å) and bond angles (°) for HIntsc-N ¹ -Me (H ² L).	[101]
Table-14	Crystallographic data of [CuCl(η ¹ -S-Hintsc)(Ph ₃ P) ₂] (12).	[102]
Table-15	Bond Lengths (Å) 12 .	[103]
Table-16	Crystallographic data of [CuI(η ¹ -S-5-MeOHIntsc-N-Me)(Ph ₃ P) ₂] 19 and [CuBr(η ¹ -S-5-MeOHIntsc-N-Me)(Ph ₃ P) ₂].CH ₃ CN 20 .	[106]
Table-17	Bond Length (Å) 19 .	[107]
Table-18	Bond Lengths for (Å) 20 .	[110]

Table-19	Crystallographic data of $[\text{Cu}_2(\mu_2\text{-I})_2(\text{HIntsc-N-Me})_2(\text{Ph}_3\text{P})_2]$ 13 $[\text{Cu}_2(\mu_2\text{-Br})_2(\text{HIntsc-N-Me})_2(\text{Ph}_3\text{P})_2]$ 14 .	[113]
Table-20	Bond Lengths for (Å) 13 .	[114]
Table-21	Bond Lengths for (Å) 14 .	[116]
Table-22	Crystallographic data of $[\text{AgCl}(\eta^1\text{-S-HIntsc})(\text{Ph}_3\text{P})_2]$ (22).	[120]
Table-23	Bond Lengths for (Å) (22).	[121]
Table-24	List of complexes of anthraldehyde based thiosemicarbazones.	[125]
Table-25	Important peaks in IR spectrum of Ligands (H^5L , H^6L) and their copper(I) complexes 30-35 .	[129]
Table-26	Important peaks in IR spectrum of silver(I) complexes 36-39 .	[130]
Table-27	^1H NMR signals for H^5L - H^6L (δ , ppm) and their copper(I) complexes 30-35 .	[131]
Table-28	^1H NMR signals for silver(I) and their complexes 36-39 .	[132]
Table-29	Crystallographic data of $\text{CuBr}[(\eta^1\text{-S-9-Hanttsc})(\text{Ph}_3\text{P})_2]$ 31 .	[136]
Table-30	Crystallographic data of $[\text{CuCl}(\eta^1\text{-S-9-Hanttsc-N}^1\text{-Me})(\text{Ph}_3\text{P})_2]$ 35 .	[137]
Table-31	Bond Lengths for (Å) 31 .	[138]
Table-32	Bond Lengths for (Å) 35 .	[140]
Table-33	Crystallographic data of $[\text{Ag}_2\text{Cl}_2(\mu_2\text{-S-9-Hanttsc-N}^1\text{-Me})(\text{Ph}_3\text{P})_2]$ 38 .	[145]
Table-34	Bond Length for (Å) (38).	[146]
Table-35	List of compounds (ligands and their complexes) with their codes	[149]
Table-36	Antifungal and antibacterial activity of B and its complexes B1-B5.	[154]
Table-37	Antifungal and antibacterial activity of ligand C and its complexes C1-C5.	[155]
Table-38	Antifungal and antibacterial activity of D and its complexes D1-D5.	[156]
Table-39	Antifungal and antibacterial activity of ligand A and its complexes A1-A5.	[157]
Table-40	Antifungal and antibacterial activity of ligand E and its complexes E1-E5.	[158]
Table-41	Antifungal and antibacterial activity of ligand F and its complexes F1-F5.	[159]
Table-42	Anti-tuberculosis activity of synthesised compounds (B, B1-B5).	[162]
Table-43	Anti-tuberculosis activity of synthesised compounds (C, C1-C5)	[163]

Table-44	Anti-tuberculosis activity of synthesised compounds (D, D1-D5)	[164]
Table-45	Anti-tuberculosis activity of synthesised compounds (A, A1-A5)	[165]
Table-46	Anti-tuberculosis activity of synthesised compounds (E, E1-E5)	[166]
Table-47	Anti-tuberculosis activity of synthesised compounds (F, F1-F5)	[167]
Table-48	List of ligands of Selenosemicarbazones prepared H ⁷ L- H ¹¹ L and dimerized azo compounds H ¹² L - H ¹⁴ L	[168]
Table-49	Important peaks in IR spectrum for cyclohexanone selenosemicarbazone and ligands H ⁷ L - H ¹¹ L.	[171]
Table-50	¹ H NMR signals for H ⁷ L - H ¹¹ L (δ, ppm).	[172]
Table-51	¹³ C NMR signals for H ⁷ L - H ¹¹ L (δ, ppm).	[173]
Table-52	¹ H NMR signals for H ¹² L - H ¹⁴ L (δ, ppm).	[177]
Table-53	¹³ C NMR signals for H ¹² L - H ¹⁴ L (δ, ppm).	[178]
Table-54	Crystallographic data of 1,2-bis(3-chlorobenzyl)hydrazine H ¹³ L.	[185]
Table-55	Crystallographic data of 1,2-bis(4-chlorobenzyl)hydrazine H ¹⁴ L.	[186]
Table-56	Bond distance (Å) and bond angles (°) for 1,2-bis(3-chlorobenzyl)hydrazine H ¹³ L.	[187]
Table-57	Bond distance (Å) and bond angles (°) for 1, 2-bis(4-chlorobenzyl)hydrazine H ¹⁴ L.	[188]
Table-58	List of complexes of selenosemicarbazones.	[189]
Table-59	Important peaks in IR spectrum for complexes 40-47 cyclohexanone selenosemicarbazone and ligands H ⁸ L - H ¹⁰ L.	[191]
Table-60	¹ H NMR signals for H ⁸ L -H ¹⁰ L (δ, ppm).	[192]

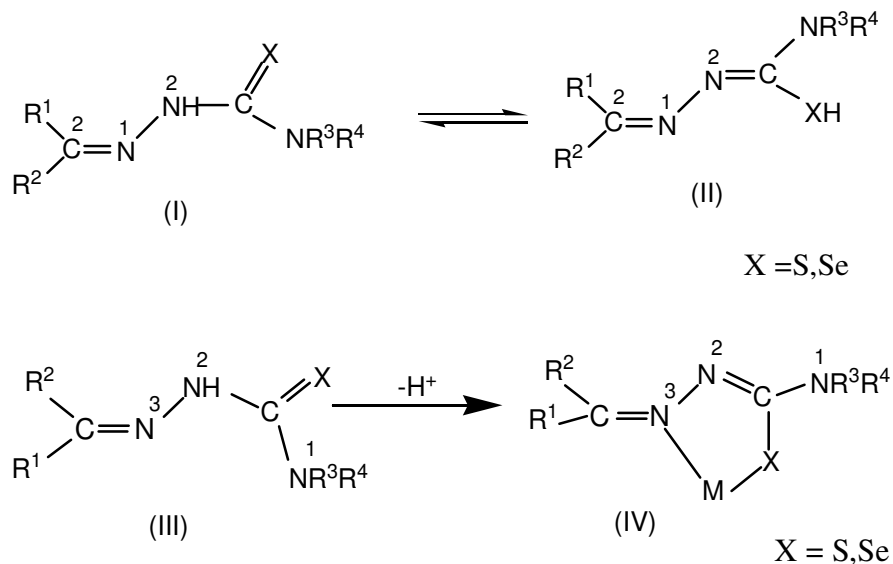
GLOSSARY OF ABBREVIATION

H ₂ itsc	Isatin thiosemicarbazones
H ₂ itsc-N-Me	Isatin-3-Methyl
H ₂ itsc-N-Et	Isatin-3-Ethyl
HIntsc	Indole-3-thiosemicarbazone
HIntsc-N ¹ -Me	Indole-N ¹ -methyl-3-thiosemicarbazone
5-MeOHIntsc	5-methoxy indole-3-thiosemicarbazone
5-MeOHIntsc-N ¹ -Me	5-methoxy indole-N ¹ -methyl-3-thiosemicarbazone
9-Hantsc	9-anthraldehde thiosemicarbazone
9-Hantsc-N ¹ -Me	9-anthraldehyde-N ¹ -methyl-3-thiosemicarbazone
PPh ₃	Triphenylphosphine
CuI	Copper Iodide
CuBr	Copper Bromide
CuCl	Copper Chloride
KI	Potassium Iodide
KBr	Potassium Bromide
KCl	Potassium Chloride
FTIR	Fourier Transformer Infrared
s	Sharp
w	Weak
PPh ₃	Triphenylphosphine
NMR	Nuclear Magnetic Resonance
DMSO- <i>d</i> ₆	Deuterated Dimethyl Sulfoxide
s	Singlet
d	Doublet
t	Triplet
MIC	Minimum inhibitory concentration
NCIM	National collection of industrial microorganisms
ppm	Parts per million
S	Sensitive
R	Resistant

CHAPTER 1

INTRODUCTION

Chalcogens of semicarbazones, i.e. $\{R^1R^2-N^3-N^2H-C^1(=X)N^1R^3R^4\}$ ($X = S, Se$) (I) constitutes an important class of N, S/Se- donor ligands. They exhibit tautomerism (thione-thiole tautomerism in sulphur) (II). They can bind to metal centre in neutral form (III) or in anionic form (IV).



Complexes of thiosemicarbazones are extensively studied and are known to exhibit variable bonding mode in both neutral (Chart 1) and anionic form (Chart 2). In neutral form, it binds via terminal S atom (η^1-S) (V), bridging S atom (μ_2-S) (VI), terminal N^3 , S- chelation (VII), N^3 , S- chelation-cum-S-bridging (VIII). If additional donor sites are present then η^3-X , N^3 , S- chelation (IX), η^4-X , N^3 , S- chelation and S-bridging (X), and η^4-X , N^3 , S- chelation and X-bridging (XI) (e.g. $X=N, O$) bonding modes are also possible [1–10].

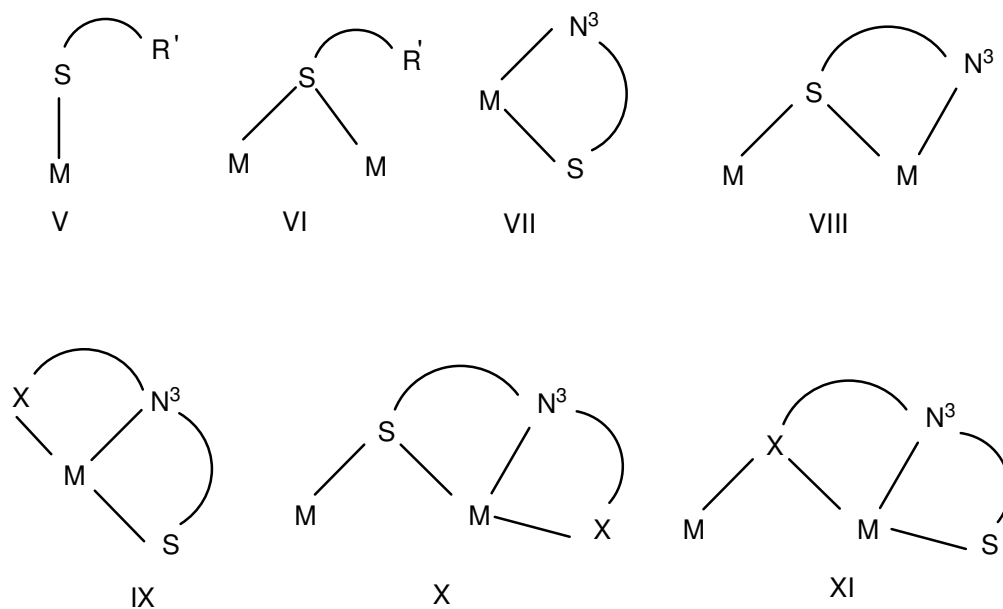


Chart 1

Apart from above mentioned modes, anionic ligands also exhibit, η^2 -N², S- chelation (XII) and N², S-bridging-cum-S-bridging modes (XIII) (Chart 2) [11, 12]. A rare mode is also known, where thiosemicarbazone act as pentadentate ligand (XIV) [12].

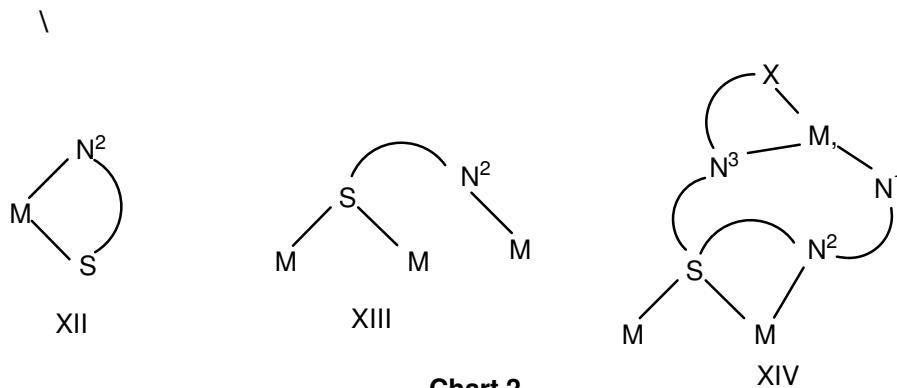


Chart 2

Since the study of selenosemicarbazone-complexes is limited, only few bonding modes are reported till now [13-17]. These modes are given in Chart 3.

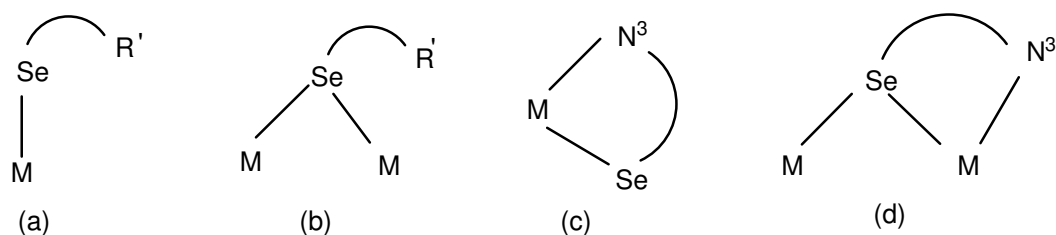


Chart 3

Apart from their variable bonding modes, thio- and selenosemicarbazone show numerous biological applications. For example, 2-Benzoylpyridine thiosemicarbazone exhibits antifungal activity against various strains of the pathogenic fungi [18], thiophene-2-carbaldehyde thiosemicarbazone exhibited cytotoxicity against Friend Leukemia Cells and MelanomaB16F10 cell lines [19], Vit. K3 thiosemicarbazone, showed similar cytotoxicity as cisplatin against cisplatin sensitive cell line A2780 and ten times more against cisplatin-resistant cell line A2780 [20] etc. Thiosemicarbazones having pyridine ring are known antitumor compounds and inhibitors of DNA synthesis, and this activity is attributed to their ability to inhibit the DNA topoisomerase II enzyme responsible for the regulation of the topology of DNA [2]. The derivatives of isatin-3-thiosemicarbazone exhibit a broad spectrum of biological activity. They are active against virology and influenza viruses. Some of the derivatives exhibit anticancer, anti histamine, analgesic and anti bacterial activity. Selenosemicarbazones have shown higher antitumor activity [21, 22], antimicrobial activity [23, 24] and antiviral activity [25], than thiosemicarbazones [26-32]. Selenosemicarbazone complexes exhibits string dose-dependent cytotoxicity against a panel of several human tumors cell lines, and this effect was comparable to that of cisplatin [33-34].

CHAPTER 2

REVIEW OF LITERATURE

2.1 Literature Survey

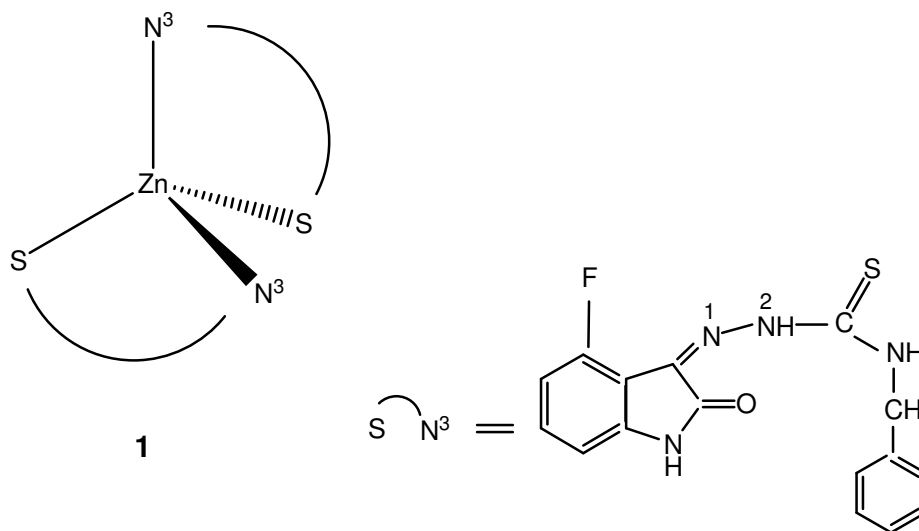
The literature survey is discussed in following parts:

- (i) Metal-complexes of thiosemicarbazones containing fused rings
- (ii) Silver complexes of thiosemicarbazones:
- (iii) Metal-complexes of selenosemicarbazones.

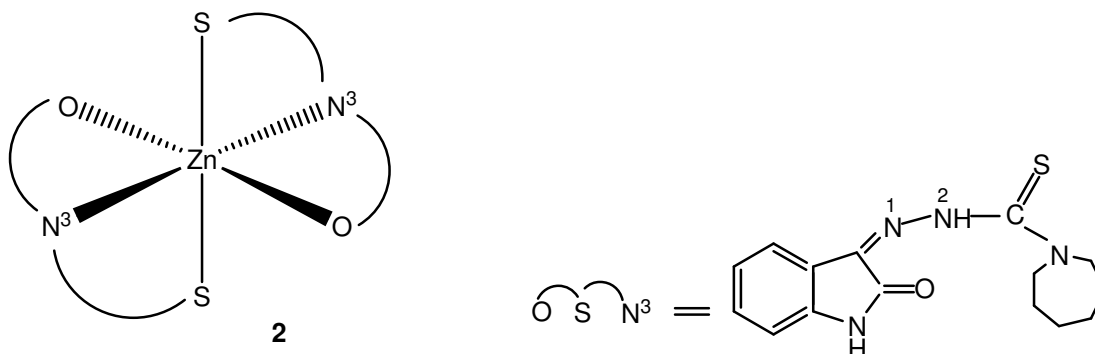
2.1.1 Metal-complexes of thiosemicarbazones containing fused rings:

Although lot of complexes were reported with thiosemicarbazones, but the study is limited with thiosemicarbazone containing fused ring. Only few complexes are x-ray characterized till now and these are mentioned below:

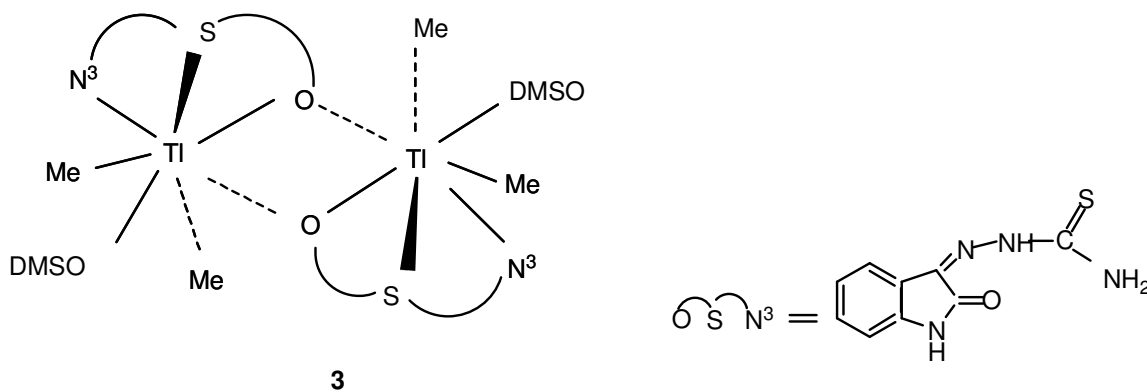
Isatin-3-thiosemicarbazone and its derivatives are extensively studied fused ring compounds. They form complexes of variable geometries and nuclearities with different metal ions. For example, 5-fluoro-isatin-3-(N-benzyl thiosemicarbazone) (HL) form tetrahedral complex, $[Zn(L)_2]$ **1** with zinc. Ligand is acting as N,S- donor in this complex.



An octahedral complex, $[Zn(L)_2]$ **2** of Zn(II) is also known with isatin-3- N-hexaminyll-thiosemiosemicarbazone (HL) [35]. Ligand is tridentate, coordinating via thione sulfur, imine nitrogen and oxygen on isatin ring

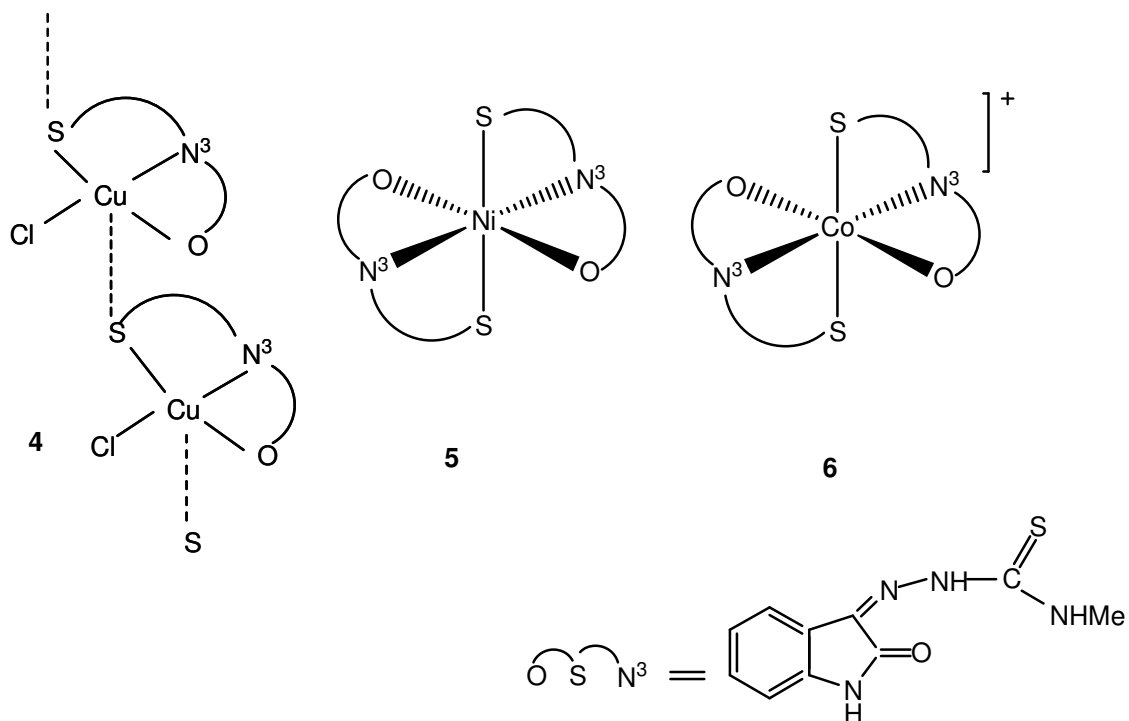


A dimer of thallium, $[TlMe_2(L)(DMSO)]$ **3** was obtained on reaction with dimethyl thallium(III) acetate and isatin-3-thiosemicarbazone (HL) [36]. This complex was recrystallized in DMSO. Metal atom has pentagonal bipyramidal structure and ligand coordinated via S, N³, O- donor atoms. Dimerization has been occurred via intermolecular $Tl \cdots O$ interaction.

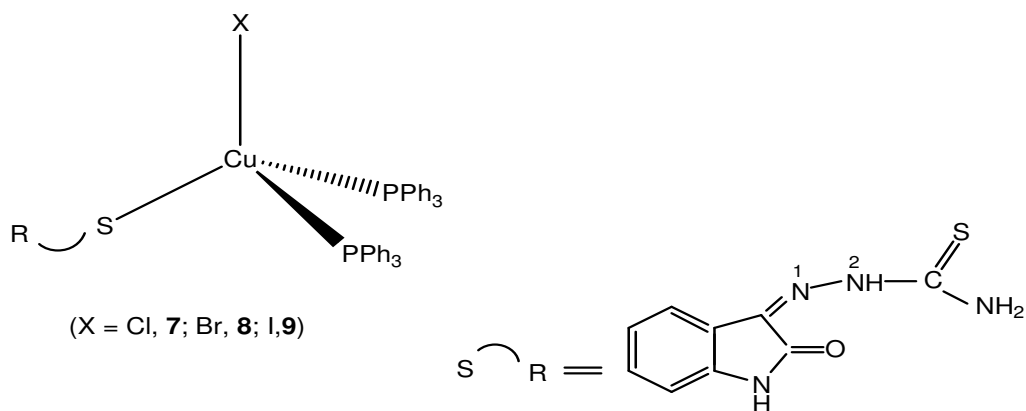


Complexes of copper, nickel and cobalt with 1-methylisatin-3-thiosemicarbazone (HL) has been formed with stoichiometry $[CuCl(L)]_n$ **4**, $[Ni(L)_2]$ **5** and $[CoL_2]_2[CoCl_4] \cdot 2EtOH$ **6** respectively [37]. In all these complexes ligand behaves as mono-anionic tridentate coordinating via O, N, S- donor atoms. In complex 4, the coordination geometry is square-pyramidal with the

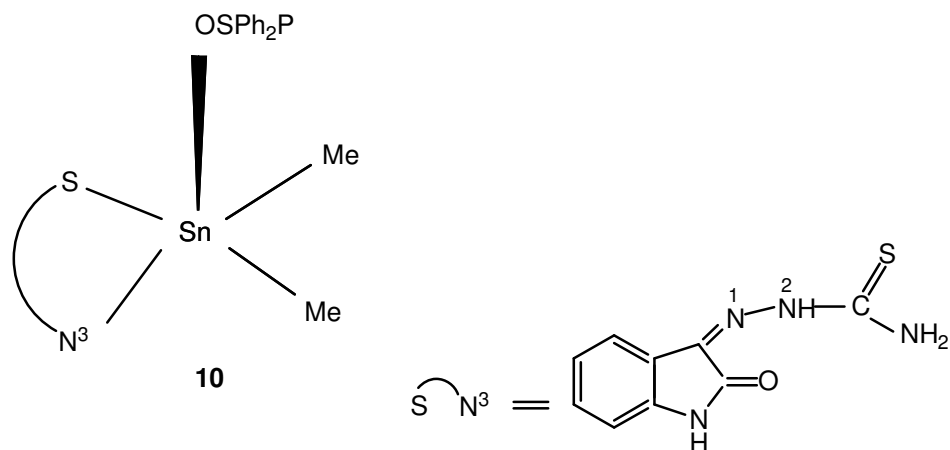
ligand and a chlorine lying on the basal plane; a bridging sulphur atom in axial position forms polymeric chains. In **5**, nickel atom is surrounded by six donor atoms of two ligand moieties in a distorted octahedral fashion. Compound **6** consists of octahedral $[\text{CoL}_2]^+$ cations, $[\text{CoCl}_4]^{2-}$ anions and ethanol molecules as solvent of crystallization.



Tetrahedral monomeric complexes of copper(I) having formula $[\text{CuX}(\text{HL})(\text{Ph}_3\text{P})_2]$ ($\text{X} = \text{Cl}$, **7**; Br , **8**; I , **9**) are known [38, 39]. In these complexes, ligand is neutral and coordinates via thione sulphur only.

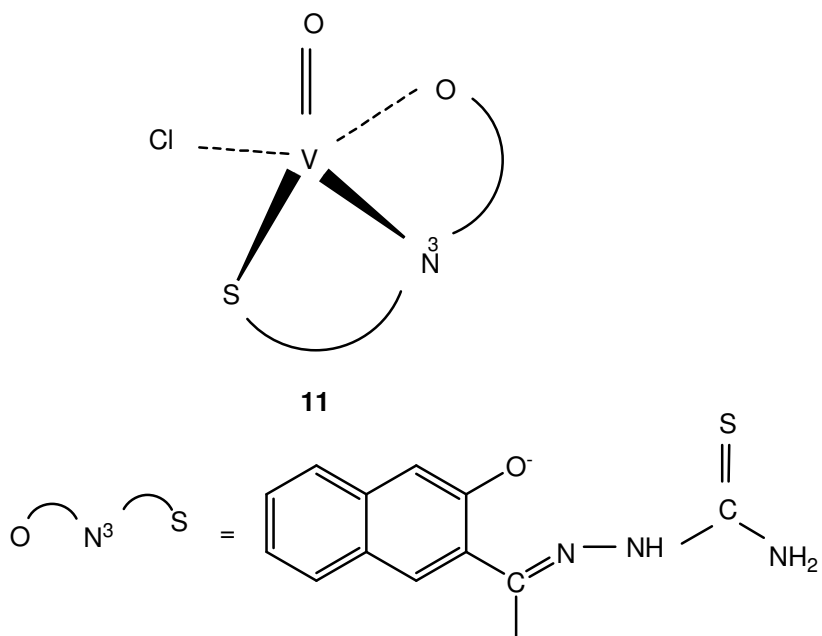


Organotin(IV) formed square planer complex with isatin-3-thiosemicarbazone (HL) having formula $[\text{SnMe}_2(\text{L})(\text{Ph}_2\text{PSO})]$ **10** [40]. The oxygen from diphenylthio - phosphinato $\{\text{Ph}_2\text{P}(=\text{S})\text{O}^-\}$ occupy the axial sites. Ligand coordinates via N^3 , S- donor atoms.

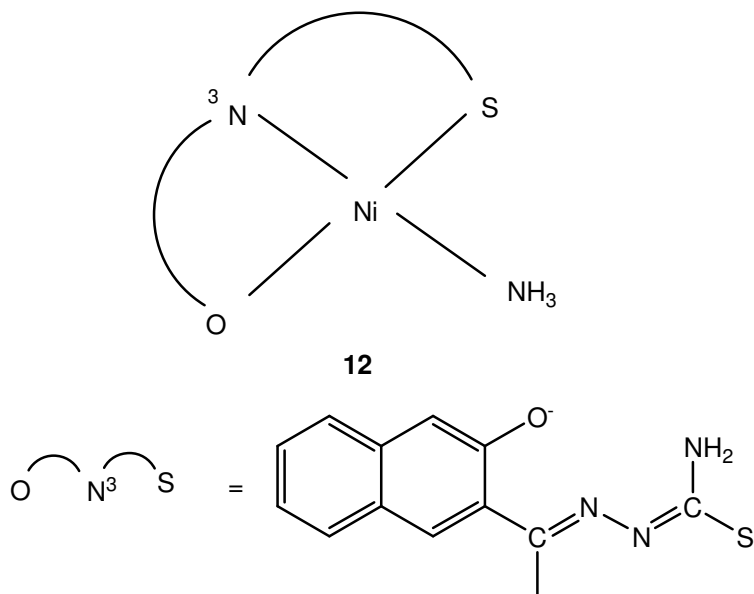


Apart from isatin-3-thiosemicarbazone and its derivative some other fused ring based thiosemicarbazone has been found to form complex with transition metals.

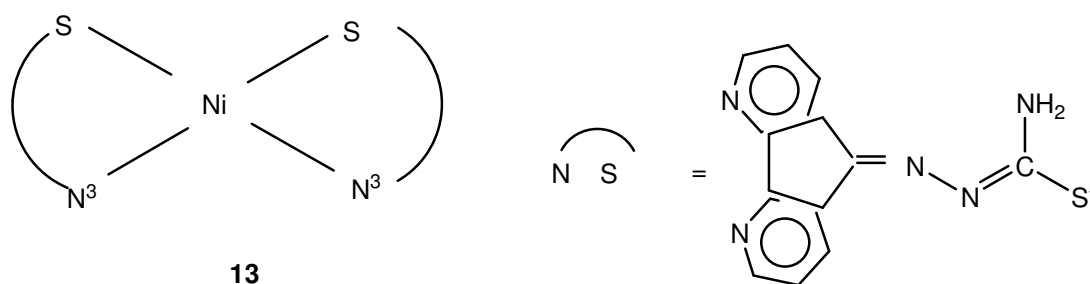
Vanadium form complexes with 3-hydroxy-naphthalene-2-carbaldehyde thiosemicarbazone (H_2L), namely, $[\text{V}^{\text{IV}}\text{OLCl}]$ **11**. This complex has distorted square pyramidal geometry with oxo group in apical position. Ligand is monoanionic tridentate, coordinating via O, N^3 , S donor atoms. [41]



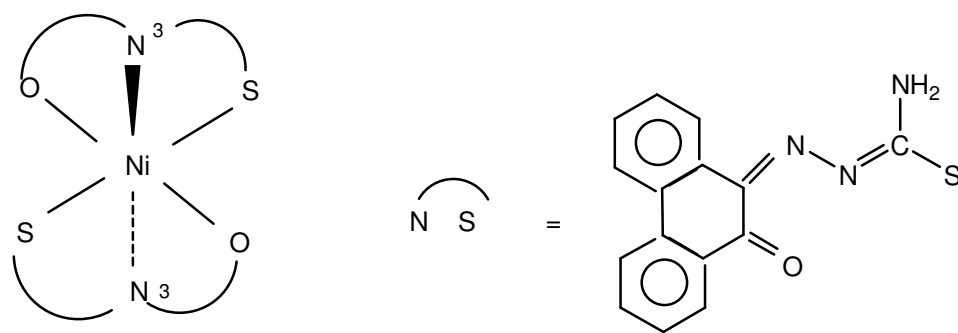
It also form square planer complex with Ni(II) having formula, $[\text{NiL}(\text{NH}_3)]$ **12** [42]. In this complex deprotonation of both $-\text{N}^2\text{H}$ and OH group takes place.



Ni(II) formed square planar complex with florenone-thiosemicarbazone (HL) of stoichiometry, $[\text{NiL}_2]$ **13** [43]. In this complex, two anionic thiosemicarbazone ligands bind via N³, S- donor atoms. Both the ligands have occupied cis-position in complex.

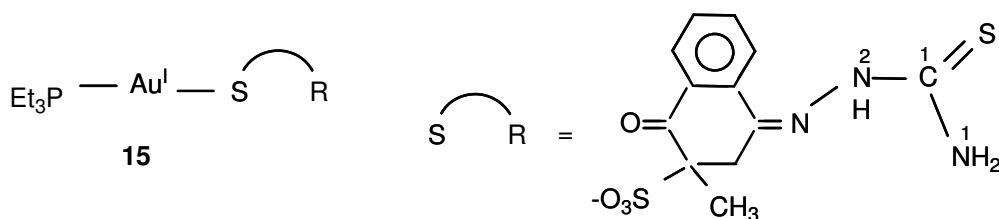


Octahedral complex of Ni(II) with phenanthrene-dione based thiosemicarbazone (HL), $[\text{NiL}_2]$ **14** had formed, where ligand coordinated to metal center via thione sulfur, ketonic oxygen and imine nitrogen [44].

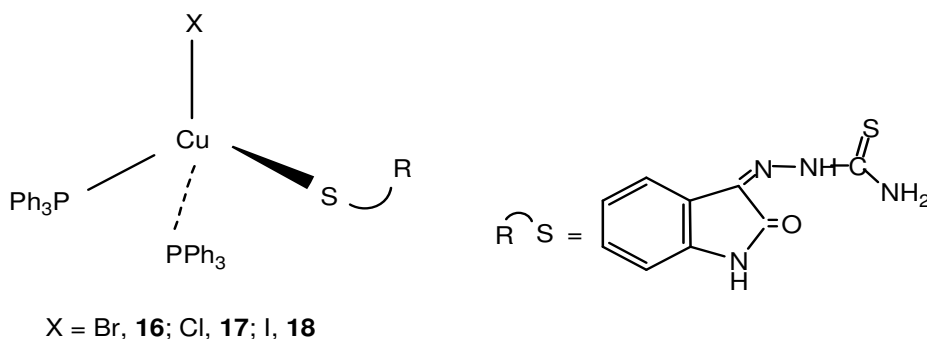


14

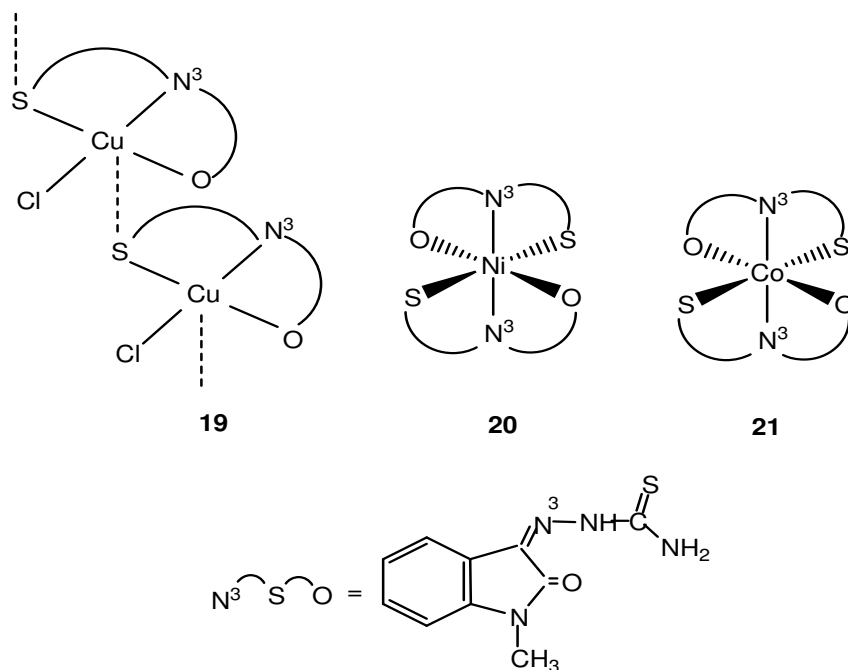
Gold(I) complex $[\text{Au}(\text{PEt}_3)(\text{HL})]$ **15** (HL = vitamin K3 thiosemicarbazone) has linear geometry around gold atom. [45]. Ligand here acted as neutral unidentate coordinating via thione sulfur only. Second site of metal has been occupied by phosphorous of triethylphosphine ligand.



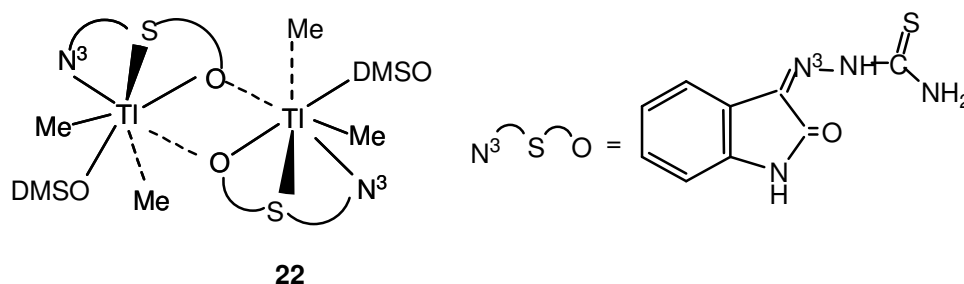
Isatin-3-thiosemicarbazone (H_2L) formed distorted tetrahedron geometrical complex with copper(I) halides having stoichiometry, $[\text{CuX}(\text{H}_2\text{L})(\text{Ph}_3\text{P})_2] \cdot 2\text{CH}_3\text{CN}$ (X= Br, **16**; Cl, **17**) and $[\text{CuI}(\text{H}_2\text{L})(\text{Ph}_3\text{P})_2] \cdot \text{CH}_3\text{CN}$ **18** [46]. The four corners of tetrahedron are occupied by two P atoms from two Ph_3P ligands, a halide ion and one thione sulfur of thiosemicarbazone ligand. Isatin-3-thiosemicarbazone coordinating via sulfur only, and thereby acts as neutral, monodentate ligand. In complex **16** and **17** two molecules of CH_3CN are present as a solvent of crystallization while only one molecule of CH_3CN is present in complex **18**.



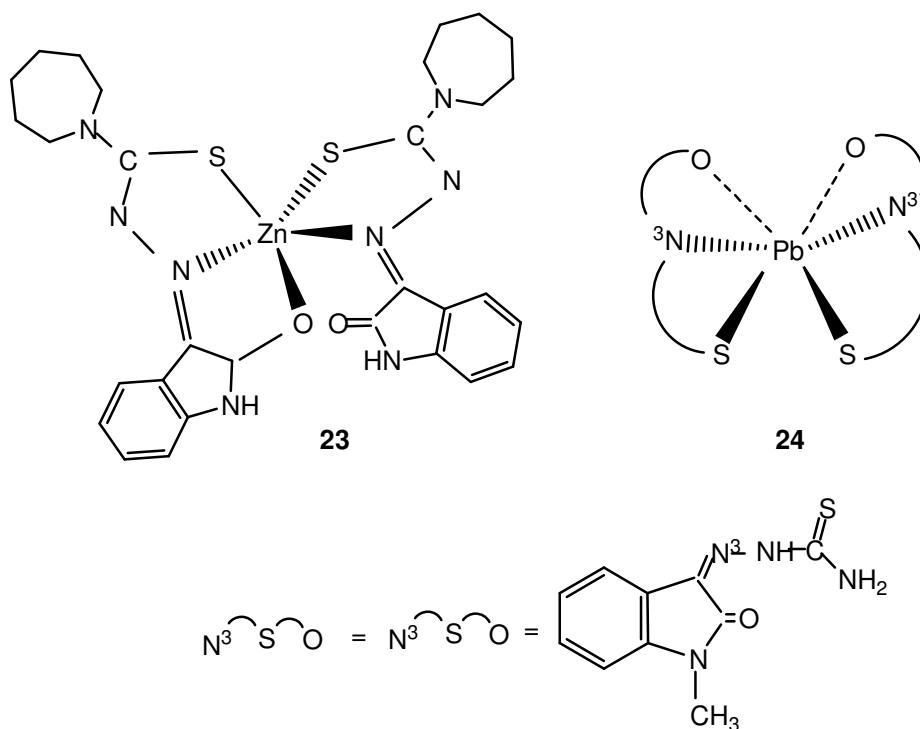
1-methyl isatin-3-thiosemicarbazone (H_2L) formed complexes with copper having stoichiometry $[CuCIL]_n$ **19**, with nickel $[NiL_2]$ **20** and cobalt $[CoL_2]^+$ $[CoCl_4]^{2-}$ **21** in presence of chloride or acetate ions[47]. In complex **19**, copper atom has square pyramid geometry having penta-coordinate coordination and coordinating in a tridentate manner via S, N and O atoms. The chlorine atom and three coordinating atoms of the ligand constitute the square base while the sulfur atom belonging to other molecule occupies the axial site while the tridentate ligand and the chlorine atom are lying at the basal plane. In complex **20**, nickel is having distorted octahedral geometry surrounded by six donor atoms of two ligand moieties coordinating via S, N, O- donor atoms of the ligand. The carbonyl oxygen of the isatin moiety and nitrogen from the hydrazine chain are arranged in a distorted octahedral fashion while the ligands are in meridional configuration with O and S atoms trans to each other. The molecular structure of Cobalt in complex **21** is having octahedral geometry consisting of $[CoL_2]^+$ cations and $[CoCl_4]^{2-}$ anions. The cobalt atom is surrounded by two ligands chelating in a SNO fashion. $[CoL_2]^+$ cations and $[CoCl_4]^{2-}$ anions has three cobalt atoms lying on binary axes while the third cobalt is the part of tetra chlorocobaltate(II) anion.



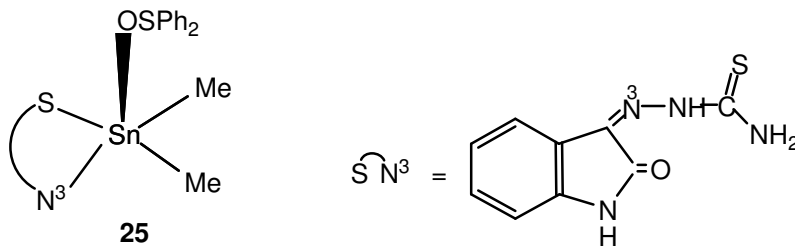
In complex **22** Isatin-3-thiosemicarbazone (H_2L) reacted with dimethylthallium(III) acetate to form complex of stoichiometry, $[TlMe_2(HL)]$, this was subsequently re-crystallized from DMSO molecules to form, $[TlMe_2(HL)(DMSO)]$ **22**[48]. The central metal thallium is having distorted pentagonal bipyramidal environment. In this complex the Tl atom is bound to two methyl C atoms and to the N(3), S and O atoms of an N(2)- deprotonated thiosemicarbazones besides a weakly bonded dimer is observed due to additional $Tl \cdots O_{HL}$ interaction with a neighboring molecule.

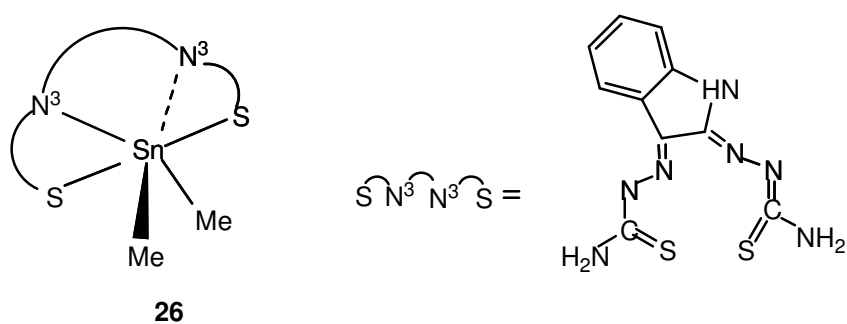


Isatin 3-hexamethyleneiminylthiosemicarbazone (HL) reacted with zinc(II) to form complex $M(L)_2$ (**23**)[49]. The two ligands coordinate giving square pyramidal geometry with a 20% distortion towards a trigonal bipyramid. One ligand acts as anionic, tridentate ligand coordinating via imine nitrogen, amide oxygen and thione sulfur and, whereas the second thiosemicarbazone bind via thione sulfur and imine nitrogen. One of ligand with N, N, S- donor atoms made the basal plane while the axial positions are occupied by thione S and amide oxygen of other ligand. In other reaction Pb reacts with Isatin 3-hexamethyleneiminylthiosemicarbazone (HL) to form complex $M(L)_2$ **24**[49]. The two coordinating ligands form a square pyramidal geometry with only 4% distortion towards a trigonal bipyramid around the central metal and the lone pair on the lead atom at the apical position. The greater bond distance observed in case of two oxygen atoms suggests weak interaction with Pb(II) center.

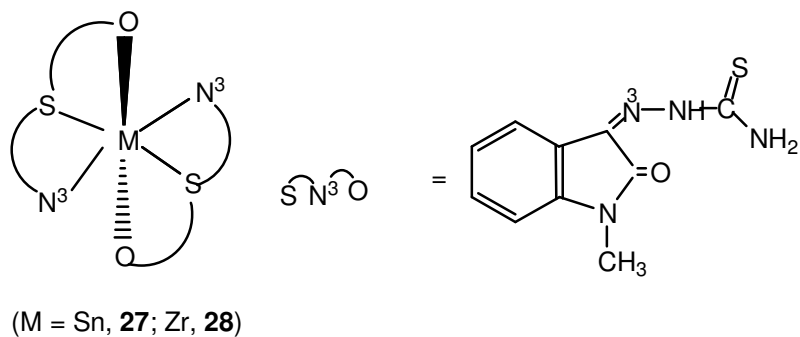


Isatin-3-thiosemicarbazone (HL) reacted with SnMe_2O to form complex, $[\text{SnMe}_2(\text{L})\text{OS}(\text{Ph})_2] \cdot \text{EtOH}$ **25** yielding a highly distorted trigonal bipyramidal geometry with weak $\text{Sn} \cdots \text{O}$ interaction. Monothiophosphinato anion in this complex is O-monodentate. In other complex reaction of SnMe_2O with isatin-2,3-bis(thiosemicarbazone) (HL) yielded, $[\text{SnMe}_2\text{L}]$ **26**, in which ligand is coordinating via, N_2S_2 donor atoms[50].

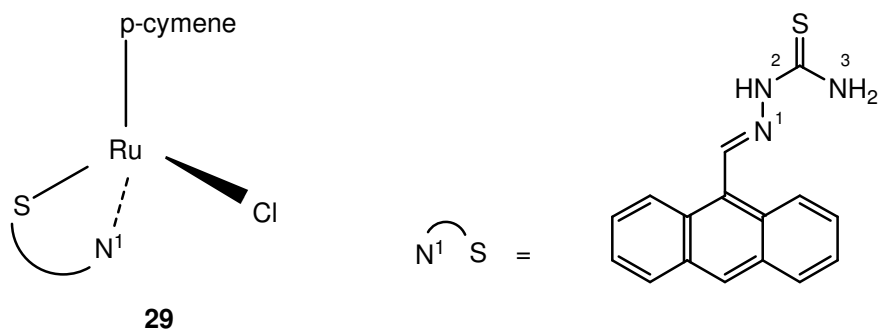




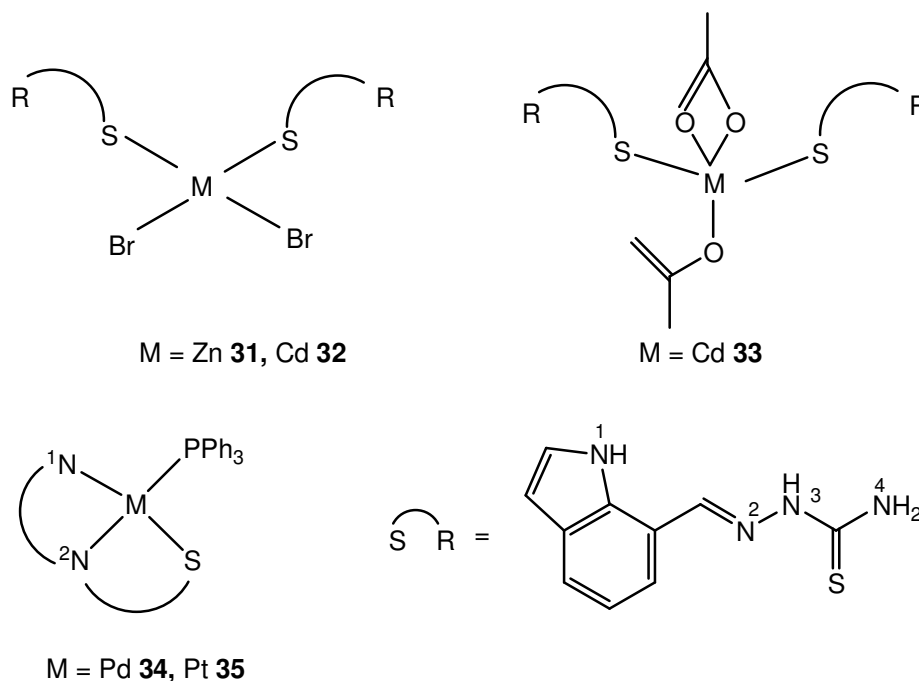
Octahedral geometry was observed in the complexes of N-Methyl-isatin-3-thiosemicarbazone (HL) with $M[L_2]Cl_2$ ($M = Sn^{IV}$, **27**; Zr^{IV} **28**)[51]. Two five membered chelation of isatin thiosemicarbazone with the central atom was observed coordinating through thiol sulfur, azomethine, nitrogen and carbonyl oxygen.



Reaction of $[(\eta^6\text{-p-cymene}) RuCl_2]_2$ with 9-anthraldehydethiosemicarbazone results in the complex with stoichiometry $(\eta^6\text{-p-cymene})Ru(NS)Cl]^+$ **29** yielding a distorted octahedral geometry[52]. The ligand 9-anthraldehydethiosemicarbazone chelates around the central atom ruthenium and coordinates via N^1 -S atoms. The other two position of the octahedra occupied by p-cymene asymmetrically and a terminal chloride.



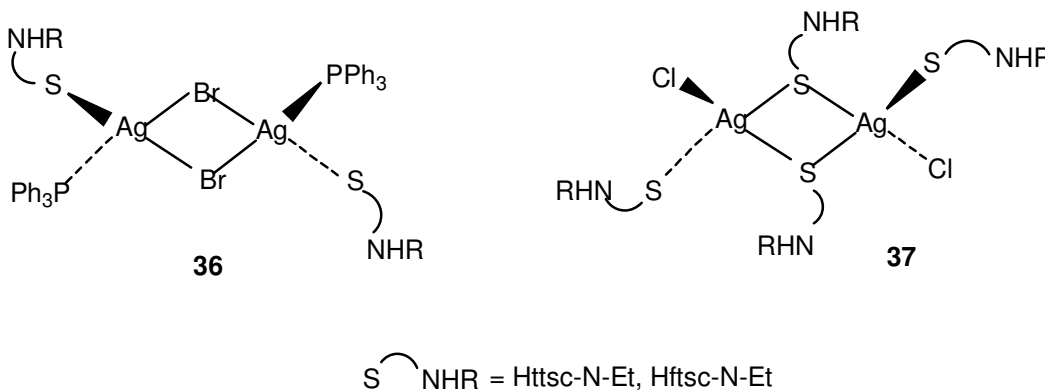
Indole-7-carbaldehyde (L) was reacted with Zn(II) **31**, Cd(II) **32,33** Pd(II) **34**, and Pt(II) **35** and resulted in complex with stoichiometry $\text{MX}_2(\text{L}_1)$ ($\text{X} = \text{Cl}, \text{Br}, \text{OAc}$)[54]. Reaction of ZnBr_2 with indole-7-carbaldehyde yield complex with stoichiometry $\text{ZnBr}_2(\text{L}).\text{CH}_3\text{OH}$ **31**. The thiosemicarbazones ligand behaves as a monodentate ligand, deprotonated at hydrazine and indole nitrogen, coordinating to the central atom via S- atom. The ligands are almost planar with respect to central atom. CdCl_2 reacts with ligand (L) yielding complex with stoichiometry $\text{CdCl}_2(\text{L})_2.\text{CH}_3\text{OH}$ **32**. The complex has a planar geometry resembling complex **31** coordinating via S atom of the ligand. $\text{Cd}(\text{OAc})_2$ reacts with Indole-7-carbaldehyde resulting in a distorted square pyramidal geometry with stoichiometry $\text{Cd}(\text{OAc})_2(\text{L})_2.2\text{CH}_3\text{OH}$ **33**. The two thiosemicarbazones ligands behave as monodentate ligand and coordinate via S- atom with the central metal. One bidentate acetate and one monodentate group and two S- atoms of ligand complete the five coordination geometry. Reaction of Pd(II) and Pt(II) with the same ligand(L) and Ph_3P as co-ligand form a square planar geometry with stoichiometry $\text{M}(\text{L})\text{Ph}_3\text{P}$ ($\text{M} = \text{Pd}$ **34**, Pt **35**).The ligand coordinates the central metal via N, N¹, S tridentate manner creating a five and six membered ring.



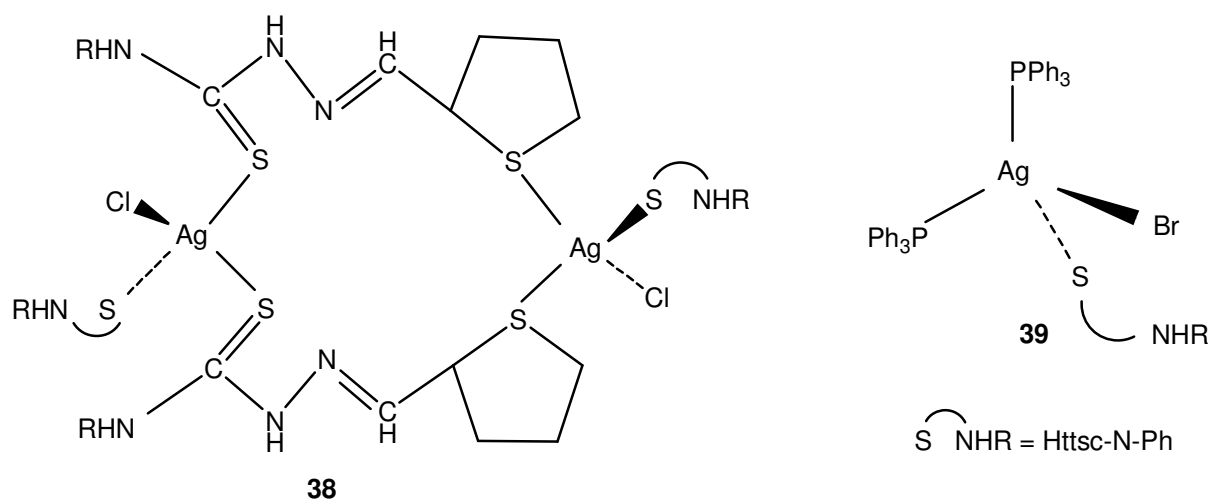
2.1.2 Silver complexes of thiosemicarbazones:

Literature survey reveals only few complexes of Ag(I) with thiosemicarbazones and fewer or almost no complexes with fused ring thiosemicarbazones.

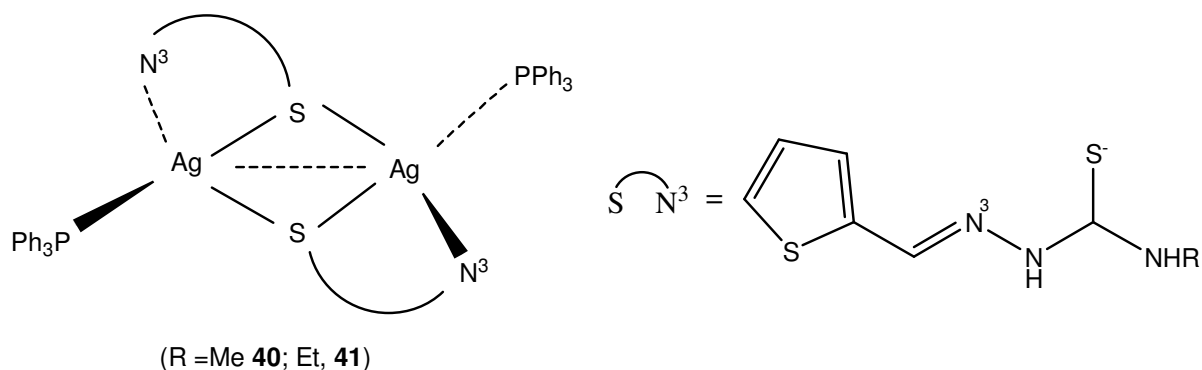
Rekha et al., recently reported reaction of various complexes of silver(I)halide acetate with thiophene-2-carbaldehyde/*N*¹-substituted acetaldehyde thiosemicarbazones and Ph₃P as coligand. *N*¹-Ethyl substituted thiosemicarbazones Httsc-NEt (HL) with Ag(I)X resulted in the formation of a halogen bridged dinuclear complex with stoichiometry [M₂(μ-X)₂(κ¹-S¹-HL)₂](X= Br) **36**[54]. Two bromine halides are involved in bridging with two Ag centres. Central metal Ag in this parallelogram is further coordinated with one terminal P of Ph₃P and the ligand(L) via S-coordination, trans to each other. However reaction of Ag(I)X with Hftsc-NEt (L) (X= Br, Hftsc = furan thiosemicarbazones) in presence of coligand Ph₃P resulted in a dinuclear complex with stoichiometry [Ag₂X(μ-S-L)₂(κ¹-S-L)₂] **37**[54]. Two ligands coordinating via κ¹-S and μ-S modes. In this Ag₂S₂ core parallelogram each Ag atom is coordinated with one chloride, one terminal sulphur atom and two bridging sulphur atoms of the ligand.



Reaction of Ag(I)X (X=Cl **38**, Br **39**) with Httsc-NPh (N-Phenyl thiosemicarbazone)(L) resulted in the complex with stoichiometry [Ag₂Cl₂(κ¹-S-L)₂(μ-S,S-L)₂] **38**, and [AgBr(κ¹-S-L)(Ph₃P)₂] **39**[54]. In complex **38** two thione sulphur (Ag-S), one chloride (Ag-Cl), and one thiophene ring sulphur (Ag-S⁴) coordinate to each silver metal center yielding a flattened tetrahedron geometry. However in complex **39** the reaction resulted in a distorted tetrahedral complex. Each Ag atom is coordinated with, two P of Ph₃P, one bromine halide while the ligand coordinating via S- mode.

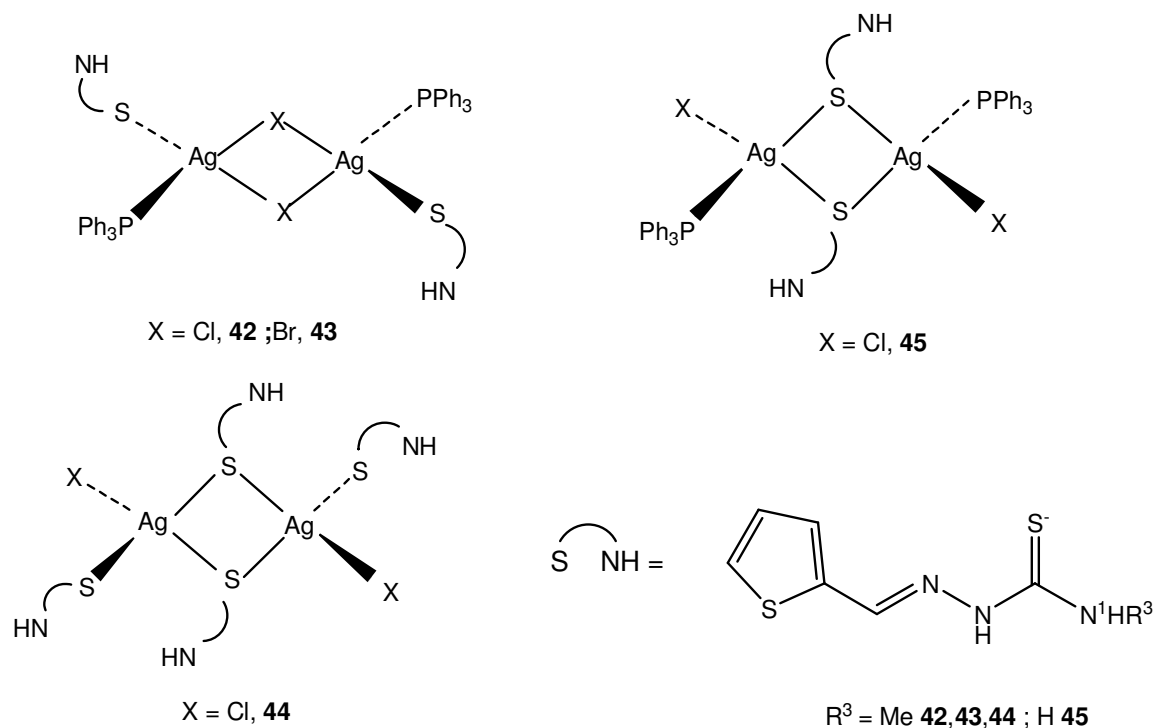


Silver(I) acetate reacted with thiophene-2-carbaldehyde thiosemicarbazones (Httsc-N-R)(L) (R = Me **40**; Et, **41**) in presence of Ph₃P as coligand, resulting in a S- bridged complex with stoichiometry [Ag₂(μ₃-N,S-LR)₂(Ph₃P)₂] (R = Me **40**; Et, **41**)[54]. Both the complexes have distorted tetrahedral geometry with central metal in both the complexes coordinated via N³ atom of terminal ligand, one P atom of coligand (Ph₃P) and S- coordinated bridged ligand forming a dimer. N³-S chelation of terminal ligand with the bridging ligand is also observed.

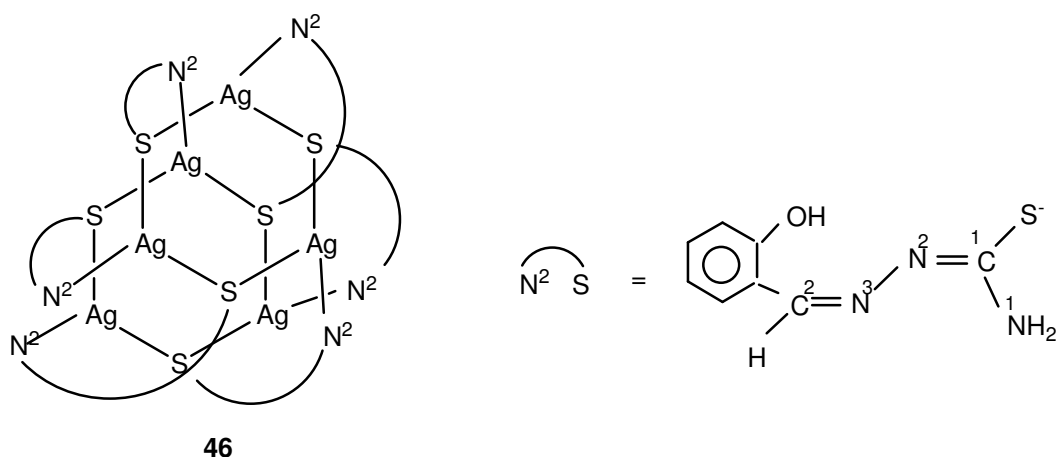


Thiophene-2-carbaldehyde N¹ methyl thiosemicarbazones (HttscMe) (L) reacted with Ag(I)X (X = Cl, **42**; Br, **43**) in presence of triphenylphosphine (Ph₃P) which yielded complex with stoichiometry Ag₂((μ-X)₂(η¹-S-L) (X = Cl, **42**; Br, **43**, L = HttscMe)[318]. Complex **42** and **43** are both halogen bridged dimers with almost square planar geometry around the central metal. Each silver is terminally coordinated with one P of triphenylphosphine and one S- of the ligand.. In a similar reaction of Ag(I)X (X = Br) **44** with 2,2'-bipyridine yielded a bridged dimer with a

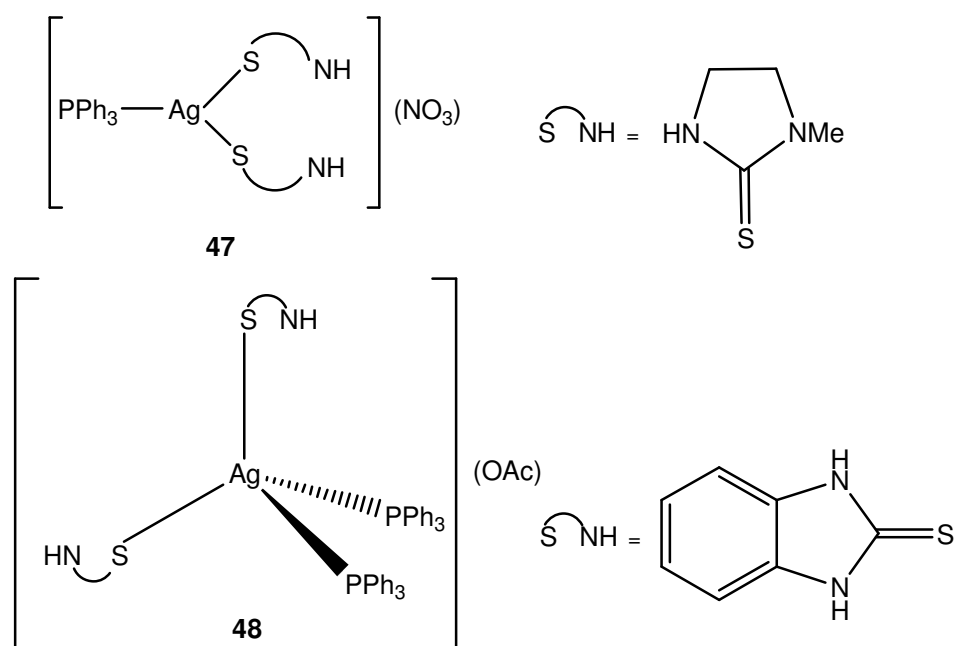
distorted tetrahedral geometry around the central metal having stoichiometry $[\text{Ag}_2(\mu\text{-S-L})(\eta\text{-L})_2] \cdot 2\text{CHCl}_3$ $\text{L} = \text{HttscMe}$ **44**. Silver metal is terminally coordinated with one sulphur and one chloride atom and two bridging sulfur giving a distorted tetrahedra. Reaction of Ag(I)X ($\text{X} = \text{Cl}$) **45** with (HttscMe) yields a sulfur bridged dimer having stoichiometry $\text{Ag}_2\text{Cl}_2(\mu\text{-S-L})(\text{Ph}_3\text{P})_2 \cdot 2\text{CH}_3\text{CN}$. Terminal chlorine has intra molecular H-bonded with imino group of the S- bridged ligand.[54]



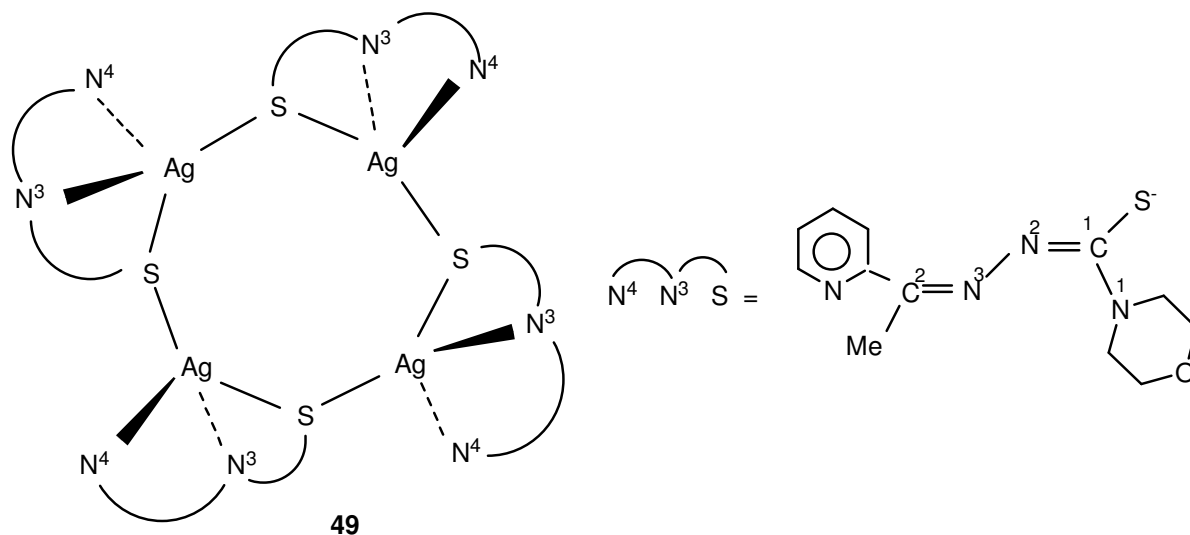
Dilworth et al. reported the first complex of silver with salicaldehyde thiosemicarbazones (L), which was structurally characterized. STSC(L) reacts with Ag(I) atom in DMF to form complex with stoichiometry $[\text{Ag}_6(\text{L})_6]$ ($\text{L} = \text{STSC}$) **46** [55]. Each Ag atom is three coordinated via two atoms of thiosemicarbazones forming bridge between two Ag centres and one N^2 donor atom. This hexanuclear complex with three S- atom of anionic thiosemicarbazones ligand and three Ag atoms form a six membered ring. Two such rings are connected by N^2 atom of salicaldehyde thiosemicarbazones.



Reaction of AgNO_3 with 1-methyl-imidazoline-2-thione (L-N-Me-S) (HL) in presence of Ph_3P resulted in a three coordinated monomer of stoichiometry $[\text{Ag}(\text{HL})_2(\text{Ph}_3\text{P})]\text{X}$ ($\text{X} = \text{NO}_3$) **47**[55]. The geometry around the central metal atom is distorted trigonal planar while NO_3 lying outside the sphere of coordination. The trigonal geometry is completed by one P of triphenylphosphine and S- coordinated two ligands. Reaction of silver(I) acetate with benzimidazole-2-thione(LNHS) yielded distorted tetrahedral arrangement with stoichiometry $[\text{Ag}(\text{LNHS})_2(\text{PPh}_3)_2]\text{OAc}\cdot\text{H}_2\text{O}$ **48**[55]. Each silver atom is surrounded by two P from Ph_3P and the ligand coordinating via S-atom.



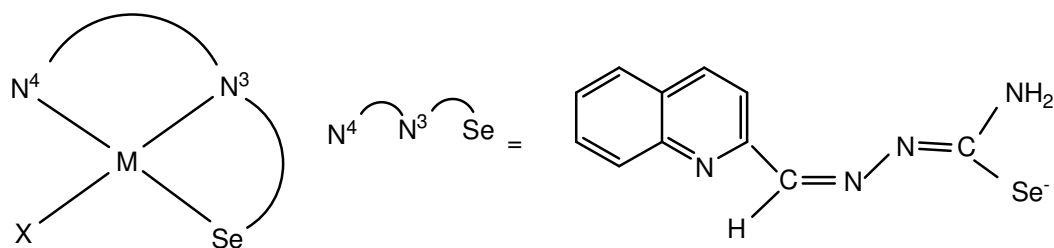
Reaction of Ag(L) (L = 2-pyrrolidine-5-carboxylate) with thiosemicarbazones resulted in the formation of a neutral tetrameric Ag(I) cluster with stoichiometry $[\text{Ag}(\text{L})]_4 \cdot 2\text{CHCl}_3$ **49**[56]. The ligand 2-pyrrolidine-5-carboxylate coordinates in a uninegative tridentate manner via N, N, S-donor atoms.



2.1.3 Metal-complexes of selenosemicarbazones:

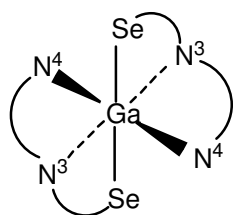
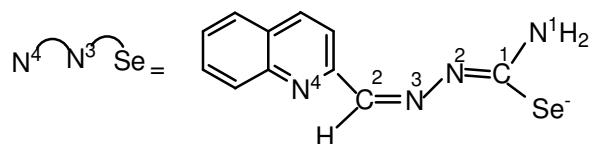
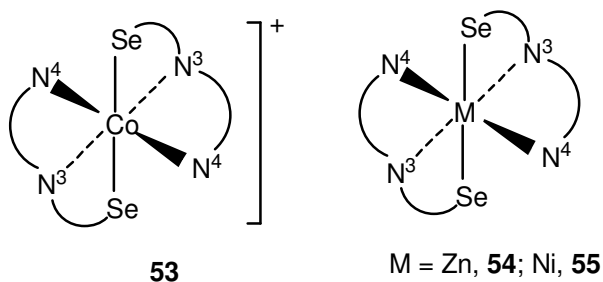
The complexes of selenosemicarbazone with transition metals are limited because C=Se bond is less stable than C=S. Due to the larger size of selenium atom, the overlap between C-S (both sigma and pi) is not very strong. Thus only few x-ray characterized complexes are known in literature. A brief description of these complexes is given below:

2-Quinolinecarboxaldehyde selenosemicarbazone (Hqasesc) formed square planar complexes with Pt(II) and Pd(II) namely, $[\text{M}(\text{qasesc})\text{Cl}]$ (M = Pt, **50**; Pd, **51**) and with Cd(II), $[\text{Cd}(\text{qasesc})(\text{OAc})] \cdot \text{H}_2\text{O}$ **52** [57, 58]. In these complexes ligand is anionic, tridentate coordinating via N^4 , N^3 , Se- donor atoms.

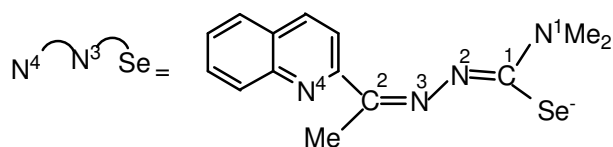


M = Pt, X = Cl, **50**; Pd, Cl, **51**;
Cd, OAc; **52**

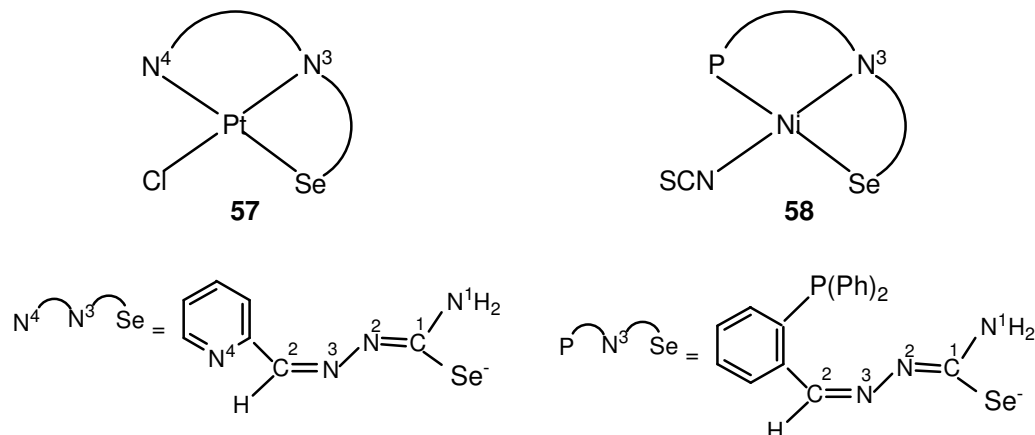
Octahedral complexes with Co(III), Zn(II) and Ni(II), [Co(qasesc)₂] BF₄·2H₂O **53**, [Zn(qasesc)₂]·3H₂O **54** and [Ni(qasesc)₂] **55** respectively, were formed with same ligand [58,64]. 2-acetylpyridine-N-dimethyl thiosemicarbazone (HapySeMe₂) also formed octahedral complex, [Ga(hapySeMe₂)₂] **56** with gallium [58].



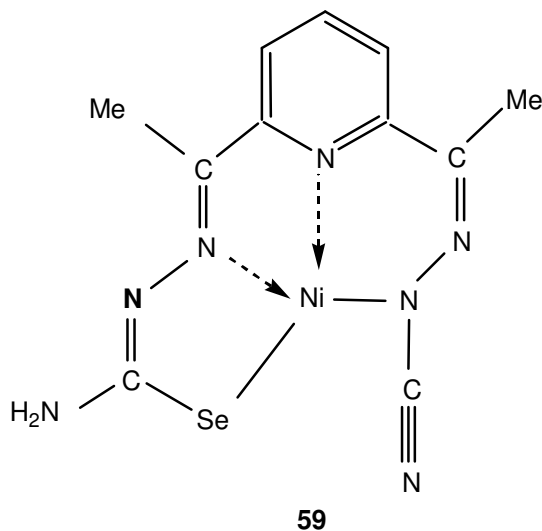
56



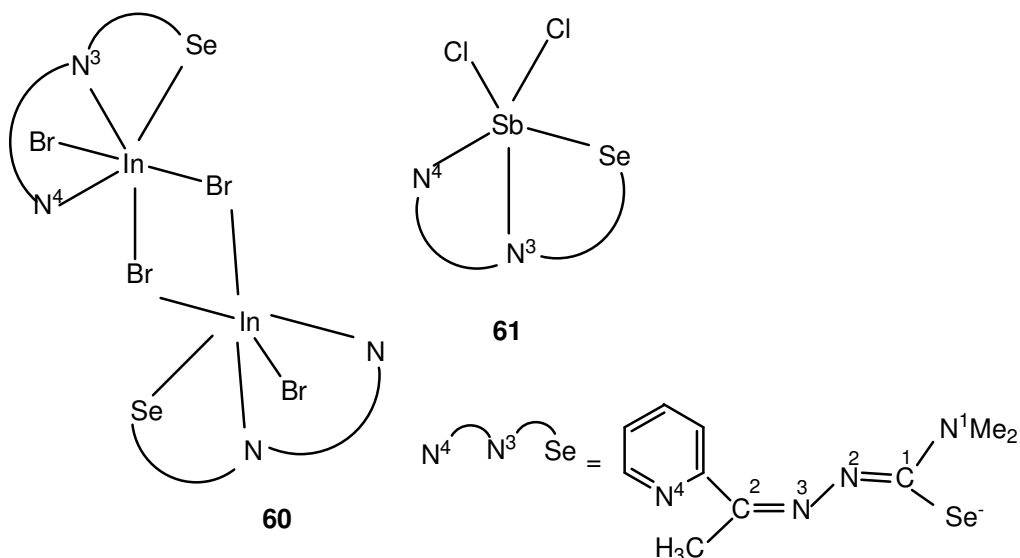
Pyridine-2-carbaldehyde selenosemicarbazone (Hpysesc) and 2-(diphenylphosphino)benzaldehyde selenosemicarbazone (HL) formed four coordinated complex, [Pt(pysesc)Cl] **57** and [Ni(L)SCN] [48, 49]. Ligand is coordinated to metal center via imine nitrogen, nitrogen of pyridine and thionate sulfur in complex **57** and imine nitrogen, phosphorous of diphenylphosphine and thionate sulfur in complex **58**. Moreover complex **58** is diamagnetic.



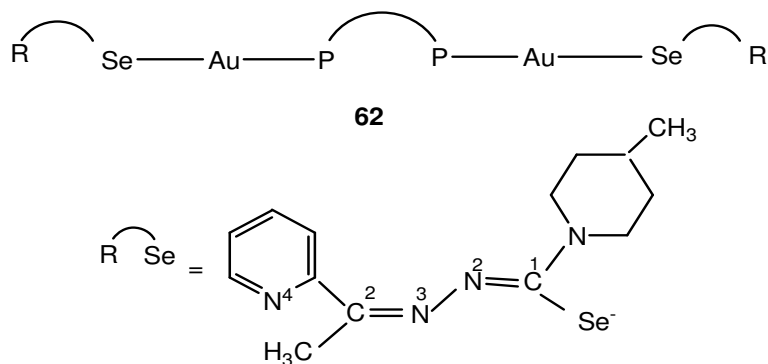
2,6-diacetylpyridine-bis(selenosemicarbazone) reacted with Ni(Oac) \cdot 4H₂O, a part of side chain of symmetrical ligand was modified with evolution of hydrogen selenide resulting in the formation of complex of Ni(II) with 2-{1-[6-(1-selenosemicarbazonoethyl)-2-pyridyl]ethylidene} hydrazine carbonitrile **59**. Ligand Acts as quardentate coordinating via N₃Se donor atoms [51].



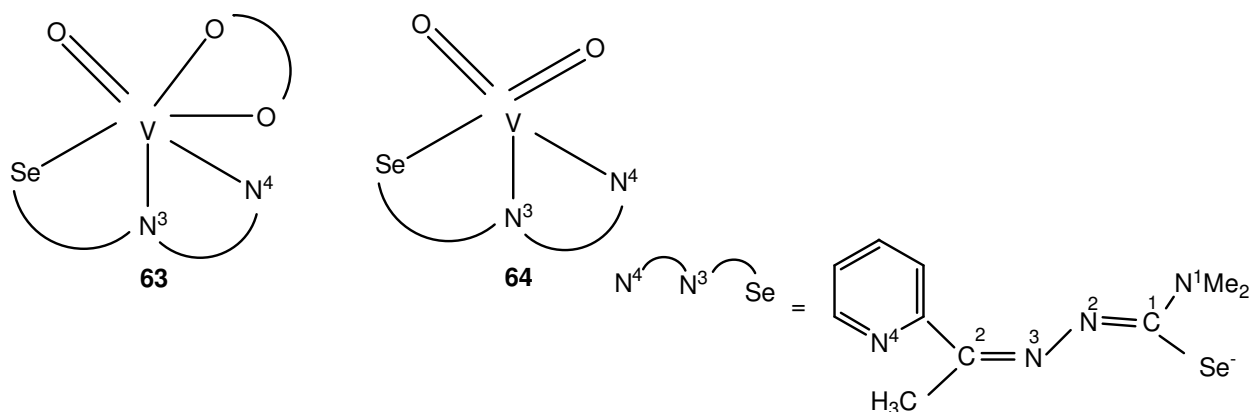
In(III) and Sb(III) formed complexes with pyridine based selenosemicarbazone, namely, $[\text{In}(\text{L})\text{Br}_2]$ **60** and $[\text{Sb}(\text{L})\text{Cl}_2]$ **61** respectively [67]. In complex **60**, dimer is formed by a weak interaction with a bromide ligand from a neighboring molecule. In complex **61**, the chloride ligands on the axial positions are bent slightly towards the selenosemicarbazone ligands.



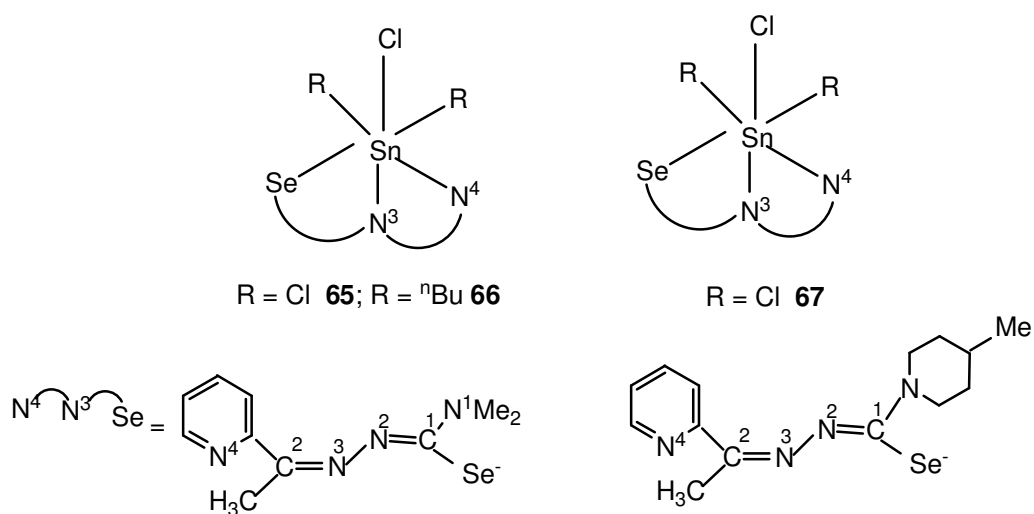
A dinuclear complex of gold(I) phosphine with acetylpyridyl based selenosemicarbazone (HL), $[\text{Au}_2(\text{L})_2(\mu\text{-dppf})]$ **62** was formed and tested for antimalarial activity against chloroquine sensitive strain of *plasmodium falciparum*. IC₅₀ results show moderate antimalarial activity of these compounds [41].



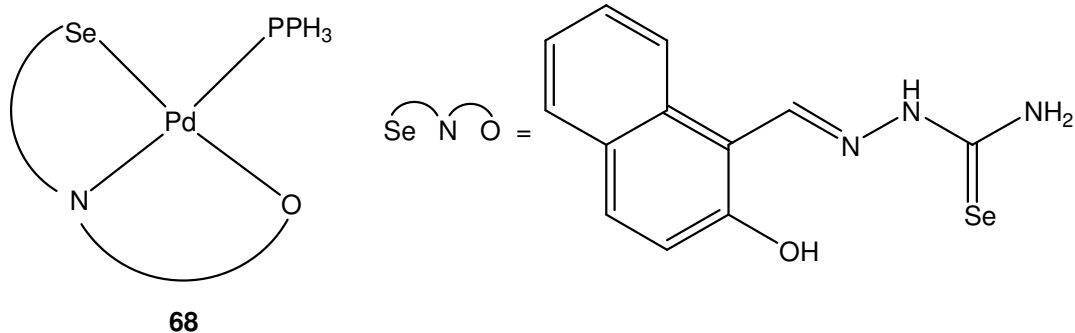
Oxovanadium(IV) and dioxovanadium(V) form complexes with pyridine based selenosemicarbazone(HL), $[\text{VO}(\text{acac})(\text{L})]$ **63** and $[\text{VO}_2(\text{L})]$ **64** [69].



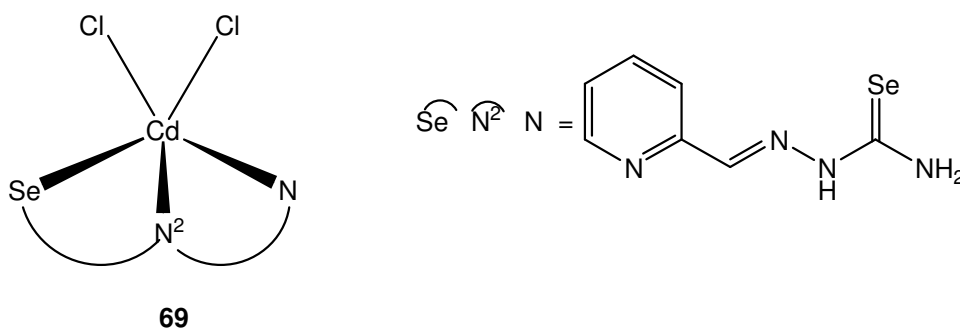
A series of tin(IV) complexes of type, [SnLCIR₂] **65-67** (R = ⁿBu, Me, Cl) containing pyridyl functionalized selenosemicarbazone was known. In vitro cytotoxicity of these compounds was evaluated in three different human tumor cell lines [43].



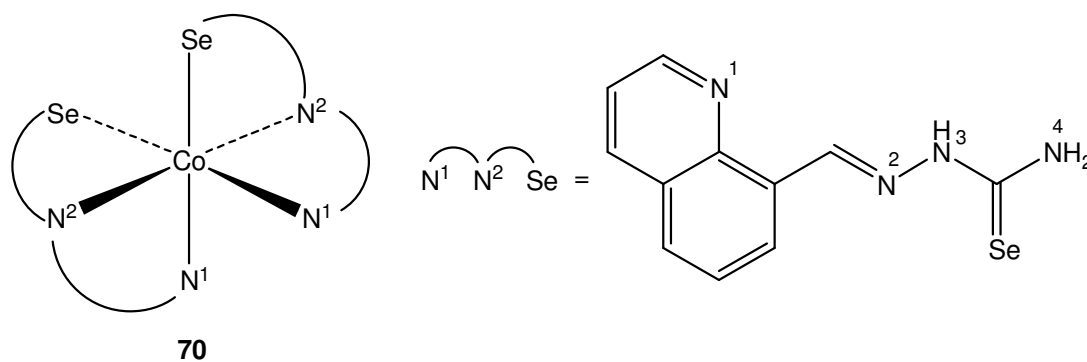
Reaction of 2-hydroxynaphthaldehyde selenosemicarbazone (HL) reacts with Pd in presence of triphenylphosphine and forms complex of stoichiometry [Pd(HL)PPh₃] **68**[60] having a square planar geometry. Pd is coordinated via Se⁻ of the ligand, O⁻, imine nitrogen, and P of PPh₃ which is trans to imine nitrogen.



Reaction of 2-formalpyridine selenosemicarbazone (Hfpsesc) (HL) with Cd(II) yields a square pyramidal geometry with stoichiometry $[CdCl_2(HL)]$ **69**[61]. Ligand is coordinated to the central metal via Se-, pyridine and azomethine nitrogen forming N, N, Se chelation. Two chloride around the central metal complete the five-coordination.



8-quinonecarboxyaldehyde selenosemicarbazone (H8qsasc) (HL) reacted with Co(III) yielding an octahedral complex with stoichiometry $[Co(HL)_2]^+$ **70**[62]. Ligand coordinates with the central metal via Se-, imine nitrogen and quinoline in a tridentate manner resulting N^1, N^2, Se - chelation.



2.2 Significance:

From the above literature survey, it is clear that only few complexes of fused ring thiosemicarbazone are characterized by x-ray. There is a large scope in this area. Moreover, extensive conjugation can impart fluorescence to these complexes. Coordination chemistry of selenosemicarbazone is a challenge for synthetic chemist and need to be explored to know the bonding modes, possible nuclearities and geometries possible for such ligands. Selenosemicarbazone shows number of biological activities, and activity of these ligands get enhanced on complexation.

2.3 Objectives:

From the literature survey it is clear that structure of only few complexes of fused ring thiosemicarbazone complexes are known till date. Moreover, no study is made on selenosemicarbazone interaction with d^{10} metal ions (Cu^{I} and Ag^{I}). Keeping all these points in mind the following objectives have been planned for current research work:

1. Synthesis and characterization (CHN, IR, NMR) of fused ring thiosemicarbazone given in Chart-4
2. Synthesis and characterization of complexes of copper(I) and silver(I) with fused ring thiosemicarbazone (CHN analysis, IR, NMR, single crystal X-ray (wherever possible)).
3. Synthesis and characterization (CHN, IR, NMR, single crystal X-ray) of selenosemicarbazone listed in Chart-5.
4. Synthesis and characterization (CHN, IR, NMR, single crystal x-ray (if possible) of complexes of copper(I) and silver(I) with selenosemicarbazones.
5. To study the antibacterial, antifungal, anti- tuberculosis and antitumor study of some of synthesized ligands and complexes.

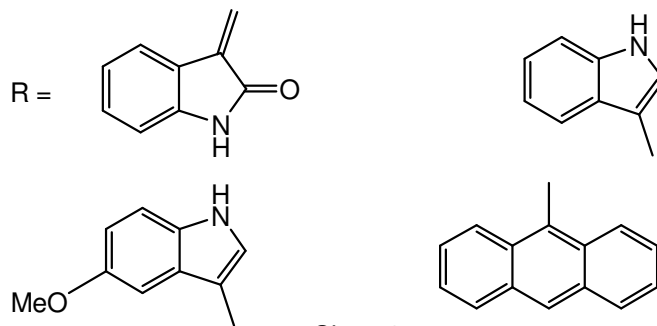
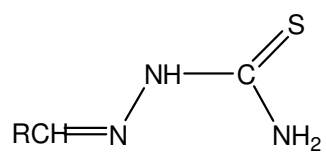


Chart 4

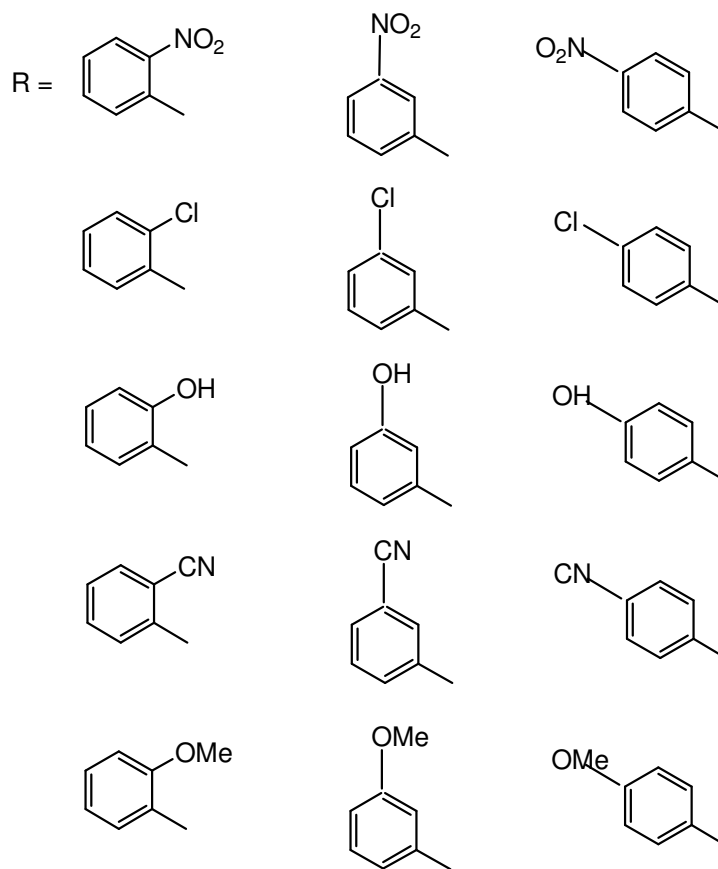
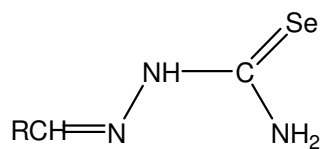


Chart 5

CHAPTER 3

GENERAL EXPERIMENTAL

This chapter gives general details of instruments, analytical, spectroscopic and structural techniques used. In addition methods of preparation of ligands and metal salts and procurement of various materials are described.

3.1 Instrumentation:

NMR Spectroscopy: ^1H NMR and ^{13}C NMR spectra of free ligands and their complexes were recorded on an AV500 FT spectrometer operating at a frequency of 500MHz and 400MHz (model no.D 205/52-2382 Avance 500) in $\text{d}^6\text{-dmsO}/\text{CDCl}_3$ mixture with TMS as a internal reference from IIM (Srinagar) J&K.

Elemental analysis: C, H and N elemental analysis of complexes were obtained from thermo electro FLASHEA 1112 micro-analyzer from Guru Nanak Dev University and Punjab University, Punjab.

Infrared spectroscopy: Infrared (IR) spectra of free ligands and their complexes were recorded using KBr pellets by SHIMADZU FTIR 8400S, Fourier Transform, Infrared spectrophotometer from Department of Chemistry, Lovely Professional University, Punjab.

Crystal Snaps: Crystal snaps of complex $[\text{CuX}(\text{H}_2\text{itsc-N}^1\text{-R})(\text{Ph}_3\text{P})]$, ($\text{X} = \text{I, Cl, Br}$) ($\text{R}=\text{Me, Et}$) (**A**), $[\text{CuX}(\text{Ph}_3\text{P})_3]$ (**B**) and yellow needles of free ligand ($\text{H}_2\text{itsc-N}^1\text{-R}$) ($\text{R}=\text{Me, Et}$) (**C**) were taken from OLYMPUS Magnus MLX Camera (40x and 100x) from Department of Biotechnology, Lovely Professional University, Punjab.

X-Ray: A single crystal was used for data collection with Agilent, Eos, Gemini (**2**) and *X'calibur* CCD (H_2L^1), equipped with graphite monochromated Mo-K α radiation ($\lambda = 0.71073 \text{ \AA}$). Crystal data was collected at 173(2) (**2**) and 293(2) (H_2L^1) K. Data was processed with CrysAlisPro, Agilent Technologies (**2**), CrysAlisPro, Oxford Diffraction Ltd (H_2L^1) (data collection) and CrysAlisPro RED (cell refinement, data reduction). For structure solution program SHELXS-97 (H_2L^1) was used, whereas structure refinement was done by SHELXL (**2**) and SHELXL-97 (H_2L^1). Atomic scattering factors taken from "International Tables for Crystallography." (**2**) Department of Physics & Electronics, University of Jammu (Jammu Tawi), J&K.

For **12, 13, 14, 19, 20, 22, 31, 35, 38, HL⁷** single crystal was used for data collection with Agilent, Eos, Gemini equipped with graphite monochromated Mo-K α radiation ($\lambda = 0.71073$ Å) (**12, 31**) ($\lambda = 1.54184$ Å) (**13, 14, 19, 20, 22, 35, 38, HL⁷**). Crystal data was collected at 173(2) K (**12, 13, 14, 19, 20, 22, 31, 35, 38**). Data was processed with CrysAlisPro, Agilent Technologies, (cell refinement, data collection, reduction). For structure solution program (Superflip (Palatinus & Chapuis, 2007; Palatinus & van der Lee, 2008; Palatinus et al., 2012) **12, 13, 20, 22, 31** and ShelXT (Sheldrick, 2015) (**19, 35, 38, HL⁷**) was used, whereas structure refinement was done by SHELXL-(Sheldrick, 2008) (**12, 13, 19, 20, 22, 31, 35, 38**) 'ShelXL (Sheldrick, 2015)(**14, HL⁷**). Atomic scattering factors were taken from “International Tables for Crystallography.”

Cytotoxicity studies: L123 (human lung cells) and HepG2 (Human hepatocellular carcinoma cells) was cultured in Dulbecco's modified Eagle's medium with 10% fetal bovine serum (heat inactivated), 100 units mL⁻¹ penicillin, 100 μ g mL⁻¹ streptomycin, and 2.5 μ g mL⁻¹ amphotericin B, at 37 °C in a saturated humidity atmosphere containing 95% air/5% CO₂. The cell lines were harvested when they reached 80% confluence to maintain exponential growth from School of Chemistry and Biochemistry, Thapar University (Patiala), Punjab.

Anti-TB activity: The anti mycobacterial activity of compounds were assessed against *M.Tuberclulosis* H₃₇RV strain ATCC 27294 using micro plate alamar blue assay (MABA) from Maratha Mandal Dental College (Belgaun), Mumbai.

Antifungal and Antibacterial activity: The anti-microbial tests were conducted on two fungal species *Aspergillus fumigates* and *Pencillium chrysogenum* (NCIM, 902 & 738) and on two bacterial species *Salmonella typhimurium* and *E.coli* (NCIM, 2501 & 2563) using disk-diffusion method from Department of Biotechnology, Lovely Professional University, Punjab.

Docking studies: Compounds were built using the builder tool kit of the software package Argus Lab 4.0.1.23 (www.arguslab.com) and energy minimized with semi-empirical quantum mechanical method PM3. Crystal coordinates of Hodgkin lymphoma enzyme and DNA were downloaded from protein data bank and in the molecule tree view of the software, the monomeric structures of the crystal co-ordinate was selected and the active site was defined

as 15 Å around the ligand from School of Chemistry and Biochemistry, Thapar University (Patiala), Punjab.

3.2 Experimental

3.2.1 Synthesis of Copper(I) and Silver(I) halides

Synthesis of copper(I) iodide: Dissolved $\text{CuSO}_4 \cdot 5\text{H}_2\text{O}$, (5 g, 20 mmol) in 50 ml of warm distilled water. To it was added KI, (3.14 g, 20 mmol) and stirred with glass rod until clear solution was formed. To this solution pass SO_2 gas in excess (SO_2 was produced by addition of H_2SO_4 to Na_2SO_3), white coloured precipitate were separated out in solution. Wash the precipitate three four times with distilled water and then two-three times with methanol. Filtered them and dried in vacuo.

Synthesis of copper(I) bromide: Dissolved $\text{CuSO}_4 \cdot 5\text{H}_2\text{O}$, (5 g, 20 mmol) in 50 ml of warm distilled water. To it was added KBr, (2.38 g, 20 mmol) and stirred with glass rod until clear solution was formed. To this solution pass SO_2 gas in excess (SO_2 was produced by addition of H_2SO_4 to Na_2SO_3), white coloured precipitate were separated out in solution. Wash the precipitate three-four times with distilled water and then two-three times with methanol. Filtered them and dried in vacuo.

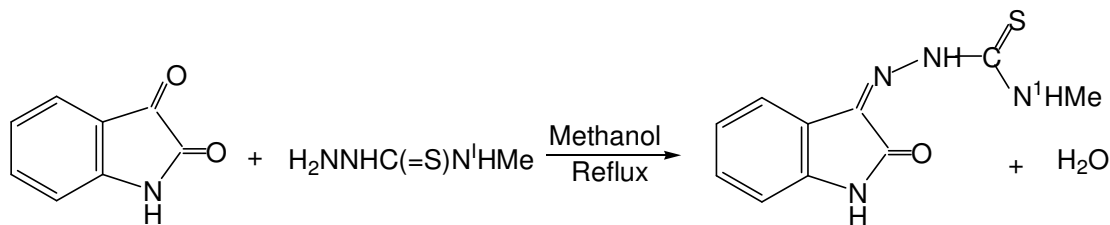
Synthesis of copper(I) chloride: Dissolved $\text{CuSO}_4 \cdot 5\text{H}_2\text{O}$, (5 g, 20 mmol) in 50 ml of warm distilled water. To it was added KCl, (1.49 g, 20 mmol) and stirred with glass rod until clear solution was formed. To this solution pass SO_2 gas (SO_2 was produced by addition of H_2SO_4 to Na_2SO_3), white coloured precipitate were separated out in solution. Wash the precipitate three four times with distilled water and then two-three times with methanol. Filtered them and dried in vacuo.

Synthesis of Silver(I) Chloride: Equimolar quantities of AgNO_3 solution with KCl/NaCl were dissolved in water resulting in the formation of white precipitates of AgCl. The precipitates were collected by filtration. Dried in vacuo and stored.

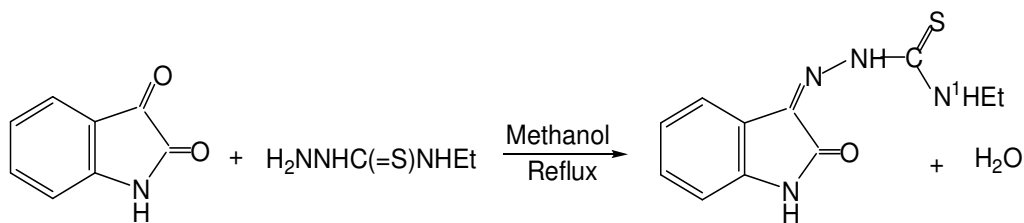
Synthesis of Silver(I) Bromide: Equimolar quantities of AgNO_3 solution with salts of KBr/NaBr were dissolved in water resulting in the formation of light green precipitates of AgBr. The precipitates were collected by filtration. Dried in vacuo and stored.

3.2.2 Synthesis of ligands (Thio- and Selenosemicarbazones):

Synthesis of N-methyl-isatin-3-thiosemicarbazone (H₂itsc-N¹-Me): Dissolved 4-Methyl-3-thiosemicarbazide, (0.5 g, 4.7 mmol) in 75 ml of methanol by refluxing for half an hour (tsc is not completely soluble in methanol alone, along with 1ml acetic acid has to be added). To it was slowly added isatin, (0.7 g, 4.7 mmol) and the reaction mixture was refluxed for 4-5 hours. On cooling at room temperature, yellow crystalline product was separated out, which was filtered and re-crystallized from methanol. Yellow needles, Yield, 86 %, m.p, 192-194°C. Main IR peaks (KBr, cm⁻¹): ν(N-H) 3304m, 3271m; ν(-NH-) 3149m; (NH, pyrrole) 3070m; ν(C-H_{Ph}), 2980m; ν(C-H_{Me}), 2872m; ν(C=O) 1689s; δ(NH₂) + ν(C=N) + ν(C-C) 1618, 1541s, 1464s; ν(C=S) 825s (thioamide moiety), ¹H NMR (d⁶-dmso, δ ppm.): 12.60 s (1H, NH, pyrrole), 11.22 s (1H, N²H), 9.263 s (1H, N¹H), 7.64 s (1H, C⁵H), 7.37 s (1H, C⁶H), 7.11 s (1H, C⁷H), 6.94 (1H, C⁸H), 3.17 m (3H, CH₃).

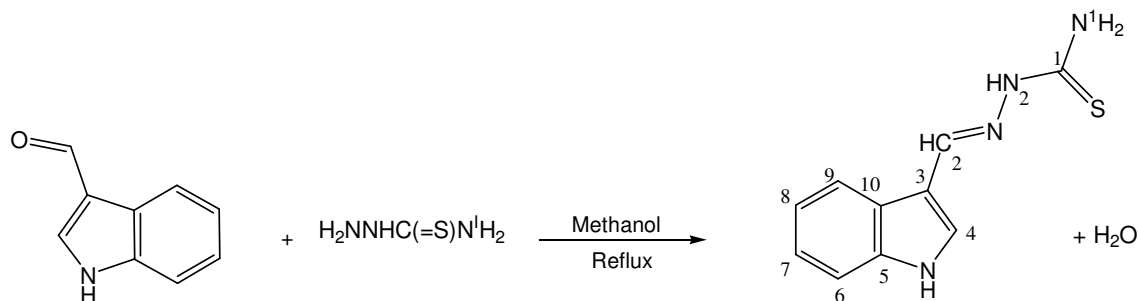


Synthesis of N-ethyl-isatin-3-thiosemicarbazone (H₂itsc-N¹-Et): Dissolved 4-Ethyl-3-thiosemicarbazide, (0.5 g, 4.2 mmoles) in 75 ml of methanol by refluxing for half an hour. To it was slowly added isatin, (0.61g, 4.2 mmoles) and the reaction mixture was refluxed for 4-5 hours. On cooling yellowish coloured crystalline product was separated out. Filtered them and recrystallized from methanol. Yellow needles, Yield, 87%, Highly soluble in CH₃OH, partially soluble in CH₃CN, CH₂Cl₂ and CHCl₃, m.p, 190-192° C. Main IR peaks (KBr, cm⁻¹): ν(N-H) 3244m; ν(-NH-) 3140m; (NH, pyrrole) 3070m; ν(C-H_{Ph}), 2945m; ν(C-H_{Me}), 2827; ν(C=O) 1695s; δ(NH₂) + ν(C=N) + ν(C-C), 1622, 1541s, 1473s; ν(C=S) 837s (thioamide moiety). ¹H NMR (d⁶-dmso, δ ppm.): 12.55 s (1H, NH, pyrrole), 11.22 s (1H, N²H), 9.3 s (1H, N¹H), 7.66 s (1H, C⁵H), 7.36 s (1H, C⁶H), 7.10 s (1H, C⁷H), 6.94 s (1H, C⁸H), 2.5 t (3H, CH₃), 1.19 q (2H, CH₂).



Synthesis of indole-3-thiosemicarbazone (HIntsc):

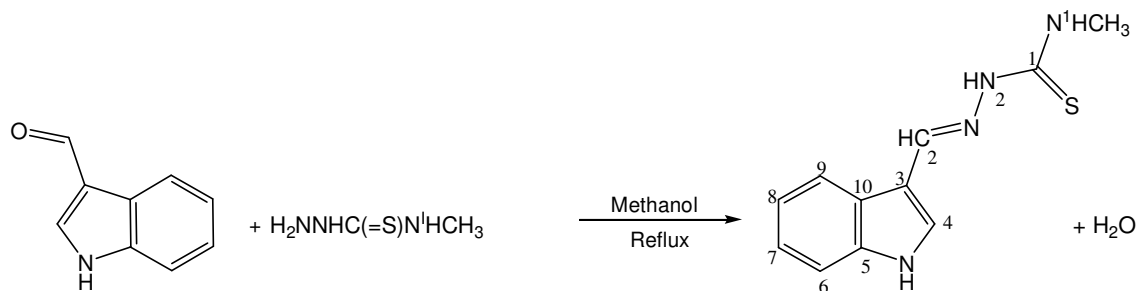
Thiosemicarbazide, (0.31 g, 3.44 mmol) was dissolved in 75 ml of ethanol with heating. To it was added Indole-3-carboxyaldehyde (0.5 g, 3.44 mmol) and the mixture was refluxed for 5-6 hours. Solution was filtered and kept for crystallization at room temperature. Light brown crystalline product was separated out after 3-4 days. Yield, 86 %, m.p, 165-168° C. Main IR peaks (KBr, cm^{-1}): $\nu(\text{N-H})$ 3311m, 3232m; $\nu(-\text{NH}-)$ 3146m; (NH, indole) 3039m; $\delta(\text{NH}_2)$ + $\nu(\text{C=N})$ + $\nu(\text{C-C})$ 1612m, 1579s, 1444s; $\nu(\text{C=S})$ 837s (thioamide moiety). $^1\text{H NMR}$ (δ , ppm; J , Hz; CDCl_3): 10.07 s (1H, N^2H), 8.33 s (1H, N^4H), 3.48 s (1H, N^1H), 7.83 s (1H, C^2H), 7.86 s (1H, C^4H), 7.46 d (2H, $J = 8$ Hz, $\text{C}^{6,9}\text{H}$), 7.29 d (2H, $J = 8$ Hz, $\text{C}^{7,8}\text{H}$).



Synthesis of indole- N^1 -methyl-3-thiosemicarbazone (HIntsc- N^1 -Me):

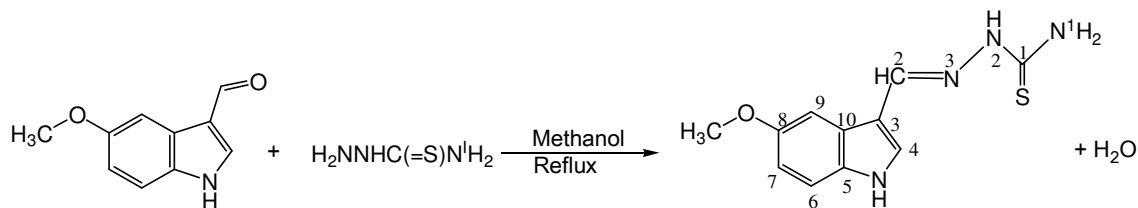
4-methyl thiosemicarbazide (0.80 g, 3.44 mmol) was dissolved in 75 ml of ethanol with heating. To it was added Indole-3-carboxyaldehyde (0.5 g, 3.44mmol) and the mixture was refluxed for 5-6 hours. Solution was filtered and kept for crystallization at room temperature. Pale white crystalline product was separated out after 3-4 days. Yield, 86 %, m.p, 185-188° C; Main IR peaks (KBr, cm^{-1}): Main IR peaks (KBr, cm^{-1}): $\nu(\text{N-H})$ 3363m, 3238m; $\nu(-\text{NH}-)$ 3188m; (NH, indole) 3051m; $\nu(\text{C-H}_{\text{Me}})$, 2978m; $\delta(\text{NH}_2)$ + $\nu(\text{C=N})$ + $\nu(\text{C=C})$ 1656m, 1546s, 1498s; $\nu(\text{C=S})$ 831s (thioamide moiety). $^1\text{H NMR}$ (δ , ppm; J , Hz; CDCl_3): 11.24 s (1H, N^2H), 10.95 s (1H, N^4H), 7.39 s (1H, N^1H), 8.10 s (1H, C^4H), 7.14 m (2H, $J = 8$ Hz, $\text{C}^{6,9}\text{H}$), 7.46 d

(2H, $J = 7.2$ Hz, $C^{7,8}H$), 3.16 m (3H, $-CH_3$). ^{13}C NMR (δ , ppm; $CDCl_3$): 176.8 (C^1) 148.4 (C^2), 129.8 (C^3), 129.8 (C^4), 136.9 (C^5), 123.9 ($C^{6,9}$), 120.4 (C^7), 122.4 (C^8), 121.5 (C^{10}).



Synthesis of 5-methoxy indole-3-thiosemicarbazone (5-MeOIntsc):

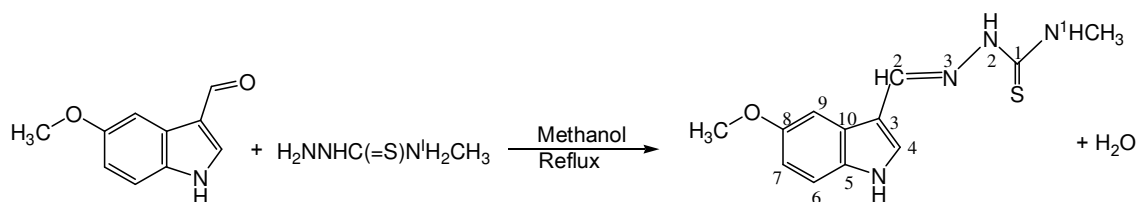
Thiosemicarbazide (0.25 g, 2.85 mmol,) was dissolved in 75 ml of ethanol with heating. To it was added 5-Methoxy Indole-3-carboxyaldehyde (0.5 g, 2.85 mmol) and the mixture was refluxed for 5-6 hours. Solution was filtered and kept for crystallization at room temperature. Pale white crystalline product was separated out after 3-4 days. Yield, 88 %, m.p, 243-246° C; Main IR peaks (KBr, cm^{-1}) $\nu(N-H)$ 3437s, 3362s; $\nu(-NH-)$ 3134m; $\nu(N-H_{Indole})$ 3047m; $\nu(C-H_{Ph})$, 2985m; $\nu(C=C)$ 1616s; $\delta(NH_2) + \nu(C=N) + \nu(C=C)$ 1616s, 1589s, 1475s; $\nu(C=S)$ 854s (thioamide moiety). 1H NMR (δ , ppm; J , Hz; $CDCl_3$): 10.04 s (1H, N^2H), 7.32 d (2H, CH), 8.61 s (1H, C^2H), 7.78-6.95 m ($C^{4,6,9}H + N^1H + PH^3P$), 7.29 d (1H $J = 8$ Hz, C^7H), 3.88-3.86 m (3H, O- CH_3). ^{13}C NMR (δ , ppm; $CDCl_3$): 185.4 (C^1), 136.1, (C^2) 103.4 (C^3), 135.6 (C^4), 115.2, (C_5), 112.4 (C^6), 115.4 (C^7), 131.8 (C^8), 125.4 (C^9), 119.7 (C^{10}), 55.9, ($-OCH_3$).



Synthesis of 5-methoxy indole- N^1 -methyl-3-thiosemicarbazone (5-MeOHIntsc- N^1 -Me):

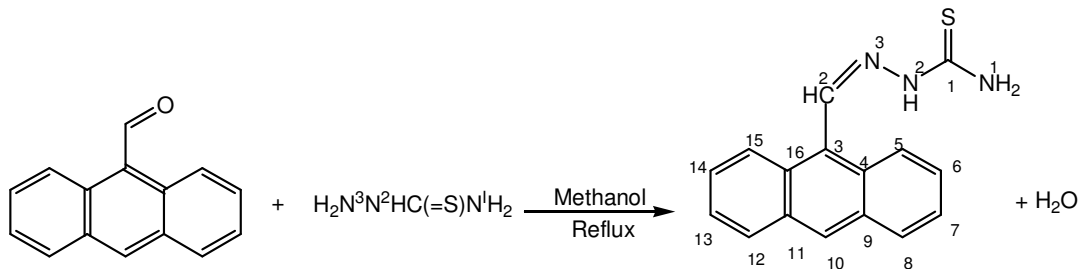
4-Methyl thiosemicarbazide (0.66 g, 2.85 mmol,) was dissolved in 75 ml of ethanol with heating. To it was added 5-Methoxy Indole-3-carboxyaldehyde (0.5 g, 2.85 mmol) and the mixture was refluxed for 5-6 hours. Solution was filtered and kept for crystallization at room temperature. Pale white crystalline product was separated out after 3-4 days. Yield, 84 %, m.p, 243-246° C;

m.p, 198-200° C; Main IR peaks (KBr, cm^{-1}): $\nu(\text{N-H})$ 3371s, 3230m; $\nu(-\text{NH}-)$ 3151m; (NH , indole) 3012m; $\nu(\text{C-H}_{\text{Me}})$ 2955m; $\nu(\text{C-H}_{\text{Ph}})$, 2897m; $\delta(\text{NH}_2) + \nu(\text{C=N}) + \nu(\text{C=C})$ 1614m, 1572s, 1479s; $\nu(\text{C=S})$ 831s (thioamide moiety). $^1\text{H NMR}$ (δ , ppm; CDCl_3): 10.01 s (1H, N^2H), 8.94d (1H, N^4H), 8.84 s (1H, C^2H), 7.78-6.94 m ($\text{C}^{4,6,9}\text{H} + \text{N}^1\text{H} + \text{Ph}^3\text{P}$), 6.94 s (1H, C^7H), 3.87s (3H, $-\text{OCH}_3$), 1.57 s (1H, $-\text{CH}_3$). $^{13}\text{C NMR}$ (δ , ppm; CDCl_3): 185.4 (C^1), 156.8 (C^2), 135.7 (C^4), 131.1 C (C^8) 125.4 (C^9), 119.7.1 (C^{10}), 115.4 (C^7), 112.4 (C^6), 103.4 (C^3), 55.9 ($-\text{OCH}_3$), 31.5 ($-\text{CH}_3$).



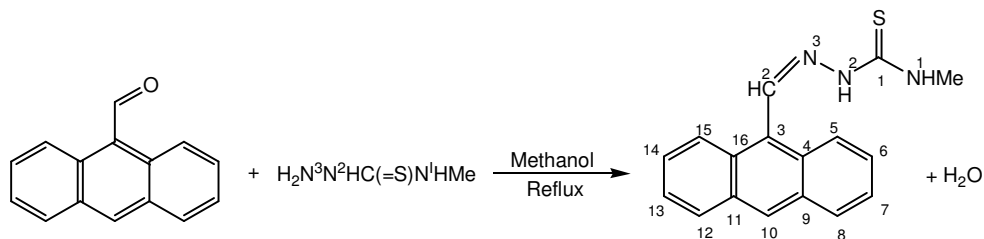
Synthesis of 9-anthraldehyde thiosemicarbazone (9-Hantsc):

Thiosemicarbazide, (0.22 g, 2.42 mmol) was dissolved in 75 ml of ethanol with heating. To it was added 9-anthraldehyde (0.5 g, 2.42 mmol) and the mixture was refluxed for 5-6 hours. Solution was filtered and kept for crystallization at room temperature. Yellow crystalline product was separated out after 3-4 days. Yellow needles, Yield, 85%, m.p, 163-165°C. Main IR peaks (KBr, cm^{-1}): $\nu(\text{N-H})$, 3437s, 3271s; $\nu(-\text{NH}-)$, 3155m; $\nu(\text{C-H}_{\text{Ph}})$, 3030m; $\delta(\text{NH}_2) + \nu(\text{C=N}) + \nu(\text{C=C})$ 1670s, 1599s, 1487s; $\nu(\text{C=S})$ 846s (thioamide moiety). $^1\text{H NMR}$ (δ , ppm; J , Hz; CDCl_3): 10.43 s (1H, N^2H), 8.49 s (1H, N^1H), 9.05 s (1H, C^2H), 8.41 d (2H, $J = 12$ Hz, $\text{C}^{5,15}\text{H}$), 8.50 s (1H, C^{10}H), 8.41 d (2H, $J = 12$ Hz, $\text{C}^{5,15}\text{H}$), 8.00 d (2H, $J = 8$ Hz, $\text{C}^{8,12}\text{H}$), 7.68-7.66 m (4H, $\text{C}^{6,7,13,14}\text{H} + \text{N}^1\text{H}_2$). $^{13}\text{C NMR}$ (δ , ppm; CDCl_3): 179.0 (C^1), 142.7 (C^2), 131.4 (C^{16}), 130.4 (C^4), 130.3 (C^9), 129.4 (C^{11}), 129.2 (C^5), 127.4 (C^{15}), 130.2 (C^{10}), 130.0 (C^3), 129.1 (C^8), 128.6 (C^{12}), 127.6 (C^6), 125.6 (C^{14}), 124.6 (C^7), 124.2 (C^{13}).



Synthesis of 9-anthraldehyde-N¹-methyl-3-thiosemicarbazone (9-Hanttsc-N¹-Me):

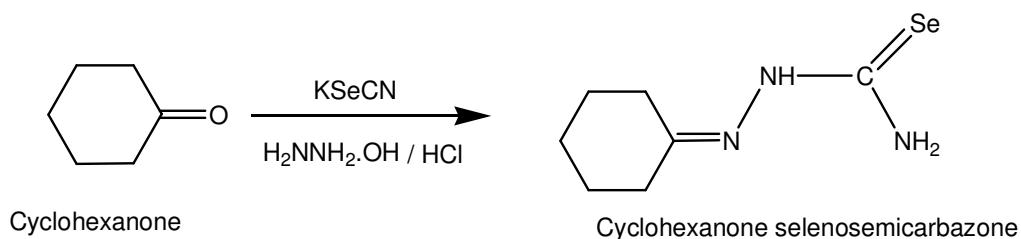
4-methyl thiosemicarbazide, (0.25 g, 2.42 mmol) was dissolved in 75 ml of ethanol with heating. To it was added 9-anthraldehyde (0.5 g, 2.42 mmol) and the mixture was refluxed for 5-6 hours. Solution was filtered and kept for crystallization at room temperature. Yellow crystalline product was separated out after 3-4 days. Yield, 84%, m.p, 145-147°C; Main IR peaks (KBr, cm⁻¹): $\nu(\text{N-H})$ 3398s, 3207s; $\nu(-\text{NH}-)$ 3113s; $\nu(\text{C-H}_{\text{Ph}})$, 3039m; $\nu(\text{C-H}_{\text{Me}})$ 2933m; $\delta(\text{NH}_2) + \nu(\text{C=N}) + \nu(\text{C=C})$ 1620s, 1529s, 1489s; $\nu(\text{C=S})$ 840s (thioamide moiety). ¹H NMR (δ , ppm; *J*, Hz; CDCl₃): 9.71 s (1H, N²H), 7.24 s (1H, N¹H), 8.89 s (1H, C²H), 8.53 d (2H, *J* = 8 Hz, C^{5,15}H), 8.56 s (1H, C¹⁰H), 8.06 d (2H, *J* = 8 Hz, C^{8,12}H), 7.57-7.47 m (4H, C^{6,7,13,14}H), 3.23 s (3H, -CH₃). ¹³C NMR (δ , ppm; CDCl₃): 178.9 (C¹), 140.8 (C²), 131 (C¹⁶), 139.7 (C⁴), 130.4 (C⁹), 130.2 (C¹¹), 129.4 (C¹⁰), 129.3 (C³), 127.8 (C⁵), 127.3 (C⁸), 127.3 (C¹⁵), 126.1 (C¹²), 125.7 (C¹⁴), 124.9 (C⁶), 124.6 (C⁷), 124.3 (C¹³), 30.3 (-CH₃).



Synthesis of Cyclohexanoneselenosemicarbazone:

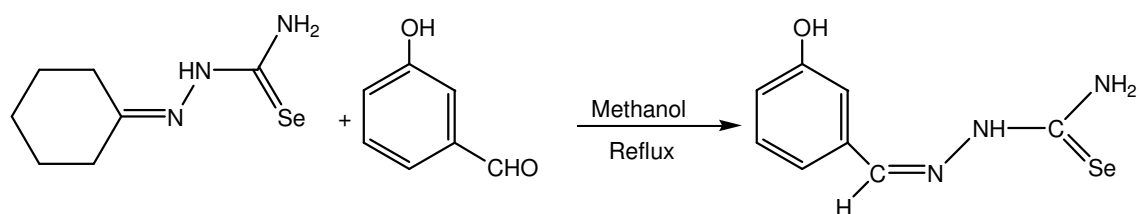
Cyclohexanone was prepared with minor modification of already reported method [71]. A solution of hydrazine hydrate, 3.75 g in a mixture of ethanol (100 ml) and water (12.5 ml) was prepared. To it was added mixture of KSeCN (3.6 g) dissolved in 25 ml of water and 8 ml cyclohexanone. The resulting mixture was refluxed for 2-3 hours. During refluxing pH was maintained upto 2.6 by adding HCl. The mixture is filtered to avoid any grey selenium (if deposited). The filtrate was evaporated in rotary evaporator until pale coloured oil left. Oil solidifies on cooling and was dissolved in CHCl₃. After evaporation white solid was formed and collected. Yield, 87%, m.p, 155-158°C. Main IR peaks (KBr, cm⁻¹): $\nu(\text{NH}_2)$ 3362s, 3252s; $\nu(-\text{NH}-)$ 3159s; $\nu(\text{C-H}_{\text{cyclo}})$, 2929s, 2856s; $\nu(\text{C=N}) + \nu(\text{C=C}) + \delta(\text{NH}_2)$ 1639, 1597s, 1491s; $\nu(\text{C=Se})$ 856s (selenoamide moiety). ¹H NMR (δ , ppm; CDCl₃): 9.12 s (1H, NH), 8.45 s (1H, NH₂), 7.66 s (1H, NH₂), 2.35 m (2H, Cy ring), 2.29 t (3H, *J* = 8Hz, Cy ring), 1.80-1.67 m (4H, Cy ring). ¹³C NMR (δ , ppm; CDCl₃): 185.4 (C¹), 136.1, (C²) 103.4 (C³), 135.6 (C⁴),

115.2, (C⁵), 112.4 (C⁶), 115.4 (C⁷), 131.8 (C⁸), 125.4 (C⁹), 119.7 (C¹⁰), 55.9, (-OCH₃), 31.53, (-CH₃).



Synthesis of 3-hydroxybenzaldehyde selenosemicarbazone [3-OH-Hbsesc]:

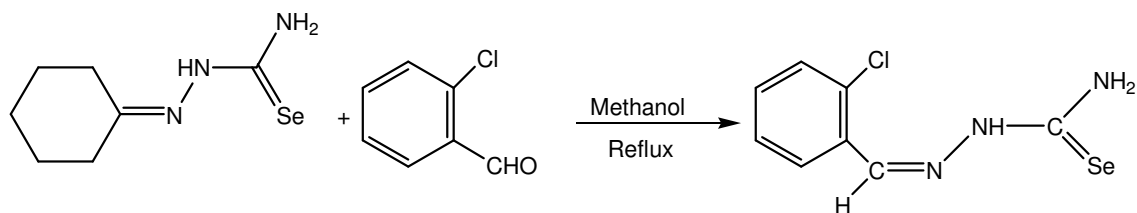
Cyclohexanone selenosemicarbazone, (0.5 g, 2.29 mmol) was dissolved in 50 ml of ethanol with heating. To it was added 3-hydroxybenzaldehyde (0.554 g, 2.29 mmol) and the mixture was refluxed for 1-2 hours. 1 ml of glacial acetic acid was added during refluxing. Yellow coloured clear solution was filtered and kept for crystallization at room temperature. Yield, 58%, m.p, 200-203° C. Main IR peaks (KBr, cm⁻¹): $\nu(\text{NH}_2)$ 3423w, 3226w; $\nu(-\text{NH}-)$ 3043w; $\nu(\text{C}=\text{N}) + \nu(\text{C}=\text{C}) + \delta \delta(\text{NH}_2)$ 1645s, 1564w, 1454s; $\nu(\text{C}=\text{Se})$ 835s (selenoamide moiety). ¹H NMR (δ , ppm; CDCl₃): 11.36 s (1H, N²H), 8.89 s (1H, C²H), obscured by ring protons (1H, N¹H₂), 7.55-6.93 m (Ring protons). ¹³C NMR (δ , ppm; CDCl₃): 164.9 (C¹), 160.0 (C²), 133.6 (C⁴), 132.78 (C³), 119.0 (C⁵), 117.5 (C⁸), 117.3 (C⁶).



Synthesis of 2-Nitrobenzaldehyde selenosemicarbazone [2-NO₂-Hbsesc]:

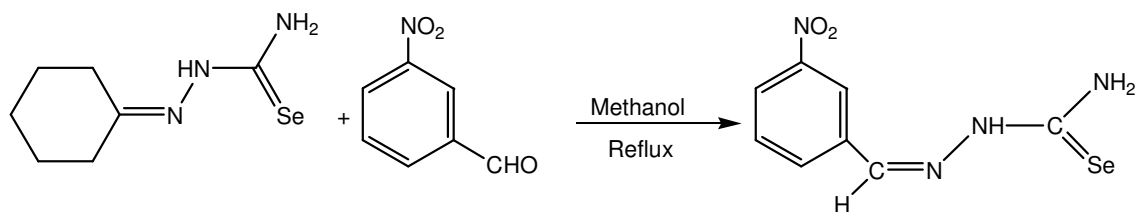
Cyclohexanone selenosemicarbazone, (0.5 g, 2.29 mmol) was dissolved in 50 ml of ethanol with heating. To it was added 2-nitrobenzaldehyde (0.34 g, 2.29 mmol) and the mixture was refluxed for 1-2 hours. 1 ml of glacial acetic acid was added during refluxing. Orange coloured clear solution was filtered and kept for crystallization at room temperature. Yield, 53%, m.p, 258-260°C. Main IR peaks (KBr, cm⁻¹): $\nu(\text{NH}_2)$ 3406s, 3250s; $\nu(-\text{NH}-)$ 3109s; $\nu(\text{C}=\text{N}) + \nu(\text{C}=\text{C}) + \delta(\text{NH}_2)$ 1602s, 1566s, 1477s; $\nu(\text{C}=\text{Se})$ 848s (selenoamide moiety). ¹H NMR (δ , ppm; CDCl₃): 11.94 s (1H, N²H), 8.62 s (1H, C²H), (obscured by ring protons) (1H,

N^1H_2), 8.38-7.48 m (Ring protons). ^{13}C NMR (δ , ppm; $CDCl_3$): 174.8 (C^1), 157.8 (C^2), 147.9 (C^4), 139.31 (C^3), 133.3 (C^5), 128.1 (C^8), 127.8 (C^6).



Synthesis of 3-Nitrobenzaldehyde selenosemicarbazone [3- NO_2 -Hbsesc]:

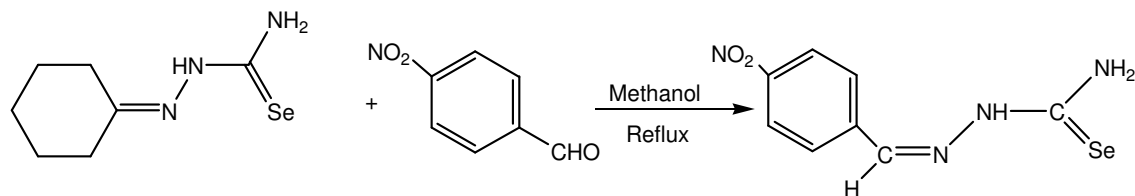
Cyclohexanone selenosemicarbazone, (0.5 g, 2.29 mmol) was dissolved in 50 ml of ethanol with heating. To it was added 2-nitrobenzaldehyde (0.34 g, 2.29 mmol) and the mixture was refluxed for 1-2 hours. 1 ml of glacial acetic acid was added during refluxing. Orange coloured clear solution was filtered and kept for crystallization at room temperature. Yield, 53%, m.p, 212-215° C. Main IR peaks (KBr, cm^{-1}): $\nu(NH_2)$ 3408m, 3232m; $\nu(-NH-)$ 3128m; $\nu(C=N) + \nu(C=C) + \delta \delta(NH_2)$ 1614w, 1597s, 1479s; $\nu(C=Se)$ 835s (selenoamide moiety). 1H NMR (δ , ppm; d^6 -dms $o/CDCl_3$): 11.79 s (1H, N^2H), 8.63 s (1H, C^2H), obscured by ring protons (1H, N^1H_2), 8.48-7.54 m (Ring protons). ^{13}C NMR (δ , ppm; d^6 -dms $o/CDCl_3$): 174.4 (C^1), 160.0 (C^2), 148.24 (C^4), 141.31 (C^3), 135.8 (C^5), 130.1 (C^8), 125.3 (C^6).



Synthesis of 4-Nitrobenzaldehyde selenosemicarbazone [4- NO_2 -Hbsesc]:

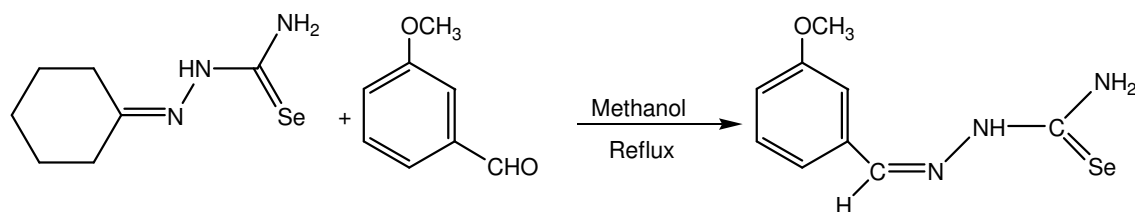
Cyclohexanone selenosemicarbazone, (0.5 g, 2.29 mmol) was dissolved in 50 ml of ethanol with heating. To it was added 2-nitrobenzaldehyde (0.34 g, 2.29 mmol) and the mixture was refluxed for 1-2 hours. 1 ml of glacial acetic acid was added during refluxing. Orange coloured clear solution was filtered and kept for crystallization at room temperature. Yield, 53%, m.p, 230-233° C. Main IR peaks (KBr, cm^{-1}): $\nu(NH_2)$ 3428m, 3252m; $\nu(-NH-)$ 3138m; $\nu(C=N) + \nu(C=C) + \delta \delta(NH_2)$ 1674sh, 1587s, 1497s; $\nu(C=Se)$ 855s (selenoamide moiety). 1H NMR (δ , ppm; d^6 -dms $o/CDCl_3$): 10.30 s (1H, N^2H), 8.54 s (1H, C^2H), obscured by ring

protons (1H, N¹H₂), 8.34-7.24 m (Ring protons). ¹³C NMR (δ, ppm; CDCl₃) :190.4 (C¹), 151.1 (C²), 151.19-123.61, (ring protons).



Synthesis of 3-methoxybenzaldehyde selenosemicarbazone [3-MeO-Hbsesc]:

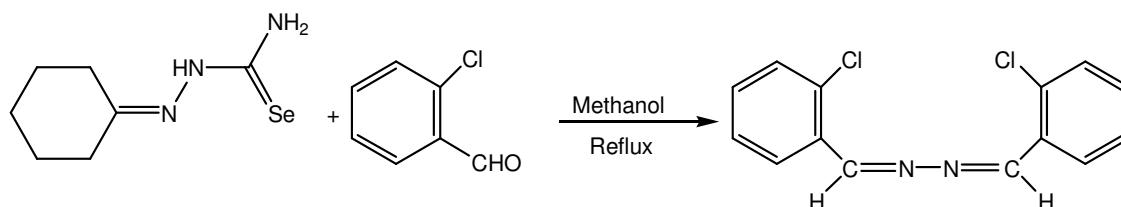
Cyclohexanone selenosemicarbazone, (0.5 g, 2.29 mmol) was dissolved in 50 ml of ethanol with heating. To it was added 3-methoxybenzaldehyde (0.314 g, 2.29 mmol) and the mixture was refluxed for 1-2 hours. 1 ml of glacial acetic acid was added during refluxing. Yellow coloured clear solution was filtered and kept for crystallization at room temperature. Yield, 58%, m.p, 118-120° C. Main IR peaks (KBr, cm⁻¹): ν(NH₂) 3383s, 3246s; ν(-NH-) 3047s; ν(C=N) + ν(C=C) + δ δ(NH₂) 1600s, 1541s, 1464s; ν(C=Se) 868s (selenoamide moiety). ¹H NMR (δ, ppm; d⁶-dmsO/CDCl₃): 8.55 s (1H, C²H), (obscured by ring protons) (1H, NH₂), 7.39 s (1H, C⁸), 7.29 m (2H, C^{4,6}), 6.96 m (1H, C⁵), 2.5 s (3H, OCH₃). ¹³C NMR (δ, ppm; d⁶-dmsO/CDCl₃) :166.9 (C¹), 161.1 (C²), 134.79-111.7, (ring protons), 54.88 (OCH₃).



Synthesis of 1, 2-bis(2-chlorobenzylidene)hydrazine:

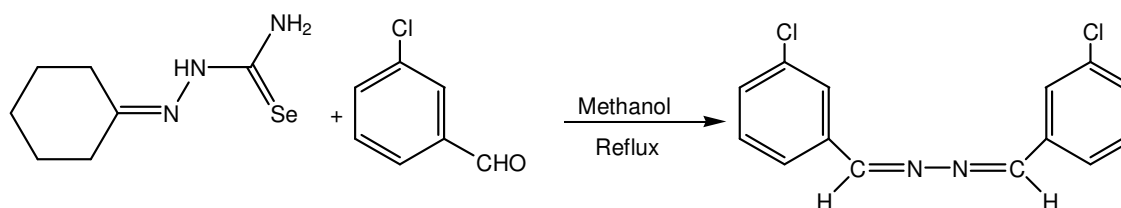
Cyclohexanone selenosemicarbazone, (0.5 g, 2.29 mmol) was dissolved in 50 ml of ethanol with heating. To it was added 2-Chlorobenzaldehyde (0.32 g, 2.29 mmol) and the mixture was refluxed for 1-2 hours. 1 ml of glacial acetic acid was added during refluxing. Yellow coloured clear solution was filtered and kept for crystallization at room temperature. Yield,

57%, m.p, 147-149° C. Main IR peaks (KBr, cm^{-1}): $\nu(\text{NH}_2)$ 3444w, 3232w; $\nu(-\text{NH}-)$ 3147m; $\nu(\text{C}=\text{N}) + \nu(\text{C}=\text{C}) + \delta \delta(\text{NH}_2)$ 1614s, 1559s, 1433s; $\nu(\text{C}=\text{Se})$ 855s (selenoamide moiety). ^1H NMR (δ , ppm; d^6 -dms o/CDCl_3): 9.06 s (1H, CH), 8.20 d (1H, C^3H), 7.53-7.20 m (3H, $\text{C}^{4,5,6}$). ^{13}C NMR (δ , ppm; d^6 -dms o/CDCl_3): 159.2 (C^1), 136.0 (C^3) 132.4 (C^2), 131.6 (C^5), 130.2 (C^7), 128.5 (C^4), 127.2 (C^6).



Synthesis of 1, 2-bis(3-chlorobenzylidene)hydrazine :

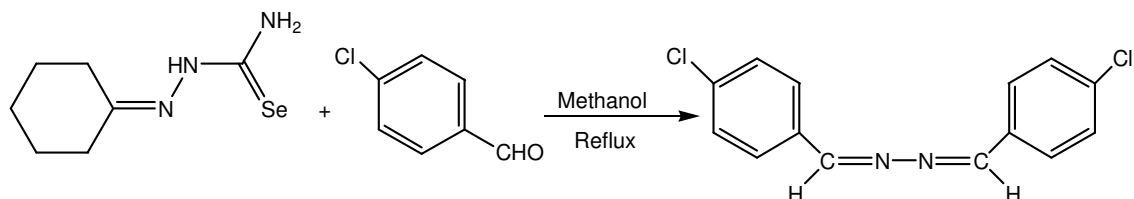
Cyclohexanone selenosemicarbazone, (0.5 g, 2.29 mmol) was dissolved in 50 ml of ethanol with heating. To it was added 3-Chlorobenzaldehyde (0.32 g, 2.29 mmol) and the mixture was refluxed for 1-2 hours. During refluxing 1 ml of glacial acetic acid was added. Yellow coloured clear solution was filtered and kept for crystallization at room temperature. Yield, 58%, m.p, 146-148° C. Main IR peaks (KBr, cm^{-1}): $\nu(\text{NH}_2)$ 3452w, 3240w; $\nu(-\text{NH}-)$ 3138m; $\nu(\text{C}=\text{N}) + \nu(\text{C}=\text{C}) + \delta \delta(\text{NH}_2)$ 1627s, 1593s, 1469s; $\nu(\text{C}=\text{Se})$ 886s (selenoamide moiety). ^1H NMR (δ ppm; d^6 -dms o/CDCl_3): 8.57 s (1H, CH), 7.85 s (1H, C^2H), 7.71 s (1H, C^6H), 7.57-7.35 m (4H, $\text{H}^{4,5}$). ^{13}C NMR (δ ppm; d^6 -dms o/CDCl_3): 161.0 (C^1), 135.9 (C^4) 135.2 (C^2), 131.5 (C^5), 130.28 (C^6), 128.3 (C^3), 127.2 (C^7).



Synthesis of {1, 2-bis(4-chlorobenzylidene)hydrazine}:

Cyclohexanone selenosemicarbazone, (0.5 g, 2.29 mmol) was dissolved in 50 ml of ethanol with heating. To it was added 4-Chlorobenzaldehyde (0.32 g, 2.29 mmol) and the mixture was refluxed for 1-2 hours. 1 ml of glacial acetic acid was added during refluxing. Yellow coloured clear solution was filtered and kept for crystallization at room temperature. Yield, 58%, m.p, 190-193° C. Main IR peaks (KBr, cm^{-1}): $\nu(\text{NH}_2)$ 3416w, 3240w; $\nu(-\text{NH}-)$ 3070m;

$\nu(\text{C}=\text{N}) + \nu(\text{C}=\text{C}) + \delta \delta(\text{NH}_2)$ 1626s, 1593s, 1479s; $\nu(\text{C}=\text{Se})$ 862s (selenoamide moiety). ^1H NMR (δ , ppm; $\text{d}^6\text{-dmsO}/\text{CDCl}_3$): 8.58 s (1H, CH), 7.76 m (2H, $\text{C}^{3,5}$), 7.49 m (2H, $\text{C}^{2,6}$). ^{13}C NMR (δ , ppm; $\text{d}^6\text{-dmsO}/\text{CDCl}_3$): 161.0 (C^1), 137.0 (C^5) 132.7 (C^2), 129.9 ($\text{C}^{3,7}$), 129.3 ($\text{C}^{4,6}$).



3.2.3 Synthesis of metal complexes:

[CuI($\eta^2\text{-N}^3$, S-H₂itsc-N¹-Me)(Ph₃P)] 1. To a solution of CuI (0.050 g, 0.26 mmol) in 15 ml of acetonitrile was added, solid Ph₃P (0.068 g, 0.26 mmol) and stirred for 2-3 hrs. The white ppt. of [CuI(Ph₃P)] were formed. The acetonitrile was decanted off from the reaction and precipitates were dissolved in 15 ml chloroform. To it was added, solid H₂itsc-N¹-Me (0.061 g, 0.26 mmol) and the reaction mixture was stirred for 3-4 h. Yellow colour clear solution thus obtained was filtered and kept for crystallization on slow evaporation at room temperature. The product thus obtained was recrystallized from acetonitrile. Yield: 0.061g, 68%; m.p. 218-220°C. Elemental analysis: Found: C, 48.5; H, 3.7; N, 8.04; S, 4.36. C₂₈H₂₆N₄PSOCuI requires, C, 48.9; H, 3.8; N, 8.16; S, 4.66%. Main IR peaks (KBr, cm⁻¹), $\nu(\text{N-H})$, 3468s, 3402s; $\nu(\text{-NH-})$ 3217m; (NH, isatin) 3142s; $\nu(\text{C-H}_{\text{Ph}})$, 3051s; $\nu(\text{C-H}_{\text{Me}})$, 2814; $\nu(\text{C}=\text{O})$ 1687s; $\delta(\text{NH}_2) + \nu(\text{C}=\text{N}) + \nu(\text{C}-\text{C})$, 1597, 1554s; $\nu(\text{C}=\text{S})$ 826s (thioamide moiety), $\nu(\text{P}-\text{C}_{\text{Ph}})$, 1095s. ^1H NMR ($\text{d}^6\text{-dmsO}$, δ ppm.): 12.64s (1H NH_{isatin}), 11.23s (1H, N²H), 9.33s (1H N¹H), 7.67-6.93m (19H, C^{5,7,8,6}H+Ph₃P), 2.50m (3H, CH₃).

[CuBr($\eta^2\text{-N}^3$, S-H₂itsc-N¹-Me)(Ph₃P)] 2. To a solution of CuBr (0.050 g, 0.35 mmol) in 15 ml of acetonitrile was added, solid Ph₃P (0.081 g, 0.35 mmol) and stirred for 2-3 hrs. The white ppt. of [CuI(Ph₃P)] were formed. The acetonitrile was decanted off from the reaction and precipitates were dissolved in 15 ml chloroform. To it was added, solid H₂itsc-N¹-Me (0.061 g, 0.26 mmol) and the reaction mixture was stirred for 3-4 h. Red colour clear solution thus obtained was filtered and kept for crystallization on slow evaporation at room temperature. The product thus obtained was recrystallized from acetonitrile. Yield: 0.080g, 76%; m.p. 182-185°C. Elemental analysis, Found: C, 53.5; H, 4.0; N, 9.76; S,

4.39. $C_{28}H_{26}N_4SOPCuBr \cdot 0.5CH_3CN$ requires: C, 53.0; H, 4.2; N, 9.54; S, 4.84. Main IR peaks (KBr, cm^{-1}), $\nu(N-H)$, 3306s, 3207s, 3051s, 3026s; (NH, isatin) 2983m; $\nu(C-H_{Me})$, 2935s; $\nu(C-H_{Ph})$, 3026; $\nu(C=O)$ 1707s; $\delta(NH_2) + \nu(C=N) + \nu(C-C)$, 1614s, 1556m, 1479m, 1464m; $\nu(C=S)$ 826 s (thioamide moiety), $\nu(P-C_{Ph})$, 1095s. 1H NMR (d^6 -dmsO, δ ppm.): 11.25 s (1H, NH_{isatin}), 9.50 s (1H, N^2H), 7.80 s (1H N^1H), 7.39-6.89 m (19H $C^{5,7,8,6}H+Ph_3P$), 3.06 m (3H, CH_3).

[CuCl(η^2-N^3 , S- $H_2itsc-N^1-Me$)(Ph_3P)] 3. To a solution of CuCl (0.050 g, 0.50 mmol) in 15 ml of acetonitrile was added, solid Ph_3P (0.131 g, 0.50 mmol) and stirred for 2-3 hrs. The white ppt. of $[CuI(Ph_3P)]$ were formed. The acetonitrile was decanted off from the reaction and precipitates were dissolved in 15 ml chloroform. To it was added, solid $H_2itsc-N^1-Me$ (0.117 g, 0.50 mmol) and the reaction mixture was stirred for 3-4 h. Red colour clear solution thus obtained was filtered and kept for crystallization on slow evaporation at room temperature. The product thus obtained was recrystallized from acetonitrile. Yield: 0.115g, 72 %; m.p. 182-185°C. Elemental analysis: Found: C, 56.2; H, 4.4; N, 11.00, S, 4.99. $C_{28}H_{25}N_4SOPCuCl \cdot CH_3CN$ requires, C, 56.6; H, 4.4; N, 11.26; S, 5.03. Main IR peaks (KBr, cm^{-1}), $\nu(N-H)$, 3470s, 3402s, 3215m; $\nu(-NH-)$ 3132m; (NH, isatin) 2982m; $\nu(C-H_{Me})$, 2893, 2823; $\nu(C=O)$ 1687s; $\delta(NH_2) + \nu(C=N) + \nu(C-C)$, 1653, 1620s, 1543s, 1467s; $\nu(C=S)$ 827s (thioamide moiety), $\nu(P-C_{Ph})$, 1103s. 1H NMR (d^6 -dmsO, $CDCl_3$ δ ppm.): 11.23 s (1H, NH_{isatin}) 9.42 s (1H, N^2H), 7.78 s (1H, N^1H), 7.39-6.91 m (19H, $C^{5,7,8,6}H+Ph_3P$), 3.10 m (3H, CH_3).

[CuI(η^2-N^3 , S- $H_2itsc-N^1-Et$)(Ph_3P)] 4. To a solution of CuI (0.050 g, 0.26 mmol) in 15 ml of acetonitrile was added, solid Ph_3P (0.068 g, 0.26 mmol) and stirred for 2-3 hrs. The white ppt. of $[CuI(Ph_3P)]$ were formed. The acetonitrile was decanted off from the reaction and precipitates were dissolved in 15 ml chloroform. To it was added, solid $H_2itsc-N^1-Et$ (0.064 g, 0.26 mmol) and the reaction mixture was stirred for 3-4 h. Yellow colour clear solution thus obtained was filtered and kept for crystallization on slow evaporation at room temperature. The product thus obtained was recrystallized from acetonitrile. Yield: 0.065g, 71%; m.p. 197-200°C. Elemental analysis, Found: C, 49.5; H, 3.8; N, 7.96; S, 4.53. $C_{29}H_{28}N_4SOPCuI$ requires, C, 49.6; H, 3.9; N, 7.98; S, 4.56. Main IR peaks (KBr, cm^{-1}), $\nu(N-H)$, 3306s, 3273s; $\nu(-NH-)$ 3180m; (NH, isatin) 3053s; $\nu(C-H_{Ph})$, 2982w, 2929w; $\nu(C-H_{Et})$, 2829; $\nu(C=O)$ 1685s; $\delta(NH_2) + \nu(C=N) + \nu(C-C)$, 1651s, 1591m, 1543s; $\nu(C=S)$ 827s (thioamide

moiety), $\nu(\text{P}-\text{C}_{\text{Ph}})$, 1094s. $^1\text{H NMR}$ (d^6 -dmsO, δ ppm.): 11.24 s (1H, $\text{NH}_{\text{isatin}}$), 9.5 s (1H, N^2H), 7.8 s (1H, N^1H), 7.46-6.9 m (19H, $\text{C}^{5,7,8,6}\text{H}+\text{Ph}_3\text{P}$), 2.5 t (3H, CH_3), 1.206 m (2H, CH_2).

[CuBr(η^2 - N^3 , S- $\text{H}_2\text{itsc-N}^1$ -Et)(Ph_3P)] 5. To a solution of CuBr (0.050 g, 0.34 mmol) in 15 ml of acetonitrile was added, solid Ph_3P (0.091 g, 0.34 mmol) and stirred for 2-3 hrs. The white ppt. of $[\text{CuI}(\text{Ph}_3\text{P})]$ were formed. The acetonitrile was decanted off from the reaction and precipitates were dissolved in 15 ml chloroform. To it was added, solid $\text{H}_2\text{itsc-N}^1$ -Et (0.086 g, 0.34 mmol) and the reaction mixture was stirred for 3-4 h. Red colour clear solution thus obtained was filtered and kept for crystallization on slow evaporation at room temperature. The product thus obtained was recrystallized from acetonitrile. Yield: 0.087g, 74%; m.p. 182-185°C. Elemental analysis, Found: C, 53.4; H, 4.0; N, 9.17; S, 4.81. $\text{C}_{29}\text{H}_{28}\text{N}_4\text{PSOCuBr}\cdot 0.5\text{CH}_3\text{CN}$ requires, C, 53.5; H, 4.4; N, 9.36; S, 4.75. Main IR peaks (KBr , cm^{-1}), $\nu(\text{N}-\text{H})$, 3308s; $\nu(-\text{NH}-)$ 3176s; (NH , isatin) 3049s, 3012s 2980m; $\nu(\text{C}-\text{H}_{\text{Ph}})$, 2928s; $\nu(\text{C}-\text{H}_{\text{Et}})$, 2889; $\nu(\text{C}=\text{O})$ 1705s; $\delta(\text{NH}_2) + \nu(\text{C}=\text{N}) + \nu(\text{C}-\text{C})$, 1614s, 1570m, 1543s, 1523m, 1458s; $\nu(\text{C}=\text{S})$ 828s (thioamide moiety), $\nu(\text{P}-\text{C}_{\text{Ph}})$, 1094s. $^1\text{H NMR}$ (d^6 -dmsO, δ ppm.): 11.23 s (1H, $\text{NH}_{\text{isatin}}$), 9.56 s (1H, N^2H), 7.9 s (1H, N^1H), 7.34-6.90 m (19H, $\text{C}^{5,7,8,6}\text{H}+\text{Ph}_3\text{P}$), 2.5 t (3H, CH_3), 1.179 m (2H, $-\text{CH}_2-$).

[CuCl(η^2 - N^3 , S- $\text{H}_2\text{itsc-N}^1$ -Et)(Ph_3P)] 6. To a solution of CuCl (0.050 g, 0.50 mmol) in 15 ml of acetonitrile was added, solid Ph_3P (0.091 g, 0.50 mmol) and stirred for 2-3 hrs. The white ppt. of $[\text{CuI}(\text{Ph}_3\text{P})]$ were formed. The acetonitrile was decanted off from the reaction and precipitates were dissolved in 15 ml chloroform. To it was added, solid $\text{H}_2\text{itsc-N}^1$ -Et (0.124 g, 0.50 mmol) and the reaction mixture was stirred for 3-4 h. Red colour clear solution thus obtained was filtered and kept for crystallization on slow evaporation at room temperature. The product thus obtained was recrystallized from acetonitrile. Yield: 0.018 g, 72%; m.p. 182-184°C. Elemental analysis, Found: C, 57.2; H, 4.3; N, 10.07; S, 4.62. $\text{C}_{29}\text{H}_{28}\text{N}_4\text{PSOCuCl}\cdot\text{CH}_3\text{CN}$ requires, C, 57.3; H, 4.8; N, 10.78; S, 4.93. Main IR peaks (KBr , cm^{-1}), $\nu(\text{N}-\text{H})$, 3306m; $\nu(-\text{NH}-)$ 3161m; (NH , isatin) 2982m; $\nu(\text{C}-\text{H}_{\text{Et}})$, 2929; $\nu(\text{C}=\text{O})$ 1687s; $\delta(\text{NH}_2) + \nu(\text{C}=\text{N}) + \nu(\text{C}-\text{C})$, 1653, 1620s, 1543s, 1467s; $\nu(\text{C}=\text{S})$ 827s (thioamide moiety), $\nu(\text{P}-\text{C}_{\text{Ph}})$, 1093s. $^1\text{H NMR}$ (d^6 -dmsO, CDCl_3 δ ppm.): 11.23 s (1H, $\text{NH}_{\text{isatin}}$), 9.46 s (1H, N^2H), 7.80 s (1H, N^1H), 7.38-6.91 m (19H, $\text{C}^{5,7,8,6}\text{H}+\text{Ph}_3\text{P}$), 2.53 t (3H, CH_3), 1.18 m (2H, CH_2).

[AgCl(η^1 -S-H₂itsc-N-Me)(Ph₃P)] 7. To a solution of AgCl (0.050 g, 0.34 mmol) in 15 ml of acetonitrile was added solid H₂itsc-N-Me (0.079 g, 0.34 mmol) and the reaction mixture was stirred for 3-4 h at room temperature. To this was added solid Ph₃P (0.089 g, 0.34 mmol) and stirred for 5-10 minutes. Yellow coloured clear solution thus obtained was filtered and kept for crystallization on slow evaporation at room temperature. Yield: 80%; m.p. 202-205°C. Main IR peaks (KBr, cm⁻¹), ν (N-H), 3470s, 3402s, (NH, pyrrole) 3216m, 3137m; ν (C-H_{Me}), 2820w, 2894s; ν (C-H_{Ph}), 3077m, 2894m; ν (C=O) 1684s; δ (NH₂) + ν (C=N) + ν (C-C), 1621s, 1558m, 1478m, 1464m; ν (C=S) 837s (thioamide moiety), ν (P-C_{Ph}), 1044s. ¹H NMR (d⁶-dmso, CDCl₃ δ ppm.): 14.84s (1H NH_{isatin}), 12.63s (1H, N²H), 11.73 s(1H N¹H), 11.60-10.94 m (19H, C^{5,7,8,6}H+Ph₃P), 5.29 m (3H, CH₃).

[AgBr(η^1 -S-H₂itsc-N-Me)(Ph₃P)] 8. To a solution of AgBr (0.050 g, 0.26 mmol) in 15 ml of acetonitrile was added solid H₂itsc-N-Me (0.061 g, 0.26 mmol) and the reaction mixture was stirred for 3-4 h at room temperature. To this was added solid Ph₃P (0.068 g, 0.26 mmol) and stirred for 5-10 minutes. Yellow coloured clear solution thus obtained was filtered and kept for crystallization on slow evaporation at room temperature. Yield: 80%; m.p. 208-210°C. Main IR peaks (KBr, cm⁻¹), ν (N-H), 3468s, 3400s, (NH, pyrrole) 3215m, 3136m; ν (C-H_{Me}), 2818w, 2895s; ν (C-H_{Ph}), 3026m, 2933m; ν (C=O) 1685s; δ (NH₂) + ν (C=N) + ν (C-C), 1622s, 1556m, 1462m, 1435m; ν (C=S) 837s (thioamide moiety), ν (P-C_{Ph}), 1045s. ¹H NMR (d⁶-dmso, CDCl₃ δ ppm.): 15.92s (1H NH_{isatin}), 13.12s (1H, *J* = 4 Hz, N²H), 12.79 s(1H N¹H), 12.32-12.15 m (19H, C^{5,7,8,6}H+Ph₃P), 5.51 m (3H, CH₃).

[CuI(η^1 -S-Hintsc)(Ph₃P)₂] 10. To a solution of CuI (0.050 g, 0.26 mmol) in 15 ml of acetonitrile was added solid Indole-3-Carboxyaldehyde thiosemicarbazone (0.057 g, 0.34 mmol) and the reaction mixture was stirred for 24 hrs at room temperature. To this was added solid Ph₃P (0.068 g, 0.26 mmol) and stirred for 5-10 minutes. Transparent clear solution thus obtained was filtered and kept for crystallization on slow evaporation at room temperature. Yield: 81%; m.p 289-291°C. Main IR peaks (KBr, cm⁻¹), ν (N-H), 3465s, 3426s; ν (-NH-) 3180m; ν (NH, indole), 3040m; δ (NH₂) + ν (C=N) + ν (C-C), 1627s, 1570m, 1489s; ν (C=S) 840s (thioamide moiety), ν (P-C_{Ph}), 1095s. ¹H NMR (δ , ppm; *J*, Hz; CDCl₃): 15.65 s (1H, N²H), 13.79 s (1H, N⁴H), 4.15 s (1H, N¹H), 7.69 s (1H, C²H), 12.98 d, (1H, C⁴H), 10.69 d (2H, *J* = 8 Hz, C^{6,9}H), 7.84 s (2H, C^{7,8}H). ¹³C NMR (δ , ppm; CDCl₃): 175.6 (C¹), 160.1 140.6 (C⁵), 120.8 (C⁶), (C²), 131.2 (C⁴), 127.5 (C⁹), 126.9 (C¹⁰), 122.9 (C⁸), 121.0 (C⁷), 112.4 (C³).

[CuBr(η^1 -S-Hintsc)(Ph₃P)₂] 11. To a solution of CuBr (0.050 g, 0.34 mmol) in 15 ml of acetonitrile was added solid Indole-3-Carboxyaldehyde thiosemicarbazone (0.075 g, 0.34 mmol) and the reaction mixture was stirred for 24 hrs at room temperature. To this was added solid Ph₃P (0.090 g, 0.34 mmol) and stirred for 5-10 minutes. Clear solution thus obtained was filtered and kept for crystallization on slow evaporation at room temperature. Yield: 85%; m.p 287-290°C. Elemental analysis, Found: C, 54.11; H, 4.23; N, 10.50; S, 4.84. C₄₆H₄₂ClCuN₄OP₂S requires 56.13; H, 4.21; N, 10.52; S, 4.81. Main IR peaks (KBr, cm⁻¹), ν (N-H), 3455s, 3436s; ν (-NH-) 3160m; ν (NH, indole), 3052m; δ (NH₂) + ν (C=N) + ν (C-C), 1617s, 1590m, 1479s; ν (C=S) 841s (thioamide moiety), ν (P-C_{Ph}), 1096s. ¹H NMR (δ , ppm; *J*, Hz; CDCl₃): 15.50 s (1H, N²H), 13.19 s (1H, N⁴H), 4.65 s (1H, N¹H), 7.88 t (1H, C²H), 12.28 s (1H, C⁴H), 11.68 d (2H, *J* = 8 Hz, C^{6,9}H), 7.24 s (2H, C^{7,8}H). ¹³C NMR (δ , ppm; CDCl₃): 177.6 (C¹), 162.1 141.6 (C⁵), 121.6 (C⁶), (C²), 132.9 (C⁴), 128.0 (C⁹), 127.9 (C¹⁰), 123.9 (C⁸), 120.0 (C⁷), 110.4 (C³).

[CuCl(η^1 -S-Hintsc)(Ph₃P)₂] 12. To a solution of CuCl (0.050 g, 0.50 mmol) in 15 ml of acetonitrile was added solid indole-3-carboxyaldehyde thiosemicarbazone (0.011 g, 0.50 mmol) and the reaction mixture was stirred for 24 hrs. at room temperature. To this was added solid Ph₃P (0.131 g, 0.50 mmol) and stirred for 5-10 minutes. A clear solution thus obtained was filtered and kept for crystallization at room temperature. Yield: 80%; m.p 290-293°C. Elemental analysis, Found: C, 56.24; H, 4.54; N, 9.40; S, 5.38. C₄₆H₄₂ClCuN₄OP₂S requires 56.18; H, 4.51; N, 9.36; S, 5.35. Main IR peaks (KBr, cm⁻¹), ν (N-H), 3443s, 3321s; ν (-NH-), 3197m; ν (NH, indole), 3091m; δ (NH₂) + ν (C=N) + ν (C-C), 1614s, 1554m, 1478s; ν (C=S) 847s (thioamide moiety), ν (P-C_{Ph}), 1091s. ¹H NMR (δ , ppm; *J*, Hz; CDCl₃): 11.71 s (1H, N²H), 10.78 s (1H, N⁴H), 8.22 s (1H, C⁴H), 7.92 d (2H, *J* = 6.8 Hz, C^{6,9}H), 7.75 s (2H, C^{7,8}H), 3.21 s (1H, N²H). ¹³C NMR (δ , ppm; CDCl₃): 173.6 (C¹), 167.3 (C²), 133.4 (C⁴), 122.7 (C⁷), 120.8 (C⁵), 120.7 (C⁶), 123.9 (C⁸), 129.1 (C¹⁰), 128.1 (C⁹), 111.7 (C³).

[Cu₂(μ_2 -I)₂(HIntsc-N¹-Me)₂(Ph₃P)₂] 13. To a solution of CuI (0.050 g, 0.26 mmol) in 15 ml of acetonitrile was added solid indole-N¹-methyl-3-thiosemicarbazone (0.06 g, 0.26 mmol) and the reaction mixture was stirred for 24 hrs at room temperature. To this was added solid Ph₃P (0.068 g, 0.26 mmol) and stirred for 5-10 minutes. Light green coloured solution thus obtained was filtered and kept for crystallization on slow evaporation at room temperature.

Yield: 80%; m.p 243-245°C. Main IR peaks (KBr, cm^{-1}), $\nu(\text{N-H})$, 3359s, 3336s; $\nu(-\text{NH-})$ 3183m; (NH, indole) 3053m; $\nu(\text{C-H}_{\text{Me}})$, 2903m, 2780m, $\delta(\text{NH}_2) + \nu(\text{C=N}) + \nu(\text{C-C})$, 1610s, 1507s, 1480s; $\nu(\text{C=S})$ 849s (thioamide moiety), $\nu(\text{P-C}_{\text{Ph}})$, 1098s. $^1\text{H NMR}$ (δ , ppm; J , Hz; CDCl_3): 11.03 s (1H, N^2H), 10.64 s (1H, N^4H), 8.36 s (1H, C^2H), 7.90 s (1H, C^4H), 6.95 d (2H, $J = 8$ Hz, $\text{C}^{6,9}\text{H}$), 7.33-7.24 m ($\text{C}^{7,8}\text{H}$), 2.99 s (3H, $-\text{CH}_3$). $^{13}\text{C NMR}$ (δ , ppm; CDCl_3): 172.4 (C^1) 142.5 (C^2), 133.6 (C^3), 130.7 (C^4), 137.1 (C^5), 116.3 (C^6), 120.9 (C^7), 129.6 (C^8), 121.4 (C^{10}), 110.9 (C^9) 30.5 ($-\text{CH}_3$).

[Cu₂(μ_2 -Br)₂(HIntsc-N¹-Me)₂(Ph₃P)₂] 14. To a solution of CuBr (0.050 g, 0.34 mmol) in 15 ml of acetonitrile was added solid indole-N¹-methyl-3-thiosemicarbazone (0.078 g, 0.34 mmol) and the reaction mixture was stirred for 24 hrs at room temperature. To this was added solid Ph₃P (0.089 g, 0.34 mmol) and stirred for 5-10 minutes. Red coloured solution thus obtained was filtered and kept for crystallization on slow evaporation at room temperature. Yield: 80%; m.p 260-263°C. Main IR peaks (KBr, cm^{-1}), $\nu(\text{N-H})$, 3362s, 3318s; $\nu(-\text{NH-})$ 3136m; (NH, indole) 3056m; $\nu(\text{C-H}_{\text{Me}})$ 2900m, 2787; $\delta(\text{NH}_2) + \nu(\text{C=N}) + \nu(\text{C-C})$, 1617s, 1574s, 1479s; $\nu(\text{C=S})$ 843s (thioamide moiety), $\nu(\text{P-C}_{\text{Ph}})$, 1094s. $^1\text{H NMR}$ (δ , ppm; J , Hz; CDCl_3): 11.57 s (1H, N^2H), 11.36 s (1H, N^4H), 7.54 s (1H, N^1H), 8.44 s (1H, C^2H), 8.10 s (1H, C^4H), 7.09 m (2H, $J = 7.2$ Hz, $\text{C}^{6,9}\text{H}$), 7.79 d (2H, $J = 8.4$ Hz, $\text{C}^{7,8}\text{H}$), 3.19 m (3H, $-\text{CH}_3$). $^{13}\text{C NMR}$ (δ , ppm; CDCl_3): 172.1 (C^1) 142.5 (C^2), 133.2 (C^3), 129.3 (C^4), 136.7 (C^5), 111.4 (C^6), 120.4 (C^7), 128.4 (C^8), 110.5 (C^9) 122.4 (C^{10}) 30.2 ($-\text{CH}_3$).

[Cu₂(μ_2 -Cl)₂(HIntsc-N¹-Me)₂(Ph₃P)₂] 15. To a solution of CuCl (0.050 g, 0.50 mmol) in 15 ml of acetonitrile was added solid indole-N¹-methyl-3-thiosemicarbazone (0.11 g, 0.50 mmol) and the reaction mixture was stirred for 24hrs at room temperature. To this was added solid Ph₃P (0.13 g, 0.50 mmol) and stirred for 5-10 minutes. Yellow coloured solution thus obtained was filtered and kept for crystallization on slow evaporation at room temperature. Yield: 80%; m.p 262-264°C. Main IR peaks (KBr, cm^{-1}), $\nu(\text{N-H})$, 3425s, 3362s; $\nu(-\text{NH-})$ 3148m; (NH, indole) 3058m; $\nu(\text{C-H}_{\text{Me}})$, 2936m, 2797m; $\delta(\text{NH}_2) + \nu(\text{C=N}) + \nu(\text{C-C})$, 1616s, 1576s, 1434s; $\nu(\text{C=S})$ 846s (thioamide moiety), $\nu(\text{P-C}_{\text{Ph}})$, 1094s. $^1\text{H NMR}$ (δ , ppm; J , Hz; CDCl_3): 11.99 s (1H, N^2H), 11.20 s (1H, N^4H), 7.35 s (1H, N^1H), 8.33 s (1H, C^2H), 8.08 s (1H, C^4H), 7.25 m (2H, $J = 8$ Hz, $\text{C}^{6,9}\text{H}$), 7.47 d (2H, $J = 10$ Hz, $\text{C}^{7,8}\text{H}$), 3.19 m (3H, $-\text{CH}_3$). $^{13}\text{C NMR}$ (δ , ppm; CDCl_3): 173.5 (C^1) 142.2 (C^2), 132.9 (C^3), 129.0 (C^4), 136.9 (C^5), 120.4 (C^6), 121.4 (C^7), 128.1 (C^8), 111.0 (C^9), 127.4 (C^{10}), 30.3 ($-\text{CH}_3$).

[CuI(η^1 -S-5-MeOHIntsc)(Ph₃P)₂] 16. To a solution of CuI (0.050 g, 0.26 mmol) in 15 ml of acetonitrile was added solid 5-methoxy indole-3-thiosemicarbazone (0.064 g, 0.26 mmol) and the reaction mixture was stirred for 24hrs at room temperature. To this was added solid Ph₃P (0.068 g, 0.26 mmol) and stirred for 5-10 minutes. Light yellow thus obtained was filtered and kept for crystallization on slow evaporation at room temperature. Yield: 80%; m.p 175-177°C. Main IR peaks (KBr, cm⁻¹), ν (N-H), 3422w, 3352w; ν (-NH-) 3178w; ((N-H)_{Indole}) 3070m; ν (C-H_{phenyl}), 2851m, δ (NH₂) + ν (C=N) + ν (C-C), 1616s, 1579s, 1476s; ν (C=S) 852s (thioamide moiety), ν (P-C_{Ph}), 1095s. ¹H NMR (δ , ppm; *J*, Hz; d⁶-dmsO, CDCl₃): 11.16 s (1H, N²H), 8.35 d (2H, N⁴H), 8.19 s (2H, C²H), 8.34-7.57 m (2H, C^{4,6,9}H+N¹H+Ph³P), 7.42 d (2H, *J* = 4 Hz, C⁷H), 3.79-3.77m (3H, -OCH₃).

[CuBr(η^1 -S-5-MeOHIntsc)(Ph₃P)₂] 17. To a solution of CuBr (0.050 g, 0.34 mmol) in 15 ml of acetonitrile was added solid 5-methoxy indole-3-thiosemicarbazone (0.084 g, 0.34 mmol) and the reaction mixture was stirred for 24 hrs at room temperature. To this was added solid Ph₃P (0.089 g, 0.26 mmol) and stirred for 5-10 minutes. Clear solution Light yellow solution thus obtained was filtered and kept for crystallization on slow evaporation at room temperature. Yield: 80%; m.p 170-172°C. Main IR peaks (KBr, cm⁻¹), ν (N-H), 3421w, 3362w; ν (-NH-) 3117w; ((N-H)_{Indole}) 2985m; ν (C-H_{Me}), 2899m, 2829m, δ (NH₂) + ν (C=N) + ν (C-C), 1624s, 1543s, 1317s; ν (C=S) 850s (thioamide moiety), ν (P-C_{Ph}), 1091s. ¹H NMR (δ , ppm; *J*, Hz; CDCl₃): 10.01 s (1H, N²H), 9.53 s (2H, N⁴H), 8.49 s (1H, C²H), 8.48-8.11 m (C^{4,6,9}H+N¹H+Ph₃P), 7.66 d (1H, C⁷H), 3.65-3.58m (3H, -OCH₃).

[CuCl(η^1 -S-5-MeOHIntsc)(Ph₃P)₂] 18. To a solution of CuI (0.050 g, 0.50 mmol) in 15 ml of acetonitrile was added solid 5-methoxy indole-3-thiosemicarbazone (0.124 g, 0.50 mmol) and the reaction mixture was stirred for 24 hrs at room temperature. To this was added solid Ph₃P (0.131 g, 0.50 mmol) and stirred for 5-10 minutes. Yellow solution thus obtained was filtered and kept for crystallization on slow evaporation at room temperature. Yield: 80%; m.p 175-177°C. Main IR peaks (KBr, cm⁻¹), ν (N-H), 3431m, 3375m; ν (-NH-) 3196m; ((N-H)_{Indole}) 3057m; ν (C-H_{phenyl}), 2899m; δ (NH₂) + ν (C=N) + ν (C-C), 1614s, 1585s, 1481s; ν (C=S) 850s (thioamide moiety), ν (P-C_{Ph}), 1091s. ¹H NMR (δ , ppm; *J*, Hz; CDCl₃): 10.00 s (1H, N²H), 9.51 s (1H, N⁴H), 8.51 s (1H, C²H), 8.50-8.23 m (C^{4,6,9}H+N¹H+Ph₃P), 7.68 d (2H, *J* = 8 Hz, C⁷H), 3.63-3.56m (3H, -OCH₃).

[CuI(η^1 -S-5-MeOHIntsc-N¹-Me)(Ph₃P)₂] 19. To a solution of CuI (0.050 g, 0.26 mmol) in 15 ml of acetonitrile was added solid 5-methoxy indole-N¹-methyl-3-thiosemicarbazone (0.068 g, 0.26 mmol) and the reaction mixture was stirred for 24hrs at room temperature. To this was added solid Ph₃P (0.068 g, 0.26 mmol) and stirred for 5-10 minutes. Orange coloured solution thus obtained was filtered and kept for crystallization on slow evaporation at room temperature. Yield: 80%; m.p 262-265°C Main IR peaks (KBr, cm⁻¹), ν (N-H) 3437m, 3338m; ν (-NH-) 3184m; (NH, indole) 3012m; ν (C-H_{Ph}), 2897m; ν (C-H_{Me}) 2947m; δ (NH₂) + ν (C=N) + ν (C=C) 1611s, 1557s, 1477s; ν (C=S) 849s (thioamide moiety) ν (P-C_{Ph}), 1095s. ¹H NMR (δ , ppm; *J*, Hz; CDCl₃): 11.37 s (1H, N²H), 8.36 s (1H, N⁴H), 8.34 s (1H, C²H), 7.67 -7.40 m (20H, C^{4,6,9}+N¹H₂+Ph₃P), 6.81 d (1H, C⁷H), 3.06 d (1H, *J* = 8 Hz -OCH₃). 1.95 t (1H, *J* = 8 Hz -CH₃). ¹³C NMR (δ , ppm; CDCl₃): 171.3 (C1), 154.6 (C2), 143.7 (C8), 133.4 (C5), 132.6 (C3), 131.9 (C10), 129.4(C5), 128.1 (C4), 128.0 (C3), 124.3 (C7), 112.2 (C7), 110.8 (C6), 103.9 (C9), 55.0 (-OCH₃), 30.85 (-CH₃).

[CuBr(η^1 -S-5-MeOHIntsc-N¹-Me)(Ph₃P)₂].CH₃CN 20. To a solution of CuBr (0.050 g, 0.34 mmol) in 15 ml of acetonitrile was added solid 5-methoxy indole-N¹-methyl-3-thiosemicarbazone (0.089 g, 0.34 mmol) and the reaction mixture was stirred for 24 hrs at room temperature. To this was added solid Ph₃P (0.089 g, 0.34 mmol) and stirred for 5-10 minutes. Light green coloured solution thus obtained was filtered and kept for crystallization on slow evaporation at room temperature. Yield: 80%; m.p 243-245°C. Main IR peaks (KBr, cm⁻¹), ν (N-H), 3377s, 3229s; ν (-NH-) 3119m; (NH, indole) 3010m; ν (C-H_{Me}), 2992m, 2824m, δ (NH₂) + ν (C=N) + ν (C-C), 1610s, 1559s, 1481s; ν (C=S) 843s (thioamide moiety), ν (P-C_{Ph}), 1092s. ¹H NMR (δ , ppm; *J*, Hz; CDCl₃): 11.75 s (1H, N²H), 8.93 s (1H, N⁴H), 8.28 s (1H, C²H), 7.47 -7.30 m (20H, C^{4,6,9}+N¹H₂+Ph₃P), 6.89 d (1H, C⁷H), 3.09 d (1H, *J* = 8 Hz -OCH₃). 1.60 s (1H, *J* = 8 Hz -CH₃). ¹³C NMR (δ , ppm; CDCl₃): 174.8 (C1), 156.3 (C2), 140.8 (C8), 133.9(C5) 132.8 (C3), 130.9 (C10), 129.5(C5) 128.2 (C4) 125.55 (C3) 117.4 (C7), 113.7 (C7), 112.8 (C6), 104.9 (C9), 55.0 (-OCH₃), 30.55 (-CH₃).

[CuCl(η^1 -S-5-MeOHIntsc-N¹-Me)(Ph₃P)₂] 21. To a solution of CuCl (0.050 g, 0.50 mmol) in 15 ml of acetonitrile was added solid 5-methoxy indole-N¹-methyl-3-thiosemicarbazone (0.013 g, 0.50 mmol) and the reaction mixture was stirred for 24 hrs at room temperature. To this was added solid Ph₃P (0.013 g, 0.50 mmol) and stirred for 5-10 minutes. Yellow solution thus obtained was filtered and kept for crystallization on slow evaporation at room

temperature. Yield: 80%; m.p 240-242°C. Main IR peaks (KBr, cm^{-1}), $\nu(\text{N-H})$, 3417s, 3363s; $\nu(-\text{NH}-)$ 3129m; $\nu(\text{NH, indole})$ 3010m; $\nu(\text{C-H}_{\text{phenyl}})$ 2831m; $\nu(\text{C-H}_{\text{Me}})$ 2940m; $\delta(\text{NH}_2) + \nu(\text{C=N}) + \nu(\text{C-C})$, 1617s, 1537m, 1482s; $\nu(\text{C=S})$ 854s (thioamide moiety), $\nu(\text{P-C}_{\text{Ph}})$, 1094s. $^1\text{H NMR}$ (δ , ppm; J , Hz; CDCl_3): 11.76 s (1H, N^2H), 8.95 s (1H, N^4H), 8.20 s (1H, C^2H), 7.57-7.30 m (20H, $\text{C}^{4,6,9} + \text{N}^1\text{H}_2 + \text{Ph}_3\text{P}$), 6.87 d (1H, C^7H), 3.11 d (1H, $J = 8$ Hz - OCH_3). 1.60 s (1H, $J = 8$ Hz - CH_3). $^{13}\text{C NMR}$ (δ , ppm; J , Hz; CDCl_3): 174.0 (C^1), 155.3 (C^2), 142.5 (C^8), 134.5 (C^5), 132.1 (C^3), 130.5 (C^{10}), 129.5 (C^5), 128.8 (C^4), 125.15 (C^3), 115.4 (C^7), 112.7 (C^7), 112.6 (C^6), 104.7 (C^9), 56.0 (- OCH_3), 30.75 (- CH_3).

[AgCl(η^1 -S-HIntsc)(Ph₃P)₂] 22. To a solution of AgCl (0.050 g, 0.34 mmol) in 15 ml of acetonitrile was added solid indole-3-carboxyaldehyde thiosemicarbazone (0.074 g, 0.34 mmol) and the reaction mixture was stirred for 24 hrs. at room temperature. To this was added solid Ph₃P (0.089 g, 0.34 mmol) and stirred for 5-10 minutes. White solution thus obtained was filtered and kept for crystallization at room temperature. Yield: 80%; m.p 180-183°C. Main IR peaks (KBr, cm^{-1}), $\nu(\text{N-H})$, 3441s, 3315s; $\nu(-\text{NH}-)$ 3142m, $\nu(\text{NH, indole})$, 3053m; $\delta(\text{NH}_2) + \nu(\text{C=N}) + \nu(\text{C-C})$, 1616s, 1587m, 1435s; $\nu(\text{C=S})$ 846s (thioamide moiety), $\nu(\text{P-C}_{\text{Ph}})$, 1095s. $^1\text{H NMR}$ (δ , ppm; J , Hz; d^6 -dmsO, CDCl_3): 15.93 s (1H, N^2H), 13.14 s (1H, N^4H), 6.69 s (1H, N^1H), 7.87 s (1H, C^2H), 12.92 s (1H, C^4H), 12.03 d (2H, $J = 8$ Hz, $\text{C}^{6,9}\text{H}$), 7.24 s (2H, $\text{C}^{7,8}\text{H}$). $^{13}\text{C NMR}$ (δ , ppm; d^6 -dmsO, CDCl_3): 173.4 (C^1), 142.3 (C^2), 132.9 (C^4), 120.0 (C^7), 136.45.8 (C^5), 120.9 (C^6), 122.0 (C^8), 129.9 (C^{10}), 128.9 (C^9), 110.3 (C^3).

[AgBr(η^1 -S-HIntsc)(Ph₃P)₂] 23. To a solution of AgBr (0.050 g, 0.26 mmol) in 15 ml of acetonitrile was added solid indole-3-carboxyaldehyde thiosemicarbazone (0.056 g, 0.26 mmol) and the reaction mixture was stirred for 24 hrs. at room temperature. To this was added solid Ph₃P (0.068 g, 0.26 mmol) and stirred for 5-10 minutes. White solution thus obtained was filtered and kept for crystallization at room temperature. Yield: 80%; m.p 190-193°C. Elemental analysis: Main IR peaks (KBr, cm^{-1}), $\nu(\text{N-H})$, 3473s, 3315s; $\nu(-\text{NH}-)$ 3140m, $\nu(\text{NH, indole})$, 3053m; $\delta(\text{NH}_2) + \nu(\text{C=N}) + \nu(\text{C-C})$, 1616s, 1585m, 1477s; $\nu(\text{C=S})$ 846s (thioamide moiety), $\nu(\text{P-C}_{\text{Ph}})$, 1097s. $^1\text{H NMR}$ (δ , ppm; J , Hz; d^6 -dmsO, CDCl_3): 15.83 s (1H, N^2H), 13.11 s (1H, N^4H), 6.97 s (1H, N^1H), 7.89 s (1H, C^2H), 12.11 s (1H, C^4H), 11.92 d (2H, $J = 8$ Hz, $\text{C}^{6,9}\text{H}$), 7.15 s (2H, $\text{C}^{7,8}\text{H}$). $^{13}\text{C NMR}$ (δ , ppm; CDCl_3): 175.4 (C^1), 148.3 (C^2),

135.9 (C⁴), 123.0 (C⁷), 138.95.8 (C⁵), 127.6 (C⁶), 125.0 (C⁸), 132.6 (C¹⁰), 125.9 (C⁹), 117.3 (C³).

[AgCl(η^1 -S-HIntsc-N¹-Me)(Ph₃P)₂] 24. To a solution of AgCl (0.050 g, 0.34 mmol) in 15 ml of acetonitrile was added solid indole-N¹-methyl-3-thiosemicarbazone (0.78 g, 0.34 mmol) and the reaction mixture was stirred for 24hrs at room temperature. To this was added solid Ph₃P (0.089 g, 0.34 mmol) and stirred for 5-10 minutes. Clear solution thus obtained was filtered and kept for crystallization on slow evaporation at room temperature. Yield: 80%; m.p 178-180°C. Main IR peaks (KBr, cm⁻¹), ν (N-H), 3364s, 3234s; ν (-NH-) 3182m; ν (NH, indole), 3053m; ν (C-H_{Me}), 2934m; δ (NH₂) + ν (C=N) + ν (C-C), 1608s, 1549m, 1498s; ν (C=S) 833s (thioamide moiety), ν (P-C_{Ph}), 1094s. ¹H NMR (δ , ppm; *J*, Hz; CDCl₃): 13.18 s (1H, N²H), 12.78 s (1H, N⁴H), 8.00 s (1H, C²H), 12.35 s (1H, C⁴H), 11.80 m (2H, *J* = 7.2 Hz, C^{6,9}H), 7.69-7.77 d (2H, *J* = 8.4 Hz, C^{7,8}H + N¹H (obscured by ring protons)), 7.55 m (3H, -CH₃). ¹³C NMR (δ , ppm; CDCl₃): 173.1 (C¹) 143.9 (C²), 134.9 (C³), 133.1 (C⁴), 137.7 (C⁵), 121.8 (C⁶), 123.6 (C⁷), 130.3 (C⁸), 112 (C⁹) 129.0 (C¹⁰) 31.5 (-CH₃).

[AgBr(η^1 -S-HIntsc-N¹-Me)(Ph₃P)₂] 25. To a solution of AgBr (0.050 g, 0.26 mmol) in 15 ml of acetonitrile was added solid indole-N¹-methyl-3-thiosemicarbazone (0.060 g, 0.26 mmol) and the reaction mixture was stirred for 24hrs at room temperature. To this was added solid Ph₃P (0.068 g, 0.26 mmol) and stirred for 5-10 minutes. Clear solution thus obtained was filtered and kept for crystallization on slow evaporation at room temperature. Yield: 80%; m.p 167-170°C. Main IR peaks (KBr, cm⁻¹), ν (N-H), 3363s, 3239s; ν (-NH-) 3179m; ν (NH, indole), 3052m; ν (C-H_{Me}), 2928m; δ (NH₂) + ν (C=N) + ν (C-C), 1609s, 1530m, 1434s; ν (C=S) 850s (thioamide moiety), ν (P-C_{Ph}), 1094s. ¹H NMR (δ , ppm; *J*, Hz; CDCl₃): 13.19 s (1H, N²H), 12.80 s (1H, N⁴H), 8.01 s (1H, C²H), 12.12 s (1H, C⁴H), 12.12 s (1H, C⁴H), 11.99 s, 11.88 m (2H, *J* = 7.2 Hz, C^{6,9}H), 7.79-7.77 d (2H, *J* = 8.4 Hz, C^{7,8}H + N¹H), 7.87 m (3H, -CH₃). ¹³C NMR (δ , ppm; CDCl₃): 172.1 (C¹), 142.5 (C²), 133.1 (C³), 131.9 (C⁴), 136.7 (C⁵), 120.4 (C⁶), 122.4 (C⁷), 129.3 (C⁸), 110 (C⁹), 128.0 (C¹⁰), 30.2 (-CH₃).

[AgCl(η^1 -S-5-MeOHIntsc)(Ph₃P)₂] 26. To a solution of AgCl (0.050 g, 0.34 mmol) in 15 ml of acetonitrile was added solid 5-methoxy indole-3-thiosemicarbazone (0.084 g, 0.34 mmol) and the reaction mixture was stirred for 24 hrs. To this was added solid Ph₃P (0.089 g, 0.34 mmol) and stirred for 5-10 minutes. Clear solution thus obtained was filtered and kept for crystallization at room temperature. Yield, 86%; m.p 248-250°C. Main IR peaks (KBr, cm⁻¹) :

$\nu(\text{N-H})$ 3434s, 3362s; $\nu(-\text{NH}-)$ 3176m; $\nu(\text{N-H}_{\text{Indole}})$ 3017sh; $\nu(\text{C-H}_{\text{Ph}})$, 2985sh; $\nu(\text{C=C})$ 1661s; $\delta(\text{NH}_2) + \nu(\text{C=N}) + \nu(\text{C=C})$ 1616s, 1588s, 1480s; $\nu(\text{C=S})$ 857s (thioamide moiety) $\nu(\text{P-C}_{\text{Ph}})$, 1094s. $^1\text{H NMR}$ (δ , ppm; J , Hz; d^6 -dmsO, CDCl_3): 11.37 s (1H, N^2H), 8.31 d (2H, $J = 6$ Hz, N^4H), 7.95 s (2H, $J = 7.2$ Hz, C^2H) 8.31-7.63 m ($\text{C}^{4,6,9}\text{H} + \text{N}^1\text{H} + \text{PH}_3\text{P}$), 6.78 d (2H, $J = 8.4$ Hz, C^7H), 3.79-3.77 m (3H, $-\text{OCH}_3$). $^{13}\text{C NMR}$ (δ , ppm; d^6 -dmsO, CDCl_3): 175.4 (C1), 154.4 (C2), 141.8 (C8), 134.8 (C5), 134.6 (C8), 132.7 (C4), 131.8 (C6), 129.0 (C10) 128.8 (C3), 110.6 (C7), 103.7 (C9), 55.2, ($-\text{OCH}_3$).

[AgBr(η^1 -S-5-MeOHIntsc)(Ph₃P)₂] 27. To a solution of AgBr (0.050 g, 0.26 mmol) in 15 ml of acetonitrile was added solid 5-methoxy indole-3-thiosemicarbazone (0.064 g, 0.26 mmol) and the reaction mixture was stirred for 24 hrs at room temperature. To this was added solid Ph₃P (0.068 g, 0.26 mmol) and stirred for 5-10 minutes. Clear solution thus obtained was filtered and kept for crystallization at room temperature. Yield, 86 %; m.p 244-246°C; Main IR peaks (KBr, cm^{-1}) $\nu(\text{N-H})$ 3430s, 3362s; $\nu(-\text{NH}-)$ 3186m; $\nu(\text{N-H}_{\text{Indole}})$ 3027sh; $\nu(\text{C-H}_{\text{Ph}})$, 2975w; $\nu(\text{C=C})$ 1681s; $\delta(\text{NH}_2) + \nu(\text{C=N}) + \nu(\text{C=C})$ 1626s, 1598s, 1485s; $\nu(\text{C=S})$ 857s (thioamide moiety) $\nu(\text{P-C}_{\text{Ph}})$, 1095s. $^1\text{H NMR}$ (δ , ppm; J , Hz; d^6 -dmsO, CDCl_3): 11.30 s (1H, N^2H), 8.30 d (2H, $J = 6$ Hz, N^4H), 7.96 s (2H, $J = 7.2$ Hz, C^2H), 8.30-7.96 m ($\text{C}^{4,6,9}\text{H} + \text{N}^1\text{H} + \text{PH}_3\text{P}$), 6.70 d (1H, $J = 8.4$ Hz, C^7H), 3.79-3.78 m (3H, $-\text{CH}_3$). $^{13}\text{C NMR}$ (δ , ppm; J , Hz; d^6 -dmsO, CDCl_3): 175.8 (C1), 153.4 (C2), 142.8 (C8), 134.9 (C5), 134.2, (C8), 132.9 (C4), 131.1 (C6), 129.9 (C10) 128.2 (C3), 112.6 (C7), 105.7 (C9), 55.7, ($-\text{OCH}_3$).

[AgCl(η^1 -S-5-MeOHIntsc-N¹-Me)(Ph₃P)₂] 28. To a solution of CuBr (0.050 g, 0.34 mmol) in 15 ml of acetonitrile was added solid 5-methoxy indole-N¹-methyl-3-thiosemicarbazone (0.09 g, 0.34 mmol) and the reaction mixture was stirred for 24 hrs at room temperature. To this was added solid Ph₃P (0.09 g, 0.34 mmol) and stirred for 5-10 minutes. Transparent solution thus obtained was filtered and kept for crystallization on slow evaporation at room temperature. Yield: 80% m.p 253-256°C. Main IR peaks (KBr, cm^{-1}), $\nu(\text{N-H})$, 3374s, 3228s, 3134s; $\nu(-\text{NH}-)$ 3051m; (NH, indole) 2991m; $\delta(\text{NH}_2) + \nu(\text{C=N}) + \nu(\text{C-C})$, 1608s, 1558m, 1477s; $\nu(\text{C=S})$ 747s (thioamide moiety), $\nu(\text{P-C}_{\text{Ph}})$, 1094s.

[AgBr(η^1 -S-5-MeOHIntsc-N¹-Me)(Ph₃P)₂] 29. To a solution of CuI (0.050 g, 0.26 mmol) in 15 ml of acetonitrile was added 5-methoxy indole-N¹-methyl-3-thiosemicarbazone (0.068 g, 0.26 mmol) and the reaction mixture was stirred for 24hrs at room temperature. To this was added solid Ph₃P (0.068 g, 0.26 mmol) and stirred for 5-10 minutes. Transparent solution thus

obtained was filtered and kept for crystallization on slow evaporation at room temperature. Yield: 80%; m.p 240-243°C. Main IR peaks (KBr, cm^{-1}), $\nu(\text{N-H})$, 3374s, 3228s, 3134s; $\nu(-\text{NH}-)$ 3051m; $\delta(\text{NH}_2)$ + $\nu(\text{C=N})$ + $\nu(\text{C-C})$, 1608s, 1558m, 1477s; $\nu(\text{C=S})$ 747s (thioamide moiety), $\nu(\text{P-C}_{\text{Ph}})$, 1094s.

[Cu₂(μ_2 -I)₂(η^1 -S-9-Hanttsc)(Ph₃P)₂] 30. To a solution of CuI (0.050 g, 0.26 mmol) in 15 ml of acetonitrile was added solid 9-anthraldehde thiosemicarbazone (0.07 g, 0.26 mmol) and the reaction mixture was stirred for 24 hrs at room temperature. To this was added solid Ph₃P (0.06 g, 0.26 mmol) and stirred for 5-10 minutes. Light green coloured solution thus obtained was filtered and kept for crystallization on slow evaporation at room temperature. Yield: 80%; m.p 280-283°C. Main IR peaks (KBr, cm^{-1}), $\nu(\text{N-H})$, 3444s, 3297s; $\nu(-\text{NH}-)$ 3147m; $\delta(\text{NH}_2)$ + $\nu(\text{C=N})$ + $\nu(\text{C-C})$, 1651s, 1575m, 1476s; $\nu(\text{C=S})$ 852s (thioamide moiety), $\nu(\text{P-C}_{\text{Ph}})$, 1094s. ¹H NMR (δ , ppm; CDCl₃): 10.73 s (1H, N²H), 6.97 s (1H, N¹H₂), 9.63 s (1H, C²H), 7.68-7.61 m (3H, C^{5,10,15}H), 7.50-7.44 m (2H, C^{8,12}H), 7.68-7.66 m (4H, C^{6,7,13,14}H + PH₃P). ¹³C NMR (δ , ppm; CDCl₃): 178.0 (C¹), 1423.7 (C²), 133.4 (C¹⁶), 132.4 (C⁴), 131.3 (C⁹), 130.4 (C¹¹), 129.9 (C⁵), 128.4 (C¹⁵), 130.8 (C¹⁰), 130.1 (C³), 129.1 (C⁸), 128.6 (C¹²), 127.6 (C⁶), 125.4 (C¹⁴), 124.8 (C⁷), 124.6 (C¹³).

[Cu₂(μ_2 -Br)₂(η^1 -S-9-Hanttsc)(Ph₃P)₂] 31. To a solution of CuBr (0.050 g, 0.34 mmol) in 15 ml of acetonitrile was added solid 9-anthraldehde thiosemicarbazone (0.094 g, 0.34 mmol) and the reaction mixture was stirred for 24 hrs. at room temperature. To this was added solid Ph₃P (0.089 g, 0.34 mmol) and stirred for 5-10 minutes. Orange coloured solution thus obtained was filtered and kept for crystallization on slow evaporation at room temperature. Yield: 80% m.p 280-283°C. Main IR peaks (KBr, cm^{-1}), $\nu(\text{N-H})$, 3449s, 3300s; $\nu(-\text{NH}-)$ 3139m; $\delta(\text{NH}_2)$ + $\nu(\text{C=N})$ + $\nu(\text{C-C})$, 1628s, 1595m, 1468s; $\nu(\text{C=S})$ 852s (thioamide moiety), $\nu(\text{P-C}_{\text{Ph}})$, 1095s. ¹H NMR (δ , ppm; *J*, Hz; CDCl₃): 12.54 s (1H, N²H), 7.08 s (1H, N¹H₂), 9.52 s (1H, C²H), 8.01 d (2H, *J* = 8 Hz, C^{5,15}H), 8.49 d (1H, *J* = 8 Hz, C¹⁰H), 7.56-7.50 m (2H, C^{8,12}H), 7.35-7.30 m (4H, C^{6,7,13,14}H). ¹³C NMR (δ , ppm; CDCl₃): 175.4 (C¹), 146.4 (C²), 131.2 (C¹⁶), 134.2 (C⁴), 130.7 (C⁹), 130.6 (C¹¹), 133.2 (C⁵), 131.4 (C¹⁵), 129.9 (C¹⁰), 129.2 (C³), 128.8 (C⁸), 128.7 (C¹²), 127.8 (C⁷), 127.3 (C¹³), 125.7 (C¹⁴), 124.9 (C⁶).

[Cu₂(μ_2 -Cl)₂(η^1 -S-9-Hanttsc)(Ph₃P)₂] 32. To a solution of CuCl (0.050 g, 0.50 mmol) in 15 ml of acetonitrile was added solid 9-anthraldehde thiosemicarbazone (0.139 g, 0.50 mmol) and the reaction mixture was stirred for 24 hrs at room temperature. To this was added solid

Ph₃P (0.131 g, 0.50 mmol) and stirred for 5-10 minutes. Orange coloured solution thus obtained was filtered and kept for crystallization on slow evaporation at room temperature. Yield: 80%; m.p 288-290°C. Main IR peaks (KBr, cm⁻¹), $\nu(\text{N-H})$, 3423s, 3244s; $\nu(-\text{NH}-)$ 3136m; $\delta(\text{NH}_2) + \nu(\text{C=N}) + \nu(\text{C-C})$, 1672s, 1562m, 1431s; $\nu(\text{C=S})$ 852s (thioamide moiety), $\nu(\text{P-C}_{\text{Ph}})$, 1095s. ¹H NMR (δ , ppm; CDCl₃): 12.34 s (1H, N²H), 7.48 s (1H, N¹H₂) 9.32 s (1H, C²H), 8.59-8.61 m (3H, C^{5,10,15}H), 7.56-7.50 m (2H, C^{8,12}H), 7.25-7.30 m (4H, C^{6,7,13,14}H+PH₃P). ¹³C NMR (δ , ppm; CDCl₃): 175.9 (C¹), 147.4 (C²), 131.9 (C¹⁶), 134.8 (C⁴), 130.2 (C⁹), 130.6 (C¹¹), 133.6 (C⁵), 131.6 (C¹⁵), 129.8 (C¹⁰), 129.3 (C³), 128.9 (C⁸), 128.8 (C¹²), 127.8 (C⁷), 127.4 (C¹³), 125.9 (C¹⁴), 124.1 (C⁶).

[CuI(η^1 -S-9-Hanttsc-N¹-Me)(Ph₃P)₂] 33. To a solution of CuI (0.050 g, 0.26 mmol) in 15 ml of acetonitrile was added solid 9-anthraldehyde-N¹-methyl-3-thiosemicarbazones (0.076 g, 0.26 mmol) and the reaction mixture was stirred for 24hrs at room temperature. To this was added solid Ph₃P (0.068 g, 0.26 mmol) and stirred for 5-10 minutes. Yellow coloured solution thus obtained was filtered and kept for crystallization on slow evaporation at room temperature. Yield: 80%; m.p 280-283°C. Main IR peaks (KBr, cm⁻¹), $\nu(\text{N-H})$, 3377s, 3205s; $\nu(-\text{NH}-)$ 3140m; $\nu(\text{C-H}_{\text{Me}})$ 2997m; $\delta(\text{NH}_2) + \nu(\text{C=N}) + \nu(\text{C-C})$, 1631s, 1562m, 1433s; $\nu(\text{C=S})$ 840s (thioamide moiety), $\nu(\text{P-C}_{\text{Ph}})$, 1097s. ¹H NMR (δ , ppm; *J*, Hz; d⁶-dmsO, CDCl₃): 11.74 s (1H, N²H), 9.30 s (1H, C²H), 8.53 d (2H, *J* = 8 Hz, C^{5,15}H), 8.11 s (1H, C¹⁰H), 7.84 d (2H, *J* = 8 Hz, C^{8,12}H), 7.63-7.32 m (4H, C^{6,7,13,14}H + N¹H + PPh₃), 2.99 s (3H, -CH₃). ¹³C NMR (δ , ppm; CDCl₃): 176.9 (C¹), 144.9 (C²), 135.4 (C¹⁶), 134.6 (C⁴), 134.5 (C⁹), 132.8 (C¹¹), 131.6 (C⁵), 130.8 (C¹⁵), 132.4 (C¹⁰), 131.5 (C³), 129.8 (C⁸), 125.8 (C¹²), 128.4 (C⁶), 128.5 (C¹⁴), 127.8 (C⁷), 125.6 (C¹³), 31.8 (-CH₃).

[CuBr(η^1 -S-9-Hanttsc-N¹-Me)(Ph₃P)₂] 34. To a solution of CuBr (0.050 g, 0.34 mmol) in 15 ml of acetonitrile was added solid 9-anthraldehyde-N¹-methyl-3-thiosemicarbazones (0.099 g, 0.34 mmol) and the reaction mixture was stirred for 24hrs at room temperature. To this was added solid Ph₃P (0.089 g, 0.34 mmol) and stirred for 5-10 minutes. Orange coloured solution thus obtained was filtered and kept for crystallization on slow evaporation at room temperature. Yield: 80%; m.p 262-264°C. Main IR peaks (KBr, cm⁻¹), $\nu(\text{N-H})$, 3383s, 3205s; $\nu(-\text{NH}-)$ 3124m; $\nu(\text{C-H}_{\text{Me}})$, 2998m; $\delta(\text{NH}_2) + \nu(\text{C=N}) + \nu(\text{C-C})$, 1621s, 1563m, 1433s; $\nu(\text{C=S})$ 840s (thioamide moiety), $\nu(\text{P-C}_{\text{Ph}})$, 1093s. ¹H NMR (δ , ppm; *J*, Hz; d⁶-dmsO, CDCl₃): 12.66 s (1H, N²H), 9.56 s (1H, C²H), 8.48 d (2H, *J* = 2.8 Hz, C^{5,15}H), 8.45 s (1H,

C¹⁰H), 8.01 d (2H, $J = 8$ Hz, C^{8,12}H), 7.56-7.45 m (4H, C^{6,7,13,14}H + N¹H + PPh₃), 3.16 t (3H, -CH₃). ¹³C NMR (δ , ppm; J , Hz; CDCl₃): 175.2 (C¹), 145.3 (C²), 134.2 (C¹⁶), 134.1 (C⁴), 133.3 (C⁹), 132.8 (C¹¹), 131.5 (C⁵), 130.5 (C¹⁵), 130.0 (C¹⁰), 130.2 (C³), 129.1 (C⁸), 125.3 (C¹²), 128.9 (C⁶), 128.8 (C¹⁴), 127.4 (C⁷), 125.7 (C¹³), 30.3 (-CH₃).

[CuCl(η^1 -S-9-Hanttsc-N¹-Me)(Ph₃P)₂] 35. To a solution of CuCl (0.050 g, 0.50 mmol) in 15 ml of acetonitrile was added solid 9-anthraldehyde-N¹-methyl-3-thiosemicarbazones (0.146 g, 0.50 mmol) and the reaction mixture was stirred for 24hrs at room temperature. To this was added solid Ph₃P (0.131 g, 0.50 mmol) and stirred for 5-10 minutes. Orange coloured solution thus obtained was filtered and kept for crystallization on slow evaporation at room temperature. Yield: 80%; m.p 256-258°C. Main IR peaks (KBr, cm⁻¹), ν (N-H), 3316s, 3230m; ν (-NH-) 3123m; ν (C-H_{Me}), 2961m; δ (NH₂) + ν (C=N) + ν (C-C), 1624s, 1560m, 1479s; ν (C=S) 840s (thioamide moiety), ν (P-C_{Ph}), 1094s. ¹H NMR (δ , ppm; J , Hz; CDCl₃): 12.92 s (1H, N²H), 9.39 s (1H, C²H), 8.00 d (2H, $J = 8$ Hz, C^{5,15}H), 8.45 s (1H, C¹⁰H), 8.06 d (2H, $J = 8$ Hz, C^{8,12}H), 7.53-7.63 m (4H, C^{6,7,13,14}H + N¹H + PPh₃), 3.78 t (3H, -CH₃). ¹³C NMR (δ , ppm; CDCl₃): 176.2 (C¹), 144.5 (C²), 134.4 (C¹⁶), 134.3 (C⁴), 134.2 (C⁹), 132.0 (C¹¹), 131.5 (C⁵), 130.4 (C¹⁵), 132.3 (C¹⁰), 131.5 (C³), 129.9 (C⁸), 125.6 (C¹²), 128.6 (C⁶), 128.5 (C¹⁴), 127.2 (C⁷), 125.3 (C¹³), 30.8 (-CH₃).

[AgCl(η^1 -S-9-Hanttsc)(Ph₃P)₂] 36. To a solution of AgCl (0.050 g, 0.34 mmol) in 15 ml of acetonitrile was added solid 9-anthraldehyde thiosemicarbazone (0.094 g, 0.34 mmol) and the reaction mixture was stirred for 24hrs at room temperature. To this was added solid Ph₃P (0.089 g, 0.34 mmol) and stirred for 5-10 minutes. Yellow coloured solution thus obtained was filtered and kept for crystallization on slow evaporation at room temperature. Yield: 80%; m.p 297-300°C. Main IR peaks (KBr, cm⁻¹), ν (N-H), 3433s, 3296s; ν (-NH-) 3140m; δ (NH₂) + ν (C=N) + ν (C-C), 1670s, 1537m, 1442m; ν (C=S) 840s (thioamide moiety), ν (P-C_{Ph}), 1066s. ¹H NMR (δ , ppm; J , Hz; CDCl₃): 12.35 s (1H, N²H), 9.65 s (1H, C²H), 8.44 d (2H, $J = 8$ Hz, C^{5,15}H), 8.51 d (1H, $J = 8$ Hz, C¹⁰H), 8.11 d (2H, $J = 8$ Hz, C^{8,12}H), 7.79-7.73 m (4H, C^{6,7,13,14}H + N¹H₂). ¹³C NMR (δ , ppm; CDCl₃): 173.7 (C¹), 148.9 (C²), 135.6 (C¹⁶), 135.1 (C⁴), 134.4 (C⁹), 133.4 (C¹¹), 130.9 (C⁵), 130.7 (C¹⁵), 132.2 (C¹⁰), 131.7 (C³), 129.9 (C⁸), 129.0 (C¹²), 128.1 (C⁶), 128.9 (C¹⁴), 127.2 (C⁷), 127.9 (C¹³).

[AgBr(η^1 -S-9-Hanttsc)(Ph₃P)₂] 37. To a solution of AgBr (0.050 g, 0.26 mmol) in 15 ml of acetonitrile was added solid 9-anthraldehde thiosemicarbazone (0.072 g, 0.26 mmol) and the reaction mixture was stirred for 24 hrs at room temperature. To this was added solid Ph₃P (0.068 g, 0.26 mmol) and stirred for 5-10 minutes. Yellow coloured solution thus obtained was filtered and kept for crystallization on slow evaporation at room temperature. Yield: 80%; m.p 278-280°C Main IR peaks (KBr, cm⁻¹), ν (N-H), 3447s, 3281s; ν (-NH-) 3150m; δ (NH₂) + ν (C=N) + ν (C-C), 1622s, 1594m, 1479s; ν (C=S) 851s (thioamide moiety), ν (P-C_{Ph}), 1094s. ¹H NMR (δ , ppm; *J*, Hz; CDCl₃): 12.40 s (1H, N²H), 9.74 s (1H, C²H), 8.52 d (2H, *J* = 8 Hz, C^{5,15}H), 8.52 d (1H, *J* = 8 Hz, C¹⁰H), 8.31 d (2H, *J* = 8 Hz, C^{8,12}H), 7.71-7.63 m (4H, C^{6,7,13,14}H + N¹H₂). ¹³C NMR (δ , ppm; CDCl₃): 175.7 (C¹), 146.9 (C²), 134.3 (C¹⁶), 134.1 (C⁴), 132.4 (C⁹), 132.4 (C¹¹), 130.4 (C⁵), 130.3 (C¹⁵), 132.7 (C¹⁰), 131.4 (C³), 129.0 (C⁸), 128.9 (C¹²), 128.7 (C⁶), 128.6 (C¹⁴), 127.5 (C⁷), 127.4 (C¹³).

Ag₂Cl₂(μ_2 -S-9-Hanttsc-N¹-Me)(Ph₃P)₂] 38. To a solution of AgCl (0.050 g, 0.34 mmol) in 15 ml of acetonitrile was added solid 9-anthraldehyde-N¹-methyl-3-thiosemicarbazone (0.099 g, 0.34 mmol) and the reaction mixture was stirred for 24hrs at room temperature. To this was added solid Ph₃P (0.089 g, 0.34 mmol) and stirred for 5-10 minutes. Orange coloured solution thus obtained was filtered and kept for crystallization on slow evaporation at room temperature. Yield: 80% m.p 218-220°C Main IR peaks (KBr, cm⁻¹), ν (N-H), 3435m, 3362s; ν (-NH-) 3109s; ν (C-H_{Me}), 2993m; δ (NH₂) + ν (C=N) + ν (C-C), 1668s, 1558s, 1479s; ν (C=S) 844s (thioamide moiety), ν (P-C_{Ph}), 1089s. ¹H NMR (δ , ppm; *J*, Hz; CDCl₃): 13.01 s (1H, N²H), 9.74 s (1H, C²H), 8.49 d (2H, *J* = 8 Hz, C^{5,15}H), 8.40 s (1H, C¹⁰H), 7.93 d (2H, *J* = 8 Hz, C^{8,12}H), 7.53-7.45 m (4H, C^{6,7,13,14}H + N¹H + PPh₃), 3.18 s (3H, -CH₃). ¹³C NMR (δ , ppm; CDCl₃): 175.8 (C¹), 143.3 (C²), 134.4 (C¹⁶), 134.3 (C⁴), 132.3 (C⁹), 132.0 (C¹¹), 130.6 (C⁵), 130.5 (C¹⁵), 130.5 (C¹⁰), 130.4 (C³), 129.1 (C⁸), 129.0 (C¹²), 127.8 (C⁶), 125.5 (C¹⁴), 125.3 (C⁷), 125.2 (C¹³), 30.2 (-CH₃).

Ag₂Br₂(μ_2 -S-9-Hanttsc-N¹-Me)(Ph₃P)₂] 39. To a solution of AgBr (0.050 g, 0.26 mmol) in 15 ml of acetonitrile was added solid 9-anthraldehyde-N¹-methyl-3-thiosemicarbazone (0.076 g, 0.26 mmol) and the reaction mixture was stirred for 24 hrs at room temperature. To this was added solid Ph₃P (0.068 g, 0.26 mmol) and stirred for 5-10 minutes. Orange coloured solution thus obtained was filtered and kept for crystallization on slow evaporation at room temperature. Yield: 80%; m.p 240-242°C. Main IR peaks (KBr, cm⁻¹), ν (N-H), 3372s,

3219s; $\nu(-NH-)$ 3132m; $\nu(C-H_{Me})$, 2993m; $\delta(NH_2) + \nu(C=N) + \nu(C-C)$, 1670s, 1521s, 1490s; $\nu(C=S)$ 844s (thioamide moiety), $\nu(P-C_{Ph})$, 1094s. 1H NMR (δ , ppm; J , Hz; $CDCl_3$): 13.00 s (1H, N^2H), 9.74 s (1H, C^2H), 8.59 d (2H, $J = 8$ Hz, $C^{5,15}H$), 8.40 s (1H, $C^{10}H$), 7.97 d (2H, $J = 8$ Hz, $C^{8,12}H$), 7.63-7.53 m (4H, $C^{6,7,13,14}H + N^1H + PPh_3$), 3.22 s (3H, $-CH_3$). ^{13}C NMR (δ , ppm; $CDCl_3$): 175.3 (C^1), 143.9 (C^2), 134.8 (C^{16}), 134.3 (C^4), 132.1 (C^9), 132.6 (C^{11}), 130.5 (C^5), 130.4 (C^{15}), 130.2 (C^{10}), 130.1 (C^3), 129.8 (C^8), 129.0 (C^{12}), 127.9 (C^6), 126.5 (C^{14}), 126.3 (C^7), 126.2 (C^{13}), 31.2 ($-CH_3$).

[CuI(η^1 -Se- 2-NO₂-Hbsesc)(Ph₃P)₂] 40. To a solution of CuI (0.050 g, 0.26 mmol) in 15 ml of acetonitrile was added solid 2-nitrobenzaldehyde selenosemicarbazones (0.070 g, 0.26 mmol) and the reaction mixture was stirred for 3 hrs at room temperature. To this was added solid Ph₃P (0.068 g, 0.26 mmol) and stirred for 5-10 minutes. Red coloured solution thus obtained was filtered and kept for crystallization on slow evaporation at room temperature. Yield: 22%; m.p 147-149°C. Main IR peaks (KBr, cm^{-1}): $\nu(NH_2)$ 3450m, 3260m; $\nu(-NH-)$ 3110s; $\nu(C=N) + \nu(C=C) + \delta(NH_2)$ 1631s, 1591s, 1475s; $\nu(C=Se)$ 844s (selenoamide moiety). 1H NMR (δ , ppm; d^6 -dmsol/ $CDCl_3$): 9.13 s (1H, N^2H), 8.84 s (1H, C^2H), obscured by ring protons (1H, N^1H_2), 8.32-7.48 m (Ring protons).

[CuBr(η^1 -Se- 2-NO₂-Hbsesc)(Ph₃P)₂] 41. To a solution of CuBr (0.050 g, 0.34 mmol) in 15 ml of acetonitrile was added solid 2-nitrobenzaldehyde selenosemicarbazones (0.092 g, 0.34 mmol) and the reaction mixture was stirred for 3 hrs at room temperature. To this was added solid Ph₃P (0.090 g, 0.34 mmol) and stirred for 5-10 minutes. Red coloured solution thus obtained was filtered and kept for crystallization on slow evaporation at room temperature. Yield: 24%; m.p 147-149°C. Main IR peaks (KBr, cm^{-1}): $\nu(NH_2)$ 3437m, 3265m; $\nu(-NH-)$ 3113s; $\nu(C=N) + \nu(C=C) + \delta(NH_2)$ 1626s, 1568s, 1473s; $\nu(C=Se)$ 844s (selenoamide moiety). 1H NMR (δ , ppm; d^6 -dmsol/ $CDCl_3$): 9.09 s (1H, N^2H), 8.27 s (1H, $J = 8$ Hz, C^2H), obscured by ring protons (1H, N^1H_2), 8.32-7.24 m (Ring protons).

[CuCl(η^1 -Se- 2-NO₂-Hbsesc)(Ph₃P)₂] 42. To a solution of CuCl (0.050 g, 0.50 mmol) in 15 ml of acetonitrile was added solid 2-nitrobenzaldehyde selenosemicarbazones (0.013 g, 0.50 mmol) and the reaction mixture was stirred for 3 hrs at room temperature. To this was added solid Ph₃P (0.131 g, 0.50 mmol) and stirred for 5-10 minutes. Red coloured solution thus obtained was filtered and kept for crystallization on slow evaporation at room temperature. Yield: 20%; m.p 150-153°C. Main IR peaks (KBr, cm^{-1}): $\nu(NH_2)$ 3445m, 3265m; $\nu(-NH-)$

3139s; $\nu(\text{C}=\text{N}) + \nu(\text{C}=\text{C}) + \delta(\text{NH}_2)$ 1651s, 1583s, 1432s; $\nu(\text{C}=\text{Se})$ 850s (selenoamide moiety). $^1\text{H NMR}$ (δ , ppm; d^6 -dmsd/ CDCl_3): 9.07 s (1H, N^2H), 8.26 s (1H, $J = 8$ Hz, C^2H), obscured by ring protons (1H, N^1H_2), 8.09-7.26 m (Ring protons).

[CuI(η^1 -Se- 3-NO₂-Hbsesc)(Ph₃P)₂] 43. To a solution of CuI (0.050 g, 0.26 mmol) in 15 ml of acetonitrile was added solid 2-nitrobenzaldehyde selenosemicarbazones (0.070 g, 0.26 mmol) and the reaction mixture was stirred for 3 hrs at room temperature. To this was added solid Ph₃P (0.068 g, 0.26 mmol) and stirred for 5-10 minutes. Yellow coloured solution thus obtained was filtered and kept for crystallization on slow evaporation at room temperature. Yield: 6%; m.p 215-217°C. Main IR peaks (KBr, cm^{-1}): $\nu(\text{NH}_2)$ 3439m, 3271m; $\nu(-\text{NH}-)$ 3174s; $\nu(\text{C}=\text{N}) + \nu(\text{C}=\text{C}) + \delta(\text{NH}_2)$ 1620s, 1599s, 1473s; $\nu(\text{C}=\text{Se})$ 838s (selenoamide moiety). $^1\text{H NMR}$ (δ , ppm; d^6 -dmsd/ CDCl_3): 11.98 s (1H, N^2H), 8.82 s (1H, C^2H), obscured by ring protons (1H, N^1H_2), 8.69-7.26 m (Ring protons).

[CuBr(η^1 -Se- 3-NO₂-Hbsesc)(Ph₃P)₂] 44. To a solution of CuBr (0.050 g, 0.34 mmol) in 15 ml of acetonitrile was added solid 2-nitrobenzaldehyde selenosemicarbazones (0.092 g, 0.34 mmol) and the reaction mixture was stirred for 3 hrs at room temperature. To this was added solid Ph₃P (0.090 g, 0.34 mmol) and stirred for 5-10 minutes. Red coloured solution thus obtained was filtered and kept for crystallization on slow evaporation at room temperature. Yield: 26%; m.p 147-149°C. Main IR peaks (KBr, cm^{-1}): $\nu(\text{NH}_2)$ 3443m, 3261m; $\nu(-\text{NH}-)$ 3179s; $\nu(\text{C}=\text{N}) + \nu(\text{C}=\text{C}) + \delta(\text{NH}_2)$ 1614s, 1567s, 1433s; $\nu(\text{C}=\text{Se})$ 841s (selenoamide moiety). $^1\text{H NMR}$ (δ , ppm; J , Hz; d^6 -dmsd/ CDCl_3): 11.96 s (1H, N^2H), 8.84 s (1H, $J = 8$ Hz, C^2H), obscured by ring protons (1H, N^1H_2), 8.70-7.26 m (Ring protons).

[CuCl(η^1 -Se- 3-NO₂-Hbsesc)(Ph₃P)₂] 45. To a solution of CuCl (0.050 g, 0.50 mmol) in 15 ml of acetonitrile was added solid 2-nitrobenzaldehyde selenosemicarbazones (0.013 g, 0.50 mmol) and the reaction mixture was stirred for 3 hrs at room temperature. To this was added solid Ph₃P (0.131 g, 0.50 mmol) and stirred for 5-10 minutes. Red coloured solution thus obtained was filtered and kept for crystallization on slow evaporation at room temperature. Yield: 10%; m.p 150-153°C. Main IR peaks (KBr, cm^{-1}): $\nu(\text{NH}_2)$ 3431m, 3251m; $\nu(-\text{NH}-)$ 3181s; $\nu(\text{C}=\text{N}) + \nu(\text{C}=\text{C}) + \delta(\text{NH}_2)$ 1633s, 1589s, 1463s; $\nu(\text{C}=\text{Se})$ 851s (selenoamide moiety). $^1\text{H NMR}$ (δ , ppm; d^6 -dmsd/ CDCl_3): 11.92 s (1H, N^2H), 8.87 s (1H, C^2H), obscured by ring protons (1H, N^1H_2), 7.63-7.03 m (Ring protons).

[AgCl(η^1 -Se- 4-NO₂-Hbsesc)(Ph₃P)₂] 46. To a solution of AgCl (0.050 g, 0.34 mmol) in 15 ml of acetonitrile was added solid 4-nitrobenzaldehyde selenosemicarbazones (0.092 g, 0.34 mmol) and the reaction mixture was stirred for 24hrs at room temperature. To this was added solid Ph₃P (0.089 g, 0.34 mmol) and stirred for 5-10 minutes. Red coloured solution thus obtained was filtered and kept for crystallization on slow evaporation at room temperature. Yield: 28%; m.p 194-197°C. Yield: 10%; m.p 150-153°C. Main IR peaks (KBr, cm⁻¹): $\nu(\text{NH}_2)$ 3417m, 3275m; $\nu(-\text{NH}-)$ 3119s; $\nu(\text{C}=\text{N}) + \nu(\text{C}=\text{C}) + \delta(\text{NH}_2)$ 1681w, 1587w, 1476s; $\nu(\text{C}=\text{Se})$ 874s (selenoamide moiety). ¹H NMR (δ , ppm; d⁶-dmsO/ CDCl₃): 8.17 s (1H, $J = 8\text{Hz}$ C²H), obscured by ring protons (1H, N¹H₂), 7.75-7.24 m (Ring protons).

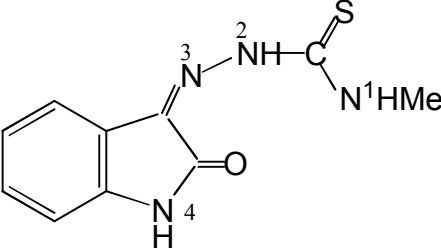
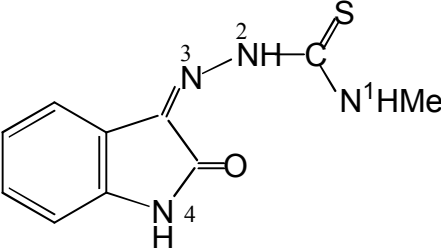
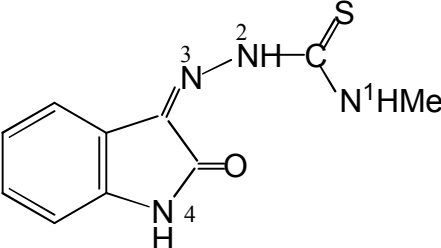
[AgBr(η^1 -Se- 4-NO₂-Hbsesc)(Ph₃P)₂] 47. To a solution of AgBr (0.050 g, 0.26 mmol) in 15 ml of acetonitrile was added solid 4-nitrobenzaldehyde selenosemicarbazones (0.070 g, 0.26 mmol) and the reaction mixture was stirred for 24 hrs at room temperature. To this was added solid Ph₃P (0.068 g, 0.26 mmol) and stirred for 5-10 minutes. Red coloured solution thus obtained was filtered and kept for crystallization on slow evaporation at room temperature. Yield: 20%; m.p 191-194°C. Main IR peaks (KBr, cm⁻¹): $\nu(\text{NH}_2)$ 3417m, 3275m; $\nu(-\text{NH}-)$ 3119s; $\nu(\text{C}=\text{N}) + \nu(\text{C}=\text{C}) + \delta(\text{NH}_2)$ 1681w, 1587w, 1476s; $\nu(\text{C}=\text{Se})$ 874s (selenoamide moiety). ¹H NMR (δ , ppm; d⁶-dmsO/ CDCl₃): 8.18 s (1H, $J = 8\text{Hz}$ C²H), obscured by ring protons (1H, N¹H₂), 7.72-7.25 m (Ring protons).

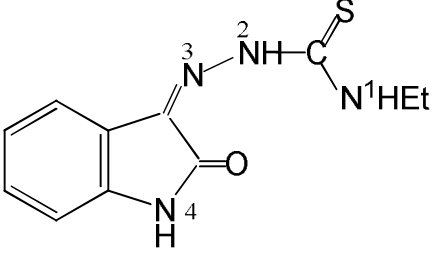
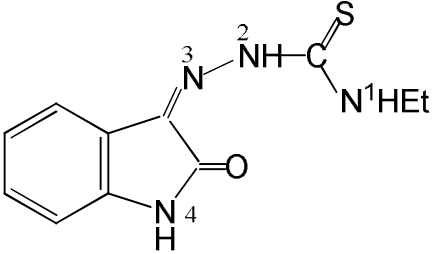
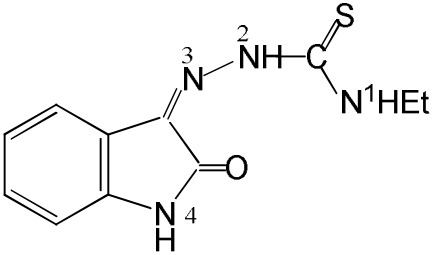
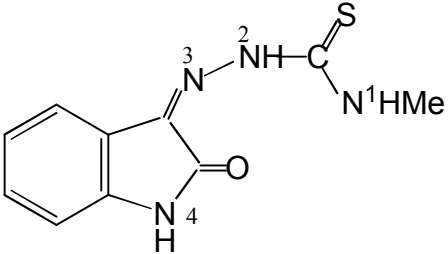
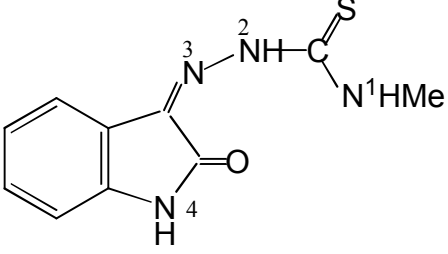
CHAPTER 4

COMPLEXES OF ISATIN-3-THIOSEMICARBAZONES

4.1. Complexes of Isatin-3-thiosemicarbazones: Complexes of isatin-3-thiosemicarbazones with copper(I) and silver(I) halides are listed in Table-1:

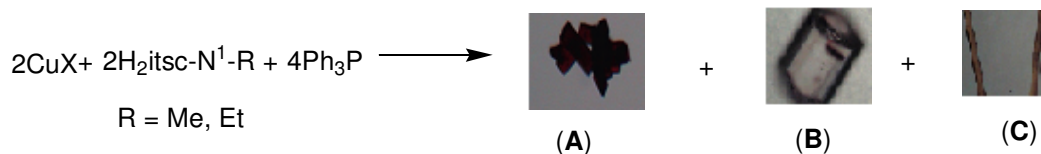
Table-1: List of complexes of isatin-3-thiosemicarbazones **1-8** with copper(I) and silver(I) halides:

Complexes	Structure of ligands
1 $[\text{CuI}(\eta^2\text{-N}^3, \text{S-H}_2\text{itsc-N}^1\text{-Me})(\text{Ph}_3\text{P})]$	 $\text{H}_2\text{itsc-N}^1\text{-Me}$
2 $[\text{CuBr}(\eta^2\text{-N}^3, \text{S-H}_2\text{itsc-N}^1\text{-Me})(\text{Ph}_3\text{P})]$	 $\text{H}_2\text{itsc-N}^1\text{-Me}$
3 $[\text{CuCl}(\eta^2\text{-N}^3, \text{S-H}_2\text{itsc-N}^1\text{-Me})(\text{Ph}_3\text{P})]$	 $\text{H}_2\text{itsc-N}^1\text{-Me}$

<p>[CuI(η^2-N³, S-H₂itsc-N¹-Et)(Ph₃P)]</p> <p>4</p>	 <p>H₂itsc-N¹-Et</p>
<p>[CuBr(η^2-N³, S-H₂itsc-N¹-Et)(Ph₃P)]</p> <p>5</p>	 <p>H₂itsc-N¹-Et</p>
<p>[CuCl(η^2-N³, S-H₂itsc-N¹-Et)(Ph₃P)]</p> <p>6</p>	 <p>H₂itsc-N¹-Et</p>
<p>[AgCl(η^1-S-H₂itsc-N¹-Me)(Ph₃P)₂]</p> <p>7</p>	 <p>H₂itsc-N¹-Me</p>
<p>[AgBr(η^1-S-H₂itsc-N¹-Me)(Ph₃P)₂]</p> <p>8</p>	 <p>H₂itsc-N¹-Me</p>

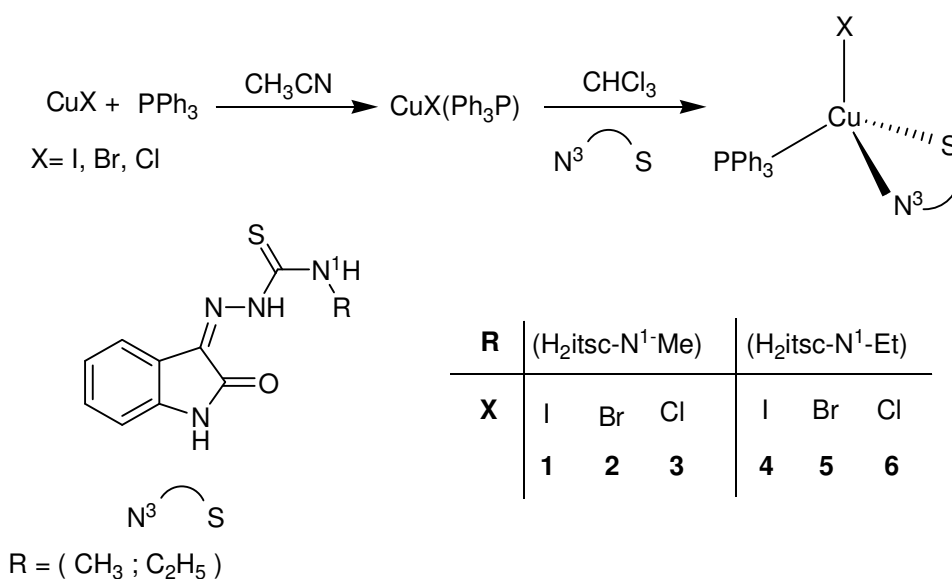
4.2. SYNTHESIS:

Reaction of un-substituted isatin-3-thiosemicarbazone (H_2itsc) with copper(I) halides and Ph_3P in 1 : 1 : 1 (M : L : PPh_3) molar ratio formed insoluble orange colored compounds. To solubilize them and to get crystalline product, one mole of Ph_3P had been further added, which formed tetrahedral monomeric complexes, $[CuX(\eta^1-S-H_2itsc)(Ph_3P)_2]$ ($X = I, Cl, Br$) [72, 73]. However, with substituted isatin-3-thiosemicarbazone ($H_2itsc-N^1-R$) ($R=Me, Et$), the similar reaction in 1 : 1 : 2 molar ratio formed three types of crystals (i) Red crystals of stoichiometry, $[CuX(H_2itsc-N^1-R)(Ph_3P)]$ (**A**), (ii) white crystals of formula, $[CuX(Ph_3P)_3]$ (**B**) and (iii) yellow needles of free ligand (**C**). (Scheme 4)



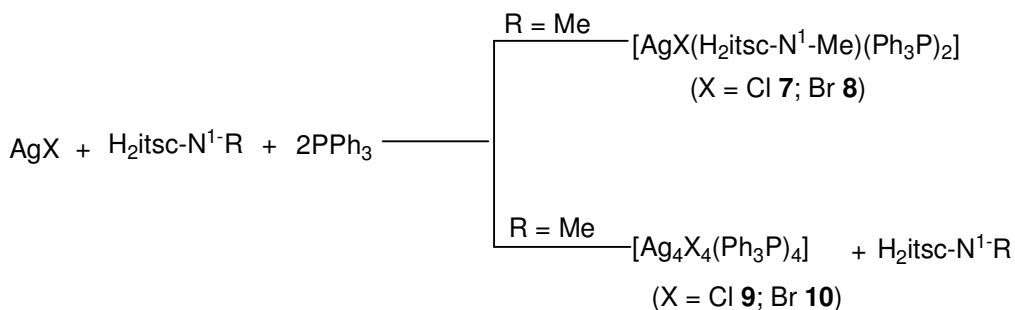
(Scheme 4)

Compounds of stoichiometry, $[CuX(H_2itsc-N^1-R)(Ph_3P)]$ were of our interest and were obtained by another route. Copper(I) halides ($X = I, Br, Cl$) were reacted with Ph_3P in 1 : 1 molar ratio to form white solid of composition, $CuX(Ph_3P)$ in acetonitrile. Acetonitrile was then removed and precipitates were dissolved in chloroform and one mole of ($H_2itsc-N^1-Me$) and ($H_2itsc-N^1-Et$) was added to get complexes of stoichiometry, $[Cu(\eta^2-N^3, S-H_2itsc-N^1-Me)(Ph_3P)]$ ($X = I, \mathbf{1}; Br, \mathbf{2}; Cl, \mathbf{3}$) and $[CuX(\eta^2-N^3, S-H_2itsc-N^1-Et)(Ph_3P)]$ ($X = I, \mathbf{4}; Br, \mathbf{5}; Cl, \mathbf{6}$) respectively. (Scheme 5)



(Scheme 5)

Silver(I) halides (X = Cl, Br) also reacted with H₂itsc-N¹-Me in 1 : 1 : 2 (M : HL : Ph₃P) molar ratio to form tetrahedral monomers, [AgX(η¹-S-H₂itsc-N¹-Me)(Ph₃P)₂] (X = Cl, **7**; Br, **8**). When an attempt was made to get the similar product with H₂itsc-N¹-Et, transparent crystals of [Ag₄X₄(Ph₃P)₄] (X = Cl, **9**; Br, **10**) were obtained. No coordination of silver(I) halides with H₂itsc-N¹-Et has been observed. (Scheme 6)



(Scheme 6)

The ν(N-H) bands in IR spectra of complexes can be divided into three categories: (i) bands between 3490–3200 cm⁻¹ due to (symmetric and asymmetric stretching mode) amino

group, (ii) band in the ranges, 3051–3081 cm^{-1} , due to NH of isatin ring, (iii) band in the ranges, 3132-3149 cm^{-1} due to amide (-NH-) group. The presence of all these bands in the complexes **1-8**, suggest that no deprotonation occurs at any nitrogen atom and ligand is coordinating in neutral form. The characteristic $\nu(\text{C}=\text{S})$ band in $\text{H}_2\text{itsc-N}^1\text{-Me}$ and $\text{H}_2\text{itsc-N}^1\text{-Et}$ appeared at 835 and 837 cm^{-1} respectively and showed shift to lower region in **1-8** (826-828 cm^{-1}). This shift indicates the binding of metal ion with thione sulfur. The presence of $\nu(\text{P-C}_{\text{Ph}})$ in the range, 1093-1103 cm^{-1} ensures the coordination of triphenylphosphine to the copper center.[72, 73]

4.3. ^1H NMR Studies:

In ^1H NMR spectra of ligands, $-\text{N}^2\text{H}-$ proton appeared at δ 11.22 ($\text{H}_2\text{itsc-N}^1\text{-Me}$) and δ 11.21 ppm ($\text{H}_2\text{itsc-N}^1\text{-Et}$), which showed an upfield shift in complexes (**2-6**) (δ 9.33 - 9.56 ppm). Similarly, the NH proton of isatin ring and N^1H proton appeared at δ 12.60 ($\text{H}_2\text{itsc-N}^1\text{-Me}$) and at δ 12.55 ($\text{H}_2\text{itsc-N}^1\text{-Et}$). Both these signals also showed an upfield shift in complexes **2-6** vis-à-vis free ligand and no change was observed in complex **1**. The presence of all these protons indicates that no deprotonation take place during complexation and isatin thiosemicarbazone ligands coordinate to the copper center in neutral form. The shift in the position of these protons also ensure complexation. The C^5H , C^6H , C^7H and C^8H ring protons of thiosemicarbazone ligands appeared in range, δ 7.67-6.89 ppm in the complexes. The CH_3 group at N^1H gives a doublet (in range δ 3.17-2.50ppm, **1-3**) and due to ethyl group a triplet (at δ 2.5ppm) and a multiplet (in the range δ 1.18-1.20ppm, **4-6**).

Peak shifts in ^1H NMR spectrum of silver(I) complexes of $\text{H}_2\text{itsc-N}^1\text{-Me}$ is different from their copper analogue. N^1H in complexes **7** and **8** appeared at δ 14.84 and 15.92 ppm respectively, which showed down field shift in contrast to a high field shift in complexes **1-6**. The CH_3 group at N^1H gives multiplet in range δ 5.29-5.51ppm (**7, 8**).

4.4. Structure of $\text{N}^1\text{-methyl-isatin-3-thiosemicarbazone}$ ($\text{H}_2\text{itsc-N}^1\text{-Me}$) and Complex **2**:

The molecular structure of ligand $\text{N}^1\text{-methyl-isatin-3-thiosemicarbazone}$ ($\text{H}_2\text{itsc-N}^1\text{-Me}$) and Complex **2** is given in Figure-1 and Figure-2 respectively. The crystallographic data and important bond parameters are given in Tables **2** and **3** respectively.

4.4.1 Structure of (H₂itsc-N¹-Me):

The ligand N¹-methyl-isatin-3-thiosemicarbazone crystallizes in monoclinic crystal system with space group P2₁/c. The two rings of isatin moiety (five and six membered) are nearly planar and the dihedral angle between mean plane of both rings is 2.08(5)°, which is close to that of N¹-ethyl-isatin-3-thiosemicarbazone, (H₂itsc-N¹-Et, 2.1°) and N¹-hexamethyleniminyl isatin-3-thiosemicarbazone, (H₂itsc-N-Hm, 0.5°)[74]. The angle describing plane of the thiosemicarbazone moiety, N(1)–N(2)–C(3)–S(1) and N(1)–N(2)–C(3)–N(3) is 1.8 and 1.6° respectively.

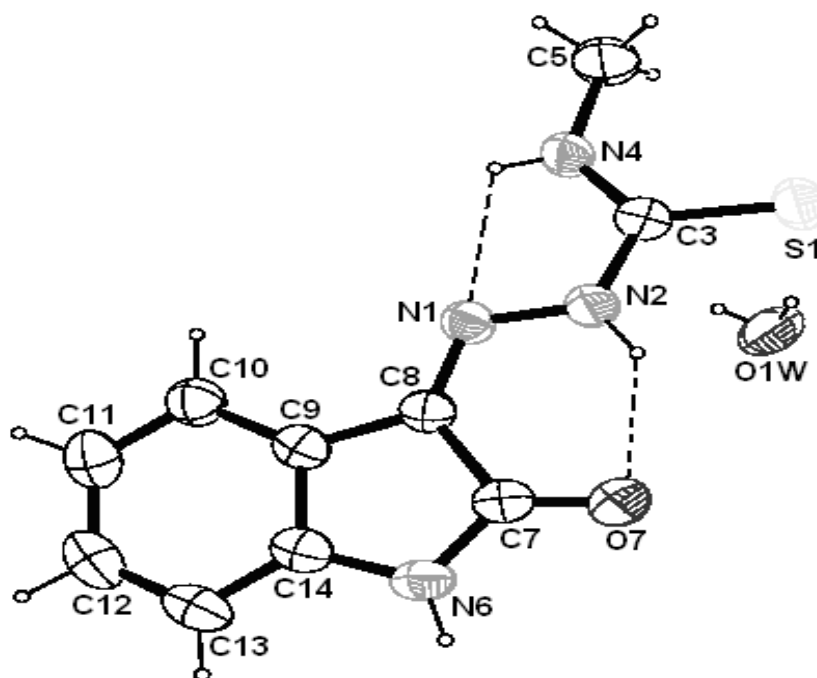


Figure-1. ORTEP view of H₂itsc-N¹-Me with numbering scheme.

H₂itsc-N¹-Me, show Z-configuration about C(8)=N(1) double bond due to intramolecular H-bonding between N(2)H of thiosemicarbazone and O(7) of isatin similar to unsubstituted and substituted isatin-3-thiosemicarbazones (Table-3).[75] The formation of five membered ring due to H-bonding between N(4)H and N(1) leads to E-configuration about N(2)-C(3) similar to H₂itsc and H₂itsc-N¹-Et, but opposite to Z-configuration in case of H₂itsc-N¹-Hm, where no such H-bonding is possible [74].

4.4.2 Structure of [CuBr(η^2 -N³, S-H₂itsc-N¹-Me)(Ph₃P)] **2**:

Complex **2** crystallizes in triclinic crystal system with space group P-1. In this complex, phosphorous atom from triphenylphosphine ligand, one bromide atom, imino nitrogen (N³) and thione sulfur of thio-ligand formed corners of tetrahedron with copper(I) in center. N¹-methylisatin-3-thiosemicarbazone coordinate as neutral ligand binding to copper(I) in N³, S- chelation mode. The Cu–S bond distance, 2.3274(10) Å is close to that of 2.3566(10) Å in [CuBr(η^1 -S-H₂itsc)(Ph₃P)₂][73], but shorter than, 2.4156(6) Å in [Cu(η^2 -N³, S-H₂itsc)Ph₃P)₂].NO₃[77]. Cu–Br bond length in **2**, 2.4219(6) Å is less than sum of ionic radii of Cu and Br (Cu⁺, Br⁻, 2.73 Å)[76]. This Cu–Br bond length is also shorter than that of 2.5459(6) Å in [CuBr(η^1 -S-H₂itsc)(Ph₃P)₂][73]. Cu-N bond distance, 2.108(3) Å is close to that found in literature.[77, 78-79] The C–S bond length, 1.689(3)Å is close to 1.6880(15)Å in free ligand (H₂itsc-N¹-Me) as well in literature [77, 78-79], which indicates binding of ligand to metal center in thione (C=S) form. The bond angles around copper in range, 84.64(8)°-121.35(3)° reveal distorted tetrahedral geometry. The maximum distortion of 121.35(3)° is found to be in P–Cu–Br angle. The Cu-S-C angle, 95.61(11)° in **2** is close to 96.91(12)° in [(Ph₃P)Cu(μ -Br)(μ_3 -S,N³-Hcptsc)CuBr(PPh₃)], where cyclohexanonethiosemicarbazone (Hcptsc) binds to metal in N³,S-chelation-cum S-bridging mode[82]. This angle is much shorter than 113.30(12)° in [CuBr(η^1 -S-H₂itsc)(Ph₃P)₂], where the thiosemicarbazone was acting as terminal monodentate ligand.[73]

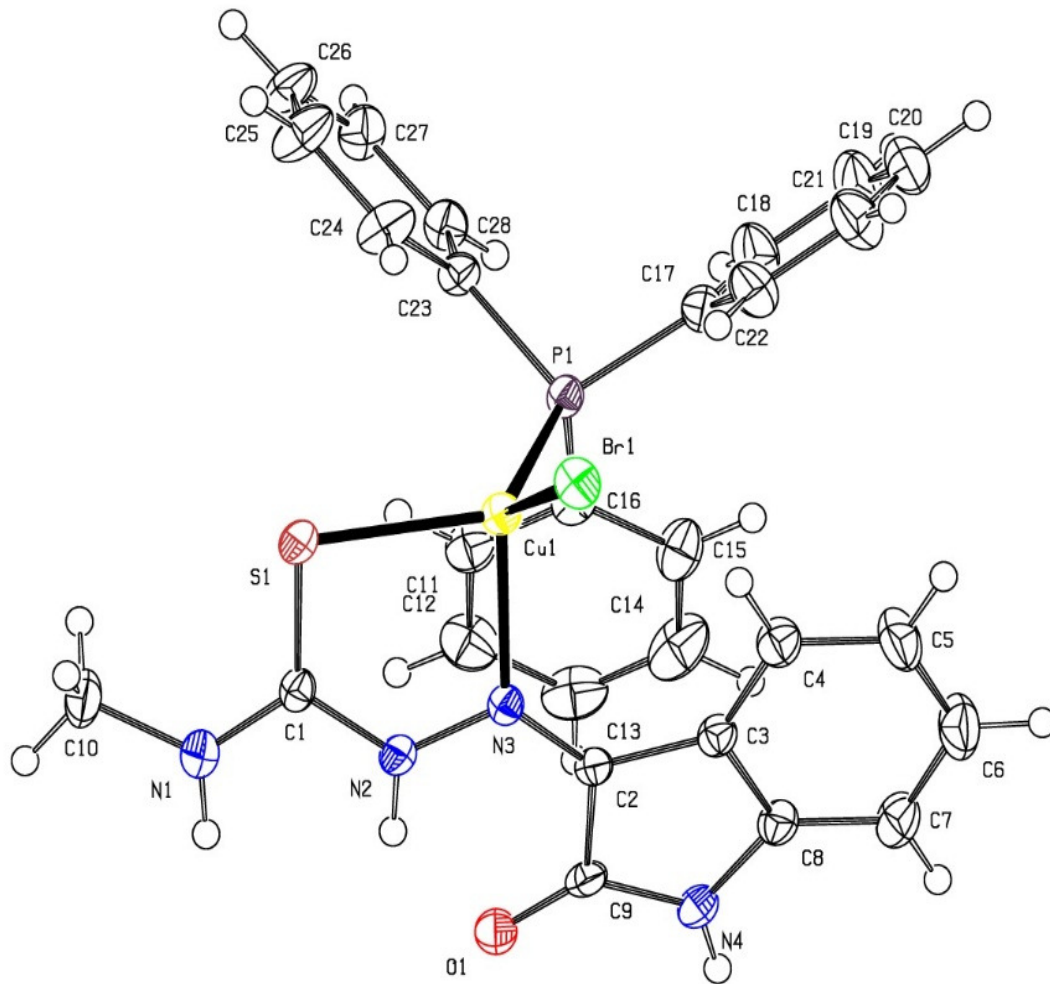


Figure-2. ORTEP view of complex **2** with numbering scheme.

In **2**, inter-molecular H-bonding between pyrrole hydrogen (N^4H) of one molecule and bromide atom of other molecule, $N^4H \cdots Br$, 2.778 \AA leads to formation of H-bonded dimer. An additional $CH \cdots HC$, 2.322 \AA interaction between phenyl ring of triphenylphosphine of two molecules is also present. These interactions are repeated to form 1D chain. Inter-molecular H-bonding between pyrrole nitrogen of one chain and Phenyl hydrogen of triphenylphosphine molecule of second chain, $HN^4 \cdots HC_{Ph}$, 2.733 \AA lead to formation of 2D sheet (Figure-3).

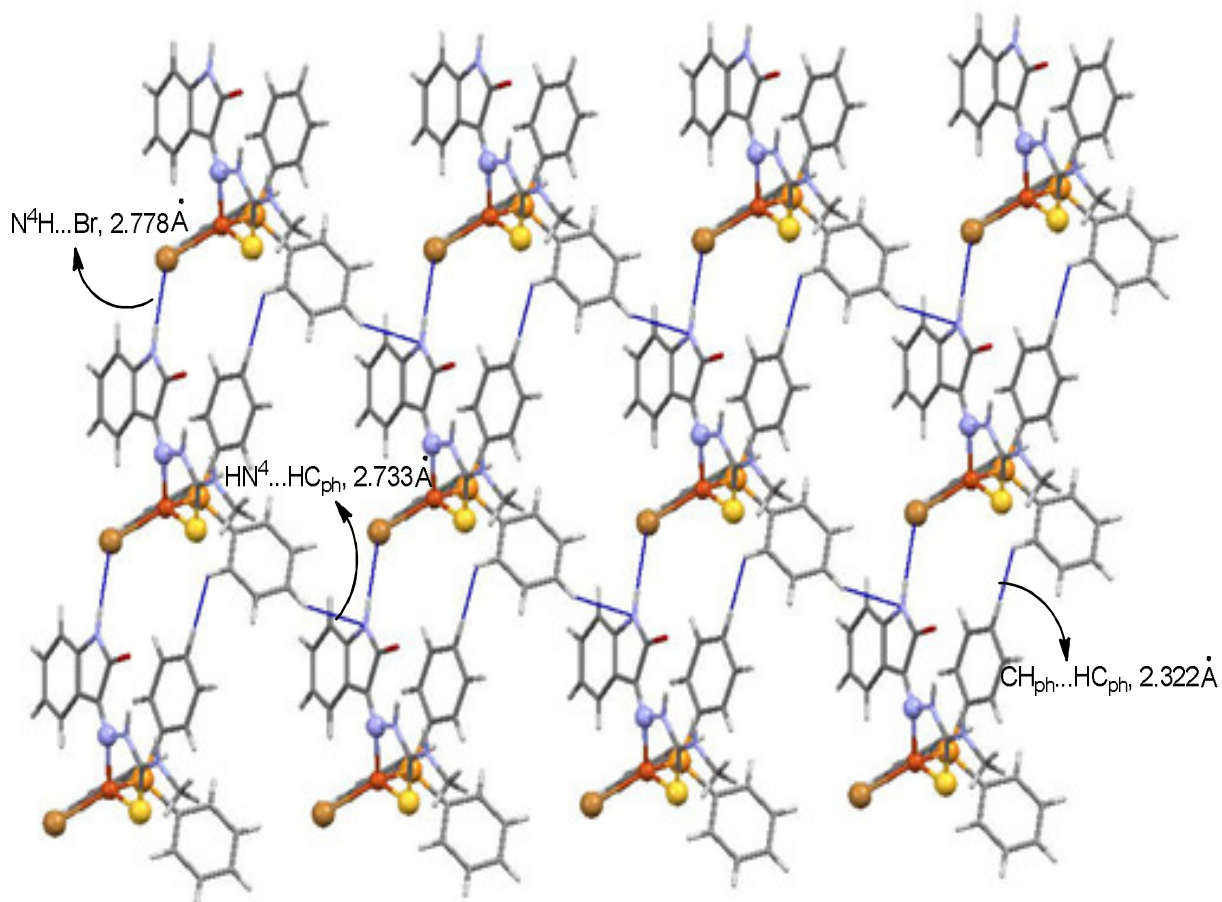


Figure-3. Packing diagram of **2** showing H-bonding and various interactions.

Table -2: Crystallographic data for $\text{H}_2\text{itsc-N}^1\text{-Me}$ and $[\text{CuBr}(\eta^2\text{-N}^3, \text{S-H}_2\text{itsc-N}^1\text{-Me})(\text{Ph}_3\text{P})]$ **2**.

	(H₂itsc-N¹-Me)	2
Crystal description	Block shaped	Prism
Crystal colour	Orange	Red
Crystal size	0.30 x 0.20 x 0.20 mm	0.34 x 0.24 x 0.12 mm
Empirical formula	$\text{C}_{10}\text{H}_{10}\text{N}_4\text{OS}\cdot\text{H}_2\text{O}$	$\text{C}_{28}\text{H}_{25}\text{BrCuN}_4\text{OPS}$
Formula weight	252.30	640.00

Radiation, Wavelength	Mo K α , 0.71073 Å	Mo K α , 0.71073 Å
Unit cell dimensions	a = 8.9306(2), b = 13.0538(3), c = 10.2347(2)Å, β = 93.105(2) $^\circ$	a = 9.8769(7), b = 11.2821(8), c = 14.1915(11)Å, α = 93.964(6), β = 102.013(6), γ = 105.636(6) $^\circ$
Crystal system	Monoclinic	Triclinic
Space group	P2 $_1$ /c	P-1
Unit cell volume	1191.39(4) Å 3	1476.3(2) Å 3
No. of molecules per unit cell, Z	4	2
Temperature	293(2) K	173(2) K
Absorption coefficient	0.268 mm $^{-1}$	2.245 mm $^{-1}$
F(000)	528	648
Scan mode	ω scan	ω scan
θ range for entire data collection	3.48 < θ < 24.99 $^\circ$	3.000< θ <32.743 $^\circ$
Range of indices	h= -10 to 10, k= -15 to 15, l= - 12 to 12	h= -14 to 14, k= -16 to 15, l= -21 to 21
Reflections collected / unique	24272 / 2083	18759 / 9734
Reflections observed (I > 2 σ (I))	1798	6849
R $_{int}$	0.0404	0.0998
R $_{sigma}$	0.0171	0.0671
Final R	0.0320	0.0998
wR(F 2)	0.0835	0.1677

Table -3: Selected bond distance (Å) and bond angles (°) for H₂itsc-N¹-Me and [CuBr(η²-N³, S-H₂itsc-N¹-Me)(Ph₃P)] **2**:

Bond distance (Å) (H ₂ itsc-N ¹ -Me)			
S(1) – C(3)	1.6880(15)	N(1) – N(2) – C(3)	120.41(13)
N(1) – C(8)	1.2906(19)	N(4) – C(3) – N(2)	116.97(14)
N(1) – N(2)	1.3561(18)	N(4) – C(3) – S(1)	125.32(12)
N(2) – C(3)	1.364(2)	N(2) – C(3) – S(1)	117.71(11)
C(3) – N(4)	1.312(2)	C(3) – N(4) – C(5)	123.80(16)
N(4) – C(5)	1.455(2)	O(7) – C(7) – N(6)	127.44(15)
C(7) – O(7)	1.236(2)	O(7) – C(7) – C(8)	126.07(14)
C(7) – C(8)	1.507(2)	N(6) – C(7) – C(8)	106.48(14)
C(8) – N(1) – N(2)	116.55(13)	N(1) – C(8) – C(9)	126.13(14)
Bond distance (Å) 2			
Br(1) – Cu(1)	2.4219(6)	C(5) – C(6)	1.395(6)
Cu(1) – S(1)	2.3274(10)	C(6) – C(7)	1.395(6)
Cu(1) – P(1)	2.2300(10)	C(7) – C(8)	1.371(5)
Cu(1) – N(3)	2.108(3)	C(11) – C(12)	1.385(6)
S(1) – C(1)	1.678(4)	C(11) – C(16)	1.382(6)
P(1) – C(16)	1.829(4)	C(12) – C(13)	1.384(7)
P(1) – C(17)	1.813(4)	C(13) – C(14)	1.370(7)
P(1) – C(23)	1.824(3)	C(14) – C(15)	1.404(7)
O(1) – C(9)	1.227(4)	C(15) – C(16)	1.389(5)
N(1) – C(1)	1.330(5)	C(17) – C(18)	1.406(6)
N(1) – C(10)	1.451(5)	C(17) – C(22)	1.380(6)
N(2) – N(3)	1.361(4)	C(18) – C(19)	1.381(6)
N(2) – C(1)	1.365(4)	C(19) – C(20)	1.370(7)

N(3) – C(2)	1.301(4)	C(20) – C(21)	1.384(7)
N(4) – C(8)	1.406(5)	C(21) – C(22)	1.393(6)
N(4) – C(9)	1.356(4)	C(23) – C(24)	1.396(5)
C(2) – C(3)	1.451(5)	C(23) – C(28)	1.389(5)
C(2) – C(9)	1.501(5)	C(24) – C(25)	1.396(5)
C(3) – C(4)	1.392(5)	C(25) – C(26)	1.361(6)
C(3) – C(8)	1.409(5)	C(26) – C(27)	1.385(6)
C(4) – C(5)	1.384(6)	C(27) – C(28)	1.387(5)
Bond Angles (°) 2:			
S(1) – Cu(1) – Br(1)	111.37(3)	C(8) – C(7) – C(6)	117.6(4)
P(1) – Cu(1) – Br(1)	121.35(3)	N(4) – C(8) – C(3)	109.8(3)
P(1) – Cu(1) – S(1)	113.66(4)	C(7) – C(8) – N(4)	128.1(3)
N(3) – Cu(1) – Br(1)	114.24(8)	C(7) – C(8) – C(3)	122.1(4)
N(3) – Cu(1) – S(1)	84.64(8)	O(1) – C(9) – N(4)	127.3(3)
N(3) – Cu(1) – P(1)	105.57(8)	O(1) – C(9) – C(2)	126.3(3)
C(1) – S(1) – Cu(1)	96.91(12)	N(4) – C(9) – C(2)	106.4(3)
C(16) – P(1) – Cu(1)	108.05(12)	C(16) – C(11) – C(12)	121.6(4)
C(17) – P(1) – Cu(1)	121.75(13)	C(13) – C(12) – C(11)	119.2(4)
C(17) – P(1) – C(16)	106.77(18)	C(14) – C(13) – C(12)	120.1(4)
C(17) – P(1) – C(23)	103.05(17)	C(13) – C(14) – C(15)	120.7(4)
C(23) – P(1) – Cu(1)	111.40(12)	C(16) – C(15) – C(14)	119.3(4)
C(23) – P(1) – C(16)	104.46(17)	C(11) – C(16) – P(1)	117.6(3)
C(1) – N(1) – C(10)	123.5(3)	C(11) – C(16) – C(15)	119.0(4)
N(3) – N(2) – C(1)	121.4(3)	C(15) – C(16) – P(1)	122.5(3)
N(2) – N(3) – Cu(1)	113.89(19)	C(18) – C(17) – P(1)	122.8(3)

C(2) – N(3) – Cu(1)	128.0(2)	C(22) – C(17) – P(1)	118.6(3)
C(2) – N(3) – N(2)	115.3(3)	C(22) – C(17) – C(18)	118.6(4)
C(9) – N(4) – C(8)	110.9(3)	C(19) – C(18) – C(17)	119.7(4)
N(1) – C(1) – S(1)	123.5(3)	C(20) – C(19) – C(18)	121.0(4)
N(1) – C(1) – N(2)	113.8(3)	C(19) – C(20) – C(21)	120.2(4)
N(2) – C(1) – S(1)	122.7(3)	C(20) – C(21) – C(22)	119.2(4)
N(3) – C(2) – C(3)	126.9(3)	C(17) – C(22) – C(21)	121.3(4)
N(3) – C(2) – C(9)	126.3(3)	C(24) – C(23) – P(1)	117.1(3)
C(3) – C(2) – C(9)	106.7(3)	C(28) – C(23) – P(1)	124.5(3)
C(4) – C(3) – C(2)	133.9(3)	C(28) – C(23) – C(24)	118.4(3)
C(4) – C(3) – C(8)	119.9(3)	C(25) – C(24) – C(23)	120.5(4)
C(8) – C(3) – C(2)	106.2(3)	C(26) – C(25) – C(24)	119.9(4)
C(5) – C(4) – C(3)	118.0(4)	C(25) – C(26) – C(27)	120.7(4)
C(4) – C(5) – C(6)	121.4(4)	C(26) – C(27) – C(28)	119.7(4)
C(5) – C(6) – C(7)	120.9(4)	C(27) – C(28) – C(23)	120.7(4)

4.4.3 Structure of [Ag₄Cl₄(Ph₃P)₄] **9**:

Complex **9** crystallizes in orthorhombic crystal system with space group Pbcn. Molecular structure of this complex is given in Figure 4 and crystallographic data and important bond parameters are given in Table 4 and 5 respectively.

In complex **9**, four silver(I) ions are connected with each other via chloride bridges (μ -Cl) to form cubane core, {Ag₄(μ -Cl)₄}. One phosphorous atom of triphenylphosphine ligand and three bridged chloride ions occupy the corners of tetrahedron around each silver atom. The structure is similar to cubane already reported in literature [80], but bond parameters are different. The Ag–Cl bond length in this complex lies in the range, 2.5395(6) - 2.7684(5) Å, which is close to the similar cubane [80] as well to the cubane, [Ag₄Cl₄(o-tolyl)₃P)₄]. [81]

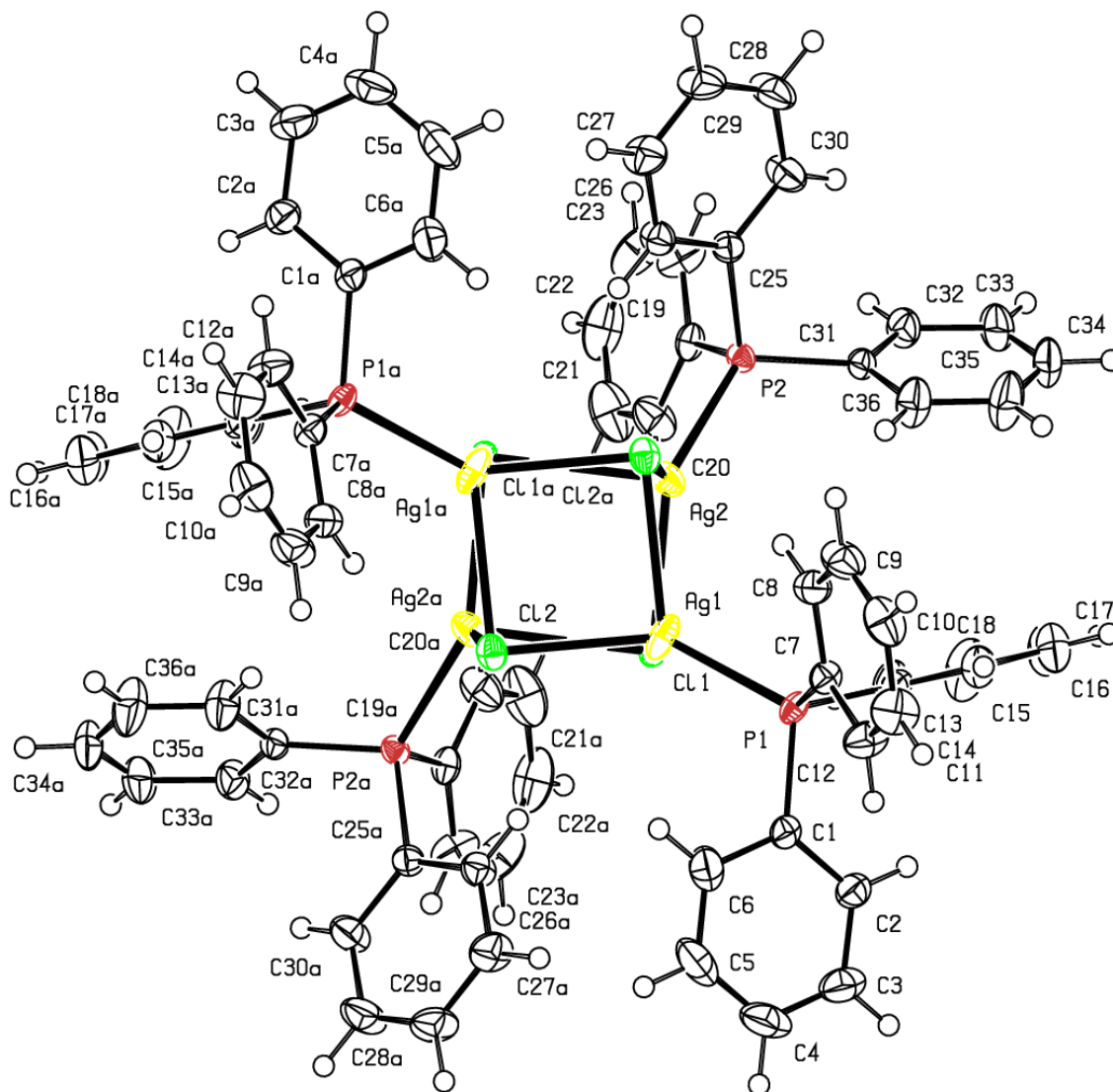


Figure-4: ORTEP view of $[Ag_4Cl_4(Ph_3P)_4]$ **9** with numbering scheme.

Out of three $Ag \cdots Ag$ contacts in cubane of complex **9**, one is 3.386 Å, which is shorter than sum of their van der Waals radii (3.44 Å), indicating $d^{10}-d^{10}$ interaction [80]. The other $Ag \cdots Ag$ contacts are found to be much larger (3.719 Å and 3.807 Å). Bond angles around each silver atom lie in the range, 86.719(17)°-139.26(2)°, indicating a highly distorted tetrahedral geometry.

Table -4: Crystallographic data for [Ag₄Cl₄(Ph₃P)₄] **9**

Empirical formula	C ₇₂ H ₆₀ Ag ₄ Cl ₄ P ₄
Formula weight	1622.36
Temperature/K	173(2)
Crystal system	Orthorhombic
Space group	Pbcn
a/Å	17.85432(16)
b/Å	20.65000(18)
c/Å	18.16054(18)
α/°	90
β/°	90
γ/°	90
Volume/Å ³	6695.64(11)
Z	4
ρ _{calc} /g/cm ³	1.609
μ/mm ⁻¹	11.936
F(000)	3232.0
Crystal size/mm ³	0.26 × 0.18 × 0.12
Radiation	CuKα (λ = 1.54184)
2θ range for data collection/°	8.158 to 142.998
Index ranges	-21 ≤ h ≤ 21, -23 ≤ k ≤ 25, -22 ≤ l ≤ 22
Reflections collected	52643
Independent reflections	6501 [R _{int} = 0.0521, R _{sigma} = 0.0235]
Data/restraints/parameters	6501/0/379
Goodness-of-fit on F ²	1.055
Final R indexes [I ≥ 2σ (I)]	R ₁ = 0.0314, wR ₂ = 0.0817
Final R indexes [all data]	R ₁ = 0.0347, wR ₂ = 0.0845

Largest diff. peak/hole / e Å ⁻³	0.98/-0.60
---	------------

Table -5: Bond distance (Å) and bond angles (°) for [Ag₄Cl₄(Ph₃P)₄] **9**

Bond distance (Å) 9			
Ag(1) – Cl(1)	2.7227(6)	C(10) – C(11)	1.376(5)
Ag(1) – Cl(2)	2.5640(6)	C(11) – C(12)	1.386(4)
Ag(1) – Cl(2) ¹	2.6587(6)	C(13) – C(14)	1.393(4)
Ag(1) – P(1)	2.3717(6)	C(13) – C(18)	1.391(4)
Ag(2) – Cl(1) ¹	2.7684(5)	C(14) – C(15)	1.383(5)
Ag(2) – Cl(1)	2.5395(6)	C(15) – C(16)	1.376(6)
Ag(2) – Cl(2) ¹	2.6814(6)	C(16) – C(17)	1.385(6)
Ag(2) – P(2)	2.3828(6)	C(17) – C(18)	1.384(5)
Cl(1) – Ag(2) ¹	2.7684(5)	C(19) – C(20)	1.384(4)
Cl(2) – Ag(1) ¹	2.6587(6)	C(19) – C(24)	1.388(4)
Cl(2) – Ag(2) ¹	2.6815(6)	C(20) – C(21)	1.388(5)
P(1) – C(1)	1.817(3)	C(21) – C(22)	1.370(6)
P(1) – C(7)	1.817(3)	C(22) – C(23)	1.372(6)
P(1) – C(13)	1.825(3)	C(23) – C(24)	1.391(5)
P(2) – C(19)	1.825(3)	C(25) – C(26)	1.389(4)
P(2) – C(25)	1.826(3)	C(25) – C(30)	1.392(4)
P(2) – C(31)	1.824(2)	C(26) – C(27)	1.392(4)
C(1) – C(2)	1.392(4)	C(27) – C(28)	1.377(5)
C(1) – C(6)	1.392(4)	C(28) – C(29)	1.380(5)
C(2) – C(3)	1.390(4)	C(29) – C(30)	1.388(4)
C(3) – C(4)	1.361(6)	C(31) – C(32)	1.388(4)

C(4) – C(5)	1.394(6)	C(31) – C(36)	1.384(4)
C(5) – C(6)	1.378(5)	C(32) – C(33)	1.393(4)
C(7) – C(8)	1.393(4)	C(33) – C(34)	1.369(5)
C(7) – C(12)	1.392(4)	C(34) – C(35)	1.381(5)
C(8) – C(9)	1.387(4)	C(35) – C(36)	1.385(5)
C(9) – C(10)	1.377(5)		
Bond Angles(°) 9			
Cl(2) – Ag(1) – Cl(1)	90.071(17)	C(12) – C(7) – P(1)	122.4(2)
Cl(2) ¹ – Ag(1) – Cl(1)	97.612(18)	C(12) – C(7) – C(8)	119.2(3)
Cl(2) – Ag(1) – Cl(2) ¹	88.792(19)	C(9) – C(8) – C(7)	119.8(3)
P(1) – Ag(1) – Cl(1)	111.889(19)	C(10) – C(9) – C(8)	120.3(3)
P(1) – Ag(1) – Cl(2)	139.26(2)	C(11) – C(10) – C(9)	120.3(3)
P(1) – Ag(1) – Cl(2) ¹	119.78(2)	C(10) – C(11) – C(12)	119.9(3)
C(11) – Ag(2) – Cl(1) ¹	91.661(17)	C(11) – C(12) – C(7)	120.4(3)
C(11) – Ag(2) – Cl(2) ¹	101.695(19)	C(14) – C(13) – P(1)	118.2(2)
Cl(2) ¹ – Ag(2) – Cl(1) ¹	86.719(17)	C(18) – C(13) – P(1)	122.8(2)
P(2) – Ag(2) – Cl(1) ¹	109.052(19)	C(18) – C(13) – C(14)	119.0(3)
P(2) – Ag(2) – Cl(1)	136.87(2)	C(15) – C(14) – C(13)	120.2(3)
P(2) – Ag(2) – Cl(2) ¹	116.46(2)	C(16) – C(15) – C(14)	120.6(4)
Ag(1) – Cl(1) – Ag(2) ¹	87.784(16)	C(15) – C(16) – C(17)	119.6(3)
Ag(2) – Cl(1) – Ag(1)	80.030(16)	C(18) – C(17) – C(16)	120.4(3)
Ag(2) – Cl(1) – Ag(2) ¹	87.473(16)	C(17) – C(18) – C(13)	120.2(3)
Ag(1) – Cl(2) – Ag(1) ¹	90.785(19)	C(20) – C(19) – P(2)	117.6(2)
Ag(1) ¹ – Cl(2) – Ag(2) ¹	78.711(16)	C(20) – C(19) – C(24)	118.5(3)
Ag(1) – Cl(2) – Ag(2) ¹	93.040(18)	C(24) – C(19) – P(2)	123.8(2)

C(1) – P(1) – Ag(1)	112.82(8)	C(19) –C(20) – C(21)	120.9(3)
C(1) – P(1) – C(7)	103.68(11)	C(22) –C(21) – C(20)	120.1(4)
C(1) – P(1) – C(13)	104.43(12)	C(21) –C(22) – C(23)	119.8(3)
C(7) – P(1) – Ag(1)	116.51(9)	C(22) –C(23) – C(24)	120.4(3)
C(7) – P(1) – C(13)	103.36(12)	C(19) –C(24) – C(23)	120.3(3)
C(13) – P(1) – Ag(1)	114.64(9)	C(26) –C(25) – P(2)	117.6(2)
C(19) – P(2) – Ag(2)	109.96(9)	C(26) –C(25) – C(30)	119.3(2)
C(19) – P(2) – C(25)	105.15(12)	C(30) –C(25) – P(2)	123.1(2)
C(25) – P(2) – Ag(2)	112.40(9)	C(25) –C(26) – C(27)	120.1(3)
C(31) – P(2) – Ag(2)	119.70(8)	C(28) –C(27) – C(26)	120.1(3)
C(31) – P(2) – C(19)	105.54(11)	C(27) –C(28) – C(29)	120.2(3)
C(31) – P(2) – C(25)	102.91(11)	C(28) –C(29) – C(30)	120.0(3)
C(2) – C(1) – P(1)	123.7(2)	C(29) –C(30) – C(25)	120.2(3)
C(2) – C(1) – C(6)	119.5(3)	C(32) –C(31) – P(2)	123.7(2)
C(6) – C(1) – P(1)	116.8(2)	C(36) –C(31) – P(2)	116.8(2)
C(3) – C(2) – C(1)	119.8(3)	C(36) –C(31) – C(32)	119.4(2)
C(4) – C(3) – C(2)	120.4(3)	C(31) –C(32) – C(33)	119.9(3)
C(3) – C(4) – C(5)	120.2(3)	C(34) –C(33) – C(32)	120.1(3)
C(6) – C(5) – C(4)	120.0(3)	C(33) –C(34) – C(35)	120.2(3)
C(5) – C(6) – C(1)	120.0(3)	C(34) –C(35) – C(36)	120.0(3)
C(8) – C(7) – P(1)	118.4(2)	C(31) –C(36) – C(35)	120.2(3)

4.5 Cytotoxic Studies

MTT assay was used to assess the % cell viability of the newly synthesized compounds (1-6) against L123 (human lung cells) and HepG2 (Hepatocellular carcinoma cells) cell lines to check their cytotoxicity profile. Cisplatin was used as a reference drug. A sub-confluent

population of L123 and HepG2 cells was treated with increasing concentration of these compounds and the number of viable cells was measured after 48 h by MTT cell viability assay. The concentration range of all the compounds was 1.55-50 μM . The cytotoxicity of complexes **1-6** was found to be concentration-dependent. The data reported in Table 6 suggest that all the complexes showed different levels of cytotoxicity. IC_{50} value for Complexes **1-6** fall in range, 8.31-25.50 μM (L123) and 18.65-22.50 μM (HepG2) (Table 6).

Table-6: Cytotoxicity profile of synthesized compounds and reference drug Cisplatin*.

<i>Compounds</i> \rightarrow ($\text{IC}_{50}\mu\text{M}$) ^a							
<i>Cell lines</i> \downarrow	1	2	3	4	5	6	Cisplatin
<i>L123</i>	18.31	25.86	22.50	18.01	24.54	22.45	8.5
<i>HepG2</i>	22.56	25.50	18.65	20.54	22.65	18.65	9.65

^a IC_{50} = the concentration of compound that inhibits 50% of cell growth.

*Each cytotoxic activity was performed in triplicate and average result is given with an error range of ± 0.05

4.5.1 Molecular modeling studies

Based on the *in vitro* anticancer activity to the Hodgkin lymphoma cell-line L1236, one of the active complex **2** was selected to evaluate the putative binding mode with amino acids in the active site of the enzyme using molecular docking technique. To confirm the binding affinity or probable binding site, docking study of cisplatin was first carried out with Hodgkin lymphoma cell line (PDB ID 1QOK) [83] using builder tool kit of software package ArgusLab 4.0.1 (www.arguslab.com).[84] It was observed that NH_2 groups of cisplatin binds with the cysteine 184 ($d = 2.51 \text{ \AA}$) and 248 ($d = 2.76 \text{ \AA}$) amino acid residues through hydrogen bonding. Moreover, it also showed binding interactions with histidine 194 ($d = 1.03 \text{ \AA}$) and glutamine 249 ($d = 2.62 \text{ \AA}$) amino acid residue. Encouraging from the results of cisplatin with Hodgkin lymphoma cell line and finding out the probable binding sites from these interactions, docking was then performed by placing complex **2** into the binding site of target-specific region (where cisplatin

showed its interactions) of the Hodgkin lymphoma cell-line (PDB ID 1QOK). The docked model of cisplatin and complex **2** with Hodgkin lymphoma enzyme was shown in Figure 5. Complex **2** is surrounded by side chains of various amino acids such as F196, H194, Y192 and Y231, indicating that the molecule is well fitted in the active pocket. The docking results revealed that the interaction of complex **2** with Hodgkin lymphoma is dominated by hydrogen bonding interactions with tyrosine (Y247), glutamine (Q249) and cysteine (C248 and C184) amino acid residues. As shown in Figure 5, NH of complex **2** showed hydrogen bonding interactions with S of cysteine (C248 and C184) amino acid residues and N of tryptophan (W195) of 1QOK (bond distance: NH...S = 2.96 Å in case of C248, NH...S = 2.73 Å in case of C184 and NH...N = 2.81 Å of W195). NH group of indole ring of complex **2** also showed hydrogen bonding interactions with oxygen of glutamine (Q249) and tyrosine (Y247) amino acid residue (bond distance: NH...O = 2.41 Å in case of Q249 and NH...O = 1.98 Å in case of Y247). Therefore, docking of complex **2** in the active site of enzyme indicated the probable mode of action for anticancer activity.

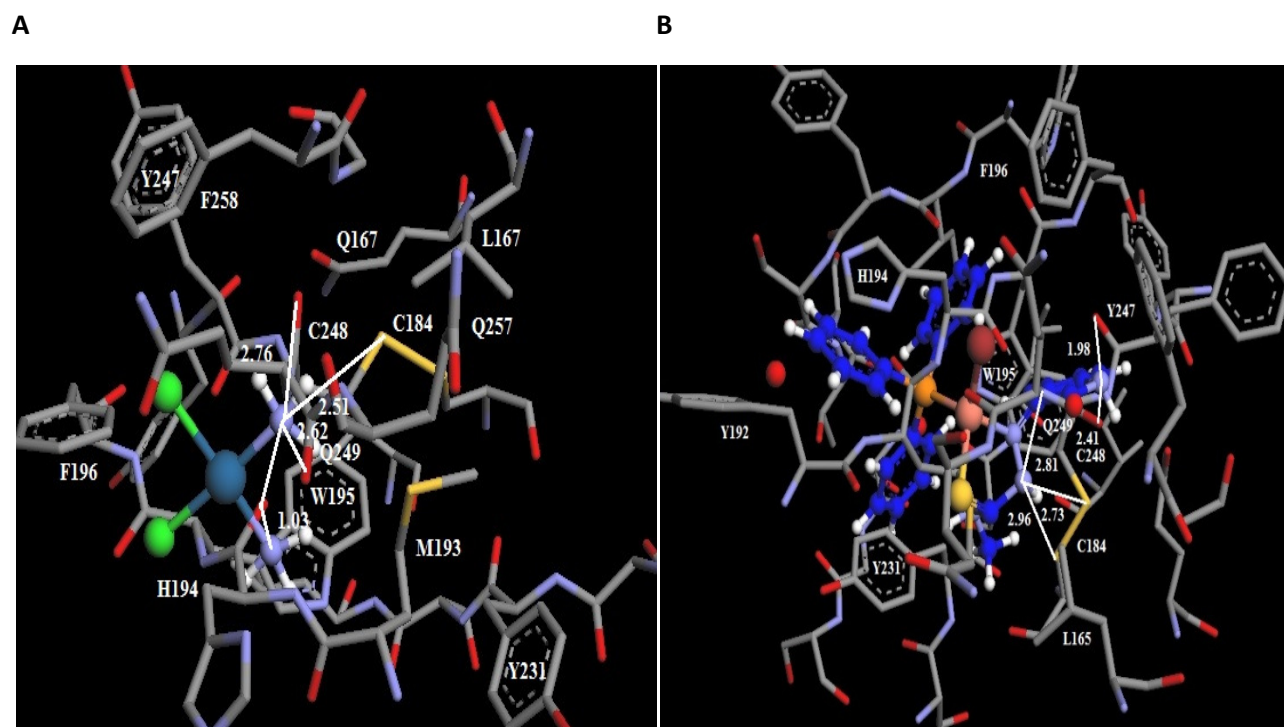
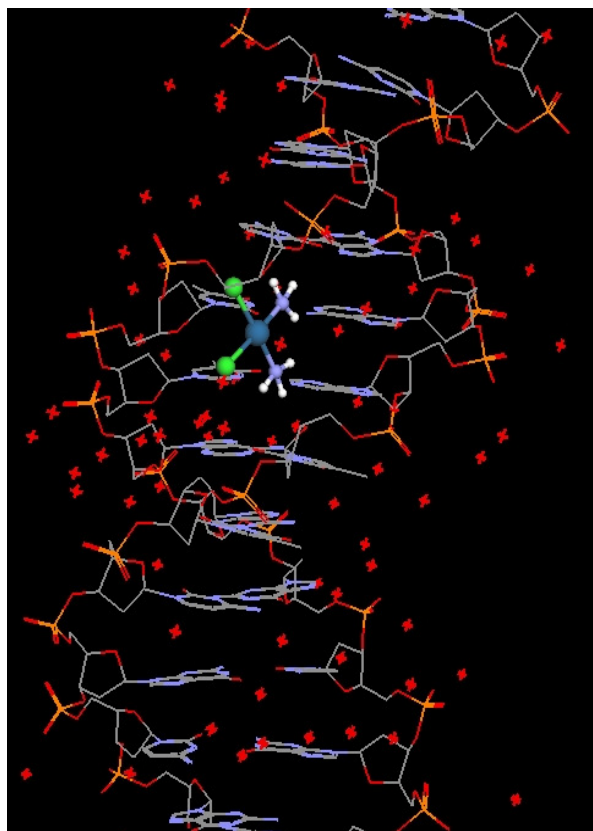


Figure-5: Docking of cisplatin (A) and complex **2** (B) in the active site of Hodgkin lymphoma (PDB ID 1QOK)

Molecular docking is an interesting tool to predict the possible drug–DNA interactions because the mode of action of cisplatin is directly associated with their binding to DNA. Thus, cisplatin showed interactions with DNA, crosslinked DNA in several different ways, interfering with cell division by mitosis and kill cells. To explore the most feasible binding site or binding affinity, docking studies have been performed on cisplatin and complex **2** with DNA (PDB ID: 1BNA). It has been demonstrated that both cisplatin and complex **2** showed interactions with DNA, the probable mode of action for anticancer activity.(Figure-5a)

A



B

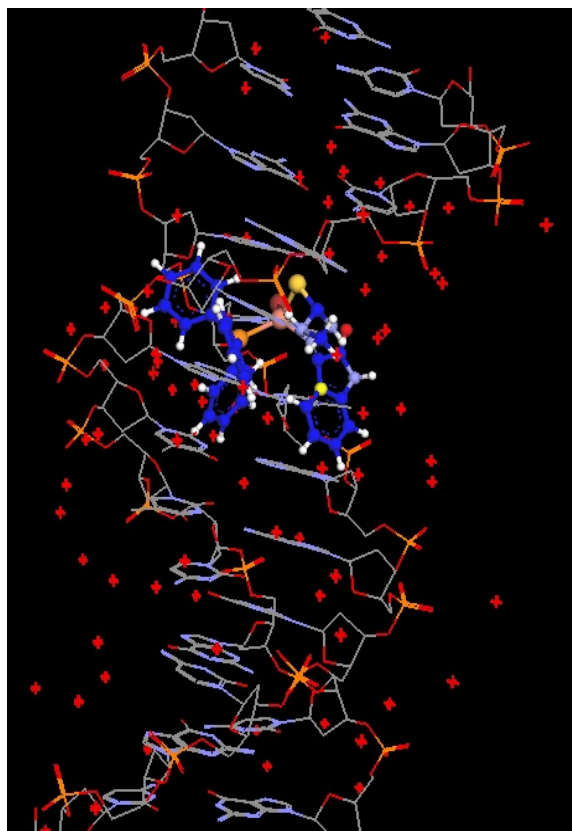


Figure-5a: Docking of cisplatin (**A**) and complex **2** (**B**) in the active site of DNA (PDB ID: 1BNA)

4.5.2 Docking studies

Compounds were built using the builder tool kit of the software package Argus Lab 4.0.1.23 and energy minimized with semi-empirical quantum mechanical method PM3. Crystal

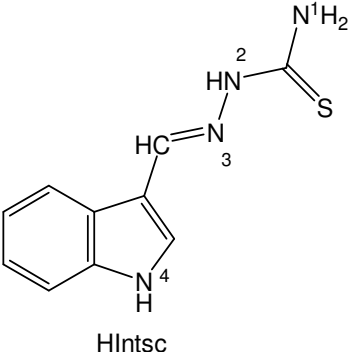
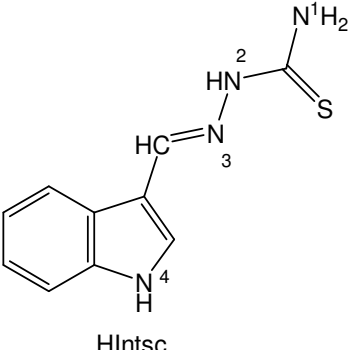
coordinates of Hodgkin lymphoma enzyme and DNA were downloaded from protein data bank and in the molecule tree view of the software, the monomeric structures of the crystal co-ordinate was selected and the active site was defined as 15 Å around the ligand. Validation of the docking programme was checked by docking the known inhibitors of the respective enzymes in their binding sites. The molecule to be docked in the active site of the enzyme was pasted in the work space carrying the structure of the enzyme. The docking programme implements an efficient grid based docking algorithm which approximates an exhaustive search within the free volume of the S19 binding site cavity. The conformational space was explored by the geometry optimization of the flexible ligand (rings were treated as rigid) in combination with the incremental construction of the ligand torsions. Thus, docking occurs between the flexible ligand parts of the compound and enzyme. The docking was repeated several times (approx. 10000 iterations) until no change in the position of the ligand and a constant value of the binding energy was observed. The ligand orientation was determined by a shape scoring function based on Ascore and the final positions were ranked by lowest interaction energy values. H-bond between the respective compound and enzyme were explored.

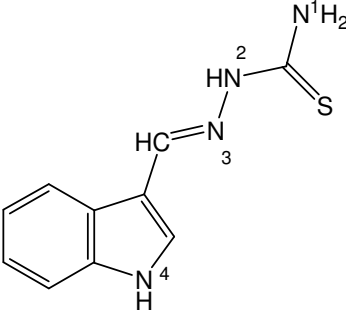
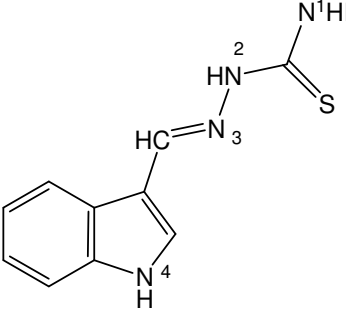
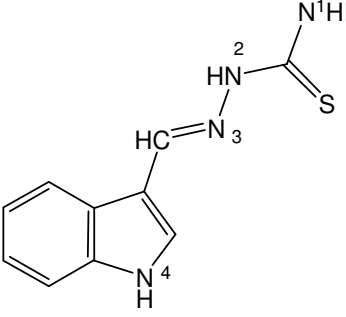
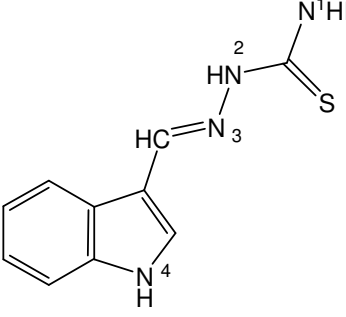
CHAPTER 5

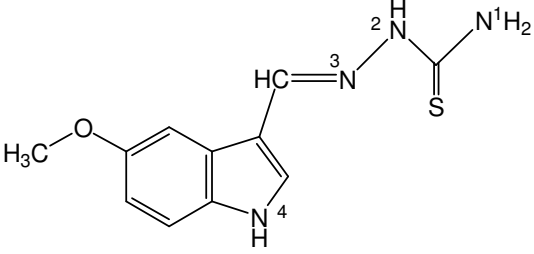
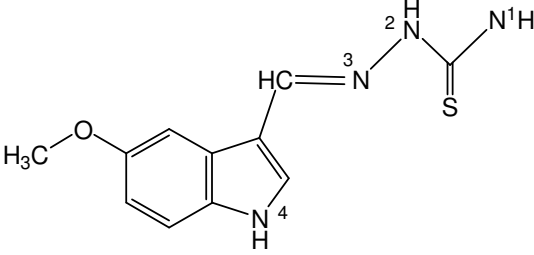
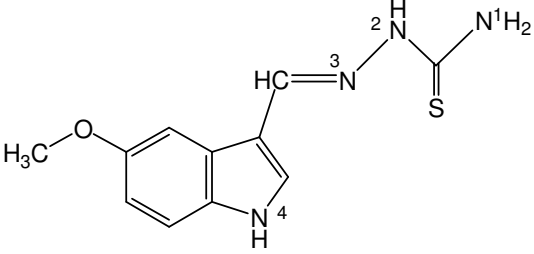
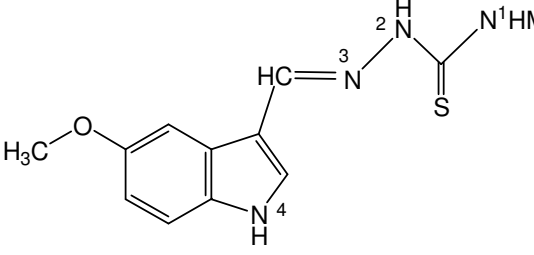
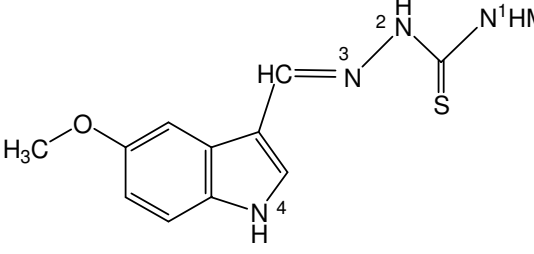
COMPLEXES OF COPPER(I) AND SILVER(I) HALIDES WITH INDOLE BASED THIOSEMICARBAZONES.

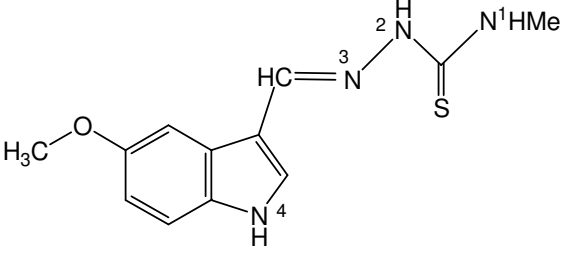
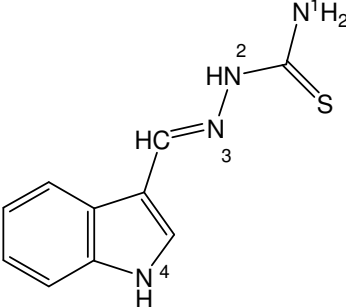
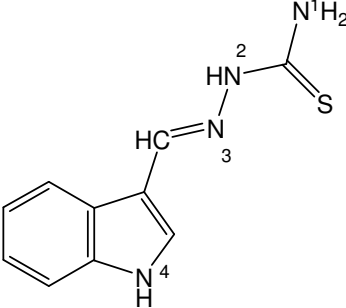
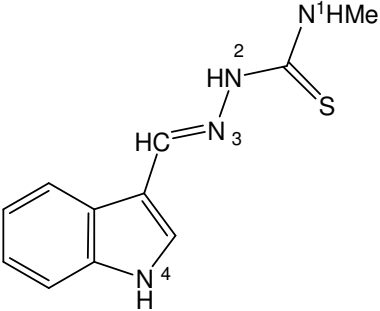
5.1 Complexes of copper(I) and silver(I) halides with indole based thiosemicarbazones: Complexes of copper(I) and silver(I) halides with indole-3-thiosemicarbazone (HIntsc), indole-N¹-methyl-3-thiosemicarbazone (HIntsc-N¹-Me), 5-methoxy indole-3-thiosemicarbazone (5-MeOHIntsc) and 5-methoxy indole-N¹-methyl-3-thiosemicarbazone (5-MeOHIntsc-N¹-Me) are listed in Table-7.

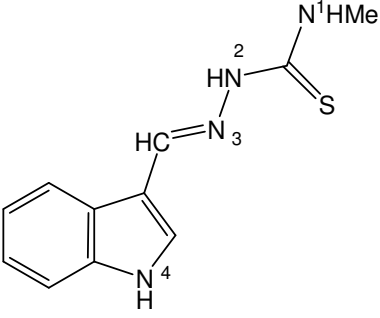
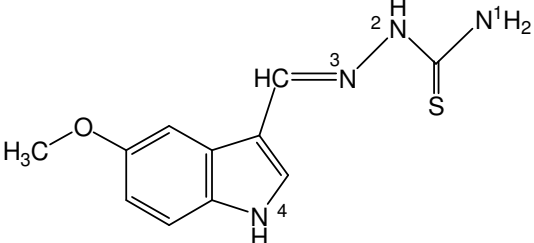
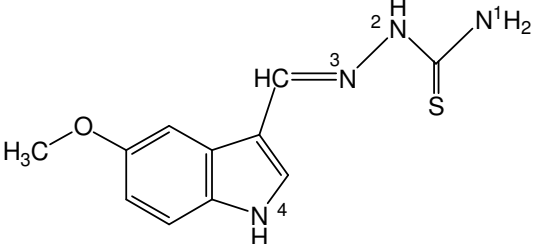
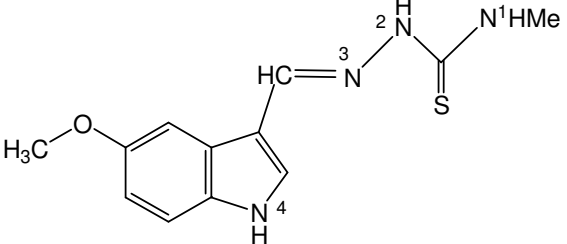
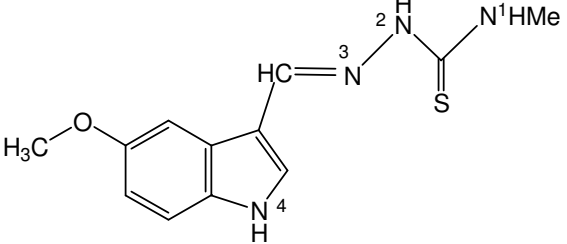
Table-7: List of copper(I) and silver(I) halide complexes of indole based thiosemicarbazones.

Complexes	Structure of ligands
<p data-bbox="240 835 581 869">$[\text{CuI}(\eta^1\text{-S-HIntsc})(\text{Ph}_3\text{P})_2]$</p> <p data-bbox="477 940 529 974">(10)</p>	 <p data-bbox="883 1163 964 1184" style="text-align: center;">HIntsc</p>
<p data-bbox="240 1201 604 1234">$[\text{CuBr}(\eta^1\text{-S-HIntsc})(\text{Ph}_3\text{P})_2]$</p> <p data-bbox="477 1306 529 1339">(11)</p>	 <p data-bbox="883 1528 964 1549" style="text-align: center;">HIntsc</p>

<p>[CuCl(η^1-S-HIntsc)(Ph₃P)₂]</p> <p>(12)</p>	 <p>HIntsc</p>
<p>[Cu₂(μ_2-I)₂(HIntsc-N¹-Me)₂(Ph₃P)₂]</p> <p>(13)</p>	 <p>HIntsc-N¹-Me</p>
<p>[Cu₂(μ_2-Br)₂(HIntsc-N¹-Me)₂(Ph₃P)₂]</p> <p>(14)</p>	 <p>HIntsc-N¹-Me</p>
<p>[Cu₂(μ_2-Cl)₂(HIntsc-N¹-Me)₂(Ph₃P)₂]</p> <p>(15)</p>	 <p>HIntsc-N¹-Me</p>

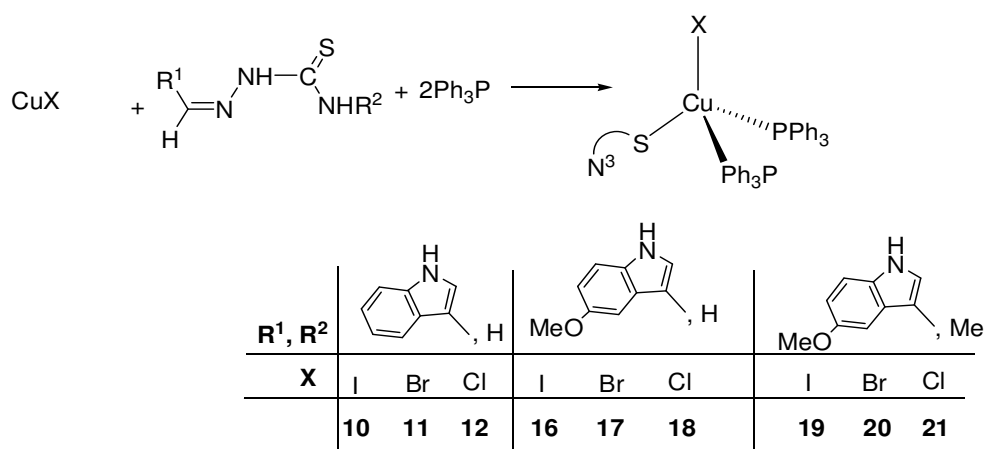
<p>[CuI(η^1-S-5-MeOHIntsc)(Ph₃P)₂]</p> <p>(16)</p>	 <p>5-MeOHIntsc</p>
<p>[CuBr(η^1-S-5-MeOHIntsc)(Ph₃P)₂]</p> <p>(17)</p>	 <p>5-MeOHIntsc</p>
<p>[CuCl(η^1-S-5-MeOHIntsc)(Ph₃P)₂]</p> <p>(18)</p>	 <p>5-MeOHIntsc</p>
<p>[CuI(η^1-S-5-MeOHIntsc-N¹-Me)(Ph₃P)₂]</p> <p>(19)</p>	 <p>5-MeOHIntsc-N¹-Me</p>
<p>[CuBr(η^1-S-5-MeOHIntsc-N¹-Me)(Ph₃P)₂].CH₃CN</p> <p>(20)</p>	 <p>5-MeOHIntsc-N¹-Me</p>

<p>[CuCl(η^1-S-5-MeOHIntsc-N¹-Me)(Ph₃P)₂]</p> <p>(21)</p>	 <p>5-MeOHIntsc-N¹-Me</p>
<p>[AgCl(η^1-S-HIntsc)(Ph₃P)₂]</p> <p>(22)</p>	 <p>HIntsc</p>
<p>[AgBr(η^1-S-HIntsc)(Ph₃P)₂]</p> <p>(23)</p>	 <p>HIntsc</p>
<p>[AgCl(η^1-S-HIntsc-N¹-Me)(Ph₃P)₂]</p> <p>(24)</p>	 <p>HIntsc-N¹-Me</p>

<p>[AgBr(η^1-S-HIntsc-N¹-Me)(Ph₃P)₂] (25)</p>	 <p>HIntsc-N¹-Me</p>
<p>[AgCl(η^1-S-5-MeOHIntsc)(Ph₃P)₂] (26)</p>	 <p>5-MeOHIntsc</p>
<p>[AgBr(η^1-S-5-MeOHIntsc)(Ph₃P)₂] (27)</p>	 <p>5-MeOHIntsc</p>
<p>[AgCl(η^1-S-5-MeOHIntsc-N¹-Me)(Ph₃P)₂] (28)</p>	 <p>5-MeOHIntsc-N¹-Me</p>
<p>[AgBr(η^1-S-5-MeOHIntsc-N¹-Me)(Ph₃P)₂] (29)</p>	 <p>5-MeOHIntsc-N¹-Me</p>

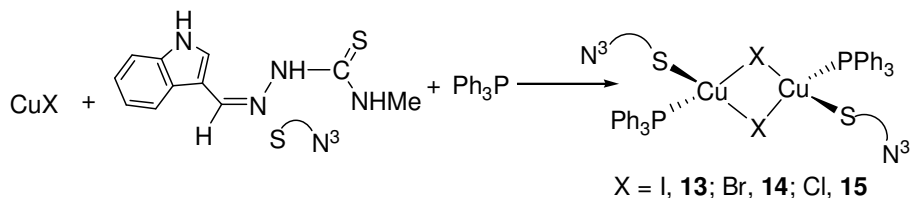
5.1.1 Synthesis

Reaction of indole-3-thiosemicarbazone (HIntsc, H¹L), 5-methoxy indole-3-thiosemicarbazone (5-MeOHIntsc, H²L) and 5-methoxy indole-N¹-methyl-3-thiosemicarbazone (5-MeOHIntsc-N¹-Me, H³L) with copper(I) halides and triphenylphosphine in 1 : 1 : 1 (M : HL : Ph₃P) ratio yielded insoluble product similar to the reaction of copper(I) iodide and bromide with isatin-3-thiosemicarbazone [46]. Addition of one extra mole of triphenylphosphine formed clear solution which on evaporation give crystalline products of stoichiometry, [CuX(HL)(Ph₃P)₂] (H¹L, X = I, **10**; Br, **11**; Cl, **12**; H²L, X = I, **16**; Br, **17**; Cl, **18**; H³L, X = I, **19**; Br, **20**; Cl, **21**) (Scheme 7).



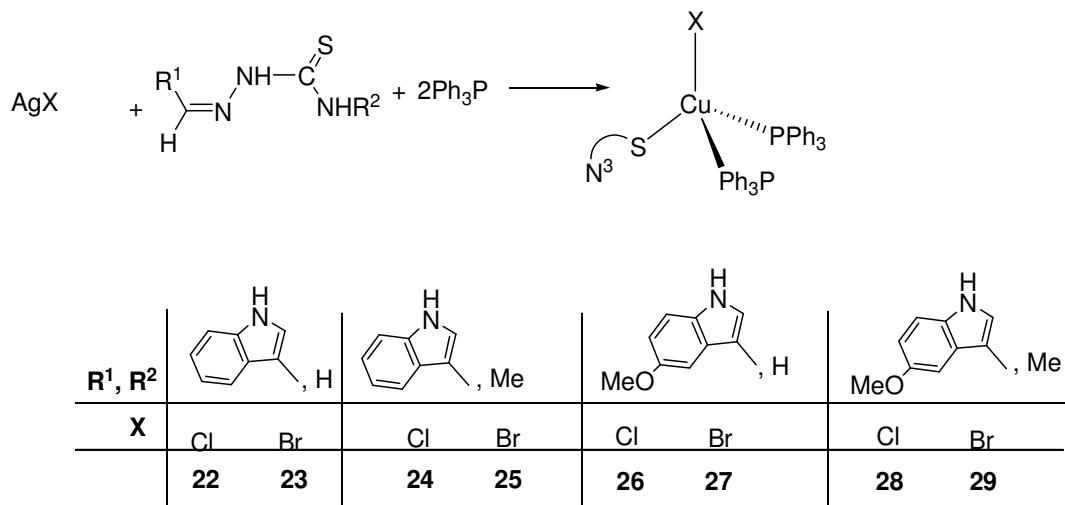
(Scheme 7)

In contrast to above, reaction of indole-N¹-methyl-3-thiosemicarbazone (HIntsc-N¹-Me, H⁴L) with copper(I) halides and triphenylphosphine in 1 : 1 : 1 (HL : M : Ph₃P) molar ratio yielded halogen bridged dimers of formula, [Cu₂(μ-X)₂(η¹-S-HIntsc-N¹-Me)₂(Ph₃P)₂] (X = I, **13**; Br, **14**; Cl, **15**) (Scheme 8). Substitution of methyl group at N¹ atom of indole-3-thiosemicarbazones has changed the nuclearity of its copper(I) complexes. This behaviour is similar to the complexes of N¹-substituted furane-2-carbaldehyde and thiophene-2-carbaldehyde thiosemicarbazones. [85, 86] X-ray quality crystals were obtained for H²L, **12**, **13**, **14**, **19** and **20**.



(Scheme 8)

Reaction of silver(I) halides (X= Cl, Br) with indole-3-thiosemicarbazone (HIntsc, H¹L), -N¹-methyl-3-thiosemicarbazone (HIntsc-N¹-Me, H⁴L), 5-methoxy indole-3-thiosemicarbazone (5-MeOHIntsc, H²L) and 5-methoxy indole-N¹-methyl-3-thiosemicarbazone (5-MeOHIntsc-N¹-Me, H³L) and triphenylphosphine in 1 : 1 : 1 (M : HL : Ph₃P) molar ratio in acetonitrile formed yellow coloured highly insoluble compound. To solubilise it, one mole of triphenylphosphine has been added. The clear solution thus formed gave complexes of stoichiometry [AgX(HL)(Ph₃P)₂] (H¹L, X = Cl(**22**), Br(**23**), H²L, X = Cl(**24**), Br(**25**), H³L, X = Cl(**26**), Br(**27**), H⁴L, X = Cl(**28**), Br(**29**) (Scheme 9). X-ray quality crystals were obtained for **22**.



(Scheme 9)

5.1.2 Discussion on IR spectroscopy:

The important IR peaks of free ligands and their copper(I) complexes are given in Table-8, and for silver(I) complexes in Table-9. $\nu(\text{N-H})$ band in free ligands of indole-3-thiosemicarbazones (H¹L, H²L, H³L and H⁴L) appeared in the range, (i) 3229-3437 cm⁻¹ due

to symmetric and asymmetric stretching of amino group, (ii) 3188-3134 cm^{-1} due to amide group and (iii) 3010-3051 cm^{-1} due to NH group of indole ring. All these band in complexes **10-29** appeared in range 3211-3473 cm^{-1} , 3188-3117 cm^{-1} and 3010-3053 cm^{-1} . Appearance of these bands in complexes indicate that no deprotonation occurred during complexation and the thio- ligands are coordinating as neutral ligands. The characteristic $\nu(\text{C}=\text{S})$ band in free ligands appeared at 837 cm^{-1} in H^1L , 831 cm^{-1} in H^2L , 854 cm^{-1} in H^3L and 857 cm^{-1} in H^4L . These bands shifted to high energy region in copper complexes **10-15** and silver complexes **22-27** and shifted to low energy region in copper complexes **16-21** and silver complexes **28-29** vis-a-vis free ligands. This shift indicates binding of metal center by thione sulfur of thio-ligands. Appearance of an additional band in the range, 1091-1098 cm^{-1} due to $\nu(\text{P}-\text{C}_{\text{ph}})$ in complexes **10-29** ensures coordination of triphenylphosphine ligand to metal center (Tables- 8,9).

Table-8: Important peaks in IR spectrum of Ligands ($\text{H}^1\text{L}-\text{H}^4\text{L}$) and their copper(I) complexes **10-21**.

Compound	$\nu(\text{N}-\text{H})$	$\nu(-\text{NH}-)$	$\nu(\text{NH}_{\text{indole}})$	$\delta(\text{NH}_2)$ + $\nu(\text{C}=\text{N})+\nu(\text{C}=\text{C})$	$\nu(\text{C}=\text{S})$	$\nu(\text{P}-\text{C}_{\text{ph}})$
Hintsc (H^1L)	3311m 3232m	3146m	3039	1612m 1579s	837s	-
10	3465s 3426s	3180m	3040	1627s 1570m	840s	1095s.
11	3455s 3436s	3160m	3052m	1617s 1590m	841s	1096s
12	3443s 3321s	3197m	3091m	1614s, 1554m	847s	1091s
(H^2L)	3363m 3238m	3188m	3051m	1656m 1546s	831s	-
13	3359s 3336s	3183m	3053m	1610s 1507s	849s	1098s
14	3362s	3136m	3056m	1617s	843s	1094s

	3318s			1574s		
15	3425s 3362s	3148m	3058m	1616s 1576s	846s	1094s.
(H³L)	3437s 3362s	3134m	3047m	1616s 1589s	854s	-
16	3422w 3352w	3178w	3070m	1616s 1579s	852s	1095s
17	3421w 3362w	3117m	3053m	1624s 1543s	850s	1091s.
18	3431m 3375m	3196m	3057m	1614s 1585s	850s	1091s
(H⁴L)	3371s 3230m	3151m	3012m	1614m 1572s	857s	-
19	3437m 3338m	3184m	3012m	1611s 1557s	849s	1095s
20	3377s 3229s	3119	3010m	1610s 1559s	843s	1092s
21	3417s 3363s	3129m	3010m	1617s 1537s	854s	1094s

s, sharp; m, medium; w, weak

Table-9: Important peaks in IR spectrum of silver(I) complexes **22-29**.

Compound	$\nu(\text{N-H})$	$\nu(-\text{NH-})$	$\nu(\text{NH, indole})$	$\nu(\text{C-H}_{\text{Me}})$	$\delta(\text{NH}_2)$ +$\nu(\text{C=N})$ +$\nu(\text{C=C})$	$\nu(\text{C=S})$	$\nu(\text{P-C}_{\text{Ph}})$
22	3441s 3315s	3142m	3053m	-	1616s 1587m	846s	1095s
23	3473s 3315s	3140m	3053m	-	1616s 1585	846s	1097s.

24	3364s 3234s	3182m	3053m	2934m	1608s 1549m	833s	1094s
25	3363s 3239s	3179m	3052m	2928m	1609s 1530m	850s	1094s
26	3434s, 3362s	3176m	3017sh	–	1616s, 1588s, 1480s	857s	1094s
27	3430s, 3362s	3186m	3027sh	–	1626s, 1598s, 1485s	857s	1095s
28	3371s 3211m	3140m	3049m	2901m	1612s 1562s	848	1093
29	3374s 3228m	3135m	3051m	2929m	1608s 1546s	831	1093s

s, sharp; m, medium; w, weak

5.1.3 Discussion on NMR spectroscopy:

Important ^1H NMR signals of spectra of ligands (H^1L - H^4L), and their copper(I) complexes are given in Table-10 and silver(I) complexes are given in Table-11. $-\text{N}^2\text{H}-$ appeared in the range of δ 10.01-11.24ppm { δ 10.07(H^1L), δ 11.24(H^4L), δ 10.04 (H^2L), δ 10.01(H^3L)} which showed a downfield shift (in range δ 11.30-15.65ppm) among all the complexes (**10-27**), except in (δ 11.03) **13**, (δ 10.01) **17** and (δ 10.00) **18** vis-a-vis free ligand. Similarly N^4H of the indole ring appeared (in range δ 7.32-10.95ppm) at δ 8.33(H^1L), δ 10.95(H^4L) δ 7.32 (H^2L), δ 8.94(H^3L), also showed downfield shift in all the complexes (ranging from δ 8.30-13.79ppm)(**10-27**), except (δ 10.64)**13** and (δ 8.36)**19**, compared to free ligand. The presence of all these protons indicate that no deprotonation take place during complexation and all the ligands coordinate to the copper center in neutral form. Signal due to ^1NH proton, in maximum of the complexes, as depicted in the table, get obscured by the phenyl ring of indole ligands. Appearance of the same, however ensured the presence of amino and amido group. Signal due to C^2H appeared as triplet in complex **11** and as singlets in the range of δ 7.11-

8.95ppm in complex **10-25** and as doublets in complex (δ 7.95)**26** and (δ 7.96)**27**. C^4H appeared as additional singlet peaks in copper complex **10-15** (in range δ 7.86-12.98ppm) and in silver complex **22-25** (in range δ 7.86-12.92ppm) while the same were obscured and appeared along with C^{6-9} peaks in complex **16-21** and **26-27**. Singlet peaks in complex (δ 1.95)**19** (δ 1.60)**20,21**, (δ 7.55)**24**, (δ 7.87)**25** a triplet peak in (δ 2.99)**13**, and multiplets (δ 3.19)**14,15** indicate the presence of $-CH_3$ group while additional peaks as multiplets in complex **16,17** and **18** in the range of δ 3.56-3.88ppm and as doublets in complex **19, 20** and **21** in the range of δ 3.06-3.11ppm indicate presence of methoxy group (Tables -10,11).

Table-10: 1H NMR signals for HL^1 - HL^5 (δ , ppm) and their copper(I) complexes **10-21**.

Complexes	(N^2H)	(N^4H)	(N^1H)	(C^2H)	Ring Protons
H¹L	10.07 s	8.33 s	3.48 s	7.83s	C^4H , 7.86 s(1H); $C^{6,9}H$, 7.46 d(2H); $C^{7,8}H$, 7.29 d (2H)
10	15.65 s	13.79 s	4.15 s	7.69s	C^4H , 12.98 s (1H); $C^{6,9}H$, 10.68d (2H); $C^{7,8}H$, 7.84s (2H)
11	15.50 s	13.19 s	4.65 s	7.88t	C^4H , 12.28 s (1H); $C^{6,9}H$, 11.68 d (2H); $C^{7,8}H$, 7.24 s (2H)
12	11.71 s	10.78 s	3.21 s	7.11	C^4H , 8.22 s (1H); $C^{6,9}H$, 7.92 d (2H); $C^{7,8}H$, 7.75 s (2H)
H⁴L	11.24 s	10.95 s	7.39 s		C^4H , 8.10 s (1H); $C^{6,9}H$, 7.14 m (2H); $C^{7,8}H$, 7.46 d (2H); $-CH_3$, 3.16 m
13	11.03 s	10.64s	(obscured by ring protons)	8.36s	C^4H , 7.90s (1H); $C^{6,9}H$, 6.95d (2H); $C^{7,8}H$, 7.33-7.24 m (2H); $-CH_3$, 2.99 s
14	11.57 s	11.36s	7.54 s	8.44s	C^4H , 8.10 s (1H); $C^{6,9}H$, 7.09 m (2H); $C^{7,8}H$, 7.79 d (2H); $-CH_3$, 3.19 m
15	11.99 s	11.20s	7.35 s	8.33s	C^4H , 8.08 s (1H); $C^{6,9}H$, 7.25 m (2H); $C^{7,8}H$, 7.47 d (2H); $-CH_3$, 3.19 m

H²L	10.04 s	7.32 d	(obscured by ring protons)	8.61 s	C ^{4,6,9} H+N ¹ H+Ph ₃ P, 7.78 - 6.95 m; C ⁷ H, 7.29 d(1H); CH ₃ , 3.88-3.86m(3H)
16	11.16 s	8.35 d	(obscured by ring protons)	8.19 s	C ^{4,6,9} H+N ¹ H+Ph ₃ P, 8.34 - 7.57 m; C ⁷ H, 7.42 d(1H); CH ₃ , 3.79-3.77m(3H)
17	10.01 s	9.53 s	(obscured by ring protons)	8.49 s	C ^{4,6,9} H+N ¹ H+Ph ₃ P, 8.48 - 8.11 m; C ⁷ H, 7.66 d(1H); CH ₃ , 3.65-3.58m(3H)
18	10.00 s	9.43 s	(obscured by ring protons)	8.51 s	C ^{4,6,9} H+N ¹ H+Ph ₃ P, 8.50 - 8.23m; C ⁷ H, 7.68 d(1H); CH ₃ , 3.63-3.56m(3H)
H³L	10.01 s	8.94 s	(obscured by ring protons)	8.84 s	C ^{4,6,9} H+N ¹ H ₂ +Ph ₃ P, 7.78 -6.94 m; C ⁷ H, 6.94 s (1H); -OCH ₃ , 3.87 s(3H); -CH ₃ , 1.57 s
19	11.37 s	8.36 s	(obscured by ring protons)	8.34 s	C ^{4,6,9} H+N ¹ H ₂ +Ph ₃ P, 7.67-7.40 m; C ⁷ H, 6.81 d (1H); -OCH ₃ , 3.06 d(3H); -CH ₃ , 1.95 t
20	11.75 s	8.93 s	(obscured by ring protons)	8.28 s	C ^{4,6,9} H+N ¹ H ₂ +Ph ₃ P, 7.47-7.30 m; C ⁷ H, 6.89 d (1H); -OCH ₃ , 3.09 d(3H); -CH ₃ , 1.60 s
21	11.76 s	8.95 s	(obscured by ring protons)	8.20 s	C ^{4,6,9} H+N ¹ H ₂ +Ph ₃ P, 7.57-7.30 m; C ⁷ H, 6.87 d (1H); -OCH ₃ , 3.11 d(3H); -CH ₃ , 1.60 s

Table-11: ¹H NMR signals for silver(I) and their complexes **22-27**.

Complexes	(N ² H)	(N ⁴ H)	(N ¹ H)	(C ² H)	Ring Protons
22	15.93 s	13.14 s	6.69 s	7.87 s	C ⁴ H, 12.92 s (1H); C ^{6,9} H, 12.03 d (2H); C ^{7,8} H, 7.25 s (2H)
23	15.83 s	13.18 s	6.68 s	7.87 s	C ⁴ H, 12.11 s (1H); C ^{6,9} H, 11.92 d (2H); C ^{7,8} H, 7.87 s (2H)

24	13.18 s	12.78 s	(obscured by ring protons)	8.00 s	C ⁴ H, 12.35 s (1H); C ^{6,9} H, 11.80 m (2H); C ^{7,8} H+ N ¹ H, 7.69-7.77 d (2H); -CH ₃ , 7.55 m
25	13.19 s	12.80 s	(obscured by ring protons)	8.01 s	C ⁴ H, 12.12 s (1H); C ^{6,9} H, 11.88 m (2H); C ^{7,8} H+ N ¹ H, 7.79-7.77 d (2H); -CH ₃ , 7.87 m
26	11.37 s	8.31 d	(obscured by ring protons)	7.95 d	C ^{4,6,9} H+N ¹ H+Ph ₃ P, 8.31 - 7.63 m; C ⁷ H, 6.78 d(1H); -OCH ₃ , 3.79-3.77m(3H)
27	11.30 s	8.30 d	(obscured by ring protons)	7.96 d	C ^{4,6,9} H+N ¹ H+Ph ₃ P, 8.30 - 7.96 m; C ⁷ H, 6.70 d(1H); -OCH ₃ , 3.79-3.78 m(3H)

5.1.4 Structure of H²L-N¹-Me (H²L):

The ligand H²L crystallizes in monoclinic crystal system with space group P2₁/c. The two rings of indole moiety (five and six membered) are nearly planer. Torsion angle between C(11)–N(4)–C(10)–C(9) and C(4)–C(5)–C(6)–C(7) is 179.44(17) and 179.80(17)° respectively. It show E –configuration about C(3)=N(1) double bond due to intramolecular H-bonding between N(3)H and N(1) atom of thiosemicarbazone moiety. (Figure-6). The C=S bond length is 1.6957(16)Å, which is close to that found in H₂itsc-N¹-Me and H₂itsc-N¹-Hm. [74] Crystallographic data and important bond parameters are given in Table-12 and Table-13 respectively.

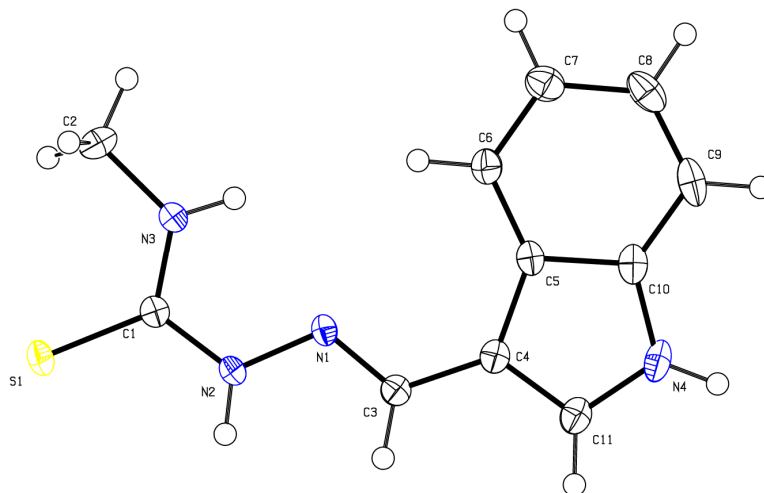


Figure-6: Structure of HIIntsc-N¹-Me with numbering scheme.

5.1.5 Structure of monomers (**12**, **19** and **20**)

Complexes [CuCl(η^1 -S-HIIntsc)(Ph₃P)₂]**12** crystallized in monoclinic crystal system with space group P2₁/c, whereas [CuI(η^1 -S-5-MeOHIntsc-N¹-Me)(Ph₃P)₂]**19** and [CuBr(η^1 -S-5-MeOHIntsc-N¹-Me)(Ph₃P)₂]**20** crystallized in orthorhombic crystal system with space group Pbca. Molecular structure of these complexes are given in Figure-7(**12**), 8(**19**), 9(**20**), packing diagrams of the complexes are given in Figures-7a(**12**), 8a(**19**), 9a(**20**), crystallographic data and important bond parameters are given in Table 14(**12**), 16(**19**, **20**) and 15(**12**), 17(**19**), 18(**20**) respectively.

In complexes **12**, **19** and **20**, four corners of tetrahedron are occupied by one halogen atom, one sulphur atom from thio- ligand and two phosphorous atom from triphenylphosphine ligands with copper(I) taking central position. The Cu–S bond length is 2.3893(5) Å (**12**), 2.3698(11) Å (**19**) and 2.3672(6) Å (**20**). This bond length is close to Cu–S bond length in similar type of tetrahedral molecules reported in literature.[46,73] This Cu–S bond length is larger than, 2.3274(10) Å in [CuBr(η^2 -N³, S-H₂Intsc-N¹-Me)(Ph₃P)] (**2**) as in this case thiosemicarbazone chelates rather than binding as terminal ligand. The copper-halogen bond distances are, Cu–I, 2.6807(6) Å (**19**); Cu–Br, 2.5179(4) Å (**20**) and Cu–Cl, 2.4301(5) Å (**12**). These distances are less than sum of the ionic radii of Cu⁺ and X⁻ (Cu⁺, I⁻, 2.97Å; Cu⁺, Br⁻, 2.73 Å; Cu⁺, Cl⁻, 2.58 Å.[73,76] The C–S bond length, 1.700(2)Å (**12**), 1.706(4)Å (**19**) and

1.700(2) Å (**20**) is close to that of HIntsc-N¹-Me (1.6957 Å), which indicate considerable C=S character in coordinated thio- ligands in these complexes as compare to thiolate, but shorter than 1.757(4)Å in [Hg(C₆H₅C₅H₄N)(btsc)] (btsc = anion of benzaldehydethiosemicarbazone) as in later ligand coordinate in thiolate form rather than thione form in former case.[87] Bond angles around copper in these monomeric complexes lie in the range, {101.640-121.029° (**12**), 104.24(3)-1176.35(4)° (**19**) and 106.60(2)-116.78(2)° (**20**)}, which suggest a distorted tetrahedral geometry around the copper centre. Cu-S-C angle in complexes are 111.72(7) (**12**), 107.73(13) (**19**) and 107.37(8) (**20**).

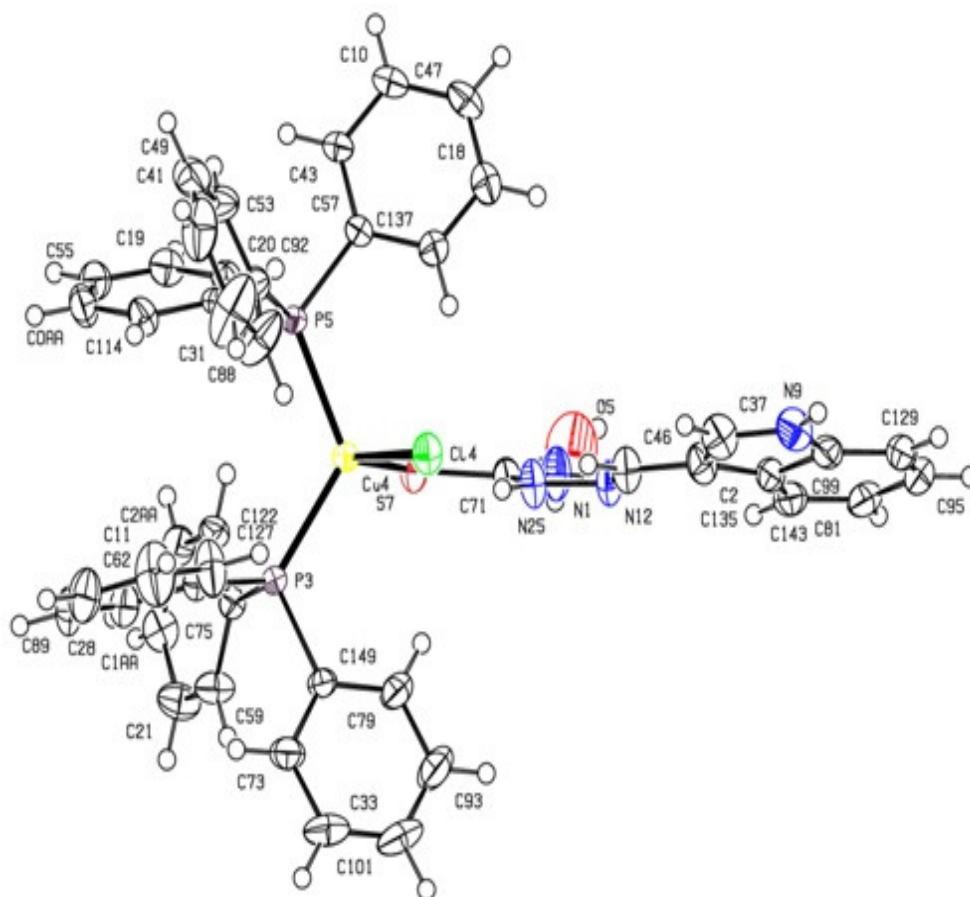


Figure-7: Structure [CuCl(η^1 -S-Hintsc)(Ph₃P)₂]**12** with numbering scheme.

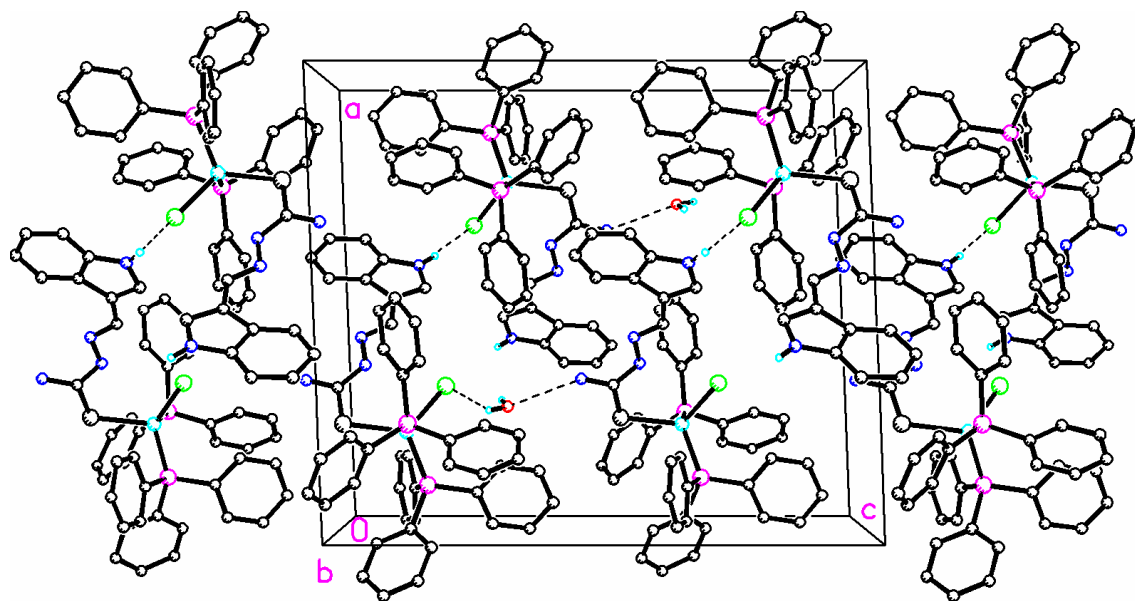


Figure-7a: Packing Diagram of $[\text{CuCl}(\eta^1\text{-S-Hintsc})(\text{Ph}_3\text{P})_2]$ **12** with numbering scheme.

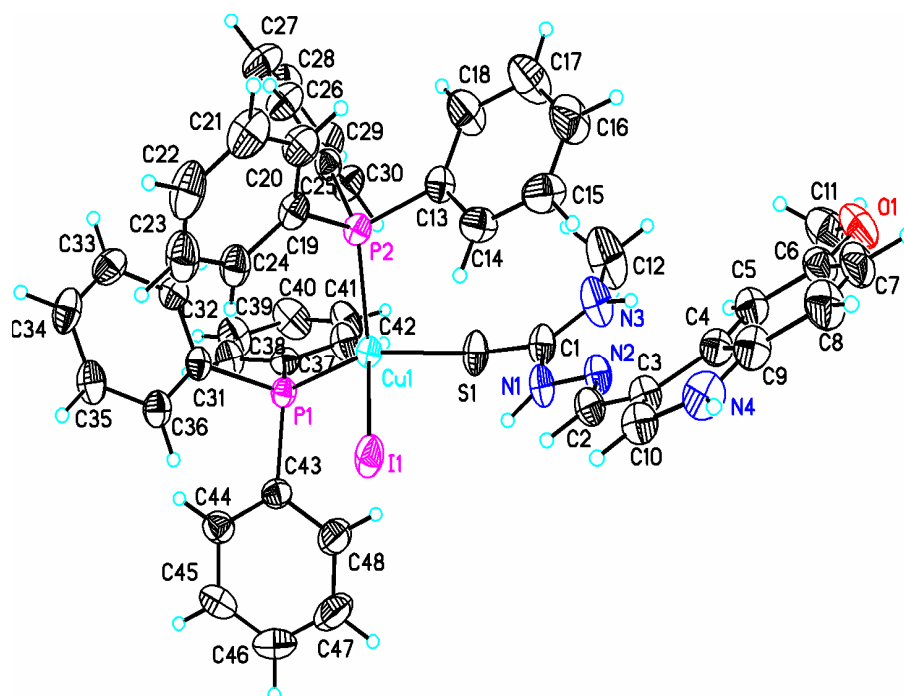


Figure-8: Structure of $[\text{CuI}(\eta^1\text{-S-5-MeOHIntsc-N-Me})(\text{Ph}_3\text{P})_2]$ **19** with numbering scheme.

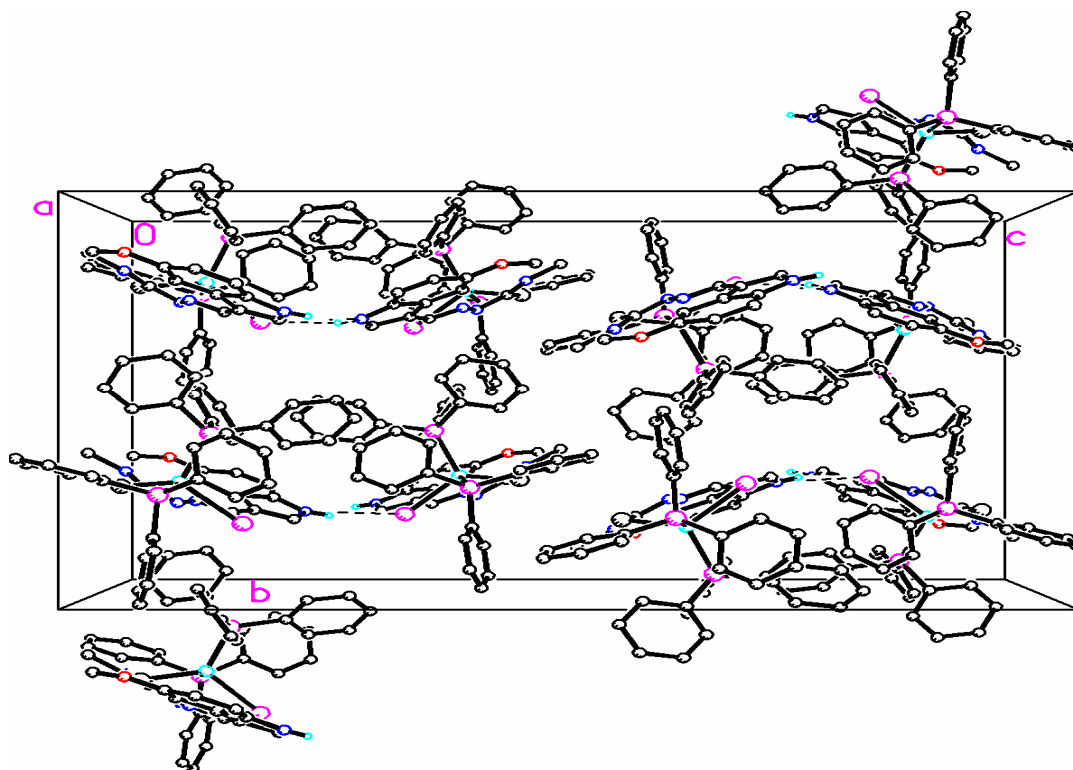


Figure-8a: Packing Diagram of $[\text{CuI}(\eta^1\text{-S-5-MeOHIntsc-N-Me})(\text{Ph}_3\text{P})_2]$ **19**.

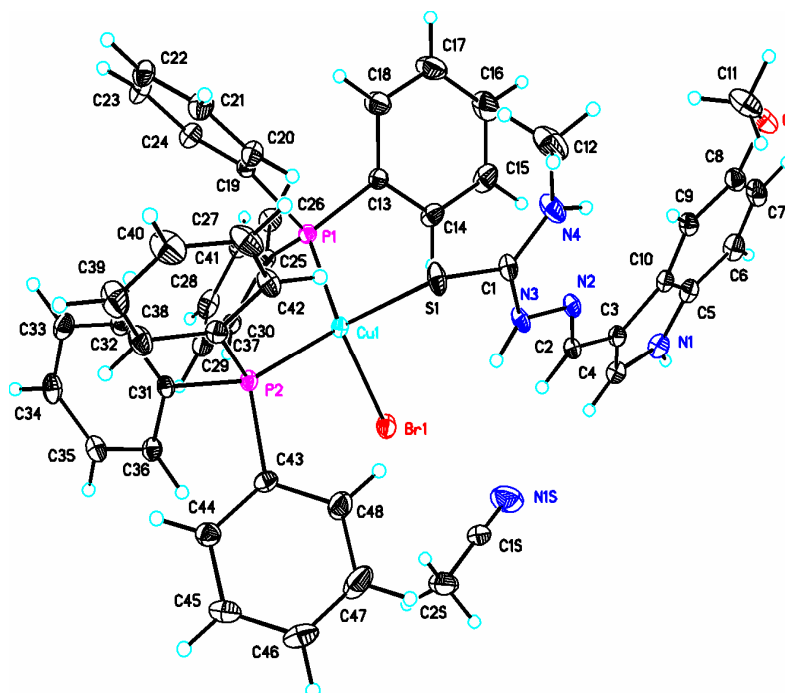


Figure-9: ORTEP view of $[\text{CuBr}(\eta^1\text{-S-5-MeOHIntsc-N-Me})(\text{Ph}_3\text{P})_2].\text{CH}_3\text{CN}$ **20** with numbering scheme.

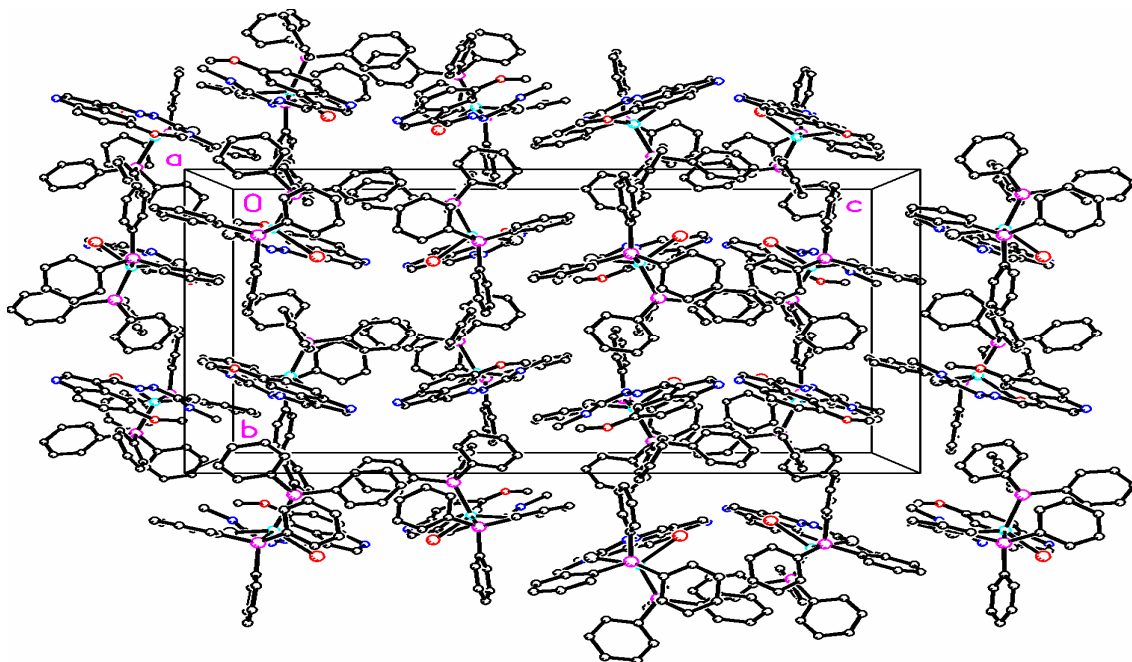


Figure-9a: Packing Diagram of $[\text{CuBr}(\eta^1\text{-S-5-MeOHIntsc-N-Me})(\text{Ph}_3\text{P})_2]\cdot\text{CH}_3\text{CN}$ **20**.

5.1.6 Structure of dimers (**13** and **14**):

Complex $[\text{Cu}_2(\mu_2\text{-I})_2(\text{HIntsc-N-Me})_2(\text{Ph}_3\text{P})_2]$ **13** and $[\text{Cu}_2(\mu_2\text{-Br})_2(\text{HIntsc-N-Me})_2(\text{Ph}_3\text{P})_2]$ **14** crystallized in monoclinic crystal system with space group $P2_1/c$. The structure of $[\text{Cu}_2(\mu_2\text{-I})_2(\text{HIntsc-N-Me})_2(\text{Ph}_3\text{P})_2]$ **13** and $[\text{Cu}_2(\mu_2\text{-Br})_2(\text{HIntsc-N-Me})_2(\text{Ph}_3\text{P})_2]$ **14** is a dimer. Molecular structure of these complexes are given in Figure-10(**13**), 11(**14**), packing diagrams of the complexes are given in Figure-10a(**13**), 11a(**14**), crystallographic data and important bond parameters are given in Table-19 (**13**, **14**) and Table-20(**13**), 21(**14**).

In halogen bridged dimers $[\text{Cu}_2(\mu_2\text{-I})_2(\text{HIntsc-N-Me})_2(\text{Ph}_3\text{P})_2]$ **13**, and $[\text{Cu}_2(\mu_2\text{-Br})_2(\text{HIntsc-N-Me})_2(\text{Ph}_3\text{P})_2]$ **14** Cu atom is bonded to one atom of thiosemicarbazones, one terminal P atom from triphenylphosphine, and two halogen atoms with central kernel, $\text{Cu}_2(\mu_2\text{-X})_2\text{Cu}$ {X = I(**13**), Br(**14**)} the two tetrahedra share halogen, halogen edge. PPh_3 and S bonded thiosemicarbazones ligands occupy trans orientation across the central kernel. The Cu–X bond distance appears at {2.6892(5), 2.7363(8) Å} (X = I, **13**) and {2.5425(5) 2.5892(5)} (X = Br, **14**). In iodo bridged dimer, the unequal Cu–I bond distance, {2.6892(5),

2.7363(8) Å} forms parallelogram of [Cu₂(μ₂-I)₂ core, similar to other iodo-bridged dimeric or polymeric complexes[88]. The Cu–I bond distance in both the cases is in conformity to Cu–I bond distances {2.6797(6) [Cu₂(μ₂-I)₂(Hftsc)₂(Ph₃P)₂ (Hftsc)] , and 2.644(2) Cu₂I₂(η²-S-Hptsc)(Ph₃P)₂] (Hftsc = furanaldehyde thiosemicarbazone, Hptsc = pyrrole-2-carbaldehyde thiosemicarbazone)}[89]. Cu–S bond distances are 2.2998 Å and 2.2908 Å in complex **13** and **14** respectively, which is longer in comparison to free ligand 1.6957 Å. These distances are much longer than, 2.240(1) and 2.251(1) Å in (Cu₃S₃) rings of hexanuclear cluster [Cu₆(Hstsc)₆] {Hstsc = salicaldehyde thiosemicarbazone –N², S- bridging-cum (μ₂-S)-bridging anionic ligand}[8]. The Cu-S bond distances in complex **13** and **14** are shorter than in monomers, 2.3274-2.3924 Å and are smaller to terminal Cu–S distance, {2.344 Å Cu₂(μ₂-I)₂(Ph₃PS)₂(MeCN)₂] [90], 2.3401(9) [Cu₂(μ₂-I)₂(Hftsc)₂(Ph₃P)₂] and 2.331(4) Cu₂I₂(η²-S-Hptsc)(Ph₃P)₂][89]. The geometry around each Cu in dimers is distorted tetrahedral as the bond angles around Cu are in range 80-118° (**13**, **14**). The Cu–X–Cu bond angles are at, ca. 80°(**13**) and 85°(**14**) while X-Cu–X angle at ca. 99°(**13**) 94°(**14**). The Cu···Cu separation in complexes **13** and **14** is 3.521 Å and 3.480 Å respectively. These Cu···Cu separations are lesser compared to that of 2.9808(8) in [Cu₂(μ₂-I)₂(Hftsc)₂(Ph₃P)₂][89], 3.0543(11) Å in [Cu₂(μ₂-Br)₂(η¹-S-Hbtsc)₂(Ph₃P)₂][21], 3.226(6) Å within 6 membered rings (Cu₃S₃) of [Cu(Hstsc)₆], 2.850(2) Å between rings {Hstsc = anion of 2-salicyldehyde thiosemicarbazone-N, S-bridging-cum-(μ₂-S)– bridging ligand}[91].

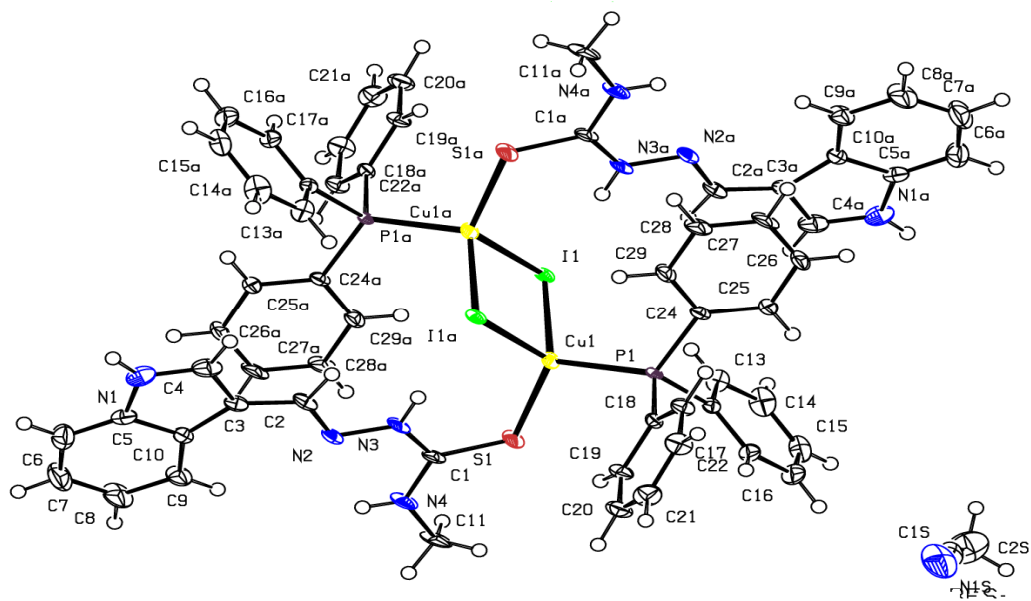


Figure 10: ORTEP view of $[\text{Cu}_2(\mu_2\text{-I})_2(\text{HIntsc-N-Me})_2(\text{Ph}_3\text{P})_2]$ **13** with numbering scheme.

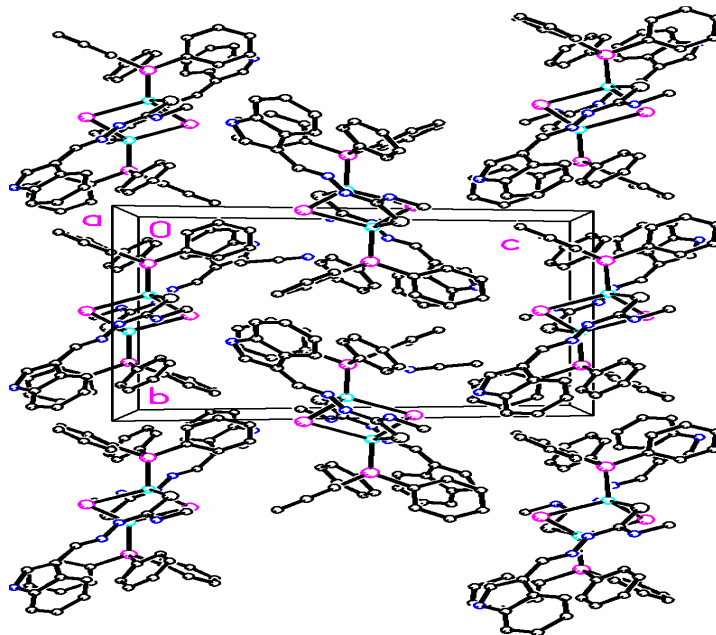


Figure-10a: Packing Diagram of $[\text{Cu}_2(\mu_2\text{-I})_2(\text{HIntsc-N-Me})_2(\text{Ph}_3\text{P})_2]$ **13**.

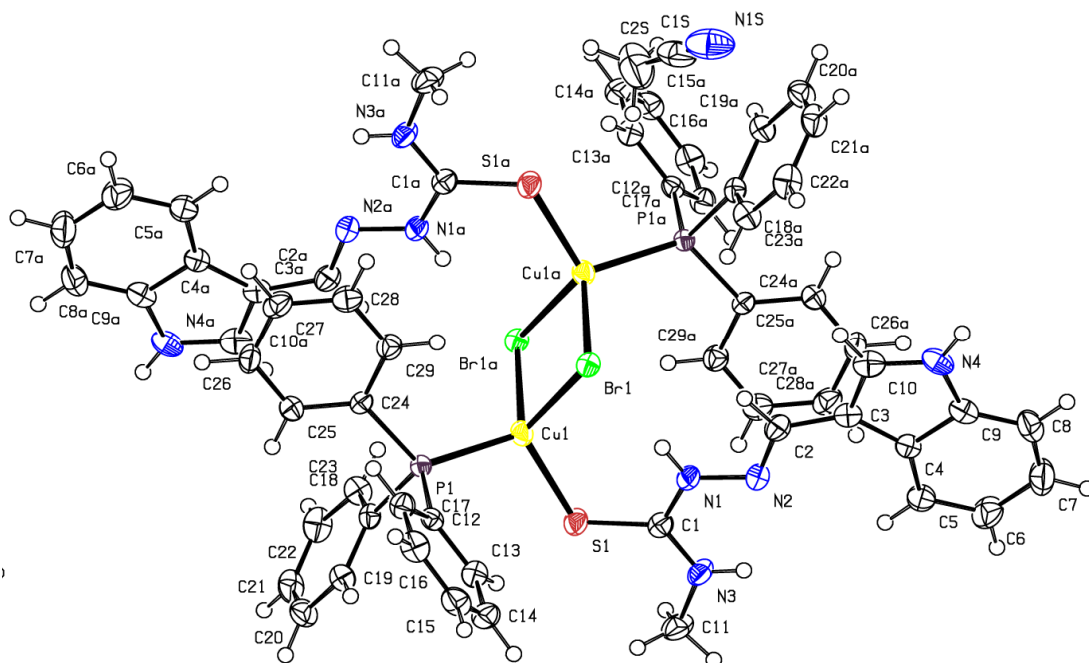


Figure-11: ORTEP view of $[\text{Cu}_2(\mu_2\text{-Br})_2(\text{HIntsc-N-Me})_2(\text{Ph}_3\text{P})_2]$ **14** with numbering scheme.

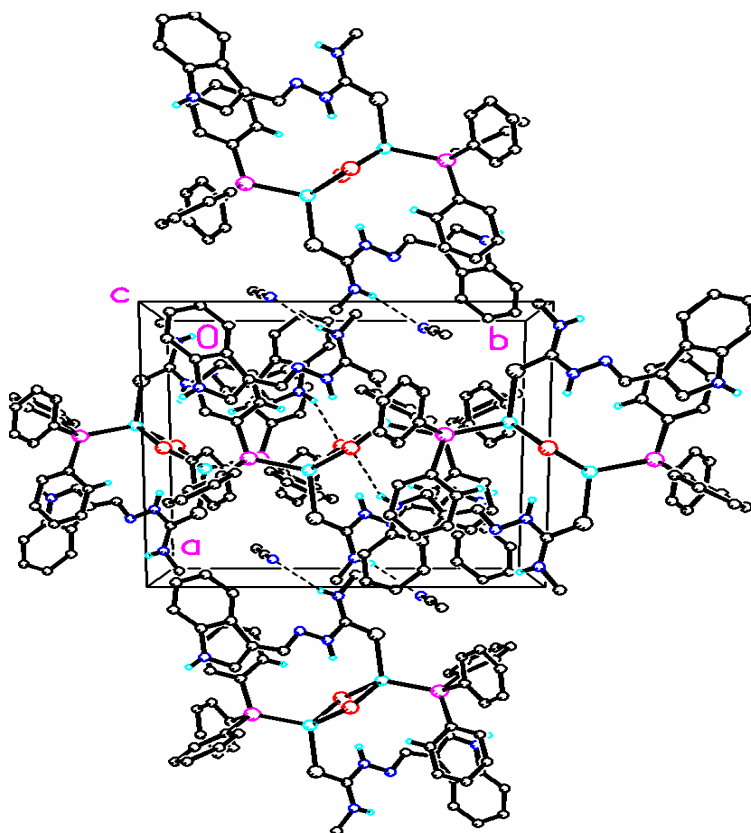


Figure-11a: Packing Diagram of $[\text{Cu}_2(\mu_2\text{-Br})_2(\text{HIntsc-N-Me})_2(\text{Ph}_3\text{P})_2]$ **14**.

Table -12: Crystallographic data for HIntsc-N¹-Me (H²L).

Empirical formula	C ₁₁ H ₁₂ N ₄ S
Formula weight	232.31
Temperature/K	173(2)
Crystal system	Monoclinic
Space group	P2 ₁ /c
a/Å	13.3962(4)
b/Å	5.12889(14)
c/Å	16.1014(4)
α/°	90.00
β/°	101.517(3)
γ/°	90.00
Volume/Å ³	1084.02(5)
Z	4
ρ _{calc} /g/cm ³	1.423
μ/mm ⁻¹	2.457
F(000)	488.0
Crystal size/mm ³	0.52 × 0.4 × 0.34
Radiation	CuKα (λ = 1.54184)
2θ range for data collection/°	6.74 to 142.5
Index ranges	-16 ≤ h ≤ 15, -4 ≤ k ≤ 6, -14 ≤ l ≤ 19
Reflections collected	3718
Independent reflections	2067 [R _{int} = 0.0217, R _{sigma} = 0.0266]
Data/restraints/parameters	2067/0/146
Goodness-of-fit on F ²	1.053
Final R indexes [I >= 2σ (I)]	R ₁ = 0.0399, wR ₂ = 0.1086
Final R indexes [all data]	R ₁ = 0.0424, wR ₂ = 0.1109
Largest diff. peak/hole / e Å ⁻³	0.26/-0.34

Table -13: Bond distance (Å) and bond angles (°) for HIntsc-N¹-Me (H²L).

Bond Length (Å) H ² L			
S(1) – C(1)	1.6957(16)	C(3) – C(4)	1.440(2)
N(1) – N(2)	1.3807(19)	C(4) – C(5)	1.445(2)
N(1) – C(3)	1.285(2)	C(4) – C(11)	1.381(2)
N(2) – H(2)	0.8800	C(5) – C(6)	1.396(2)
N(2) – C(1)	1.346(2)	C(5) – C(10)	1.415(2)
N(3) – H(3)	0.8800	C(6) – H(6)	0.9500
N(3) – C(1)	1.333(2)	C(6) – C(7)	1.386(2)
N(3) – C(2)	1.451(2)	C(7) – H(7)	0.9500
N(4) – H(4)	0.8800	C(7) – C(8)	1.402(3)
N(4) – C(10)	1.381(2)	C(8) – H(8)	0.9500
N(4) – C(11)	1.356(2)	C(8) – C(9)	1.381(3)
C(2) – H(2A)	0.9800	C(9) – H(9)	0.9500
C(2) – H(2B)	0.9800	C(9) – C(10)	1.391(3)
C(2) – H(2C)	0.9800	C(11) – H(11)	0.9500
C(3) – H(3A)	0.9500		
Bond Angle (°) H ² L			
C(3) – N(1) – N(2)	116.05(14)	C(11) – C(4) – C(3)	124.82(16)
N(1) – N(2) – H(2)	120.5	C(11) – C(4) – C(5)	106.46(14)
C(1) – N(2) – N(1)	119.02(13)	C(6) – C(5) – C(4)	134.79(15)
C(1) – N(2) – H(2)	120.5	C(6) – C(5) – C(10)	118.88(15)
C(1) – N(3) – H(3)	118.3	C(10) – C(5) – C(4)	106.33(14)
C(1) – N(3) – C(2)	123.45(15)	C(5) – C(6) – H(6)	120.4
C(2) – N(3) – H(3)	118.3	C(7) – C(6) – C(5)	119.26(17)
C(10) – N(4) – H(4)	125.3	C(7) – C(6) – H(6)	120.4
C(11) – N(4) – H(4)	125.3	C(6) – C(7) – H(7)	119.7
C(11) – N(4) – C(10)	109.49(14)	C(6) – C(7) – C(8)	120.68(18)
N(2) – C(1) – S(1)	120.71(12)	C(8) – C(7) – H(7)	119.7
N(3) – C(1) – S(1)	123.08(13)	C(7) – C(8) – H(8)	119.3
N(3) – C(1) – N(2)	116.18(14)	C(9) – C(8) – C(7)	121.47(17)

N(3) – C(2) – H(2)A	109.5	C(9) – C(8) – H(8)	119.3
N(3) – C(2) – H(2)B	109.5	C(8) – C(9) – H(9)	121.2
N(3) – C(2) – H(2)C	109.5	C(8) – C(9) – C(10)	117.54(17)
H(2)A–C(2) – H(2)B	109.5	C(10) – C(9) – H(9)	121.2
H(2) – C(2) – H(2)C	109.5	N(4) – C(10) – C(5)	107.71(15)
H(2)B– C(2) – H(2)C	109.5	N(4) – C(10) – C(9)	130.12(16)
N(1) – C(3) – H(3)A	119.5	C(9) – C(10) – C(5)	122.18(17)
N(1) – C(3) – C(4)	120.94(15)	N(4) – C(11) – C(4)	110.01(16)
C(4) – C(3) – H(3)A	119.5	N(4) – C(11) – H(11)	125.0
C(3) – C(4) – C(5)	128.67(15)	C(4) – C(11) – H(11)	125.0

Table-14: Crystallographic data of $[\text{CuCl}(\eta^1\text{-S-Hintsc})(\text{Ph}_3\text{P})_2]$ (**12**).

Empirical formula	$\text{C}_{46}\text{H}_{42}\text{ClCuN}_4\text{OP}_2\text{S}$
Formula weight	859.82
Temperature/K	173(2)
Crystal system	Monoclinic
Space group	$\text{P}2_1/\text{c}$
a/Å	17.4138(5)
b/Å	13.1467(4)
c/Å	20.1767(6)
$\alpha/^\circ$	90
$\beta/^\circ$	92.207(3)
$\gamma/^\circ$	90
Volume/Å ³	4615.7(2)
Z	4
$\rho_{\text{calc}}/\text{g}/\text{cm}^3$	1.237
μ/mm^{-1}	0.683
F(000)	1784.0
Crystal size/mm ³	0.54 × 0.51 × 0.39

Radiation	MoK α ($\lambda = 0.71073$)
2 Θ range for data collection/ $^{\circ}$	6.302 to 65.662
Index ranges	$-24 \leq h \leq 26$, $-19 \leq k \leq 14$, $-26 \leq l \leq 28$
Reflections collected	35506
Independent reflections	15292 [$R_{\text{int}} = 0.0305$, $R_{\text{sigma}} = 0.0488$]
Data/restraints/parameters	15292/0/508
Goodness-of-fit on F^2	1.072
Final R indexes [$I \geq 2\sigma(I)$]	$R_1 = 0.0477$, $wR_2 = 0.1118$
Final R indexes [all data]	$R_1 = 0.0762$, $wR_2 = 0.1227$
Largest diff. peak/hole / $e \text{ \AA}^{-3}$	0.59/-0.36

Cu(1) – C(11)	2.4301(5)	C(15) – C(16)	1.399(3)
Cu(1) – S(1)	2.3893(5)	C(17) – C(18)	1.397(2)
Cu(1) – P(1)	2.2704(5)	C(17) – C(22)	1.384(3)
Cu(1) – P(2)	2.2787(5)	C(18) – C(19)	1.382(3)
S(1) – C(1)	1.700(2)	C(19) – C(20)	1.377(3)
P(1) – C(11)	1.8264(18)	C(20) – C(21)	1.388(3)
P(1) – C(17)	1.8229(19)	C(21) – C(22)	1.386(3)
P(1) – C(23)	1.8205(19)	C(23) – C(24)	1.387(3)
P(2) – C(29)	1.8249(18)	C(23) – C(28)	1.382(3)
P(2) – C(35)	1.8345(19)	C(24) – C(25)	1.385(4)
P(2) – C(41)	1.8288(19)	C(25) – C(26)	1.366(4)
N(1) – N(2)	1.391(2)	C(26) – C(27)	1.369(3)
N(1) – C(2)	1.287(3)	C(27) – C(28)	1.391(3)
N(2) – C(1)	1.329(2)	C(29) – C(30)	1.393(3)
N(3) – C(1)	1.331(3)	C(29) – C(34)	1.392(2)
N(4) – C(4)	1.356(3)	C(30) – C(31)	1.384(3)
N(4) – C(10)	1.375(3)	C(31) – C(32)	1.387(3)

C(2) – C(3)	1.431(3)	C(32) – C(33)	1.381(3)
C(3) – C(4)	1.376(3)	C(33) – C(34)	1.388(3)
C(3) – C(5)	1.436(3)	C(35) – C(36)	1.383(3)
C(5) – C(6)	1.395(3)	C(35) – C(40)	1.389(2)
C(5) – C(10)	1.419(3)	C(36) – C(37)	1.382(4)
C(6) – C(7)	1.379(3)	C(37) – C(38)	1.388(4)
C(7) – C(8)	1.403(4)	C(38) – C(39)	1.379(3)
C(8) – C(9)	1.372(4)	C(39) – C(40)	1.385(3)
C(9) – C(10)	1.381(3)	C(41) – C(42)	1.375(3)
C(11) – C(12)	1.392(3)	C(41) – C(46)	1.385(3)
C(11) – C(16)	1.382(3)	C(42) – C(43)	1.392(4)
C(12) – C(13)	1.392(3)	C(43) – C(44)	1.370(4)
C(13) – C(14)	1.365(4)	C(44) – C(45)	1.357(4)
C(14) – C(15)	1.373(4)	C(45) – C(46)	1.376(3)
Bond Angles (°)(12)			
S(1) – Cu(1) – C(11)	111.577(19)	C(14) – C(13) – C(12)	120.4(2)
P(1) – Cu(1) – C(11)	110.097(18)	C(13) – C(14) – C(15)	119.9(2)
P(1) – Cu(1) – S(1)	103.77(2)	C(14) – C(15) – C(16)	120.3(2)
P(1) – Cu(1) – P(2)	121.096(19)	C(11) – C(16) – C(15)	120.4(2)
P(2) – Cu(1) – C(11)	101.640(19)	C(18) – C(17) – P(1)	118.46(15)
P(2) – Cu(1) – S(1)	108.780(19)	C(22) – C(17) – P(1)	123.23(14)
C(1) – S(1) – Cu(1)	111.72(7)	C(22) – C(17) – C(18)	118.26(18)
C(11) – P(1) – Cu(1)	116.01(7)	C(19) – C(18) – C(17)	120.87(19)
C(17) – P(1) – Cu(1)	112.01(6)	C(20) – C(19) – C(18)	120.22(18)
C(17) – P(1) – C(11)	103.84(8)	C(19) – C(20) – C(21)	119.7(2)
C(23) – P(1) – Cu(1)	118.45(7)	C(22) – C(21) – C(20)	119.9(2)
C(23) – P(1) – C(11)	101.33(9)	C(17) – C(22) – C(21)	121.01(19)
C(23) – P(1) – C(17)	103.37(9)	C(24) – C(23) – P(1)	117.26(16)
C(29) – P(2) – Cu(1)	116.08(6)	C(28) – C(23) – P(1)	124.84(15)

C(29) – P(2) – C(35)	104.30(8)	C(28) – C(23) – C(24)	117.78(19)
C(29) – P(2) – C(41)	101.80(8)	C(25) – C(24) – C(23)	121.4(2)
C(35) – P(2) – Cu(1)	113.34(6)	C(26) – C(25) – C(24)	119.9(2)
C(41) – P(2) – Cu(1)	117.12(6)	C(25) – C(26) – C(27)	119.9(2)
C(41) – P(2) – C(35)	102.34(9)	C(26) – C(27) – C(28)	120.3(2)
C(2) – N(1) – N(2)	113.68(17)	C(23) – C(28) – C(27)	120.7(2)
C(1) – N(2) – N(1)	120.15(16)	C(30) – C(29) – P(2)	120.56(13)
C(4) – N(4) – C(10)	109.28(18)	C(34) – C(29) – P(2)	120.99(14)
N(2) – C(1) – S(1)	120.56(15)	C(34) – C(29) – C(30)	118.26(17)
N(2) – C(1) – N(3)	116.80(18)	C(31) – C(30) – C(29)	120.86(18)
N(3) – C(1) – S(1)	122.63(15)	C(30) – C(31) – C(32)	120.3(2)
N(1) – C(2) – C(3)	123.13(19)	C(33) – C(32) – C(31)	119.46(19)
C(2) – C(3) – C(5)	130.65(18)	C(32) – C(33) – C(34)	120.25(18)
C(4) – C(3) – C(2)	122.2(2)	C(33) – C(34) – C(29)	120.83(18)
C(4) – C(3) – C(5)	106.97(19)	C(36) – C(35) – P(2)	117.00(15)
N(4) – C(4) – C(3)	109.9(2)	C(36) – C(35) – C(40)	118.67(19)
C(6) – C(5) – C(3)	135.41(19)	C(40) – C(35) – P(2)	124.25(15)
C(6) – C(5) – C(10)	118.63(19)	C(37) – C(36) – C(35)	120.4(2)
C(10) – C(5) – C(3)	105.92(18)	C(36) – C(37) – C(38)	120.8(3)
C(7) – C(6) – C(5)	118.6(2)	C(39) – C(38) – C(37)	119.0(2)
C(6) – C(7) – C(8)	121.5(2)	C(38) – C(39) – C(40)	120.1(2)
C(9) – C(8) – C(7)	121.2(2)	C(39) – C(40) – C(35)	120.93(19)
C(8) – C(9) – C(10)	117.5(2)	C(42) – C(41) – P(2)	120.29(16)
N(4) – C(10) – C(5)	107.90(18)	C(42) – C(41) – C(46)	117.73(19)
N(4) – C(10) – C(9)	129.5(2)	C(46) – C(41) – P(2)	121.93(15)
C(9) – C(10) – C(5)	122.6(2)	C(41) – C(42) – C(43)	120.7(2)
C(12) – C(11) – P(1)	123.00(15)	C(44) – C(43) – C(42)	120.3(3)
C(16) – C(11) – P(1)	118.53(15)	C(45) – C(44) – C(43)	119.4(2)
C(16) – C(11) – C(12)	118.47(18)	C(44) – C(45) – C(46)	120.6(2)

C(11) – C(12) – C(13)	120.5(2)	C(45) – C(46) – C(41)	121.2(2)
-----------------------	----------	-----------------------	----------

Table-16: Crystallographic data of [CuI(η^1 -S-5-MeOHIntsc-N-Me)(Ph₃P)₂]**19** and [CuBr(η^1 -S-5-MeOHIntsc-N-Me)(Ph₃P)₂].CH₃CN **20**.

	19	20
Empirical formula	C ₄₈ H ₄₄ CuIN ₄ OP ₂ S	C ₅₀ H ₄₇ BrCuN ₅ OP ₂ S
Formula weight	977.31	971.37
Temperature/K	173(2)	173(2)
Crystal system	Orthorhombic	Orthorhombic
Space group	Pbca	Pbca
a/Å	17.3113(2)	17.19267(16)
b/Å	17.8423(2)	17.96952(17)
c/Å	30.8800(4)	30.4528(3)
α /°	90.00	90
β /°	90.00	90
γ /°	90.00	90
Volume/Å ³	9538.1(2)	9408.22(16)
Z	8	8
ρ_{calc} /cm ³	1.361	1.372
μ /mm ⁻¹	7.066	3.035
F(000)	3968.0	4000.0
Crystal size/mm ³	0.38 × 0.33 × 0.11	0.48 × 0.32 × 0.22
Radiation	CuK α (λ = 1.54184)	CuK α (λ = 1.54184)
2 Θ range for data collection/°	7.66 to 142.76	7.686 to 142.866
Index ranges	-13 ≤ h ≤ 21, -21 ≤ k ≤ 21, -37 ≤ l ≤ 37	-21 ≤ h ≤ 20, -15 ≤ k ≤ 21, -37 ≤ l ≤ 34
Reflections collected	82420	76167
Independent reflections	9220 [R _{int} = 0.0636, R _{sigma} =	9074 [R _{int} = 0.0494, R _{sigma} =

	0.0260]	0.0212]
Data/restraints/parameters	9220/0/525	9074/0/553
Goodness-of-fit on F^2	1.090	1.081
Final R indexes [$I \geq 2\sigma(I)$]	$R_1 = 0.0514$, $wR_2 = 0.1286$	$R_1 = 0.0408$, $wR_2 = 0.1010$
Final R indexes [all data]	$R_1 = 0.0557$, $wR_2 = 0.1322$	$R_1 = 0.0446$, $wR_2 = 0.1040$
Largest diff. peak/hole / $e \text{ \AA}^{-3}$	1.92/-0.93	0.74/-0.48

Table 17: Bond Length (\AA) 19.

I(1) – Cu(1)	2.6807(6)	C(16) – C(17)	1.370(7)
Cu(1) – S(1)	2.3698(11)	C(17) – C(18)	1.391(7)
Cu(1) – P(1)	2.2736(11)	C(19) – C(20)	1.381(6)
Cu(1) – P(2)	2.2987(11)	C(19) – C(24)	1.404(6)
S(1) – C(1)	1.706(4)	C(20) – C(21)	1.393(6)
P(1) – C(31)	1.826(4)	C(21) – C(22)	1.387(8)
P(1) – C(37)	1.829(4)	C(22) – C(23)	1.376(8)
P(1) – C(43)	1.837(4)	C(23) – C(24)	1.378(6)
P(2) – C(13)	1.825(4)	C(25) – C(26)	1.382(6)
P(2) – C(19)	1.830(4)	C(25) – C(30)	1.383(5)
P(2) – C(25)	1.836(4)	C(26) – C(27)	1.394(6)
O(1) – C(6)	1.377(6)	C(27) – C(28)	1.370(7)
O(1) – C(11)	1.418(7)	C(28) – C(29)	1.376(7)
N(1) – N(2)	1.389(4)	C(29) – C(30)	1.386(6)
N(1) – C(1)	1.335(5)	C(31) – C(32)	1.387(5)
N(2) – C(2)	1.275(5)	C(31) – C(36)	1.394(5)
N(3) – C(1)	1.315(6)	C(32) – C(33)	1.388(6)
N(3) – C(12)	1.440(6)	C(33) – C(34)	1.382(7)
N(4) – C(9)	1.380(6)	C(34) – C(35)	1.378(7)
N(4) – C(10)	1.356(6)	C(35) – C(36)	1.390(6)
C(2) – C(3)	1.433(6)	C(37) – C(38)	1.391(6)

C(3) – C(4)	1.453(6)	C(37) – C(42)	1.389(6)
C(3) – C(10)	1.370(6)	C(38) – C(39)	1.381(6)
C(4) – C(5)	1.401(6)	C(39) – C(40)	1.378(7)
C(4) – C(9)	1.407(6)	C(40) – C(41)	1.374(7)
C(5) – C(6)	1.382(6)	C(41) – C(42)	1.388(6)
C(6) – C(7)	1.420(7)	C(43) – C(44)	1.390(6)
C(7) – C(8)	1.355(8)	C(43) – C(48)	1.389(6)
C(8) – C(9)	1.389(7)	C(44) – C(45)	1.392(6)
C(13) – C(14)	1.388(6)	C(45) – C(46)	1.370(7)
C(13) – C(18)	1.386(6)	C(46) – C(47)	1.385(8)
C(14) – C(15)	1.376(7)	C(47) – C(48)	1.390(7)
C(15) – C(16)	1.374(8)		
Bond Angle for (°)19			
S(1) – Cu(1) – I(1)	110.74(3)	C(18) – C(13) – C(14)	118.0(4)
P(1) – Cu(1) – I(1)	104.24(3)	C(15) – C(14) – C(13)	121.0(4)
P(1) – Cu(1) – S(1)	111.21(4)	C(16) – C(15) – C(14)	120.4(4)
P(1) – Cu(1) – P(2)	117.35(4)	C(17) – C(16) – C(15)	119.7(5)
P(2) – Cu(1) – I(1)	107.22(3)	C(16) – C(17) – C(18)	120.0(5)
P(2) – Cu(1) – S(1)	106.01(4)	C(13) – C(18) – C(17)	120.7(4)
C(1) – S(1) – Cu(1)	107.73(13)	C(20) – C(19) – P(2)	123.1(3)
C(31) – P(1) – Cu(1)	110.62(12)	C(20) – C(19) – C(24)	119.0(4)
C(31) – P(1) – C(37)	103.33(17)	C(24) – C(19) – P(2)	117.9(3)
C(31) – P(1) – C(43)	104.80(18)	C(19) – C(20) – C(21)	120.9(5)
C(37) – P(1) – Cu(1)	118.89(13)	C(22) – C(21) – C(20)	119.3(5)
C(37) – P(1) – C(43)	100.98(17)	C(23) – C(22) – C(21)	120.3(4)
C(43) – P(1) – Cu(1)	116.50(13)	C(22) – C(23) – C(24)	120.5(5)
C(13) – P(2) – Cu(1)	115.38(13)	C(23) – C(24) – C(19)	120.1(4)
C(13) – P(2) – C(19)	100.92(18)	C(26) – C(25) – P(2)	123.9(3)
C(13) – P(2) – C(25)	104.97(17)	C(26) – C(25) – C(30)	118.7(4)

C(19) – P(2) – Cu(1)	118.69(14)	C(30) – C(25) – P(2)	117.2(3)
C(19) – P(2) – C(25)	105.01(17)	C(25) – C(26) – C(27)	120.4(4)
C(25) – P(2) – Cu(1)	110.45(13)	C(28) – C(27) – C(26)	120.1(4)
C(6) – O(1) – C(11)	116.9(4)	C(27) – C(28) – C(29)	120.1(4)
C(1) – N(1) – N(2)	118.6(3)	C(28) – C(29) – C(30)	119.8(4)
C(2) – N(2) – N(1)	116.0(3)	C(25) – C(30) – C(29)	120.9(4)
C(1) – N(3) – C(12)	126.2(4)	C(32) – C(31) – P(1)	120.2(3)
C(10) – N(4) – C(9)	109.0(3)	C(32) – C(31) – C(36)	118.2(3)
N(1) – C(1) – S(1)	119.6(3)	C(36) – C(31) – P(1)	121.4(3)
N(3) – C(1) – S(1)	122.9(3)	C(31) – C(32) – C(33)	121.1(4)
N(3) – C(1) – N(1)	117.5(4)	C(34) – C(33) – C(32)	120.4(4)
N(2) – C(2) – C(3)	121.3(4)	C(35) – C(34) – C(33)	119.1(4)
C(2) – C(3) – C(4)	127.6(4)	C(34) – C(35) – C(36)	120.8(4)
C(10) – C(3) – C(2)	125.7(4)	C(35) – C(36) – C(31)	120.5(4)
C(10) – C(3) – C(4)	106.5(4)	C(38) – C(37) – P(1)	122.8(3)
C(5) – C(4) – C(3)	134.0(4)	C(42) – C(37) – P(1)	118.7(3)
C(5) – C(4) – C(9)	120.1(4)	C(42) – C(37) – C(38)	118.5(4)
C(9) – C(4) – C(3)	105.8(4)	C(39) – C(38) – C(37)	120.5(4)
C(6) – C(5) – C(4)	117.8(4)	C(40) – C(39) – C(38)	120.2(4)
O(1) – C(6) – C(5)	124.2(4)	C(41) – C(40) – C(39)	120.2(4)
O(1) – C(6) – C(7)	114.9(4)	C(40) – C(41) – C(42)	119.7(4)
C(5) – C(6) – C(7)	120.8(4)	C(41) – C(42) – C(37)	120.9(4)
C(8) – C(7) – C(6)	121.7(4)	C(44) – C(43) – P(1)	123.3(3)
C(7) – C(8) – C(9)	117.9(4)	C(48) – C(43) – P(1)	117.4(3)
N(4) – C(9) – C(4)	108.2(4)	C(48) – C(43) – C(44)	119.2(4)
N(4) – C(9) – C(8)	130.1(4)	C(43) – C(44) – C(45)	120.5(4)
C(8) – C(9) – C(4)	121.7(4)	C(46) – C(45) – C(44)	120.0(5)
N(4) – C(10) – C(3)	110.3(4)	C(45) – C(46) – C(47)	120.0(4)
C(14) – C(13) – P(2)	117.2(3)	C(46) – C(47) – C(48)	120.5(5)

C(18) – C(13) – P(2)	124.6(3)	C(43) – C(48) – C(47)	119.9(5)
----------------------	----------	-----------------------	----------

Table-18: Bond Lengths for (Å) 20

Br(1) – Cu(1)	2.5179(4)	C(17) – C(18)	1.383(4)
Cu(1) – S(1)	2.3672(6)	C(19) – C(20)	1.395(3)
Cu(1) – P(1)	2.2944(6)	C(19) – C(24)	1.386(3)
Cu(1) – P(2)	2.2708(6)	C(20) – C(21)	1.389(3)
S(1) – C(1)	1.700(2)	C(21) – C(22)	1.382(4)
P(1) – C(13)	1.823(2)	C(22) – C(23)	1.377(4)
P(1) – C(19)	1.831(2)	C(23) – C(24)	1.391(4)
P(1) – C(25)	1.827(2)	C(25) – C(26)	1.395(3)
P(2) – C(31)	1.825(2)	C(25) – C(30)	1.395(3)
P(2) – C(37)	1.833(2)	C(26) – C(27)	1.389(4)
P(2) – C(43)	1.835(2)	C(27) – C(28)	1.385(5)
O(1) – C(8)	1.369(3)	C(28) – C(29)	1.385(4)
O(1) – C(11)	1.418(4)	C(29) – C(30)	1.382(3)
N(1) – C(4)	1.351(3)	C(31) – C(32)	1.398(3)
N(1) – C(5)	1.376(3)	C(31) – C(36)	1.393(3)
N(2) – N(3)	1.388(3)	C(32) – C(33)	1.387(3)
N(2) – C(2)	1.285(3)	C(33) – C(34)	1.387(4)
N(3) – C(1)	1.342(3)	C(34) – C(35)	1.381(4)
N(4) – C(1)	1.321(3)	C(35) – C(36)	1.388(3)
N(4) – C(12)	1.448(4)	C(37) – C(38)	1.394(3)
C(2) – C(3)	1.439(3)	C(37) – C(42)	1.393(3)
C(3) – C(4)	1.381(3)	C(38) – C(39)	1.382(4)
C(3) – C(10)	1.440(3)	C(39) – C(40)	1.382(4)
C(5) – C(6)	1.391(4)	C(40) – C(41)	1.373(4)
C(5) – C(10)	1.411(3)	C(41) – C(42)	1.381(4)

C(6) – C(7)	1.373(4)	C(43) – C(44)	1.393(3)
C(7) – C(8)	1.409(4)	C(43) – C(48)	1.381(4)
C(8) – C(9)	1.390(4)	C(44) – C(45)	1.381(4)
C(9) – C(10)	1.400(3)	C(45) – C(46)	1.378(5)
C(13) – C(14)	1.385(3)	C(46) – C(47)	1.373(5)
C(13) – C(18)	1.396(4)	C(47) – C(48)	1.393(4)
C(14) – C(15)	1.389(4)	N(1)S – C(1)S	1.124(4)
C(15) – C(16)	1.364(5)	C(1)S – C(2)S	1.436(4)
C(16) – C(17)	1.388(5)		
Bond Angles for (°) 20			
S(1) – Cu(1) – Br(1)	109.48(2)	C(13) – C(14) – C(15)	120.8(3)
P(1) – Cu(1) – Br(1)	106.011(19)	C(16) – C(15) – C(14)	120.4(3)
P(1) – Cu(1) – S(1)	106.87(3)	C(15) – C(16) – C(17)	119.6(3)
P(2) – Cu(1) – Br(1)	106.60(2)	C(18) – C(17) – C(16)	120.4(3)
P(2) – Cu(1) – S(1)	110.86(2)	C(17) – C(18) – C(13)	120.2(3)
P(2) – Cu(1) – P(1)	116.78(2)	C(20) – C(19) – P(1)	116.87(18)
C(1) – S(1) – Cu(1)	107.37(8)	C(24) – C(19) – P(1)	124.16(17)
C(13) – P(1) – Cu(1)	115.33(8)	C(24) – C(19) – C(20)	118.7(2)
C(13) – P(1) – C(19)	105.32(10)	C(21) – C(20) – C(19)	120.8(2)
C(13) – P(1) – C(25)	101.20(11)	C(22) – C(21) – C(20)	119.8(2)
C(19) – P(1) – Cu(1)	110.67(7)	C(23) – C(22) – C(21)	119.9(2)
C(25) – P(1) – Cu(1)	118.13(8)	C(22) – C(23) – C(24)	120.5(2)
C(25) – P(1) – C(19)	104.85(10)	C(19) – C(24) – C(23)	120.3(2)
C(31) – P(2) – Cu(1)	111.14(7)	C(26) – C(25) – P(1)	123.52(19)
C(31) – P(2) – C(37)	103.13(10)	C(30) – C(25) – P(1)	117.59(18)
C(31) – P(2) – C(43)	105.04(11)	C(30) – C(25) – C(26)	118.9(2)
C(37) – P(2) – Cu(1)	118.48(8)	C(27) – C(26) – C(25)	120.5(3)
C(37) – P(2) – C(43)	101.33(10)	C(28) – C(27) – C(26)	119.9(3)
C(43) – P(2) – Cu(1)	116.06(8)	C(29) – C(28) – C(27)	120.0(2)

C(8) – O(1) – C(11)	117.3(2)	C(30) – C(29) – C(28)	120.2(3)
C(4) – N(1) – C(5)	109.5(2)	C(29) – C(30) – C(25)	120.6(2)
C(2) – N(2) – N(3)	115.93(19)	C(32) – C(31) – P(2)	119.58(17)
C(1) – N(3) – N(2)	118.67(19)	C(36) – C(31) – P(2)	121.41(17)
C(1) – N(4) – C(12)	125.6(2)	C(36) – C(31) – C(32)	118.6(2)
N(3) – C(1) – S(1)	120.02(18)	C(33) – C(32) – C(31)	120.4(2)
N(4) – C(1) – S(1)	123.10(19)	C(32) – C(33) – C(34)	120.3(2)
N(4) – C(1) – N(3)	116.9(2)	C(35) – C(34) – C(33)	119.7(2)
N(2) – C(2) – C(3)	120.5(2)	C(34) – C(35) – C(36)	120.2(2)
C(2) – C(3) – C(10)	128.6(2)	C(35) – C(36) – C(31)	120.7(2)
C(4) – C(3) – C(2)	124.5(2)	C(38) – C(37) – P(2)	122.49(18)
C(4) – C(3) – C(10)	106.7(2)	C(42) – C(37) – P(2)	118.91(18)
N(1) – C(4) – C(3)	109.8(2)	C(42) – C(37) – C(38)	118.6(2)
N(1) – C(5) – C(6)	130.3(2)	C(39) – C(38) – C(37)	120.2(2)
N(1) – C(5) – C(10)	108.0(2)	C(38) – C(39) – C(40)	120.4(3)
C(6) – C(5) – C(10)	121.7(2)	C(41) – C(40) – C(39)	120.0(2)
C(7) – C(6) – C(5)	117.8(2)	C(40) – C(41) – C(42)	120.1(2)
C(6) – C(7) – C(8)	121.4(2)	C(41) – C(42) – C(37)	120.8(2)
O(1) – C(8) – C(7)	115.0(2)	C(44) – C(43) – P(2)	123.33(19)
O(1) – C(8) – C(9)	124.0(2)	C(48) – C(43) – P(2)	117.52(19)
C(9) – C(8) – C(7)	121.0(2)	C(48) – C(43) – C(44)	119.0(2)
C(8) – C(9) – C(10)	118.0(2)	C(45) – C(44) – C(43)	120.3(3)
C(5) – C(10) – C(3)	106.1(2)	C(46) – C(45) – C(44)	120.5(3)
C(9) – C(10) – C(3)	134.0(2)	C(47) – C(46) – C(45)	119.6(3)
C(9) – C(10) – C(5)	120.0(2)	C(46) – C(47) – C(48)	120.4(3)
C(14) – C(13) – P(1)	117.23(19)	C(43) – C(48) – C(47)	120.2(3)
C(14) – C(13) – C(18)	118.5(2)	N(1)S – C(1)S – C(2S)	178.7(4)
C(18) – C(13) – P(1)	124.18(19)		

Table-19: Crystallographic data of $[\text{Cu}_2(\mu_2\text{-I})_2(\text{HIntsc-N-Me})_2(\text{Ph}_3\text{P})_2]$ **13** $[\text{Cu}_2(\mu_2\text{-Br})_2(\text{HIntsc-N-Me})_2(\text{Ph}_3\text{P})_2]$ **14**.

	13	14
Empirical formula	$\text{C}_{62}\text{H}_{60}\text{Cu}_2\text{I}_2\text{N}_{10}\text{P}_2\text{S}_2$	$\text{C}_{62}\text{H}_{60}\text{Br}_2\text{Cu}_2\text{N}_{10}\text{P}_2\text{S}_2$
Formula weight	1452.14	1358.16
Temperature/K	173(2)	173(2)
Crystal system	monoclinic	monoclinic
Space group	$\text{P2}_1/\text{c}$	$\text{P2}_1/\text{c}$
$a/\text{\AA}$	13.4763(3)	13.3882(3)
$b/\text{\AA}$	13.5778(3)	13.6628(3)
$c/\text{\AA}$	18.0255(4)	17.6182(4)
$\alpha/^\circ$	90	90
$\beta/^\circ$	109.128(3)	109.622(3)
$\gamma/^\circ$	90	90
Volume/ \AA^3	3116.19(13)	3035.58(14)
Z	2	2
$\rho_{\text{calc}}/\text{g/cm}^3$	1.548	1.486
μ/mm^{-1}	10.101	3.926
F(000)	1456.0	1384.0
Crystal size/ mm^3	$0.36 \times 0.32 \times 0.22$	$0.25 \times 0.23 \times 0.2$
Radiation	$\text{CuK}\alpha$ ($\lambda = 1.54184$)	$\text{CuK}\alpha$ ($\lambda = 1.54184$)
2Θ range for data collection/ $^\circ$	8.328 to 142.892	8.382 to 142.958
Index ranges	$-14 \leq h \leq 16, -16 \leq k \leq 9, -21 \leq l \leq 21$	$-10 \leq h \leq 16, -16 \leq k \leq 15, -21 \leq l \leq 21$
Reflections collected	12364	12459
Independent reflections	5950 [$R_{\text{int}} = 0.0389, R_{\text{sigma}} = 0.0473$]	5815 [$R_{\text{int}} = 0.0341, R_{\text{sigma}} = 0.0518$]
Data/restraints/parameters	5950/0/363	5815/0/364

Goodness-of-fit on F^2	1.053	1.030
Final R indexes [$I \geq 2\sigma(I)$]	$R_1 = 0.0415$, $wR_2 = 0.1031$	$R_1 = 0.0353$, $wR_2 = 0.0861$
Final R indexes [all data]	$R_1 = 0.0450$, $wR_2 = 0.1066$	$R_1 = 0.0439$, $wR_2 = 0.0909$
Largest diff. peak/hole / $e \text{ \AA}^{-3}$	1.91/-2.27	0.58/-0.39

Table-20: Bond Lengths for (\AA) 13.

I(1) – Cu(1) ¹	2.6892(5)	C(8) – C(9)	1.371(6)
I(1) – Cu(1)	2.7363(6)	C(9) – C(10)	1.407(5)
Cu(1) – I(1) ¹	2.6892(5)	C(12) – C(13)	1.400(5)
Cu(1) – S(1)	2.2998(9)	C(12) – C(17)	1.397(5)
Cu(1) – P(1)	2.2533(9)	C(13) – C(14)	1.390(6)
S(1) – C(1)	1.706(4)	C(14) – C(15)	1.396(7)
P(1) – C(12)	1.821(3)	C(15) – C(16)	1.379(7)
P(1) – C(18)	1.829(3)	C(16) – C(17)	1.398(6)
P(1) – C(24)	1.828(3)	C(18) – C(19)	1.396(5)
N(1) – C(4)	1.354(6)	C(18) – C(23)	1.387(5)
N(1) – C(5)	1.382(5)	C(19) – C(20)	1.394(5)
N(2) – N(3)	1.389(5)	C(20) – C(21)	1.385(6)
N(2) – C(2)	1.282(5)	C(21) – C(22)	1.387(6)
N(3) – C(1)	1.331(5)	C(22) – C(23)	1.395(5)
N(4) – C(1)	1.335(5)	C(24) – C(25)	1.395(5)
N(4) – C(11)	1.452(6)	C(24) – C(29)	1.381(5)
C(2) – C(3)	1.434(5)	C(25) – C(26)	1.401(5)
C(3) – C(4)	1.377(5)	C(26) – C(27)	1.378(6)
C(3) – C(10)	1.445(5)	C(27) – C(28)	1.382(6)
C(5) – C(6)	1.374(6)	C(28) – C(29)	1.397(5)
C(5) – C(10)	1.413(5)	N(1)S – C(1)S	1.128(8)
C(6) – C(7)	1.382(7)	(C(1)S – C(2)S)	1.442(9)
C(7) – C(8)	1.405(7)		

Bond Angles for (°) 13			
Cu(1) ¹ – I1 – Cu(1)	80.934(17)	C(9) – C(8)– C(7)	122.2(4)
I(1) ¹ – Cu(1) – I(1)	99.066(17)	C(8) – C(9)– C(10)	118.5(4)
S(1) – Cu(1) – I(1) ¹	118.58(3)	C(5) – C(10)– C(3)	106.8(3)
S(1) – Cu(1) – I(1)	107.00(3)	C(9) – C(10)– C(3)	134.9(4)
P(1) – Cu(1) – I(1) ¹	109.63(3)	C(9) – C(10)– C5)	118.2(3)
P(1) – Cu(1) – I(1)	111.30(3)	C(13) – C(12)– P(1)	117.4(3)
P(1) – Cu(1) – S(1)	110.62(4)	C(17) – C(12)– P(1)	123.8(3)
C(1) – S(1) – Cu(1)	113.94(14)	C(17) – C(12)– C(13)	118.8(3)
C(12) – P(1) – Cu(1)	115.89(11)	C(14) – C(13)– C(12)	120.6(4)
C(12) – P(1) – C(18)	104.17(16)	C(13) – C(14)– C(15)	119.9(4)
C(12) – P(1) – C(24)	103.15(16)	C(16) – C(15)– C(14)	120.0(4)
C(18) – P(1) – Cu(1)	109.99(11)	C(15) – C(16)– C(17)	120.3(4)
C(24) – P(1) – Cu(1)	118.55(11)	C(12) – C(17)– C(16)	120.4(4)
C(24) – P(1) – C(18)	103.48(15)	C(19) – C(18)– P(1)	117.9(3)
C(4) – N(1) – C(5)	109.5(3)	C(23) – C(18)– P(1)	122.7(3)
C(2) – N(2) – N(3)	113.7(3)	C(23) – C(18)– C(19)	119.4(3)
C(1) – N(3) – N(2)	121.1(3)	C(20) – C(19)– C(18)	120.2(3)
C(1) – N(4) – C(11)	123.8(4)	C(21) – C(20)– C(19)	120.0(4)
N(3) – C(1) – S(1)	120.4(3)	C(20) – C(21)– C(22)	119.9(4)
N(3) – C(1) – N(4)	117.5(4)	C(21) – C(22)– C(23)	120.1(4)
N(4) – C(1) – S(1)	122.1(3)	C(18) – C(23)– C(22)	120.3(3)
N(2) – C(2) – C(3)	122.8(3)	C(25) – C(24)– P(1)	122.9(3)
C(2) – C(3) – C(10)	130.5(3)	C(29) – C(24)– P(1)	117.6(3)
C(4) – C(3) – C(2)	123.3(3)	C(29) – C(24)– C(25)	119.5(3)
C(4) – C(3) – C(10)	106.0(3)	C(24) – C(25)– C(26)	119.7(4)
N(1) – C(4) – C(3)	110.4(3)	C(27) – C(26)– C(25)	120.1(4)
N(1) – C(5) – C(10)	107.3(3)	C(26) – C(27)– C(28)	120.3(3)
C(6) – C(5) – N(1)	129.6(4)	C(27) – C(28)– C(29)	119.7(4)

C(6) – C(5) – C(10)	123.1(4)	C(24) – C(29)– C(28)	120.7(4)
C(5) – C(6) – C(7)	117.9(4)	N(1)S – C(1)S– C(2)S	177.9(6)
C(6) – C(7) – C(8)	120.1(4)		

Table-21: Bond Lengths for (Å) **14**

Br(1) – Cu1	2.5425(5)	C(7) – C(8)	1.369(5)
Br(1) – Cu(1) ¹	2.5892(5)	C(8) – C(9)	1.386(4)
Cu(1) – Br(1) ¹	2.5892(5)	C(12) – C(13)	1.395(4)
Cu(1) – S(1)	2.2908(7)	C(12) – C(17)	1.388(4)
Cu(1) – P(1)	2.2368(7)	C(13) – C(14)	1.387(4)
S(1) – C(1)	1.711(3)	C(14) – C(15)	1.386(4)
P(1) – C(12)	1.832(2)	C(15) – C(16)	1.381(5)
P(1) – C(18)	1.826(3)	C(16) – C(17)	1.393(4)
P(1) – C(24)	1.825(2)	C(18) – C(19)	1.394(4)
N(1) – N(2)	1.385(3)	C(18) – C(23)	1.392(4)
N(1) – C(1)	1.343(4)	C(19) – C(20)	1.393(4)
N(2) – C(2)	1.289(4)	C(20) – C(21)	1.387(5)
N(3) – C(1)	1.320(3)	C(21) – C(22)	1.388(5)
N(3) – C(11)	1.455(4)	C(22) – C(23)	1.390(4)
N(4) – C(9)	1.380(4)	C(24) – C(25)	1.390(4)
N(4) – C(10)	1.355(4)	C(24) – C(29)	1.394(4)
C(2) – C(3)	1.439(4)	C(25) – C(26)	1.389(4)
C(3) – C(4)	1.440(4)	C(26) – C(27)	1.386(4)
C(3) – C(10)	1.372(4)	C(27) – C(28)	1.384(4)
C(4) – C(5)	1.403(4)	C(28) – C(29)	1.385(4)
C(4) – C(9)	1.411(4)	N(1)S – C(1S)	1.127(5)
C(5) – C(6)	1.378(4)	C(1)S – C(2S)	1.447(6)
C(6) – C(7)	1.409(5)		

Bond Angles for (°) 14			
Cu(1) – Br(1) – Cu(1) ¹	85.382(15)	C(7) – C(8) – C(9)	117.6(3)
Br(1) – Cu(1) – Br(1) ¹	94.617(15)	N(4) – C(9) – C(4)	107.3(2)
S(1) – Cu(1) – Br(1)	117.48(2)	N(4) – C(9) – C(8)	129.8(3)
S(1) – Cu(1) – Br(1) ¹	106.93(2)	C(8) – C(9) – C(4)	122.9(3)
P(1) – Cu(1) – Br(1) ¹	114.86(2)	N(4) – C(10) – C(3)	110.0(2)
P(1) – Cu(1) – Br(1)	112.81(2)	C(13) – C(12) – P(1)	117.7(2)
P(1) – Cu(1) – S(1)	109.45(3)	C(17) – C(12) – P(1)	123.0(2)
C(1) – S(1) – Cu(1)	113.42(10)	C(17) – C(12) – C(13)	119.2(2)
C(12) – P(1) – Cu(1)	110.18(8)	C(14) – C(13) – C(12)	120.4(3)
C(18) – P(1) – Cu(1)	115.86(8)	C(15) – C(14) – C(13)	119.9(3)
C(18) – P(1) – C1(2)	104.02(12)	C(16) – C(15) – C(14)	120.1(3)
C(24) – P(1) – Cu(1)	118.42(8)	C(15) – C(16) – C(17)	120.0(3)
C(24) – P(1) – C1(2)	103.49(11)	C(12) – C(17) – C(16)	120.3(3)
C(24) – P(1) – C1(8)	103.26(11)	C(19) – C(18) – P(1)	123.8(2)
C(1) – N(1) – N(2)	120.2(2)	C(23) – C(18) – P(1)	117.2(2)
C(2) – N(2) – N(1)	113.6(2)	C(23) – C(18) – C(19)	119.0(2)
C(1) – N(3) – C(11)	124.4(2)	C(20) – C(19) – C(18)	120.1(3)
C(10) – N(4) – C(9)	109.5(2)	C(21) – C(20) – C(19)	120.3(3)
N(1) – C(1) – S(1)	119.4(2)	C(20) – C(21) – C(22)	120.1(3)
N(3) – C(1) – S(1)	122.4(2)	C(21) – C(22) – C(23)	119.5(3)
N(3) – C(1) – N(1)	118.2(2)	C(22) – C(23) – C(18)	121.0(3)
N(2) – C(2) – C(3)	122.9(2)	C(25) – C(24) – P(1)	123.7(2)
C(2) – C(3) – C(4)	130.4(2)	C(25) – C(24) – C(29)	119.5(2)
C(10) – C(3) – C(2)	122.9(3)	C(29) – C(24) – P(1)	116.77(19)
C(10) – C(3) – C(4)	106.5(2)	C(26) – C(25) – C(24)	120.1(3)
C(5) – C(4) – C(3)	134.9(3)	C(27) – C(26) – C(25)	120.1(3)
C(5) – C(4) – C(9)	118.4(3)	C(28) – C(27) – C(26)	120.0(3)
C(9) – C(4) – C(3)	106.6(2)	C(27) – C(28) – C(29)	120.2(3)

C(6) – C(5) – C(4)	118.7(3)	C(28) – C(29) – C(24)	120.2(3)
C(5) – C(6) – C(7)	121.4(3)	N(1S)– C(1)S – C(2)S	177.9(4)
C(8) – C(7) – C(6)	121.0(3)		

5.1.7 Structure of silver(I) complex:

Complex $[\text{AgCl}(\eta^1\text{-S-HIntsc})(\text{Ph}_3\text{P})_2]$ **22** crystallized in monoclinic crystal system with space group $P2_1/c$. Molecular structure of this monomeric complex **22** is given in Figure-12 packing diagram of the complex is given in Figure-12a, crystallographic data and important bond parameters are given in Table-22 and Table-23.

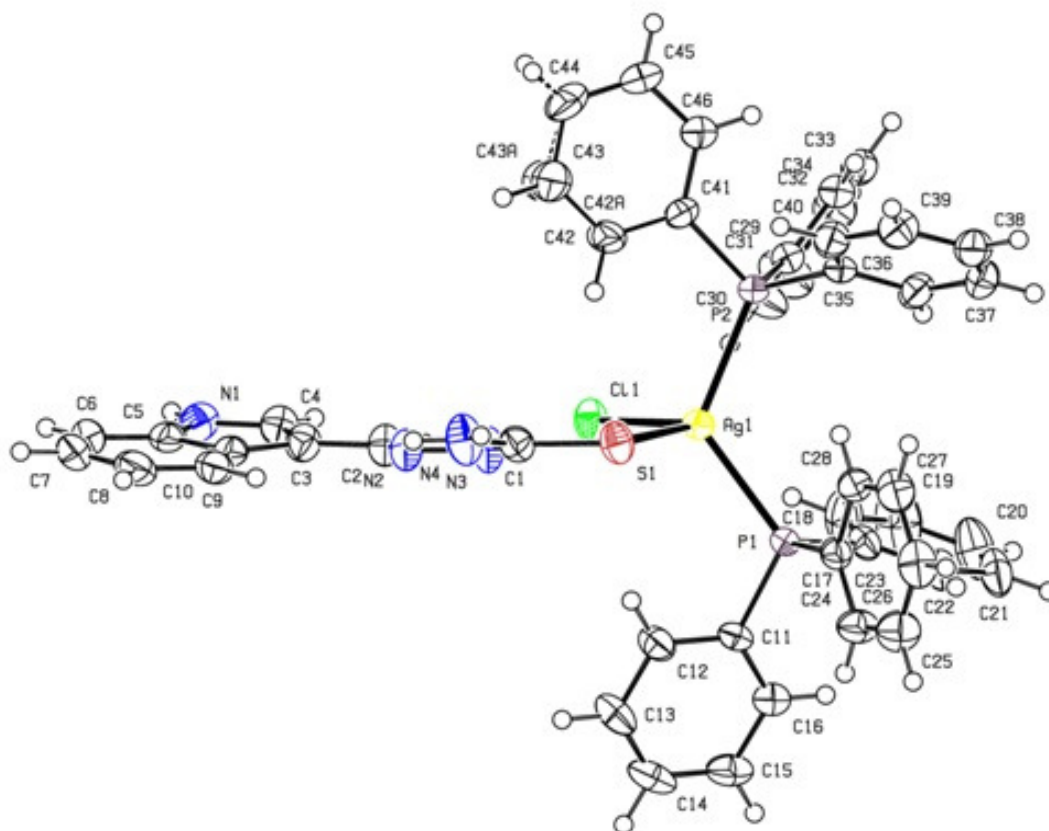


Figure-12: ORTEP view of $[\text{AgCl}(\eta^1\text{-S-HIntsc})(\text{Ph}_3\text{P})_2]$ **22** with numbering scheme.

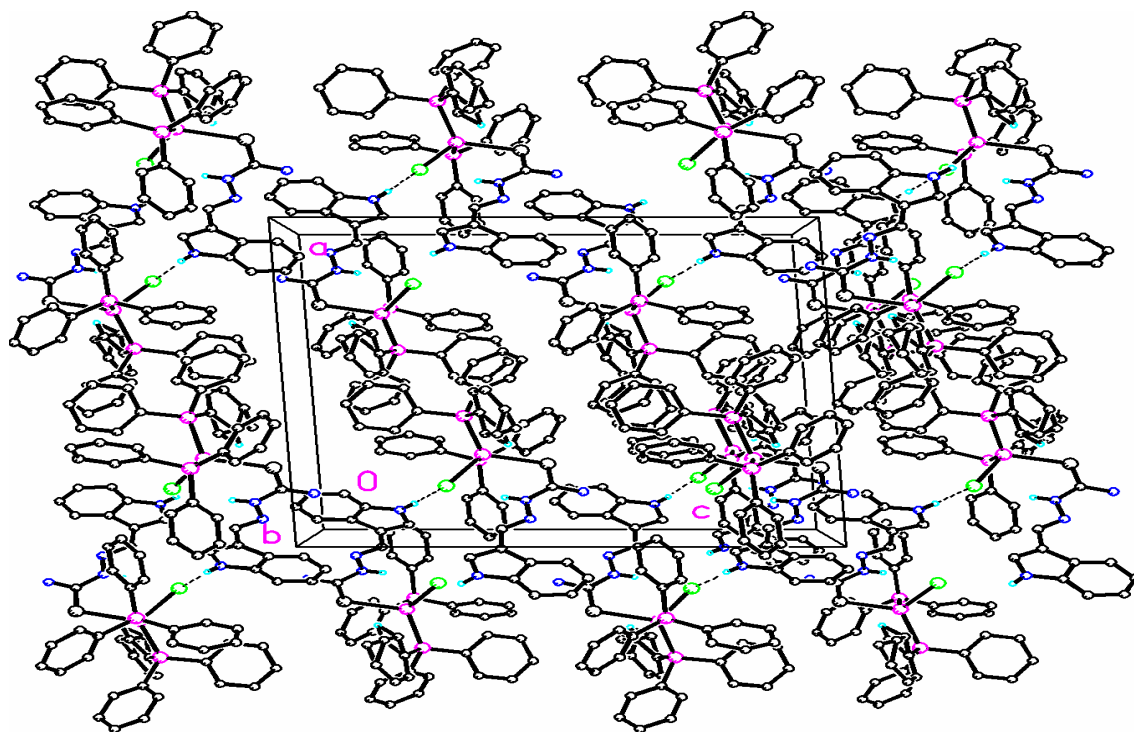


Figure-12a: Packing Diagram of $[\text{AgCl}(\eta^1\text{-S-HIntsc})(\text{Ph}_3\text{P})_2]$ **22** with numbering scheme.

In complex **22**, silver is coordinated by one chlorine, one sulphur atom of thio-ligand and two phosphorous atoms of two triphenylphosphine molecules to form tetrahedral geometry. The Ag–Cl bond distance, $\{2.6569(7) \text{ \AA}\}$ in $[\text{AgCl}(\eta^1\text{-S-HIntsc})(\text{Ph}_3\text{P})_2]$ **22** is close to the that of $\{\text{Ag–Cl}, 2.6448(7) \text{ \AA}\}$ in $[\text{AgCl}(\eta^1\text{-S-Hpytsc})(\text{Ph}_3\text{P})_2] \cdot \text{CH}_3\text{CN}$ ($\text{X} = \text{Cl}, \text{Br}$) [92] and longer than $2.595(1) \text{ \AA}$ in $[\text{Ag}(\text{Ph}_3\text{P})_2(\text{Py}_2\text{SH})\text{Cl}]$ ($\text{Py}_2\text{SH} = \text{pyridine-2-thione}$) [93]. This Ag–Cl bond distance is less than the sum of the ionic radii of Ag^+ and Cl^- (2.75 \AA) [94, 95]. The Ag–S bond length, $2.628(8) \text{ \AA}$ in **22** is close to similar tetrahedral complexes, $\{2.6284(7) \text{ \AA}\}$ in $[\text{AgCl}(\kappa^1\text{-S-L})(\text{PPh}_3)_2]$ ($\text{L} = \text{Pyridine-2-carbaldehyde thiosemicarbazone}$) [92] and $\{2.625(1) \text{ \AA}\}$ in $[\text{Ag}(\text{Ph}_3\text{P})_2(\text{Py}_2\text{SH})\text{Cl}]$, but longer than $\{2.4799(12), 2.5107(11) \text{ \AA}\}$ in $[\text{Ag}_6(\text{HL})_6]$ [8] ($\text{HL} = \text{anion of salicyldehyde thiosemicarbazone}$). The S–C bond distance, 1.705 \AA in **22** is close to that of $[\text{Ag}(\text{Ph}_3\text{P})_2(\text{Py}_2\text{SH})\text{Cl}]$, but shorter than $1.757(5) \text{ \AA}$ in $[\text{Ag}_6(\text{HL})_6]$ [11], because in the former case thiosemicarbazone is coordinating as neutral monodentate ligand bonding via S atom only whereas in later case thiosemicarbazone is anionic and coordinating via N^3 S- donor atoms to form a five membered chelate ring. The Ag–P bond lengths,

{2.4558(7)Å, and 2.4740(2) Å} are close to literature values [92, 93] and in [Ag(Ph₃P₂)(Py₂SH)Cl] [96].

The bond angle around Ag atom lies in the range of 99.9(2)°- 121.49(2)°. Presence of two bulkier Ph₃P groups around Ag causes distortion and results in a distorted tetrahedral geometry as a result P(1)–Ag–P(2) and P(1)–Ag–S bond angle is observed at 121.49(2)° and 102.79(3)° respectively. The Ag–S–C bond angle in [AgCl(η¹-S-HIntsc)(Ph₃P)₂] **22** is 111.57(11)° and is similar to 111.2(1)° in [Ag(Ph₃P₂)(Py₂SH)Cl].

Table-22: Crystallographic data of [AgCl(η¹-S-HIntsc)(Ph₃P)₂] (**22**).

Empirical formula	C ₄₆ H ₄₀ AgClN ₄ P ₂ S
Formula weight	886.14
Temperature/K	173(2)
Crystal system	Monoclinic
Space group	P2 ₁ /c
a/Å	17.5112(3)
b/Å	13.3235(2)
c/Å	20.3377(4)
α/°	90
β/°	93.3599(17)
γ/°	90
Volume/Å ³	4736.87(15)
Z	4
ρ _{calc} /cm ³	1.243
μ/mm ⁻¹	5.238
F(000)	1816.0
Crystal size/mm ³	0.32 × 0.26 × 0.14
Radiation	CuKα (λ = 1.54184)
2θ range for data collection/°	7.938 to 142.54
Index ranges	-21 ≤ h ≤ 15, -16 ≤ k ≤ 15, -19 ≤ l ≤ 24

Reflections collected	20985
Independent reflections	9040 [$R_{\text{int}} = 0.0343$, $R_{\text{sigma}} = 0.0431$]
Data/restraints/parameters	9040/0/503
Goodness-of-fit on F^2	1.027
Final R indexes [$I > 2\sigma(I)$]	$R_1 = 0.0409$, $wR_2 = 0.1059$
Final R indexes [all data]	$R_1 = 0.0519$, $wR_2 = 0.1107$
Largest diff. peak/hole / $e \text{ \AA}^{-3}$	1.29/-0.66

Table-23: Bond Lengths for (\AA) (**22**).

Ag(1) – C(11)	2.6569(7)	C(17) – C(22)	1.378(4)
Ag(1) – S(1)	2.6288(8)	C(18) – C(19)	1.388(6)
Ag(1) – P(1)	2.4558(7)	C(19) – C(20)	1.383(7)
Ag(1) – P(2)	2.4740(6)	C(20) – C(21)	1.359(6)
S(1) – C(1)	1.705(3)	C(21) – C(22)	1.397(5)
P(1) – C(11)	1.832(2)	C(23) – C(24)	1.383(4)
P(1) – C(17)	1.824(3)	C(23) – C(28)	1.398(4)
P(1) – C(23)	1.825(3)	C(24) – C(25)	1.390(5)
P(2) – C(29)	1.831(3)	C(25) – C(26)	1.373(5)
P(2) – C(35)	1.830(3)	C(26) – C(27)	1.380(5)
P(2) – C(41)	1.833(3)	C(27) – C(28)	1.385(5)
N(1) – C(4)	1.352(4)	C(29) – C(30)	1.370(5)
N(1) – C(5)	1.374(5)	C(29) – C(34)	1.403(4)
N(2) – N(3)	1.397(3)	C(30) – C(31)	1.386(5)
N(2) – C(2)	1.280(4)	C(31) – C(32)	1.380(5)
N(3) – C(1)	1.328(4)	C(32) – C(33)	1.370(5)
N(4) – C(1)	1.322(4)	C(33) – C(34)	1.373(5)
C(2) – C(3)	1.437(4)	C(35) – C(36)	1.396(4)

C(3) – C(4)	1.375(4)	C(35) – C(40)	1.377(4)
C(3) – C(10)	1.450(4)	C(36) – C(37)	1.392(4)
C(5) – C(6)	1.390(5)	C(37) – C(38)	1.374(5)
C(5) – C(10)	1.412(4)	C(38) – C(39)	1.379(5)
C(6) – C(7)	1.385(6)	C(39) – C(40)	1.400(5)
C(7) – C(8)	1.398(6)	C(41) – C(42)	1.408(7)
C(8) – C(9)	1.383(5)	C(41) – C(46)	1.390(4)
C(9) – C(10)	1.393(4)	C(41) – C(42)A	1.33(2)
C(11) – C(12)	1.396(4)	C(42) – C(43)	1.380(9)
C(11) – C(16)	1.376(4)	C(43) – C(44)	1.375(8)
C(12) – C(13)	1.403(4)	C(44) – C(45)	1.363(5)
C(13) – C(14)	1.370(5)	C(44) – C(43)A	1.51(2)
C(14) – C(15)	1.378(5)	C(45) – C(46)	1.379(4)
C(15) – C(16)	1.408(4)	C(42)A–C(43)A	1.43(3)
Bond Angles for (°) (22)			
S(1) – Ag(1)– Cl(1)	105.65(2)	C(11) – C(16) – C(15)	120.3(3)
P(1) – Ag(1)– Cl(1)	114.74(2)	C(18) – C(17) – P(1)	115.7(2)
P(1) – Ag(1)– S(1)	102.79(3)	C(22) – C(17) – P(1)	125.1(2)
P(1) – Ag(1)– P(2)	121.49(2)	C(22) – C(17) – C(18)	119.2(3)
P(2) – Ag(1)– Cl(1)	99.91(2)	C(19) – C(18) – C(17)	120.3(4)
P(2) – Ag(1) S(1)	111.58(2)	C(20) – C(19) – C(18)	119.6(4)
C(1) – S(1)– Ag(1)	111.57(11)	C(21) – C(20) – C(19)	120.5(4)
C(11) – P(1)– Ag(1)	116.13(9)	C(20) – C(21) – C(22)	120.2(4)
C(17) – P(1)– Ag(1)	116.71(10)	C(17) – C(22) – C(21)	120.2(3)
C(17) – P(1)– Cl(1)	102.67(13)	C(24) – C(23) – P(1)	123.1(2)
C(17) – P(1)– C2(3)	104.45(13)	C(24) – C(23) – C(28)	118.9(3)
C(23) – P(1)– Ag(1)	110.88(9)	C(28) – C(23) – P(1)	118.0(2)
C(23) – P(1)– Cl(1)	104.65(12)	C(23) – C(24) – C(25)	120.3(3)
C(29) – P(2)– Ag(1)	116.90(9)	C(26) – C(25) – C(24)	120.7(3)

C(29) – P(2)– C(41)	103.74(13)	C(25) – C(26) – C(27)	119.5(3)
C(35) – P(2)– Ag(1)	115.12(8)	C(26) – C(27) – C(28)	120.5(3)
C(35) – P(2)– C(29)	102.92(12)	C(27) – C(28) – C(23)	120.1(3)
C(35) – P(2)– C(41)	104.14(13)	C(30) – C(29) – P(2)	119.9(2)
C(41) – P(2)– Ag(1)	112.51(9)	C(30) – C(29) – C(34)	118.4(3)
C(4) – N(1)– C(5)	109.0(3)	C(34) – C(29) – P(2)	121.6(2)
C(2) – N(2)– N(3)	114.4(3)	C(29) – C(30) – C(31)	120.7(3)
C(1) – N(3)– N(2)	119.3(3)	C(32) – C(31) – C(30)	120.2(3)
N(3) – C(1)– S(1)	120.9(2)	C(33) – C(32) – C(31)	119.6(3)
N(4) – C(1)– S(1)	121.8(2)(C(32) – C(33) – C(34)	120.4(3)
N(4) – C(1)– N(3)	117.3(3)	C(33) – C(34) – C(29)	120.6(3)
N(2) – C(2)– C(3)	122.3(3)	C(36) – C(35) – P(2)	119.5(2)
C(2) – C(3)– C(10)	130.4(3)	C(40) – C(35) – P(2)	121.4(2)
C(4) – C(3)– C(2)	122.9(3)	C(40) – C(35) – C(36)	118.8(3)
C(4) – C(3)– C(10)	106.6(3)	C(37) – C(36) – C(35)	120.2(3)
N(1) – C(4)– C(3)	110.3(3)	C(38) – C(37) – C(36)	120.3(3)
N(1) – C(5)– C(6)	129.4(3)	C(37) – C(38) – C(39)	120.1(3)
N(1) – C(5)– C(10)	108.6(3)	C(38) – C(39) – C(40)	119.6(3)
C(6) – C(5)– C(10)	122.0(3)	C(35) – C(40) – C(39)	120.9(3)
C(7) – C(6)– C(5)	117.0(3)	C(42) – C(41) – P(2)	118.6(3)
C(6) – C(7)– C(8)	121.9(3)	C(46) – C(41) – P(2)	123.7(2)
C(9) – C(8)– C(7)	120.7(3)	C(46) – C(41) – C(42)	117.4(3)
C(8) – C(9)– C(10)	118.8(3)	C(42)A–C(41) – P(2)	113.9(8)
C(5) – C(10)– C(3)	105.5(3)	C(42)A–C(41) – C(46)	118.1(8)
C(9) – C(10)– C(3)	135.0(3)	C(43) – C(42) – C(41)	120.2(5)
C(9) – C(10)– C(5)	119.5(3)	C(44) – C(43) – C(42)	120.2(5)
C(12) – C(11)– P(1)	116.9(2)	C(45) – C(44) – C(43)	119.6(4)
C(16) – C(11)– P(1)	123.1(2)	C(45) – C(44) – C(43)A	114.0(7)
C(16) – C(11)– C(12)	120.0(2)	C(44) – C(45) – C(46)	120.4(3)

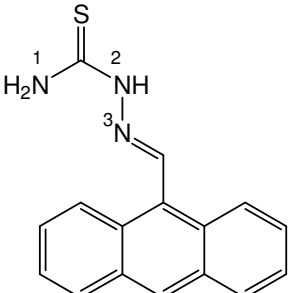
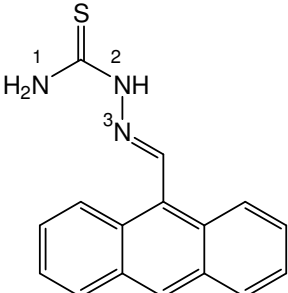
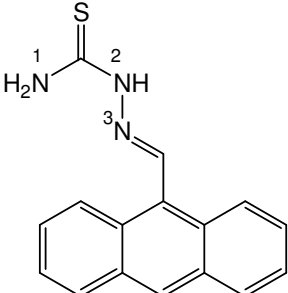
C(11) – C(12)– C(13)	119.0(3)	C(45) – C(46) – C(41)	120.8(3)
C(14) – C(13)– C(12)	120.8(3)	C(41) – C(42) A–C(43)A	120.7(15)
C(13) – C(14)– C(15)	120.4(3)	C(42)A–C(43)A– C(44)	116.3(15)
C(14) – C(15)– C(16)	119.5(3)		

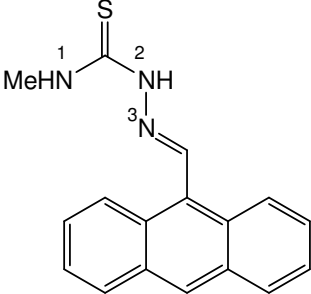
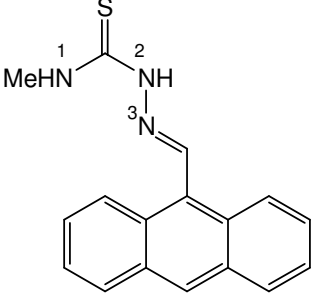
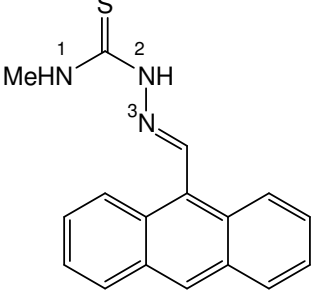
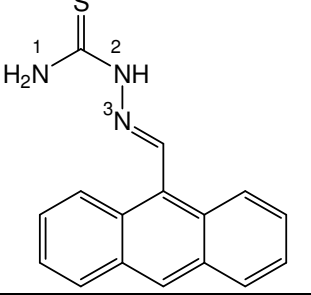
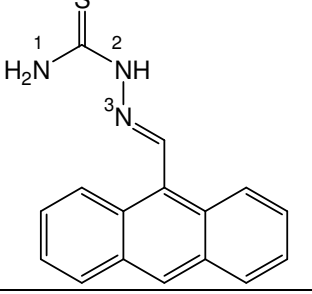
CHAPTER 6

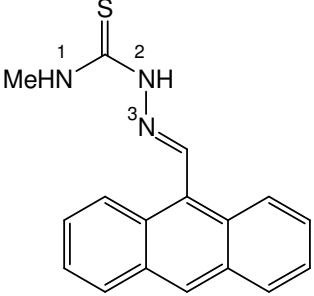
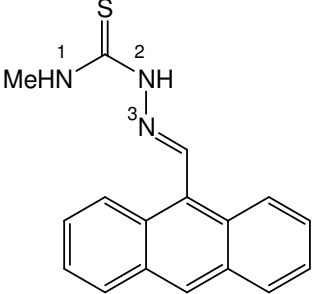
COMPLEXES OF COPPER(I) AND SILVER(I) HALIDES WITH 9- ANTHRALDEHYDE BASED THIOSEMICARBAZONES.

6.1 Complexes of Copper(I) halides and silver(I) halides with 9-anthraldehyde based thiosemicarbazones: Copper(I) and silver(I) halides formed complexes with 9-anthraldehyde thiosemicarbazone (9-Hantsc) and 9-anthraldehyde-N¹-methyl-3-thiosemicarbazone (9-Hanttsc-N¹-Me). These complexes are listed in Table-24.

Table-24: List of complexes of anthraldehyde based thiosemicarbazones.

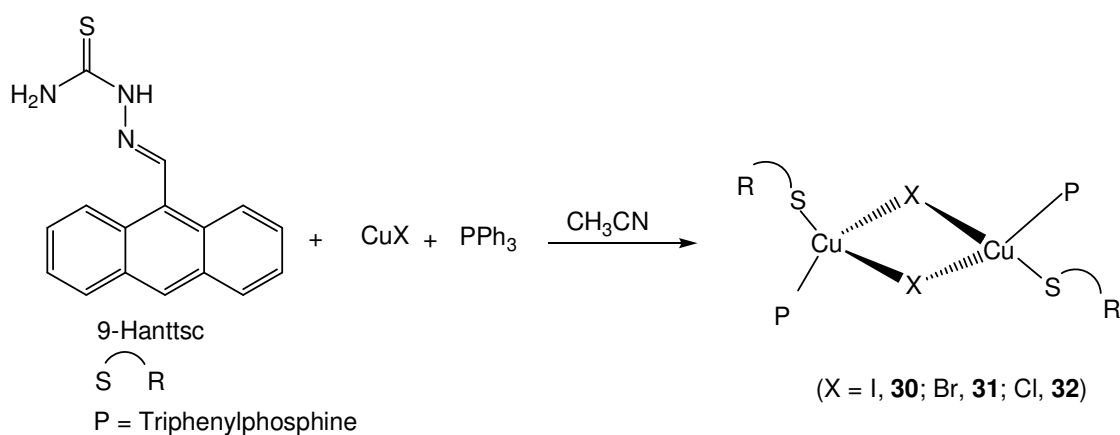
Complexes	Structure of ligands
$[\text{Cu}_2(\mu_2\text{-I})_2(\eta^1\text{-S-9-Hanttsc})(\text{Ph}_3\text{P})_2]$ <p style="text-align: center;">(30)</p>	
$[\text{Cu}_2(\mu_2\text{-Br})_2(\eta^1\text{-S-9-Hanttsc})(\text{Ph}_3\text{P})_2]$ <p style="text-align: center;">(31)</p>	
$[\text{Cu}_2(\mu_2\text{-Cl})_2(\eta^1\text{-S-9-Hanttsc})(\text{Ph}_3\text{P})_2]$ <p style="text-align: center;">(32)</p>	

<p>[CuI(η^1-S-9-Hanttsc-N¹-Me)(Ph₃P)₂]</p> <p>(33)</p>	
<p>[CuBr(η^1-S-9-Hanttsc-N¹-Me)(Ph₃P)₂]</p> <p>(34)</p>	
<p>[CuCl(η^1-S-9-Hanttsc-N¹-Me)(Ph₃P)₂]</p> <p>(35)</p>	
<p>[AgCl(η^1-S-9-Hanttsc)(Ph₃P)₂]</p> <p>(36)</p>	
<p>[AgBr(η^1-S-9-Hanttsc)(Ph₃P)₂]</p> <p>(37)</p>	

<p>[Ag₂Cl₂(μ₂-S-9-Hanttsc-N¹-Me)(Ph₃P)₂]</p> <p>(38)</p>	
<p>[Ag₂Br₂(μ₂-S-9-Hanttsc-N¹-Me)(Ph₃P)₂]</p> <p>(39)</p>	

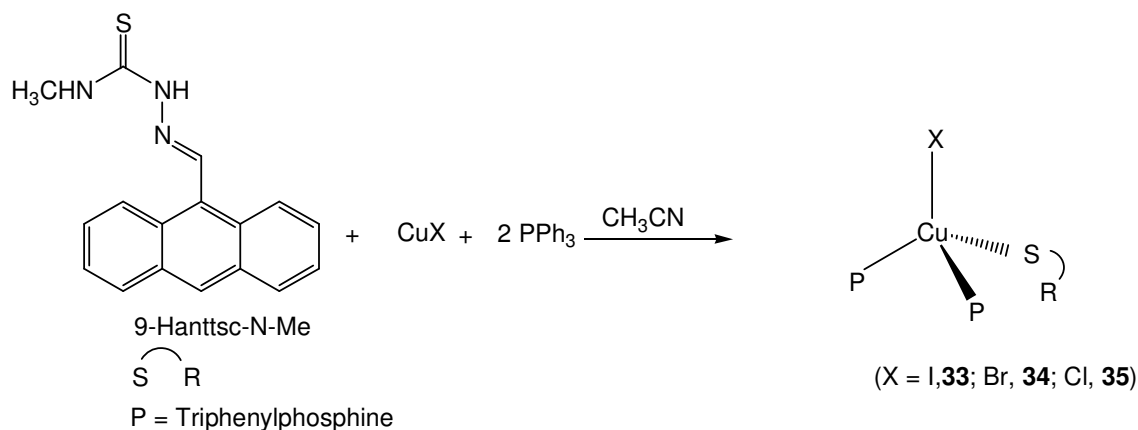
6.1.1 Synthesis

Reaction of copper(I) halides (X= I, Br, Cl) with 9-anthraldehyde thiosemicarbazone (9-Hanttsc, H⁵L) and triphenylphosphine in 1 : 1 : 1 (M : L : Ph₃P) molar ratio in acetonitrile formed orange coloured clear solution which on evaporation give crystalline products of stoichiometry [Cu₂(μ₂-X)₂(η¹-S-9-Hanttsc)(Ph₃P)₂] (X = I, **30**; Br, **31**; Cl, **32**) (Scheme 10).

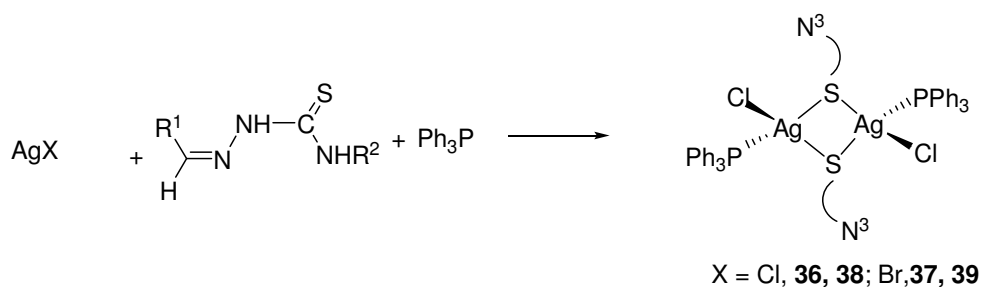


The reaction of copper(I) halides with 9-anthraldehyde-N¹-methyl thiosemicarbazone (9-Hanttsc-N¹-Me, H⁶L) and triphenylphosphine in 1 : 1 : 1 molar ratio formed insoluble

product. To solubilize it, an additional mole of triphenylphosphine was added, which resulted into formed complexes of stoichiometry, $[\text{CuCl}(\eta^1\text{-S-9-Hanttsc-N}^1\text{-Me})(\text{Ph}_3\text{P})_2]$ ($\text{X} = \text{I}$, **33**; Br , **34**; Cl , **35**) (Scheme-11). The behaviour of 9-Hanttsc- $\text{N}^1\text{-Me}$ ligand towards their copper(I) halide complexes is similar to that of isatin-3-thiosemicarbazone, indole-3-thiosemicarbazone (**10-12**), 5-methoxy indole-3-thiosemicarbazone (**16-18**) and 5-methoxy indole- $\text{N}^1\text{-methyl-3-thiosemicarbazone}$ (**19-21**) [46].



Silver (I) halides ($\text{X} = \text{Cl}$, Br) when reacted with 9-anthraldehyde-3-thiosemicarbazones (9-Hanttsc, H^5L) or 9-anthraldehyde- $\text{N}^1\text{-methyl-3-thiosemicarbazone}$ (9-Hanttsc- $\text{N}^1\text{-Me}$, H^6L) in the presence of triphenylphosphine in 1 : 1 : 1 ($\text{M} : \text{HL} : \text{Ph}_3\text{P}$) molar ratio formed sulphur bridged dimers of formula, $[\text{Ag}_2\text{X}_2(\mu_2\text{-S-9-Hanttsc-N}^1\text{-Me})_2(\text{Ph}_3\text{P})_2]$ ($\text{X} = \text{Cl}$, **36**, **38**; Br , **37**, **39**) (Scheme 12).



R^1, R^2	,H		,Me	
X	Cl	Br	Cl	Br
	36	37	38	39

(Scheme 12)

6.1.2 Discussion on IR spectroscopy:

Important IR peaks of free ligands, 9-Hanttsc (H^5L) and 9-Hanttsc- N^1 -Me (H^6L) and their copper(I) complexes are given in Table-25 and for silver complexes are given in Table-26. The $\nu(N-H)$ band of H^5L and H^6L , appeared in the range (i) $3437 - 3207\text{ cm}^{-1}$ due to symmetric and asymmetric stretching of amino group (ii) $3155-3113\text{ cm}^{-1}$ due to amide group and (iii) $3030-3039\text{ cm}^{-1}$ due to $-NH-$ group of indole ring. In complexes 30-35, these appeared in range $3205-3449\text{ cm}^{-1}$, $3147-3123\text{ cm}^{-1}$ and $3040-3053\text{ cm}^{-1}$ respectively. These bands showed high energy shift in their silver(I) complexes **36-39** ($3447 - 3207\text{ cm}^{-1}$) vis-a-vis free ligand. Appearance of all the $\nu(N-H)$ bands in complexes ensured that no deprotonation occurred during complexation and thio- ligand coordinated in neutral form. The characteristic $\nu(C=S)$ band of free ligand appeared at 846 cm^{-1} in H^5L and 841 cm^{-1} in H^6L . These bands shifted to high energy region in complexes **30-32, 37** and to low energy region in complexes **33-36, 38-39**. Appearance of an additional band in the range, $1066-1094\text{ cm}^{-1}$ due to $\nu(P-C_{ph})$ in complexes **30-39** ensured coordination of triphenylphosphine ligand to metal center (Tables - 25, 26).

Table-25: Important peaks in IR spectrum of Ligands (H^5L , H^6L) and their copper(I) complexes **30-35**.

Compound	$\nu(N-H)$	$\nu(-NH-)$	$\nu(C-H_{phenyl})$	$\nu(C-H_{Me})$	$\delta(NH_2)$ $+\nu(C=N)+\nu(C=C)$	$\nu(C=S)$	$\nu(P-C_{Ph})$
H^5L	3437s 3271s	3155m	3030m	–	1670s 1599s	846s	-
30	3444s 3297s	3147m	3040s	–	1651s 1575m	852s	1094s.
31	3449s 3300s	3139m	3047s	–	1628s 1595m	852s	1095s.
32	3423s 3244s	3136m	3049s	–	1672s 1562m	852s	1095s

H⁶L	3398s 3207s	3113s	3039m	2933m	1620s 1529s	841s	-
33	3377s 3205s	3140m	3047m	2997m	1631s 1562m	840s	1097s
34	3383s 3205s	3124m	3050m	2998M	1621s 1563m	840s	1093s
35	3316s 3230m	3123m	3053m	2961m	1624s 1560m	840s	1094s

s, sharp; m, medium; w, weak

Table-26: Important peaks in IR spectrum of silver(I) complexes **36-39**

Compound	$\nu(\text{N-H})$	$\nu(\text{-NH-})$	$\nu(\text{C-H}_{\text{phenyl}})$	$\nu(\text{C-H}_{\text{Me}})$	$\delta(\text{NH}_2)$ +$\nu(\text{C=N})$+$\nu(\text{C=C})$	$\nu(\text{C=S})$	$\nu(\text{P-C}_{\text{Ph}})$
36	3433s 3296s	3140m	3049s	-	1670s 1537m	840s	1096s
37	3447s 3281s	3150m	3029	-	1622s 1594m	851s	1094s
38	3435m 3362s	3109s	3051s	2993m	1668s 1558s	844s	1089s.
39	3372s 3219s	3132m	3051m	2993m	1670s 1521s	844s	1091s

s, sharp; m, medium; w, weak

6.1.3 Discussion on NMR spectroscopy:

In ¹H NMR spectra of ligands (H¹L-H⁴L), singlet was obtained for -N²H- proton in the range δ 9.71- 10.43 ppm, which showed a downfield shift in complexes (**30-39**) (δ 10.73- 13.01 ppm) vis-à-vis free ligand. Appearance of -N²H- protons in complexes ensured binding of ligands in neutral mode. Similarly, N¹H₂ protons in ligands H⁵L and H⁶L appeared at δ 8.49 ppm and δ 7.24 ppm respectively, however these peaks got obscured by the protons of phenyl rings of anthraldehyde as well triphenylphosphine in their complexes. Ring protons of

anthraldehyde and phenyl rings of triphenylphosphine appeared in the range δ 8.11- 7.25 ppm. The presence of methyl group at N¹ atom of thio- ligand was confirmed by the appearance of peak in the range δ 3.16-3.78 in complexes **33-35**, **38**, **39**. (Tables-27, 28).

Table-27: ¹H NMR signals for H⁵L- H⁶L (δ , ppm) and their copper(I) complexes **30-35**.

Complexes	(1H, N ² H)	(1H, N ¹ H).	(1H, C ² H)	Ring of protons
H⁵L	10.43 s	8.49 s	9.05 s	C ^{5,15} H , 8.41 d (2H); C ¹⁰ H , 8.50 s (1H); C ^{8,12} H, 8.00 d (2H); C ^{6,7,13,14} H + PH ₃ P, 7.68-7.66 m
30	10.73 s	6.97 s	9.63 s	C ^{5,10,15} H , 7.68-7.61 m (3H); C ^{8,12} H, 7.50-7.44 m (2H); C ^{6,7,13,14} H + PH ₃ P, 7.68-7.66 m
31	12.54 s	7.08 s	9.52 s	C ^{5,15} H , 8.01 d (2H); C ¹⁰ H , 8.49 d (1H); C ^{8,12} H, 7.56-7.50 m (2H); C ^{6,7,13,14} H + PH ₃ P, 7.35-7.30 m
32	12.34 s	7.48 s	9.32 s	C ^{5,10,15} H , 8.59—8.61 m (3H); C ^{8,12} H, 7.56-7.50 m (2H); C ^{6,7,13,14} H + PH ₃ P, 7.30-7.25 m
H⁶L	9.71 s	7.24 s	8.89 s	C ^{5,15} H , 8.53 d (2H); C ¹⁰ H , 8.56 s (1H); C ^{8,12} H, 8.06 d (2H); C ^{6,7,13,14} H + PH ₃ P, 7.57-7.47 m; -CH ₃ , 3.23 s (3H)
33	11.74 s	(Obscured by ring protons)	9.30 s	C ^{5,15} H , 8.31 d (2H); C ¹⁰ H , 8.11 s (1H); C ^{8,12} H, 7.84 d (2H); C ^{6,7,13,14} H + PH ₃ P, 7.63-7.32 m; -CH ₃ , 2.99 s (3H)
34	12.66 s	(Obscured by ring protons)	9.56 s	C ^{5,15} H , 8.48 d (2H); C ¹⁰ H , 8.45 s (1H); C ^{8,12} H, 8.01 d (2H); C ^{6,7,13,14} H + PH ₃ P, 7.56-7.45 m; -CH ₃ , 3.16 s (3H)
35	12.92 s	(Obscured by ring protons)	9.39 s	C ^{5,15} H , 8.00 d (2H); C ¹⁰ H , 8.45 s (1H); C ^{8,12} H, 8.06 d (2H); C ^{6,7,13,14} H + PH ₃ P, 7.63-7.53 m; -CH ₃ , 3.78 s (3H)

Table-28: ^1H NMR signals for silver(I) and their complexes **36-39**.

Complexes	(1H, N ² H)	(1H, N ¹ H).	(1H, C ² H)	Ring of protons
36	12.35 s	(Obscured by ring protons)	9.65 s	C ^{5,15} H, 8.44 d (2H); C ¹⁰ H, 8.51 d (1H) C ^{8,12} H, 8.11 d (2H); C ^{6,7,13,14} H + PH ₃ P+N ¹ H ₂ , 7.79-7.73 m
37	12.40 s	(Obscured by ring protons)	9.74 s	C ^{5,15} H, 8.52 d (2H); C ¹⁰ H, 8.52 d (1H) C ^{8,12} H, 8.31 d (2H); C ^{6,7,13,14} H + PH ₃ P+N ¹ H ₂ , 7.71-7.63 m
38	13.01 s	(Obscured by ring protons)	9.74 s	C ^{5,15} H, 8.49 d (2H); C ¹⁰ H, 8.40 s (1H); C ^{8,12} H, 7.93 d (2H); C ^{6,7,13,14} H + PH ₃ P N ¹ H ₂ , 7.53-7.45 m; -CH ₃ , 3.18 d (3H)
39	13.00	(Obscured by ring protons)	9.74 s	C ^{5,15} H, 8.59 d (2H); C ¹⁰ H, 8.40 s (1H); C ^{8,12} H, 7.97 d (2H); C ^{6,7,13,14} H + PH ₃ P N ¹ H ₂ , 7.63-7.53 m; -CH ₃ , 3.22 d (3H)

6.1.4 Structure of [Cu₂(μ₂-Br)₂](η¹-S-9-Hanttsc)(Ph₃P)₂ **31.**

The complex, [Cu₂(μ₂-Br)₂](η¹-S-9-Hanttsc)(Ph₃P)₂ **31** crystallized in triclinic crystal system with space group P-1. Its molecular structure and packing diagram are given in Figures 13 and 13a respectively. The crystallographic data and important bond parameters of complex **31** are given in Tables 29 and 31 respectively.

Each Cu atom is bonded to one P atom of triphenylphosphine, thione sulfur of thiosemicarbazone and one bromine atom. Two such units are connected by bromine bridge to form central kernel, Cu₂(μ₂-Br)₂Cu. Triphenylphosphine and thio- ligand occupy trans-orientation across the central kernel. The two unequal Cu–Br bond distances, {2.4739(3), 2.5912(4) Å} make the central kernel, Cu₂(μ₂-Br)₂Cu, a parallelogram. These Cu–Br bond distances are, {2.5425(5), 2.5892(5) Å} in **14**. The Cu–S bond distance, 2.3362(6) Å in **31** is longer than 2.2933(6) Å in [Cu₂(μ₂-Br)₂](η¹-S-HftscMe)₂(Ph₃P)₂][85]

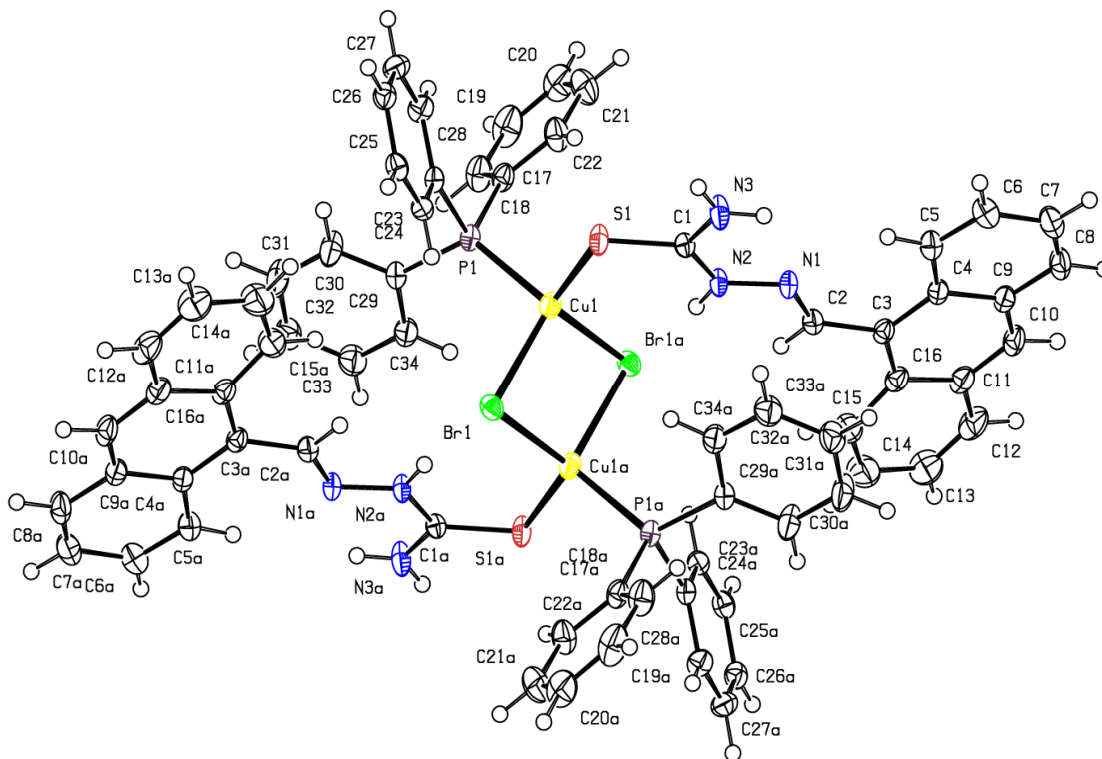


Figure-13: ORTEP view of $\text{Cu}_2(\mu_2\text{-Br})_2[(\eta^1\text{-S-9-Hanttsc})(\text{Ph}_3\text{P})_2]$ **31** with numbering scheme.

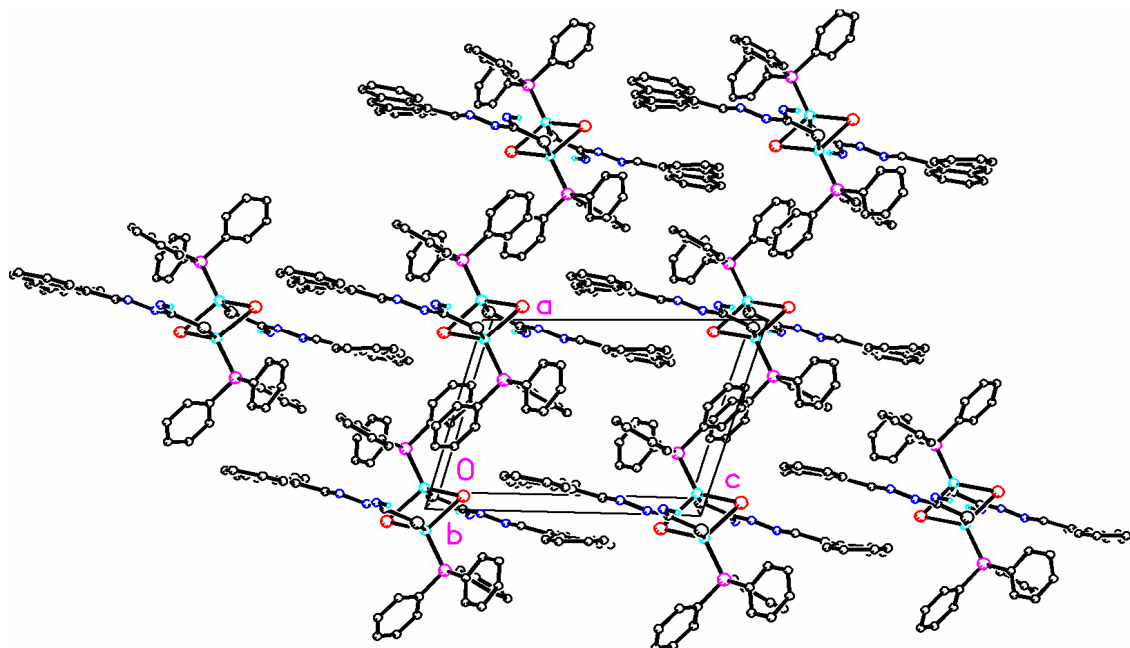


Figure-13a: Packing Diagram of $[\text{Cu}_2(\mu_2\text{-Br})_2[(\eta^1\text{-S-9-Hanttsc})(\text{Ph}_3\text{P})_2]]$ **31**.

The geometry around each Cu in dimers are in range $103.939(11)^\circ$ - $116.822(18)^\circ$ indicating distorted tetrahedral geometry. The Cu–X–Cu bond angles are at, ca. $76.062(12)^\circ$ while X–Cu–X angle at ca. $103.939(11)^\circ$. The Cu...Cu separation, 3.990 \AA in **31** is more when compared to $3.0543(11) \text{ \AA}$ in $[\text{Cu}_2(\mu_2\text{-Br})_2(\eta^1\text{-S-Hbtsc})_2(\text{Ph}_3\text{P})_2]$ [21] but comparatively lesser $3.226(6) \text{ \AA}$ in $[\text{Cu}_2(\mu_2\text{-I})_2(\text{Hftsc})_2(\text{Ph}_3\text{P})_2]$ [89].

6.1.5 Structure of monomer (**35**):

Complex $[\text{CuCl}(\eta^1\text{-S-9-Hanttsc-N}^1\text{-Me})(\text{Ph}_3\text{P})_2]$ **35** crystallized in triclinic crystal system with space group P-1. Its molecular structure and packing diagram are given in Figures-14 and Figure-14a respectively. The crystallographic data and important bond parameters of complex **35** are given in Table-30 and 32.

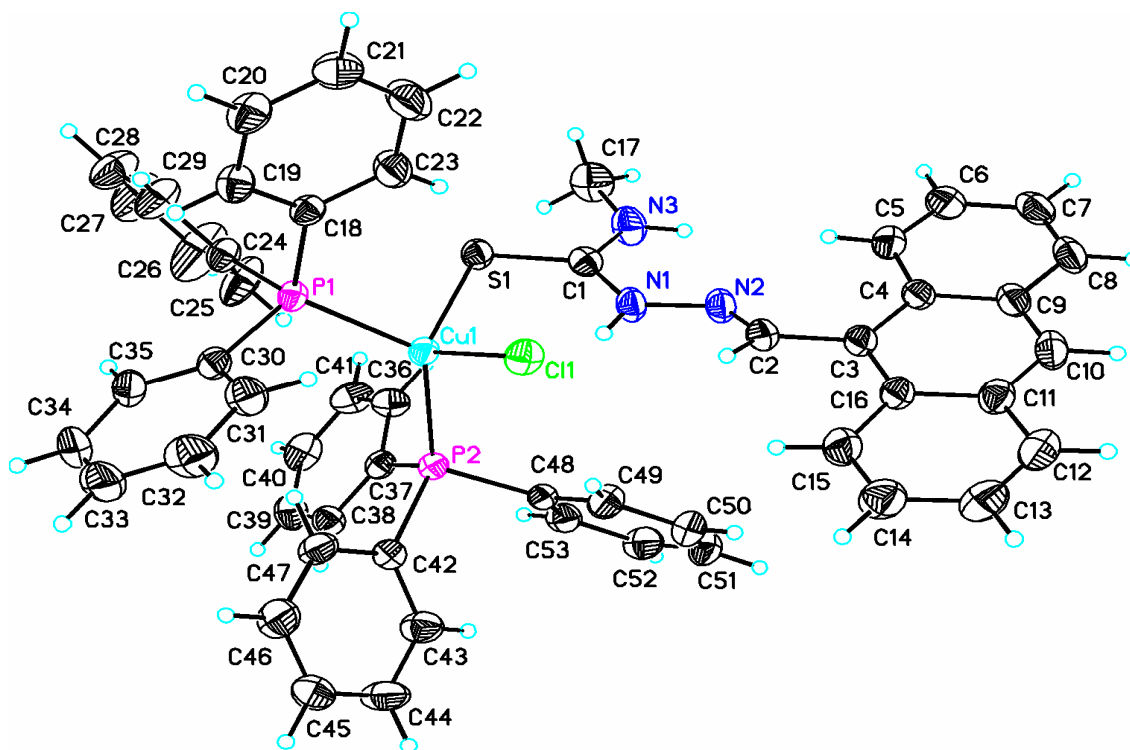


Figure-14: ORTEP view of $[\text{CuCl}(\eta^1\text{-S-9-Hanttsc-N}^1\text{-Me})(\text{Ph}_3\text{P})_2]$ **35** with numbering scheme.

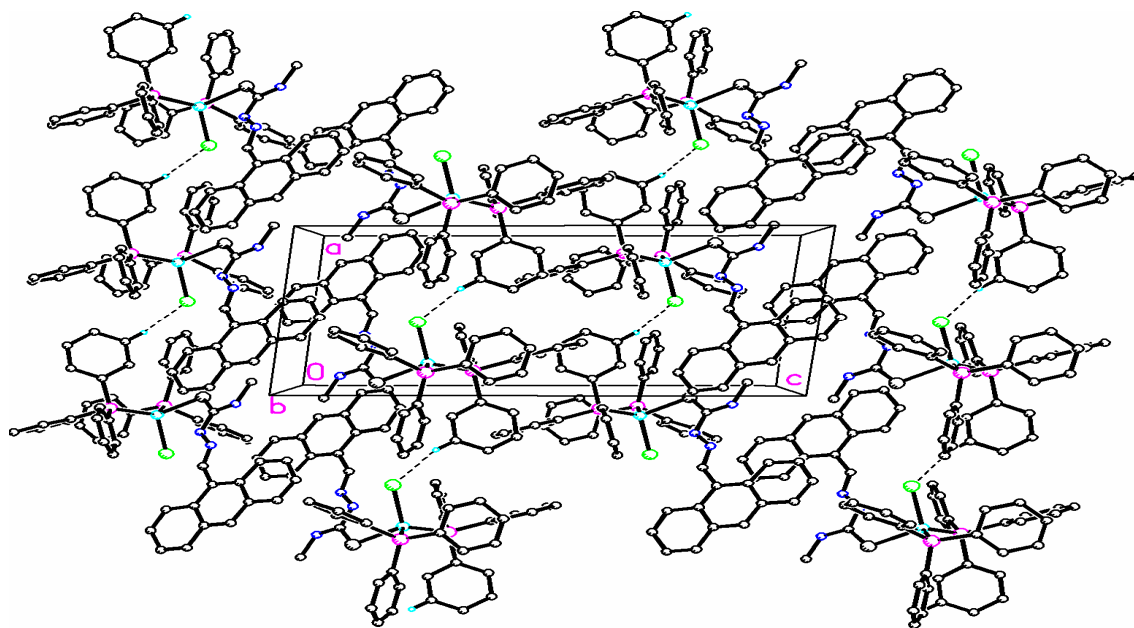


Figure-14a: Packing Diagram of $[\text{CuCl}(\eta^1\text{-S-9-Hanttsc-N}^1\text{-Me})(\text{Ph}_3\text{P})_2]$ **35**.

One chlorine atom, two P atoms from two PPh_3 ligands and one S atom from thio- ligand occupied four corners of tetrahedra. The Cu–S bond distance, 2.3942 Å in **35** is close to the 2.2598(5) Å Cu–S bond distance in $[\text{Cu}(\text{tscac})_2]$ (tscac = acetone thiosemicarbazone) [98] and other monomeric complexes of copper(I) with thiosemicarbazones reported in literature. The Cu–Cl bond distance 2.3754(6) Å is smaller 2.4301(5) Å in comparison to $[\text{CuCl}(\eta^1\text{-S-HIntsc})(\text{Ph}_3\text{P})_2]$ **12**. The (Cu–S) bond distance 2.3942(5) Å in complex **35** are however in close approximation with 2.3323(5) Å (Cu–S) bonds in complex $\text{CuCl}(\text{H}_2\text{itsc})(\text{Ph}_3\text{P})_2$. CH_3CN [38] and 2.3274(10) Å in $[\text{CuBr}(\eta^2\text{-N}^3, \text{S-H}_2\text{itsc-N}^1\text{-Me})(\text{Ph}_3\text{P})]$ (**2**). This bond length is close to Cu–S bond length in similar type of tetrahedral molecules reported in literature [46,73]. The Cu–P bond distances in complexes **35**, are 2.2741(5) Å, (Cu(1)–P(1); 2.2856(5), (Cu(1)–P(2)). The C–S bond distances 1.694(2) is close to that of $\text{HIntsc-N}^1\text{-Me}$ (1.6957 Å), which indicate considerable C=S character in coordinated thio- ligands in these complexes as compared to thiolate, but shorter than 1.757(4) Å in $[\text{Hg}(\text{C}_6\text{H}_5\text{C}_5\text{H}_4\text{N})(\text{btsc})]$ (btsc = anion of benzaldehydethiosemicarbazone) as in later ligand coordinate in thiolate form rather than thione form in former case.[87,100]

Presence of two bulky PPh_3 molecules leads to steric hindrance as a result the bond angles around copper atoms in the range ca. $102.06(2)^\circ$ - $109.65(2)^\circ$ reveal distorted tetrahedral geometry with maximum distortion $124.99(2)^\circ$ along the P–Cu–P bond angle.

Table-29: Crystallographic data of CuBr[(η^1 -S-9-Hanttsc)(Ph₃P)₂] **31**

Empirical formula	C ₆₈ H ₅₆ Br ₂ Cu ₂ N ₆ P ₂ S ₂
Formula weight	1370.14
Temperature/K	173(2)
Crystal system	Triclinic
Space group	P-1
a/Å	10.6214(6)
b/Å	11.2972(5)
c/Å	13.7145(7)
α /°	72.608(4)
β /°	70.363(5)
γ /°	75.468(4)
Volume/Å ³	1458.20(14)
Z	1
ρ_{calc} /cm ³	1.560
μ /mm ⁻¹	2.275
F(000)	696.0
Crystal size/mm ³	0.51 × 0.25 × 0.23
Radiation	MoK α (λ = 0.71073)
2 θ range for data collection/°	5.93 to 65.652
Index ranges	-15 ≤ h ≤ 15, -16 ≤ k ≤ 17, -20 ≤ l ≤ 20
Reflections collected	17833
Independent reflections	9606 [R _{int} = 0.0353, R _{sigma} = 0.0582]
Data/restraints/parameters	9606/0/370
Goodness-of-fit on F ²	1.026
Final R indexes [I >= 2 σ (I)]	R ₁ = 0.0395, wR ₂ = 0.0803
Final R indexes [all data]	R ₁ = 0.0630, wR ₂ = 0.0913
Largest diff. peak/hole / e Å ⁻³	0.60/-0.68

Table-30: Crystallographic data of [CuCl(η^1 -S-9-Hanttsc-N¹-Me)(Ph₃P)₂] **35**

Empirical formula	C ₅₃ H ₄₅ ClCuN ₃ P ₂ S
Formula weight	916.91
Temperature/K	173(2)
Crystal system	Triclinic
Space group	P-1
a/Å	9.3618(6)
b/Å	13.0317(6)
c/Å	19.9761(11)
α /°	87.840(4)
β /°	83.721(5)
γ /°	84.866(5)
Volume/Å ³	2411.8(2)
Z	2
ρ_{calc} /cm ³	1.263
μ /mm ⁻¹	2.467
F(000)	952.0
Crystal size/mm ³	0.31 × 0.29 × 0.24
Radiation	CuK α (λ = 1.54184)
2 Θ range for data collection/°	6.82 to 142.94
Index ranges	-11 ≤ h ≤ 11, -16 ≤ k ≤ 15, -21 ≤ l ≤ 24
Reflections collected	17563
Independent reflections	9186 [R _{int} = 0.0443, R _{sigma} = 0.0543]
Data/restraints/parameters	9186/0/551
Goodness-of-fit on F ²	1.031
Final R indexes [I >= 2 σ (I)]	R ₁ = 0.0431, wR ₂ = 0.1124
Final R indexes [all data]	R ₁ = 0.0487, wR ₂ = 0.1177
Largest diff. peak/hole / e Å ⁻³	0.53/-0.39

Table-31: Bond Lengths for (Å) 31			
Br(1) – Cu(1) ¹	2.4739(3)	C(11) – C(12)	1.436(3)
Br(1) – Cu(1)	2.5912(4)	C(11) – C(16)	1.435(3)
Cu(1) – Br(1) ¹	2.4739(3)	C(12) – C(13)	1.337(4)
Cu(1) – S(1)	2.3362(6)	C(13) – C(14)	1.413(4)
Cu(1) – P(1)	2.2475(6)	C(14) – C(15)	1.368(3)
S(1) – C(1)	1.704(2)	C(15) – C(16)	1.425(3)
P(1) – C(17)	1.821(2)	C(17) – C(18)	1.395(3)
P(1) – C(23)	1.829(2)	C(17) – C(22)	1.390(3)
P(1) – C(29)	1.822(2)	C(18) – C(19)	1.387(4)
N(1) – N(2)	1.385(2)	C(19) – C(20)	1.368(4)
N(1) – C(2)	1.287(3)	C(20) – C(21)	1.389(4)
N(2) – C(1)	1.332(2)	C(21) – C(22)	1.384(3)
N(3) – C(1)	1.322(3)	C(23) – C(24)	1.397(3)
C(2) – C(3)	1.457(3)	C(23) – C(28)	1.395(3)
C(3) – C(4)	1.422(3)	C(24) – C(25)	1.388(3)
C(3) – C(16)	1.426(3)	C(25) – C(26)	1.387(3)
C(4) – C(5)	1.427(3)	C(26) – C(27)	1.378(3)
C(4) – C(9)	1.435(3)	C(27) – C(28)	1.390(3)
C(5) – C(6)	1.363(3)	C(29) – C(30)	1.387(3)
C(6) – C(7)	1.413(3)	C(29) – C(34)	1.387(3)
C(7) – C(8)	1.351(3)	C(30) – C(31)	1.385(3)
C(8) – C(9)	1.429(3)	C(31) – C(32)	1.374(3)
C(9) – C(10)	1.395(3)	C(32) – C(33)	1.376(3)
C(10) – C(11)	1.386(3)	C(33) – C(34)	1.388(3)
Bond Angles for (°)31			
Cu(1) ¹ – Br(1) – Cu(1)	76.062(12)	C(10) – C(11) – C(12)	120.8(2)
Br(1) ¹ – Cu(1) – Br(1)	103.939(11)	C(10) – C(11) – C(16)	119.8(2)
S(1) – Cu(1) – Br(1) ¹	116.822(18)	C(16) – C(11) – C(12)	119.4(2)
S(1) – Cu(1) – Br(1)	103.778(19)	C(13) – C(12) – C(11)	121.3(2)

P(1) – Cu(1) – Br(1) ¹	115.884(18)	C(12) – C(13) – C(14)	119.6(2)
P(1) – Cu(1) – Br(1)	108.216(19)	C(15) – C(14) – C(13)	121.5(3)
P(1) – Cu(1) – S(1)	107.17(2)	C(14) – C(15) – C(16)	120.9(2)
C(1) – S(1) – Cu(1)	114.00(7)	C(3) – C(16) – C(11)	119.4(2)
C(17) – P(1) – Cu(1)	113.18(7)	C(15) – C(16) – C(3)	123.7(2)
C(17) – P(1) – C(23)	103.54(9)	C(15) – C(16) – C(11)	116.9(2)
C(17) – P(1) – C(29)	103.26(10)	C(18) – C(17) – P(1)	123.83(19)
C(23) – P(1) – Cu(1)	109.25(6)	C(22) – C(17) – P(1)	117.66(17)
C(29) – P(1) – Cu(1)	122.06(7)	C(22) – C(17) – C(18)	118.5(2)
C(29) – P(1) – C(23)	103.69(9)	C(19) – C(18) – C(17)	120.1(3)
C(2) – N(1) – N(2)	112.72(17)	C(20) – C(19) – C(18)	120.6(2)
C(1) – N(2) – N(1)	121.13(17)	C(19) – C(20) – C(21)	120.1(3)
N(2) – C(1) – S(1)	120.57(15)	C(22) – C(21) – C(20)	119.4(3)
N(3) – C(1) – S(1)	121.22(15)	C(21) – C(22) – C(17)	121.2(2)
N(3) – C(1) – N(2)	118.21(19)	C(24) – C(23) – P(1)	117.17(15)
N(1) – C(2) – C(3)	127.5(2)	C(28) – C(23) – P(1)	123.81(16)
C(4) – C(3) – C(2)	124.67(18)	C(28) – C(23) – C(24)	118.99(18)
C(4) – C(3) – C(16)	119.26(19)	C(25) – C(24) – C(23)	120.25(18)
C(16) – C(3) – C(2)	115.8(2)	C(26) – C(25) – C(24)	120.19(19)
C(3) – C(4) – C(5)	123.8(2)	C(27) – C(26) – C(25)	119.93(19)
C(3) – C(4) – C(9))	119.62(19)	C(26) – C(27) – C(28)	120.36(19)
C(5) – C(4) – C(9)	116.5(2)	C(27) – C(28) – C(23)	120.3(2)
C(6) – C(5) – C(4)	121.3(2)	C(30) – C(29) – P(1)	123.76(17)
C(5) – C(6) – C(7)	121.8(2)	C(30) – C(29) – C(34)	118.5(2)
C(8) – C(7) – C(6)	118.9(2)	C(34) – C(29) – P(1)	117.69(17)
C(7) – C(8) – C(9)	121.5(2)	C(31) – C(30) – C(29)	120.5(2)
C(8) – C(9) – C(4)	119.8(2)	C(32) – C(31) – C(30)	120.6(2)
C(10) – C(9) – C(4)	119.6(2)	C(31) – C(32) – C(33)	119.5(2)
C(10) – C(9) – C(8)	120.5(2)	C(32) – C(33) – C(34)	120.3(2)
C(11) – C(10) – C(9)	121.5(2)	C(29) – C(34) – C(33)	120.6(2)

Cu(1) – C(11)	2.3754(6)	C(19) – C(20)	1.389(3)
Cu(1) – S(1)	2.3942(5)	C(20) – C(21)	1.379(4)
Cu(1) – P(1)	2.2741(5)	C(21) – C(22)	1.380(4)
Cu(1) – P(2)	2.2856(5)	C(22) – C(23)	1.390(3)
S(1) – C(1)	1.694(2)	C(24) – C(25)	1.383(3)
P(1) – C(18)	1.8327(19)	C(24) – C(29)	1.383(3)
P(1) – C(24)	1.828(2)	C(25) – C(26)	1.379(4)
P(1) – C(35)	1.828(2)	C(26) – C(27)	1.397(4)
P(2) – C(37)	1.832(2)	C(27) – C(28)	1.370(4)
P(2) – C(42)	1.8380(19)	C(28) – C(29)	1.393(4)
P(2) – C(48)	1.835(2)	C(30) – C(31)	1.392(3)
N(1) – N(2)	1.373(2)	C(30) – C(35)	1.390(3)
N(1) – C(1)	1.341(3)	C(31) – C(32)	1.380(4)
N(2) – C(2)	1.276(3)	C(32) – C(33)	1.368(5)
N(3) – C(1)	1.334(3)	C(33) – C(34)	1.400(4)
N(3) – C(17)	1.442(3)	C(34) – C(35)	1.387(3)
C(2) – C(3)	1.467(3)	C(36) – C(37)	1.396(3)
C(3) – C(4)	1.424(3)	C(36) – C(41)	1.386(3)
C(3) – C(16)	1.421(3)	C(37) – C(38)	1.396(3)
C(4) – C(5)	1.429(3)	C(38) – C(39)	1.389(3)
C(4) – C(9)	1.435(3)	C(39) – C(40)	1.384(3)
C(5) – C(6)	1.361(3)	C(40) – C(41)	1.390(4)
C(6) – C(7)	1.404(4)	C(42) – C(43)	1.385(3)
C(7) – C(8)	1.351(4)	C(42) – C(47)	1.387(3)
C(8) – C(9)	1.432(3)	C(43) – C(44)	1.391(3)
C(9) – C(10)	1.387(3)	C(44) – C(45)	1.378(4)
C(10) – C(11)	1.392(3)	C(45) – C(46)	1.367(4)

C(11) – C(12)	1.432(3)	C(46) – C(47)	1.397(3)
C(11) – C(16)	1.438(3)	C(48) – C(49)	1.400(3)
C(12) – C(13)	1.351(4)	C(48) – C(53)	1.393(3)
C(13) – C(14)	1.413(4)	C(49) – C(50)	1.387(3)
C(14) – C(15)	1.360(4)	C(50) – C(51)	1.380(4)
C(15) – C(16)	1.436(3)	C(51) – C(52)	1.383(4)
C(18) – C(19)	1.394(3)	C(52) – C(53)	1.391(3)
C(18) – C(23)	1.389(3)		
Bond Angles for (°)35			
Cl(1) – Cu(1) – S(1)	107.39(2)	C(15) – C(16) – C(11)	116.3(2)
P(1) – Cu(1) – C(11)	104.63(2)	C(19) – C(18) – P(1)	122.31(16)
P(1) – Cu(1) – S(1)	102.06(2)	C(23) – C(18) – P(1)	118.52(15)
P(1) – Cu(1) – P(2)	124.99(2)	C(23) – C(18) – C(19)	119.16(19)
P(2) – Cu(1) – C(11)	107.01(2)	C(20) – C(19) – C(18)	120.5(2)
P(2) – Cu(1) – S(1)	109.65(2)	C(21) – C(20) – C(19)	120.0(2)
C(1) – S(1) – Cu(1)	108.44(7)	C(20) – C(21) – C(22)	119.8(2)
C(18) – P(1) – Cu(1)	113.97(7)	C(21) – C(22) – C(23)	120.7(2)
C(24) – P(1) – Cu(1)	115.28(7)	C(18) – C(23) – C(22)	119.8(2)
C(24) – P(1) – C(18)	104.10(9)	C(25) – C(24) – P(1)	117.30(17)
C(24) – P(1) – C(35)	104.74(10)	C(29) – C(24) – P(1)	123.63(17)
C(35) – P(1) – Cu(1)	115.41(7)	C(29) – C(24) – C(25)	119.1(2)
C(35) – P(1) – C(18)	101.76(9)	C(26) – C(25) – C(24)	120.7(2)
C(37) – P(2) – Cu(1)	113.61(6)	C(25) – C(26) – C(27)	119.8(3)
C(37) – P(2) – C(42)	103.74(9)	C(28) – C(27) – C(26)	119.7(2)
C(37) – P(2) – C(48)	103.17(9)	C(27) – C(28) – C(29)	120.1(2)
C(42) – P(2) – Cu(1)	117.98(6)	C(24) – C(29) – C(28)	120.5(2)
C(48) – P(2) – Cu(1)	115.49(6)	C(35) – C(30) – C(31)	120.7(2)
C(48) – P(2) – C(42)	100.88(9)	C(32) – C(31) – C(30)	119.7(3)
C(1) – N(1) – N(2)	119.75(17)	C(33) – C(32) – C(31)	119.9(2)
C(2) – N(2) – N(1)	114.63(18)	C(32) – C(33) – C(34)	121.1(2)

C(1) – N(3) – C(17)	124.8(2)	C(35) – C(34) – C(33)	119.3(2)
N(1) – C(1) – S(1)	119.97(15)	C(30) – C(35) – P(1)	116.30(16)
N(3) – C(1) – S(1)	122.86(17)	C(34) – C(35) – P(1)	124.21(18)
N(3) – C(1) – N(1)	117.15(19)	C(34) – C(35) – C(30)	119.3(2)
N(2) – C(2) – C(3)	125.85(19)	C(41) – C(36) – C(37)	120.8(2)
C(4) – C(3) – C(2)	123.0(2)	C(36) – C(37) – P(2)	117.41(15)
C(16) – C(3) – C(2)	116.68(19)	C(38) – C(37) – P(2)	123.86(15)
C(16) – C(3) – C(4)	120.14(19)	C(38) – C(37) – C(36)	118.66(19)
C(3) – C(4) – C(5)	124.6(2)	C(39) – C(38) – C(37)	120.36(19)
C(3) – C(4) – C(9)	118.9(2)	C(40) – C(39) – C(38)	120.6(2)
C(5) – C(4) – C(9)	116.54(19)	C(39) – C(40) – C(41)	119.5(2)
C(6) – C(5) – C(4)	121.3(2)	C(36) – C(41) – C(40)	120.2(2)
C(5) – C(6) – C(7)	121.8(2)	C(43) – C(42) – P(2)	122.65(16)
C(8) – C(7) – C(6)	119.3(2)	C(43) – C(42) – C(47)	118.63(19)
C(7) – C(8) – C(9)	121.2(2)	C(47) – C(42) – P(2)	118.71(15)
C(8) – C(9) – C(4)	119.7(2)	C(42) – C(43) – C(44)	120.8(2)
C(10) – C(9) – C(4)	120.2(2)	C(45) – C(44) – C(43)	120.0(2)
C(10) – C(9) – C(8)	120.1(2)	C(46) – C(45) – C(44)	119.9(2)
C(9) – C(10) – C(11)	121.9(2)	C(45) – C(46) – C(47)	120.5(2)
C(10) – C(11) – C(12)	120.5(2)	C(42) – C(47) – C(46)	120.2(2)
C(10) – C(11) – C(16)	119.4(2)	C(49) – C(48) – P(2)	117.12(16)
C(12) – C(11) – C(16)	120.1(2)	C(53) – C(48) – P(2)	123.62(17)
C(13) – C(12) – C(11)	120.9(2)	C(53) – C(48) – C(49)	119.2(2)
C(12) – C(13) – C(14)	119.6(2)	C(50) – C(49) – C(48)	120.1(2)
C(15) – C(14) – C(13)	121.6(2)	C(51) – C(50) – C(49)	120.4(2)
C(14) – C(15) – C(16)	121.4(2)	C(50) – C(51) – C(52)	119.9(2)
C(3) – C(16) – C(11)	119.49(19)	C(51) – C(52) – C(53)	120.4(2)
C(3) – C(16) – C(15)	124.2(2)	C(52) – C(53) – C(48)	120.0(2)

6.1.6 Structure of $[\text{Ag}_2\text{Cl}_2(\mu_2\text{-S-9-Hanttsc-N}^1\text{-Me})(\text{Ph}_3\text{P})_2]$ **38**.

Complex $[\text{Ag}_2\text{Cl}_2(\mu_2\text{-S-9-Hanttsc-N}^1\text{-Me})(\text{Ph}_3\text{P})_2]$ **38** crystallized in triclinic crystal system with space group P-1. Molecular structure of this dimeric complex **38** is given in Figures-15 packing diagram of the complex is given in Figure-15a, crystallographic data and important bond parameters are given in Table-33 and Table-34.

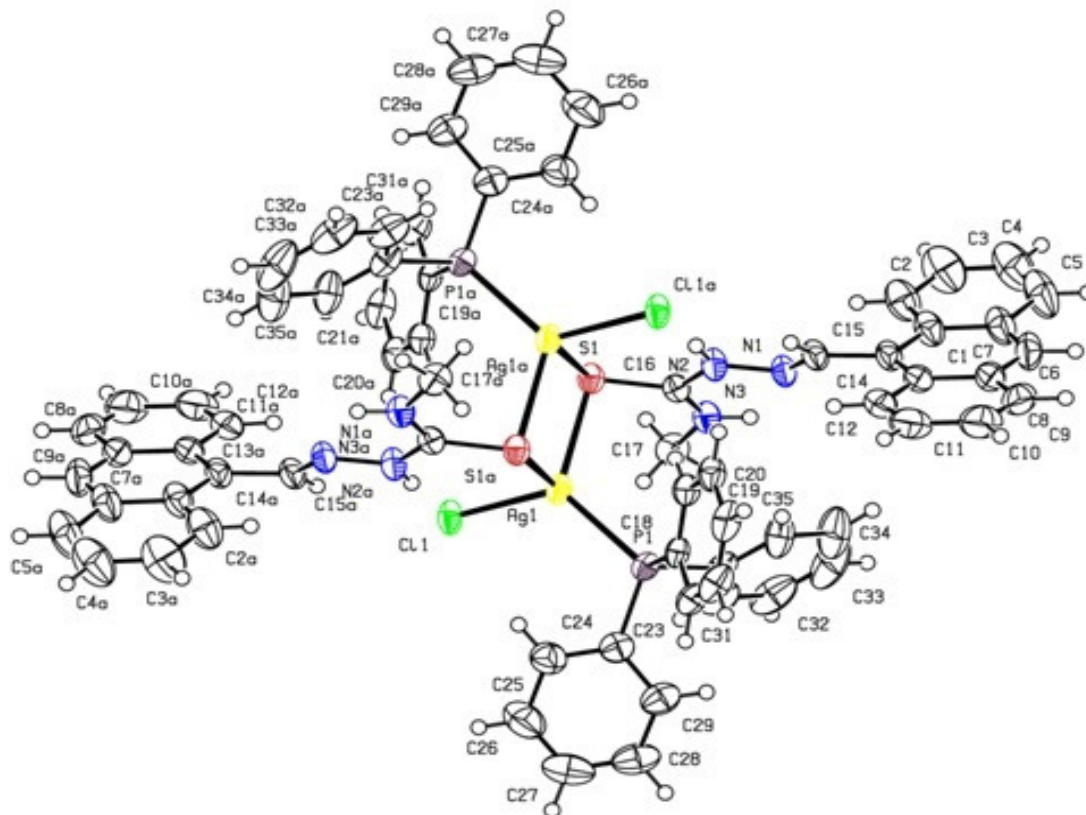


Figure-15: ORTEP view of $[\text{Ag}_2\text{Cl}_2(\mu_2\text{-S-9-Hanttsc-N}^1\text{-Me})(\text{Ph}_3\text{P})_2]$ **38** with numbering scheme.

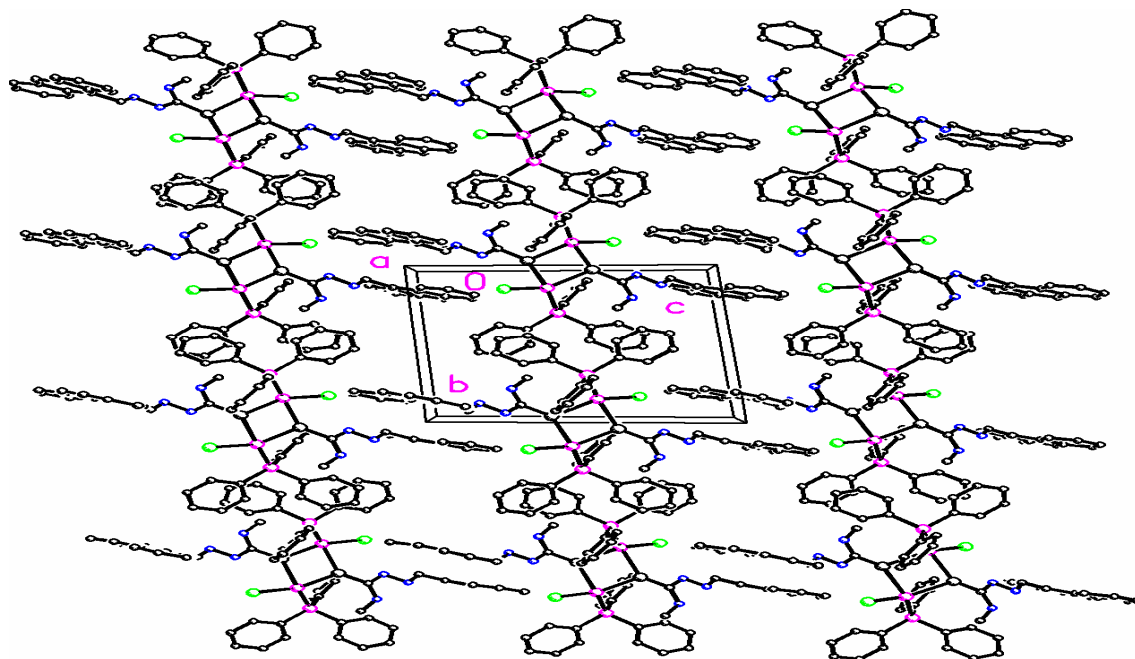


Figure-15a: Packing Diagram of $[\text{Ag}_2\text{Cl}_2(\mu_2\text{-S-9-Hanttsc-N}^1\text{-Me})(\text{Ph}_3\text{P})_2]\mathbf{38}$.

In $[\text{Ag}_2\text{Cl}_2(\mu_2\text{-S-9-Hanttsc-N}^1\text{-Me})(\text{Ph}_3\text{P})_2]$ **38** the Ag atom is bonded with one chloride halogen atom trans to each other, one P atom of PPh_3 and two S atoms from two different thiosemicarbazone ligands bridging two Ag centres, with central kernel, $\text{Ag}_2(\mu_2\text{-S})_2\text{Ag}$ and two tetrahedral share a sulphur-sulfur edge, Ph_3P and halogen ligands occupy trans orientation across the central kernel. The Ag–Cl, Ag–S1 and Ag–S bond distance $\{2.5226(7) \text{ \AA}, 2.7761(7) \text{ \AA} 2.6007(7) \text{ \AA} (\text{bridging})\}$ respectively. This unequal bond distances make the Ag_2S_2 core, a parallelogram. Ag–S bond distance in complex **38** $[\text{AgCl}(9\text{-Hanttsc-N}^1\text{-Me})(\text{Ph}_3\text{P})_2]$ are comparable and characteristic of such cores $\{2.6070(9) \text{ \AA}, 2.6851(9) \text{ \AA}$ in $\text{AgBr}(\mu_2\text{-S-Hptsc})\text{Ph}_3\text{P}$, $2.5810(10) \text{ \AA}, 2.6591(11) \text{ \AA}$ $[\text{Ag}(\mu_2\text{-S-(Hftsc)}_2)(\text{Ph}_3\text{P})_2]$ $2.6284(7), 2.6284(7) \text{ \AA}$ } in $[\text{AgIPPh}_3\text{P}_2(\text{Py}_2\text{SH})\text{Cl}][93,98]$. The $\text{Ag}\cdots\text{Ag}$ bond distance 3.578 \AA is larger than that observed 3.487 \AA in $[\text{Ag}_2\text{Cl}_2(\mu\text{-S-Httsc-N-Me})_2]$ and $3.32282(4) \text{ \AA}$ in $[\text{Ag}_2\text{Cl}_2(\mu\text{-S-Hftsc-NEt})_2(\kappa\text{-S-Hftsc-NEt})_2][101]$. The geometry around the Ag is distorted tetrahedral with the bond angles ranging around ca. $98.51(9)\text{-}122.66(2)^\circ$. The Ag–P bond distance is $2.4304(7) \text{ \AA}$ is in conformity to the reported bond distance of its analogue in $2.4393(11) \text{ \AA}$ $[\text{Ag}_2(\text{PPh}_3)\text{-S-(Bacatsc)}_2(\text{NO}_3)][94]$. The C–S bond distance $1.715(3) \text{ \AA}$ and stands in conformity with $1.697(2) \text{ \AA}$ $[\text{Ag}_2(\mu\text{-S-Hftsc--NEt})_2(\kappa\text{-S-HftscNEt})_2][101]$. The shortened bond distance indicates that these ligands are coordinating through thione form rather than thiole form. The Ag–S–Ag $83.368(19) \text{ \AA}$, bond distance are more than $74.392(18) \text{ \AA}$ $[\text{Ag}_2(\mu\text{-S-$

Hftsc--NEt)₂(κ-S-HftscNEt)₂ and S–Ag–S bond distance is 96.631(19) Å are lesser than [Ag₂(μ-S-Hftsc-NEt)₂(κ-S-HftscNEt)[101].

Table-33: Crystallographic data of [Ag₂Cl₂(μ₂-S-9-Hanttsc-N¹-Me)(Ph₃P)₂]**38**

Empirical formula	C ₇₀ H ₆₀ Ag ₂ Cl ₂ N ₆ P ₂ S ₂
Formula weight	1397.94
Temperature/K	173(2)
Crystal system	Triclinic
Space group	P-1
a/Å	10.4921(7)
b/Å	12.0020(6)
c/Å	13.8200(10)
α/°	82.287(5)
β/°	79.882(6)
γ/°	75.133(5)
Volume/Å ³	1648.60(19)
Z	1
ρ _{calc} /cm ³	1.408
μ/mm ⁻¹	6.912
F(000)	712.0
Crystal size/mm ³	0.38 × 0.18 × 0.12
Radiation	CuKα (λ = 1.54184)
2θ range for data collection/°	6.526 to 142.5
Index ranges	-12 ≤ h ≤ 12, -14 ≤ k ≤ 10, -16 ≤ l ≤ 16
Reflections collected	11774
Independent reflections	6261 [R _{int} = 0.0304, R _{sigma} = 0.0411]
Data/restraints/parameters	6261/0/380
Goodness-of-fit on F ²	1.002
Final R indexes [I >= 2σ (I)]	R ₁ = 0.0382, wR ₂ = 0.0964
Final R indexes [all data]	R ₁ = 0.0436, wR ₂ = 0.0997
Largest diff. peak/hole / e Å ⁻³	1.45/-0.48

Table-34: Bond Length for (Å) (38)			
Ag(1) – Cl(1)	2.5226(7)	C(9)– C(10)	1.351(7)
Ag(1) – S(1) ¹	2.7761(7)	C(10) – C(11)	1.406(6)
Ag(1) – S(1)	2.6007(7)	C(11) – C(12)	1.349(5)
Ag(1) – P(1)	2.4304(7)	C(12) – C(13)	1.423(5)
S(1) – Ag(1) ¹	2.7762(7)	C(13) – C(14)	1.415(5)
S(1) – C(16)	1.715(3)	C(14) – C(15)	1.476(4)
P(1) – C(18)	1.825(3)	C(18) – C(19)	1.390(4)
P(1) – C(24)	1.818(3)	C(18) – C(23)	1.389(4)
P(1) – C(30)	1.831(3)	C(19) – C(20)	1.385(4)
N(1) – N(2)	1.397(3)	C(20) – C(21)	1.383(5)
N(1) – C(15)	1.271(4)	C(21) – C(22)	1.381(5)
N(2) – C(16)	1.340(4)	C(22) – C(23)	1.390(4)
N(3) – C(16)	1.322(4)	C(24) – C(25)	1.392(5)
N(3) – C(17)	1.460(4)	C(24) – C(29)	1.398(5)
C(1) – C(2)	1.420(6)	C(25) – C(26)	1.395(5)
C(1) – C(6)	1.445(5)	C(26) – C(27)	1.376(7)
C(1) – C(14)	1.419(5)	C(27) – C(28)	1.363(7)
C(2) – C(3)	1.374(6)	C(28) – C(29)	1.370(6)
C(3) – C(4)	1.409(8)	C(30) – C(31)	1.402(5)
C(4) – C(5)	1.342(8)	C(30) – C(35)	1.384(5)
C(5) – C(6)	1.433(6)	C(31) – C(32)	1.384(6)
C(6) – C(7)	1.384(6)	C(32) – C(33)	1.368(8)
C(7) – C(8)	1.378(6)	C(33) – C(34)	1.384(8)
C(8) – C(9)	1.426(6)	C(34) – C(35)	1.396(5)
C(8) – C(13)	1.436(4)		
Bond Angles for (°) (38)			
Cl(1) – Ag(1) – S(1) ¹	102.55(2)	C(11) – C(12) – C(13)	121.0(3)

Cl(1) – Ag(1) – S(1)	105.60(2)	C(12) – C(13) – C(8)	117.4(3)
S(1) – Ag(10) – S(1) ¹	96.631(19)	C(14) – C(13) – C(8)	119.3(3)
P(1) – Ag(10) – C(11)	122.66(2)	C(14) – C(13) – C(12)	123.2(3)
P(1) – Ag(1) – S(1)	120.60(2)	C(1) – C(14) – C(15)	121.5(3)
P(1) – Ag(1) – S(1) ¹	103.73(2)	C(13) – C(14) – C(1)	121.0(3)
Ag(1) – S(1) – Ag(1) ¹	83.368(19)	C(13) – C(14) – C(15)	117.3(3)
C(16) – S(1) – Ag(1) ¹	112.11(9)	N(1) – C(15) – C(14)	122.0(3)
C(16) – S(1) – Ag(1)	98.51(9)	N(2) – C(16) – S(1)	118.7(2)
C(18) – P(1) – Ag(1)	108.66(9)	N(3) – C(16) – S(1)	123.0(2)
C(18) – P(1) – C(30)	103.48(13)	N(3) – C(16) – N(2)	118.3(3)
C(24) – P(1) – Ag(1)	114.32(11)	C(19) – C(18) – P(1)	116.4(2)
C(24) – P(1) – C(18)	107.29(13)	C(23) – C(18) – P(1)	124.5(2)
C(24) – P(1) – C(30)	102.98(15)	C(23) – C(18) – C(19)	119.1(3)
C(30) – P(1) – Ag(1)	119.07(9)	C(20) – C(19) – C(18)	121.3(3)
C(15) – N(1) – N(2)	114.2(2)	C(21) – C(20) – C(19)	119.0(3)
C(16) – N(2) – N(1)	118.4(2)	C(22) – C(21) – C(20)	120.4(3)
C(16) – N(3) – C(17)	124.6(3)	C(21) – C(22) – C(23)	120.4(3)
C(2) – C(1) – C(6)	118.0(3)	C(18) – C(23) – C(22)	119.7(3)
C(14) – C(1) – C(2)	124.0(3)	C(25) – C(24) – P(1)	117.9(2)
C(14) – C(1) – C(6)	117.8(3)	C(25) – C(24) – C(29)	119.1(3)
C(3) – C(2) – C(1)	120.9(4)	C(29) – C(24) – P(1)	123.0(3)
C(2) – C(3) – C(4)	120.7(5)	C(24) – C(25) – C(26)	119.3(4)
C(5) – C(4) – C(3)	120.5(4)	C(27) – C(26) – C(25)	120.2(5)
C(4) – C(5) – C(6)	121.5(4)	C(28) – C(27) – C(26)	120.5(4)
C(5) – C(6) – C(1)	118.3(4)	C(27) – C(28) – C(29)	120.5(4)
C(7) – C(6) – C(1)	120.2(3)	C(28) – C(29) – C(24)	120.4(4)
C(7) – C(6) – C(5)	121.5(4)	C(31) – C(30) – P(1)	118.4(3)
C(8) – C(7) – C(6)	122.3(3)	C(35) – C(30) – P(1)	122.4(2)
C(7) – C(8) – C(9)	121.8(3)	C(35) – C(30) – C(31)	118.9(3)
C(7) – C(8) – C(13)	119.3(3)	C(32) – C(31) – C(30)	120.1(4)

C(9) – C(8) – C(13)	118.8(4)	C(33) – C(32) – C(31)	120.3(4)
C(10) – C(9) – C(8)	121.5(4)	C(32) – C(33) – C(34)	120.9(4)
C(9) – C(10) – C(11)	119.2(4)	C(33) – C(34) – C(35)	119.1(5)
C(12) – C(11) – C(10)	121.9(4)	C(30) – C(35) – C(34)	120.7(4)

CHAPTER 7
BIOLOGICAL ACTIVITY

7.1 Biological activity: The thiosemicarbazones ligands and their metal complexes (Cu^I and Ag^I) were tested for antifungal, antibacterial and anti M. Tubercular activities. The codes used for compounds (ligands and their complexes) studied for various biological activities are enlisted in Table-35.

Table-35: List of compounds (ligands and their complexes) with their codes

Complex	Code used
H¹L (HIntsc)	B
[CuCl(η ¹ -S-HIntsc)(Ph ₃ P) ₂] 12	B1
[CuBr(η ¹ -S-HIntsc)(Ph ₃ P) ₂] 11	B2
[CuI(η ¹ -S-HIntsc)(Ph ₃ P) ₂] 10	B3
[AgCl(η ¹ -S-HIntsc)(Ph ₃ P) ₂] 22	B4
[AgBr(η ¹ -S-HIntsc)(Ph ₃ P) ₂] 23	B5
H²L (HIntsc-N ¹ -Me)	C
[Cu ₂ (μ ₂ -Cl) ₂ (HIntsc-N ¹ -Me) ₂ (Ph ₃ P) ₂] 15	C1
[Cu ₂ (μ ₂ -Br) ₂ (HIntsc-N ¹ -Me) ₂ (Ph ₃ P) ₂] 14	C2
[Cu ₂ (μ ₂ -I) ₂ (HIntsc-N ¹ -Me) ₂ (Ph ₃ P) ₂] 13	C3
[AgCl(η ¹ -S-HIntsc-N ¹ -Me)(Ph ₃ P) ₂] 24	C4
[AgBr(η ¹ -S-HIntsc-N ¹ -Me)(Ph ₃ P) ₂] 25	C5
H³L (5-MeOHIntsc)	D
[CuCl(η ¹ -S-5-MeOHIntsc)(Ph ₃ P) ₂] 18	D1
[CuBr(η ¹ -S-5-MeOHIntsc)(Ph ₃ P) ₂] 17	D2
[CuI(η ¹ -S-5-MeOHIntsc)(Ph ₃ P) ₂] 16	D3
[AgCl(η ¹ -S-5-MeOHIntsc)(Ph ₃ P) ₂] 26	D4
[AgBr(η ¹ -S-5-MeOHIntsc)(Ph ₃ P) ₂] 27	D5
H⁴L (5-MeOHIntsc-N ¹ -Me)	A
[CuCl(η ¹ -S-5-MeOHIntsc-N ¹ -Me)(Ph ₃ P) ₂].CH ₃ CN 21	A1

[CuBr(η^1 -S-5-MeOHIntsc-N ¹ -Me)(Ph ₃ P) ₂].CH ₃ CN 20	A2
[CuI(η^1 -S-5-MeOHIntsc-N ¹ -Me)(Ph ₃ P) ₂] 19	A3
[AgCl(η^1 -S-5-MeOHIntsc-N ¹ -Me)(Ph ₃ P) ₂] 28	A4
[AgBr(η^1 -S-5-MeOHIntsc-N ¹ -Me)(Ph ₃ P) ₂] 29	A5
H⁵L (9-Hanttsc)	E
[Cu ₂ (μ_2 -Cl) ₂ (η^1 -S-9-Hanttsc)(Ph ₃ P) ₂] 32	E1
[Cu ₂ (μ_2 -Br) ₂ (η^1 -S-9-Hanttsc)(Ph ₃ P) ₂] 31	E2
[Cu ₂ (μ_2 -I) ₂ (η^1 -S-9-Hanttsc)(Ph ₃ P) ₂] 30	E3
[AgCl(η^1 -S-9-Hanttsc)(Ph ₃ P) ₂] 36	E4
[AgBr(η^1 -S-9-Hanttsc)(Ph ₃ P) ₂] 37	E5
H⁶L (9-Hanttsc-N ¹ -Me)	F
[CuCl(η^1 -S-9-Hanttsc-N ¹ -Me)(Ph ₃ P) ₂] 35	F1
[CuBr(η^1 -S-9-Hanttsc-N ¹ -Me)(Ph ₃ P) ₂] 34	F2
[CuI(η^1 -S-9-Hanttsc-N ¹ -Me)(Ph ₃ P) ₂] 33	F3
[Ag ₂ Cl ₂ (μ_2 -S-9-Hanttsc-N ¹ -Me)(Ph ₃ P) ₂] 38	F4
[Ag ₂ Br ₂ (μ_2 -S-9-Hanttsc-N ¹ -Me)(Ph ₃ P) ₂] 39	F5

7.2 Antimicrobial activities (Antifungal and Antibacterial):

All the synthesized compounds (ligands and their complexes) were investigated for their activity against bacterial and fungal strains. The media used for this purpose are Nutrient agar media and potato dextrose media.

Media preparation: - 28 grams of nutrient agar and 39.0 grams of Potato dextrose agar was added to the 1 liter of double distilled water separately, it was mixed thoroughly and pH was adjusted at 7.5 ± 0.2 . The solution was heated to dissolve the ingredients completely after which the media was autoclaved at 121°C for 45 minutes at 15lbs pressure. After autoclaving, 15-20 ml of that media was poured into petri dish for studying antimicrobial activities.

Anti-microbial strains used:- The cultures used in this experiment were ordered from NCIM Pune (India). The anti-microbial tests were conducted on two fungal species *Aspergillus fumigates* and *Pencillium chrysogenum* (NCIM 902 & 738) (NCIM = National collection of

industrial microorganisms) and on two bacterial species *Salmonella typhimurium* and *E.coli* (NCIM, 2501 & 2563) by following standard literature reported procedure of disk-diffusion method [Jain *et al.*, 2003][102]. Whatman no. 1 filter paper disks were sterilized by autoclaving at 160⁰C for 1 h. Then the sterile disks were impregnated with the test compounds of different concentrations (125ppm, 250 ppm, 500 ppm and 1000 ppm). Cultures having 10⁵CFU/mL were used against each concentration levels. The impregnated disks were placed on the medium suitably spaced apart, and the plates were incubated at 37⁰C for 24 h and 28⁰C for fungal species. Dimethyl sulfoxide (DMSO) was used for dissolving compound. Finally the zones of inhibition were measured in mm scale. The results of anti-bacterial activities are summarized in the respective tables.

7.2.1 Discussion on Antifungal activity:

Antifungal activity of ligand Indole-3-carboxyaldehyde thiosemicarbazones (**B**) and its metal complexes, (**B1-B5**) were evaluated against *Aspergillus fumigates* (**a**) and *Pencillium chrysogenum* (**b**) and show a moderate activity vis-à-vis free ligands. The antifungal activity significantly enhanced in complexes **B3-B5**. Moreover, **B2** (MIC=7mm 1000ppm) against *Aspergillus fumigates* and **B1, B2** (MIC=7mm 1000ppm) against *Pencillium chrysogenum* show effective antifungal inhibition among **B1-B5** complexes (Table-36, Figure-16).

Compound **C** did not show any antifungal activity at all measured concentrations against and are even lesser active than **B** against *Aspergillus fumigates* and *Pencillium chrysogenum*) strains. **C1, C2** and **C5** matched their ligand in inhibiting the growth of microbes. Complex **C3** (MIC of 5mm at 1000ppm and 7mm at 1000ppm and **C4** (MIC of 7mm at 1000ppm are mildly active (Table-37, Figure-18).

Anti-fungal activity of compound **D** was found significantly high as compared to **B** and **C**. Compound **D** show considerable antifungal activity while activity of its complexes **D2-D5** increased along with the concentration and show moderate to good activity vis-à-vis free ligand. Moderate activity was observed in complex **D2, D3** and **D5** interestingly **D3** and **D5** are equipotent (MIC=8mm 1000ppm) (Table-38, Figure-20).

Compound **A** exhibit moderate antifungal activity and are effective as compared to **C**. Except for complex **A2** all the complexes are potent in inhibiting the fungal growth. Complex **A1** and **A4** were screened equipotent (MIC=7mm at 1000ppm) against *Pencillium chrysogenum*.

Copper complex **A3** and silver complexes **A4** exhibited moderate antifungal activity ranging from 3-6mm and 3-7mm respectively (Table-39, Figure-22).

Antifungal activity of compound **E** was found moderately active than **C** in inhibiting the fungal activity. Except for **E3** which show no activity against the two strains, all the other complexes of **E** (**E1-E5**) show moderate to good inhibiting activity. The activity is quite significant and equally potent in **E1** (2-7mm) and **E2** (3-7mm) (Table-40, Figure-24).

An exceptional trend was obtained in the antifungal activity of compounds **F** and **F1-F5** were in **F** and its **F1-F3** complexes exhibited no inhibiting antifungal against *Aspergillus fumigates* except for complex **F4**(MIC=4mm at 1000ppm). In contrast its complexes (**F1-F5**) were found significantly active against *Pencillium chrysogenum* strain (Table-41, Figure-26).

7.2.2 Discussion on Antibacterial activity:

Compound **B** and its complexes **B1-B5** were screened for antibacterial activity against *Salmonella typhimurium* and *E.coli*. In contrast to its antifungal activity all the **B1-B5** complexes were not effective as they did not inhibit the growth of bacteria even with increasing concentration. Except for **B4** (MIC = 2-5mm) which was found mildly active against both the strains at all measured concentrations (Table-36, Figure-17).

Compound **C** did not show any antifungal activity at all measured concentrations as was the case in **B**. All the complexes of **C**, (**C1-C5**) except for complex **C4** (MIC=5-6mm) and **C3** (MIC=2-5mm) did not show any activity. **C4** and **C5** were found active and appear to show significant yet moderate microbial inhibiting character against (gram-negative) *Salmonella typhimurium* and *E.coli*. Results probably suggest that substitution of methyl group at N¹ atom in **C** decreased antifungal as well as antibacterial activity (Table-37, Figure-19)

An interesting trend was observed in case of compound **D** and its complexes **D1-D5** compared to **C**. While, **D** did not show any antifungal activity however, to our surprise it showed considerable antibacterial activity. All the complexes **D1-D5** compared to parent ligand exhibit moderate anti bacterial activity and inhibit growth of microbes at all measured concentrations. Maximum antibacterial activity (MIC=8mm at 1000pm) was shown by **D5** against *E.coli* strain. Substitution of methoxy group present at 5th position of indole ring probably has the effect in increasing the activity against all the strains (Table-38, Figure-21).

Similarly, in compound **A** (as in the case of **D**) exhibit moderate antibacterial activity which got enhanced in complexes **A1-A5**. Interestingly, antibacterial activity screened against *Salmonella typhimurium* and *E.coli* in all the copper and silver complexes exhibited a similar trend however complex **A3** (at 125ppm, 250ppm) and **A5** (at 125ppm) did not inhibit antibacterial growth (Table-39, Figure-23).

Compound **E** and its complexes **E1-E5** shows moderate antibacterial activity and is similar to activities shown by **A(A1-A5)**. The activity in ligand got enhanced on complexation and increases with the increasing concentration. **E4** and **E5** (MIC=7mm at 1000ppm) show significant antibacterial activity except for **E3** (Table-40, Figure-25).

Compound **F** show no antifungal activity against *Salmonella typhimurium* and *E.coli*. In contrast complex **F1** (MIC=2-6mm) and **F4** (MIC=1-6mm) were screened mildly active. All the other complexes were either ineffective or show little antibacterial activity against the strains used (Table-41, Figure-27).

All the metal complexes of both copper and silver with various ligands screened for different antimicrobial (antifungal and antibacterial) activity have shown enhanced and effective inhibiting potency (MIC). Complex formation generally results in increased fungicidal and bactericidal activity. Complexes normally have more potency and enhanced activity as compared to ligands. It is suggested that formation of complexes results in deactivation of various cellular enzymes playing vital role in various metabolic pathways of pathogens. Further bridging and chelation in complexes results in increased activity possibly due to partial sharing of positive charge of the metal with the donor atoms of ligand resulting in delocalisation over the entire chelate ring. This enhanced potency in complexes increases lipophilic character thereby favouring permeation through lipid layers of microbes.

7.2.3 Antifungal and Antibacterial activity of indole-3-thiosemicarbazone (B) and its complexes (B1-B5):

Table-36: Antifungal and antibacterial activity of B and its complexes B1-B5.

	(Zone in inhibition in mm)							
	Antifungal activity				Antibacterial activity			
	<i>Aspergillus fumigates</i> (NCIM 902)		<i>Pencillium chrysogenum</i> (NCIM 738)		<i>Salmonella typhimurium</i> (NCIM 2501)		<i>Escherichia coli</i> (NCIM 2563)	
	125 (ppm)	250 (ppm)	500 (ppm)	1000 (ppm)	125 (ppm)	250 (ppm)	500 (ppm)	1000 (ppm)
B	0	0	2	4	0	0	3	5
B1	0	0	0	2	0	3	5	7
B2	0	3	5	7	2	3	5	7
B3	1	2	2	3	3	3	5	5
B4	1	2	3	3	2	2	2	5
B5	1	1	1	3	2	2	2	4

#Minimum inhibitory concentration MIC (ppm) values are given in the table, (MIC) i.e. the lowest concentration of drug which completely inhibit bacterial/fungal growth. Diameter of inhibition zone was measured in mm.

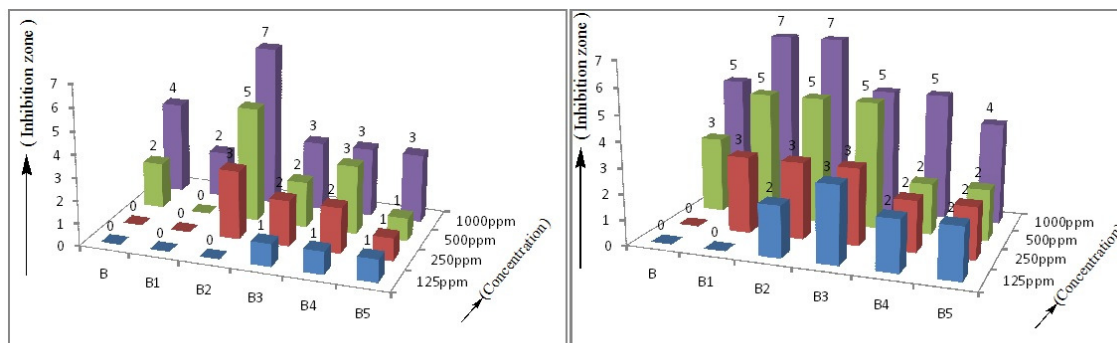


Figure-16: A comparative presentation of antifungal activity against *Aspergillus fumigates* (a) and *Pencillium chrysogenum* (b) of B and complexes B1-B5 with numbering scheme.

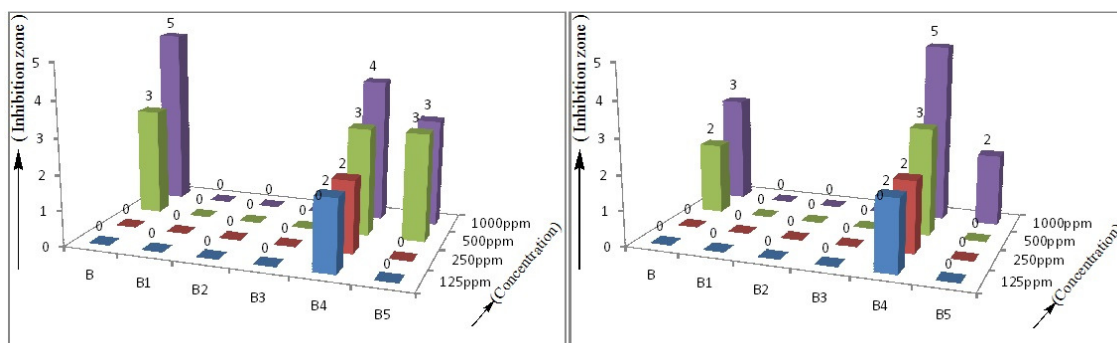


Figure-17: A comparative presentation of antibacterial activity against *Salmonella typhimurium* (c) and *E. coli* (d) of ligand B and complexes B1-B5 with numbering scheme.

7.2.4 Antifungal and Antibacterial activity of indole-N¹-methyl-3-thiosemicarbazone (C) and its complexes (C1-C5):

Table-37: Antifungal and antibacterial activity of ligand C and its complexes C1-C5.

	(Zone in inhibition in mm)							
	Antifungal activity				Antibacterial activity			
	<i>Aspergillus fumigates</i> (NCIM 902)		<i>Pencillium chrysogenum</i> (NCIM 738)		<i>Salmonella typhimurium</i> (NCIM 2501)		<i>Escherichia coli</i> (NCIM 2563)	
	125 (ppm)	250 (ppm)	500 (ppm)	1000 (ppm)	125 (ppm)	250 (ppm)	500 (ppm)	1000 (ppm)
C	0	0	0	0	0	0	0	0
C1	0	0	0	0	0	0	0	3
C2	0	0	0	5	0	0	3	5
C3	0	0	5	5	4	4	5	7
C4	2	3	5	5	3	4	5	7
C5	0	0	2	4	0	0	0	0

#Minimum inhibitory concentration MIC (ppm) values are given in the table (MIC) i.e. the lowest concentration of drug which completely inhibit bacterial/fungal growth. Diameter of inhibition zone was measured in mm.

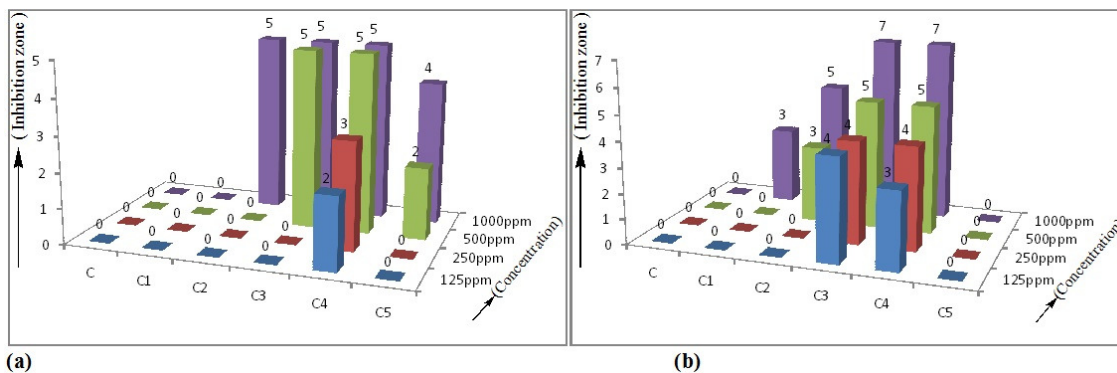


Figure-18: A comparative presentation of antifungal activity against *Aspergillus fumigates* (a) and *Pencillium chrysogenum* (b) of C and complexes C1-C5 with numbering scheme.

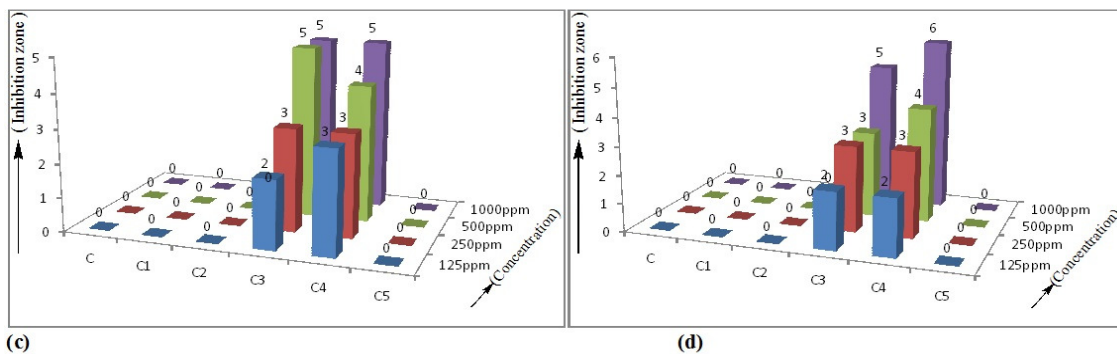


Figure-19: A comparative presentation of antibacterial activity against *Salmonella typhimurium* (c) and *E. coli* (d) of C and complexes C1-C5 with numbering scheme.

7.2.5 Antifungal and Antibacterial activity of 5-methoxy indole-3-thiosemicarbazone (D) and its complexes (D1-D5):

Table-38: Antifungal and antibacterial activity of D and its complexes D1-D5.

	(Zone in inhibition in mm)							
	Antifungal activity				Antibacterial activity			
	<i>Aspergillus fumigates</i> (NCIM 902)		<i>Pencillium chrysogenum</i> (NCIM 738)		<i>Salmonella typhimurium</i> (NCIM 2501)		<i>Escherichia coli</i> (NCIM 2563)	
	125 (ppm)	250 (ppm)	500 (ppm)	1000 (ppm)	125 (ppm)	250 (ppm)	500 (ppm)	1000 (ppm)
D	1	1	2	4	0	1	3	5
D1	2	4	6	2	3	5	5	2
D2	0	2	2	4	4	4	6	9
D3	0	2	4	7	3	5	5	8
D4	1	1	2	3	2	2	3	3
D5	1	2	2	2	1	3	5	8

#Minimum inhibitory concentration MIC (ppm) values are given in the table (MIC) i.e. the lowest concentration of drug which completely inhibit bacterial/fungal growth. Diameter of inhibition zone was measured in mm.

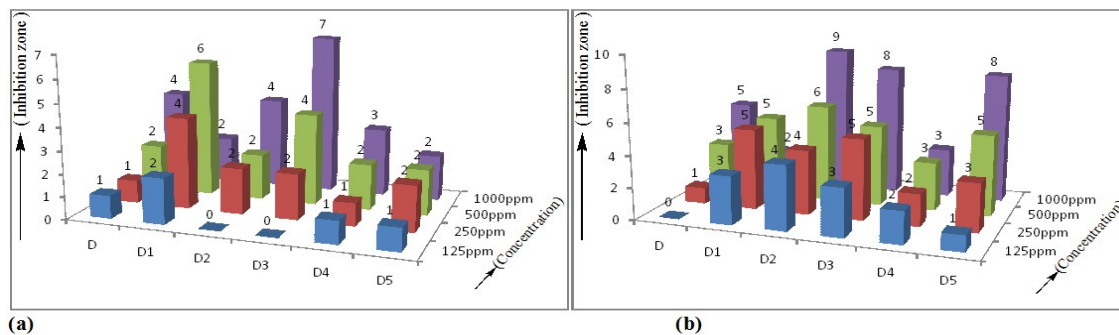


Figure-20: A comparative presentation of antifungal activity against *Aspergillus fumigates* (a) and *Pencillium chrysogenum* (b) of D and complex D1-D5 with numbering scheme.

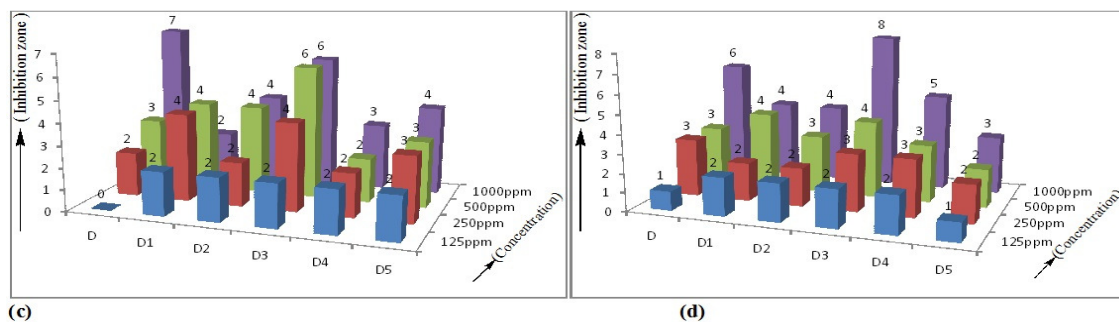


Figure-21: A comparative presentation of antibacterial activity against *Salmonella typhimurium* (c) and *E.coli* (d) of D and complex D1-D5 with numbering scheme.

7.2.6 Antifungal and Antibacterial activity of 5-methoxy indole-N¹-methyl-3-thiosemicarbazone (A) and its complexes (A1-A5):

Table-39: Antifungal and antibacterial activity of ligand A and its complexes A1-A5.

	(Zone in inhibition in mm)							
	Antifungal activity				Antibacterial activity			
	<i>Aspergillus fumigates</i> (NCIM 902)		<i>Pencillium chrysogenum</i> (NCIM 738)		<i>Salmonella typhimurium</i> (NCIM 2501)		<i>Escherichia coli</i> (NCIM 2563)	
	125 (ppm)	250 (ppm)	500 (ppm)	1000 (ppm)	125 (ppm)	250 (ppm)	500 (ppm)	1000 (ppm)
A	0	2	2	4	1	2	3	5
A1	0	3	5	7	2	2	4	7
A2	0	0	0	0	0	1	1	5
A3	3	3	5	6	2	4	4	6
A4	1	1	4	4	3	5	5	7
A5	1	1	1	3	1	1	2	2

#Minimum inhibitory concentration MIC (ppm) values are given in the table (MIC) i.e. the lowest concentration of drug which completely inhibit bacterial/fungal growth. Diameter of inhibition zone was measured in mm.

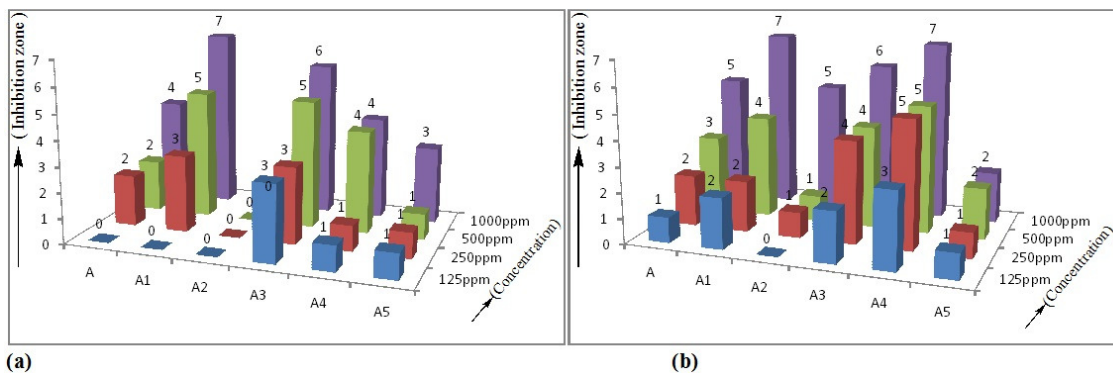


Figure-22: A comparative presentation of antifungal activity against *Aspergillus fumigates* (a) and *Pencillium chrysogenum* (b) of A and complex A1-A5 with numbering scheme.

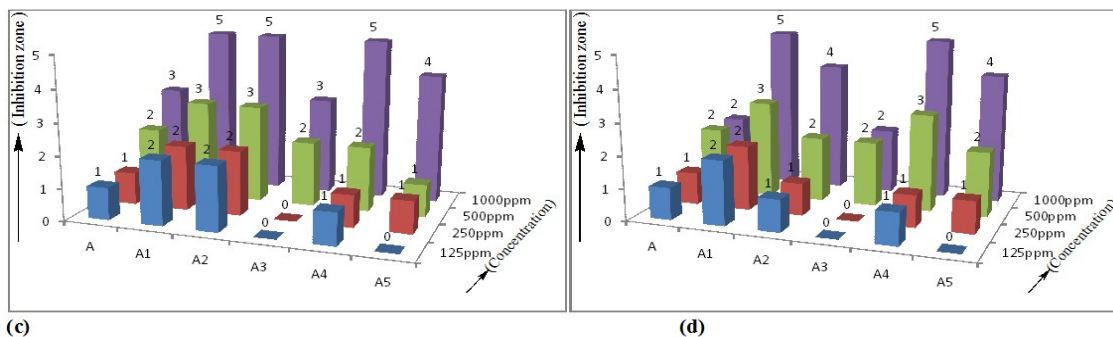


Figure-23: A comparative presentation of antibacterial activity against *Salmonella typhimurium* (c) and *E.coli* (d) of A and complex A1-A5 with numbering scheme.

7.2.7 Antifungal and Antibacterial activity of 9-anthraldehyde thiosemicarbazones (E) and its complexes (E1-E5):

Table-40 : Antifungal and antibacterial activity of ligand E and its complexes E1-E5.

	(Zone in inhibition in mm)							
	Antifungal activity				Antibacterial activity			
	<i>Aspergillus fumigates</i> (NCIM 902)		<i>Pencillium chrysogenum</i> (NCIM 738)		<i>Salmonella typhimurium</i> (NCIM 2501)		<i>Escherichia coli</i> (NCIM 2563)	
	125 (ppm)	250 (ppm)	500 (ppm)	1000 (ppm)	125 (ppm)	250 (ppm)	500 (ppm)	1000 (ppm)
E	2	3	3	5	2	2	3	4
E1	2	4	4	7	3	3	5	6
E2	2	2	3	5	3	3	5	5
E3	0	0	0	0	0	0	0	0
E4	0	1	2	3	2	2	3	5
E5	2	2	4	6	2	2	4	5

#Minimum inhibitory concentration MIC (ppm) values are given in the table (MIC) i.e. the lowest concentration of drug which completely inhibit bacterial/fungal growth. Diameter of inhibition zone was measured in mm.

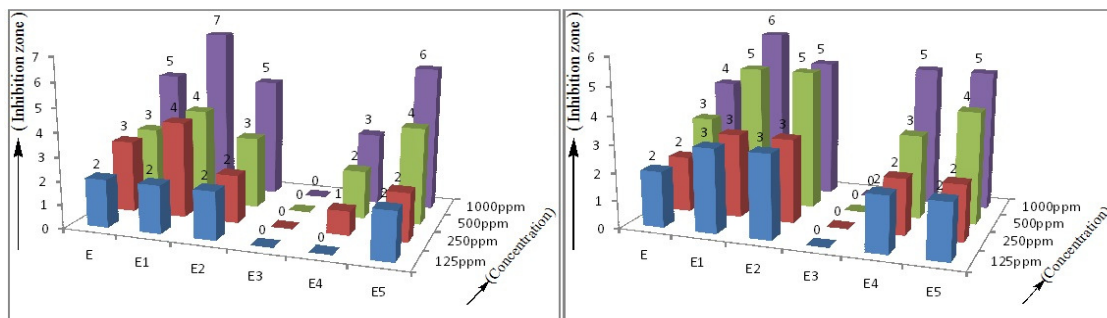


Figure-24: A comparative presentation of antifungal activity against *Aspergillus fumigates* (a) and *Pencillium chrysogenum* (b) of E and complexes E1-E5 with numbering scheme.

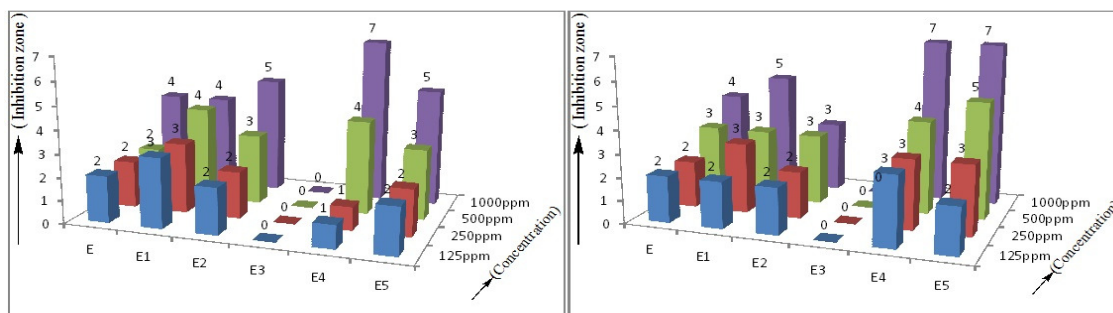


Figure-25: A comparative presentation of antibacterial activity against *Salmonella typhimurium* (c) and *E. coli* (d) of E and complexes E1-E5 with numbering scheme.

7.2.8 Antifungal and Antibacterial activity of (9-anthraldehyde-N¹-methyl-3-thiosemicarbazone (F) and complexes (F1-F5):

Table-41: Antifungal and antibacterial activity of ligand F and its complexes F1-F5.

	(Zone in inhibition in mm)							
	Antifungal activity				Antibacterial activity			
	<i>Aspergillus fumigates</i> (NCIM 902)		<i>Pencillium chrysogenum</i> (NCIM 738)		<i>Salmonella typhimurium</i> (NCIM 2501)		<i>Escherichia coli</i> (NCIM 2563)	
	125 (ppm)	250 (ppm)	500 (ppm)	1000 (ppm)	125 (ppm)	250 (ppm)	500 (ppm)	1000 (ppm)
F	0	0	0	0	0	0	0	0
F1	0	0	0	0	3	3	5	7
F2	0	0	0	0	0	1	3	5
F3	0	0	0	0	0	2	2	3
F4	2	2	2	4	2	2	2	5
F5	0	0	2	4	0	2	2	3

#Minimum inhibitory concentration MIC (ppm) values are given in the table (MIC) i.e. the lowest concentration of drug which completely inhibit bacterial/fungal growth. Diameter of inhibition zone was measured in mm.

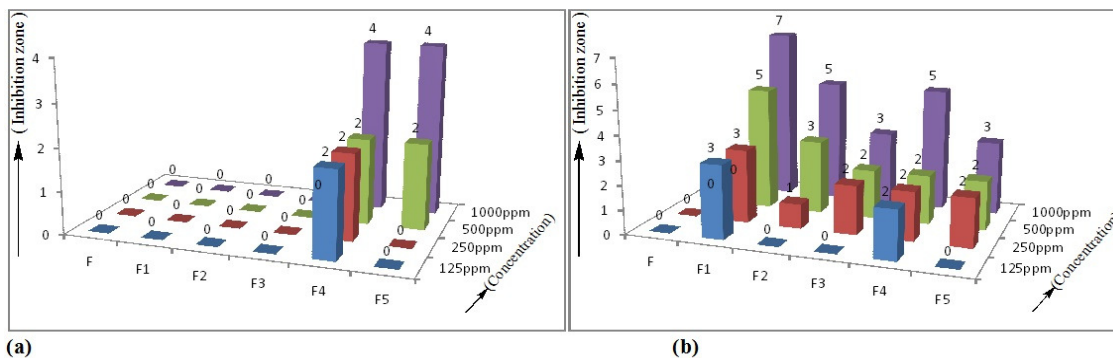


Figure-26: A comparative presentation of antifungal activity against *Aspergillus fumigates* (a) and *Pencillium chrysogenum* (b) of F and complexes F1-F5 with numbering scheme.

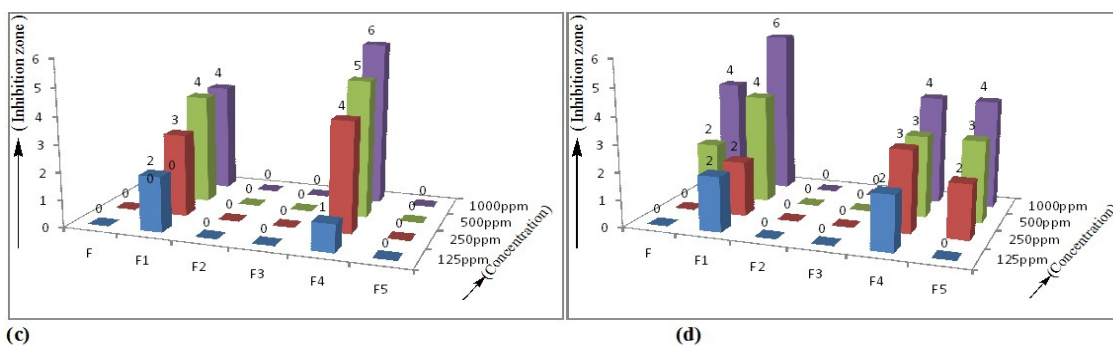


Figure-27: A comparative presentation of antibacterial activity against *Salmonella typhimurium* (c) and *E. coli* (d) of F and complexes F1-F5 with numbering scheme.

7.3 Anti-Tuberculosis Activity:

The anti mycobacterial activity of compounds (Ligands and their complexes) were assessed against *M. tuberculosis* using microplate Alamar Blue assay (MABA)[103]. This methodology used is non-toxic, uses a thermally stable reagent and show good correlation with propotional and BACTEC radiometric method. Briefly, 200µl of sterile de-ionized water was added to all outer perimeter wells of sterile 96 wells plate to minimized evaporation of medium in the test wells during incubation. The 96 wells plate received 100 µl of the Middlebrook 7H9 broth and serial dilution of compounds were made directly on plate. The final drug concentrations tested were 100 to 0.2µg/ml. Each test was carried in triplicate. Plates were covered and sealed with parafilm and incubated at 37°C for five days in sealed plastic bags with 5% CO₂ atmosphere. After this time, 25µl of freshly prepared 1:1 mixture of Almar Blue reagent and 10% tween 80 was added to the plate and incubated for 24 hrs.

A blue color in the well was interpreted as no bacterial growth, and pink color was scored as growth. The MIC was defined as lowest drug concentration which prevented the color change from blue to pink. Pyrazinamide, ciprofloxacin and streptomycin were included as standard drugs. The acceptable range, (MIC) of the standard drugs are 3.125 µg/ml, 3.125 µg/ml and 6.25 µg/ml respectively.

7.3.1 Anti-Tuberculosis activity of Indole-3-carboxyaldehyde thiosemicarbazones (B1) and complexes (B1-B5):

Anti- *M.Tuberculosis* activity of ligand (B) and their metal complexes (copper(I) and silver(I), B1-B5) was evaluated against *M.Tuberculosis* H₃₇RV strain ATCC 27294 and results for their Minimum Inhibitory Concentration (MIC) are reported in Table 42. Standard drugs (already in practice) used for comparative analysis are streptomycin, ciprofloxacin and pyrazinamide. MIC inhibition zones for these drugs are 6.25 µg/ml, 3.125 µg/ml and 3.125 µg/ml respectively (Figure-28).

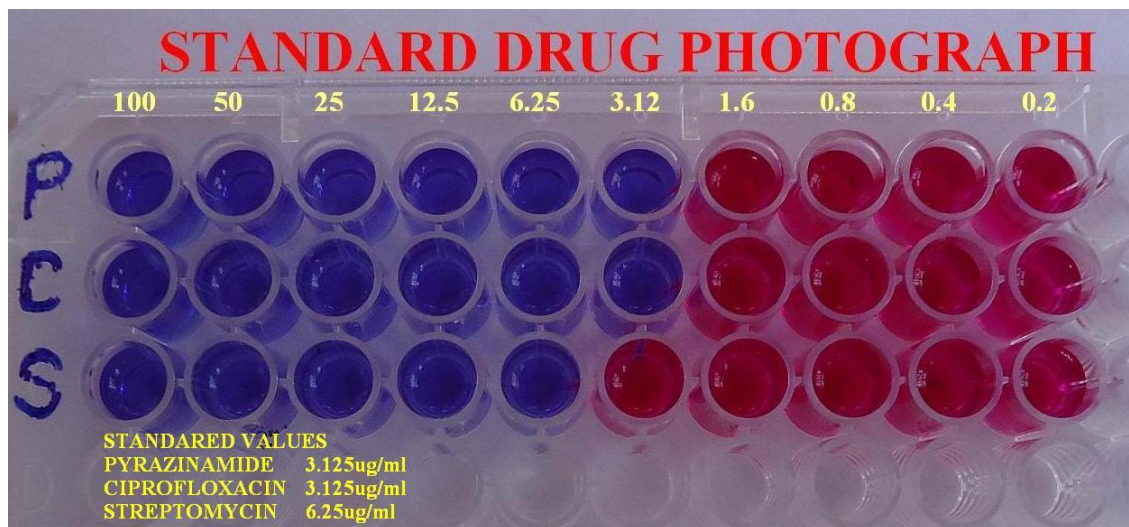


Figure-28: MIC inhibition zones ($\mu\text{g/ml}$) of standard drugs.

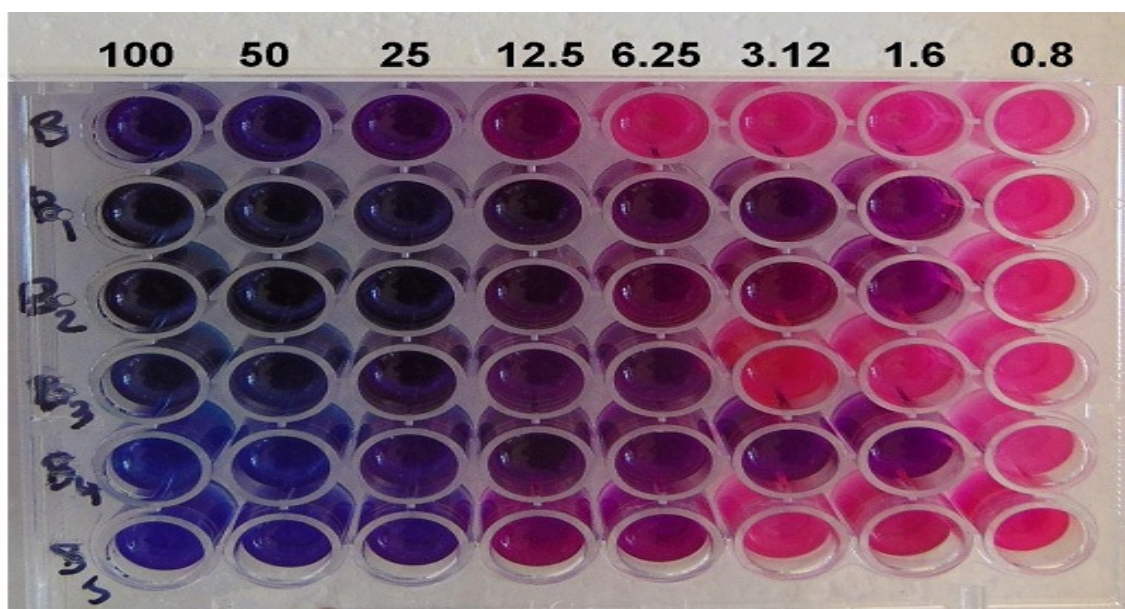


Figure-29: MIC inhibition zones ($\mu\text{g/ml}$) of compounds **B**, **B1-B5**.

The compound **B** (ligand) was found active at 12.5 $\mu\text{g/ml}$ concentration. The activity of compound **B** got enhanced on complexation with copper(I) and silver(I) **B1-B5**(Figure 29). More significant results were obtained for compounds **B1**, **B2** and **B4**(MIC = 1.6 $\mu\text{g/ml}$), where the activity was found to be not even more than the standard drugs used for comparison, but also the “second line” drugs such as streptomycin (MIC = 6.25 $\mu\text{g/ml}$) ciprofloxacin (MIC = 3.125 $\mu\text{g/ml}$) and pyrazinamide (MIC = 3.125 $\mu\text{g/ml}$) and some reported drugs viz clarithromycin (MIC = 8.0-16 $\mu\text{g/ml}$), tobramycin (MIC = 4.0-8.0 $\mu\text{g/ml}$)

[104].The observed activity of compounds **B** may be due to the presence of indole ring as reported in literature [97] or due to the N, S- donor fragment of thiosemicarbazone. The enhancement in the activity in compounds **B1-B5** can be related to: (i) Electronegativity of halides attached to metal (ii) increased electron density due to phenyl rings of triphenylphosphine molecule.

Table-42: Anti-tuberculosis activity of synthesised compounds (B, B1-B5).

S. No	Compound	Mycobacterium tuberculosis H37RV strain							
		MIC ($\mu\text{g}/\text{mL}$)							
		100	50	25	12.5	6.25	3.12	1.6	0.8
1.	B	S	S	S	S	R	R	R	R
2.	B1	S	S	S	S	S	S	S	R
3.	B2	S	S	S	S	S	S	S	R
4.	B3	S	S	S	S	S	R	R	R
5.	B4	S	S	S	S	S	S	S	R
6.	B5	S	S	S	S	S	R	R	R
7.	Pyrazinamide*	S	S	S	S	S	S	R	R
8.	Ciprofloxacin*	S	S	S	S	S	S	R	R
9.	Streptomycin*	S	S	S	S	S	R	R	R

* = Control

S= Sensitive, R = Resistant

7.3.2 Anti-Tuberculosis activity of indole-N¹-methyl-3-thiosemicarbazone (C1) and its complexes (C1-C5):

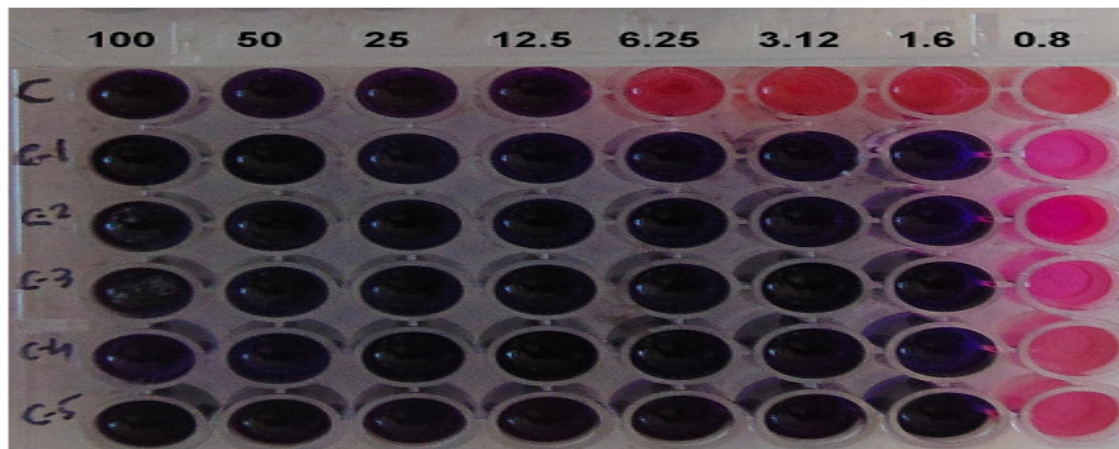


Figure-30: Anti-Tuberculosis MIC inhibition zones ($\mu\text{g}/\text{ml}$) of compounds C, C1-C5.

Compound **C** has shown similar anti-Tuberculosis activity as that of **B**. Observed MIC values for **C** is 12.5MIC $\mu\text{g}/\text{ml}$. There is unusual enhancement in anti-tuberculosis activity in all the complexes of **C** (**C1-C5**) by an equal amount (Table 43, Figure 30). The MIC value for **C1-C5** was found to be 1.6 $\mu\text{g}/\text{ml}$, which is significantly high as compare to

standard drugs used for experimental comparison as well as second line standard drugs mentioned earlier [104]. Substitution of methyl group at N¹ atom in **C** vis-à-vis **B**, enhanced the lipophilicity of compound. This increased lipophilicity facilitated the permeability of the compounds through the lipid rich bacterial wall thereby increased anti-microbial activity.

Table-43: Anti-tuberculosis activity of synthesised compounds (C, C1-C5)

S. No	Compound	Mycobacterium tuberculosis H37RV strain							
		MIC ($\mu\text{g/mL}$)							
		100	50	25	12.5	6.25	3.12	1.6	0.8
1.	C	S	S	S	S	R	R	R	R
2.	C1	S	S	S	S	S	S	S	R
3.	C2	S	S	S	S	S	S	S	R
4.	C3	S	S	S	S	S	S	S	R
5.	C4	S	S	S	S	S	S	S	R
6.	C5	S	S	S	S	S	S	S	R
7.	Pyrazinamide*	S	S	S	S	S	S	R	R
8.	Ciprofloxacin*	S	S	S	S	S	S	R	R
9.	Streptomycin*	S	S	S	S	S	R	R	R

* = Control

S= Sensitive, R = Resistant

7.3.3 Anti Tuberculosis Activity of 5-methoxy indole-3-thiosemicarbazone (D) and its complexes (D1-D5):

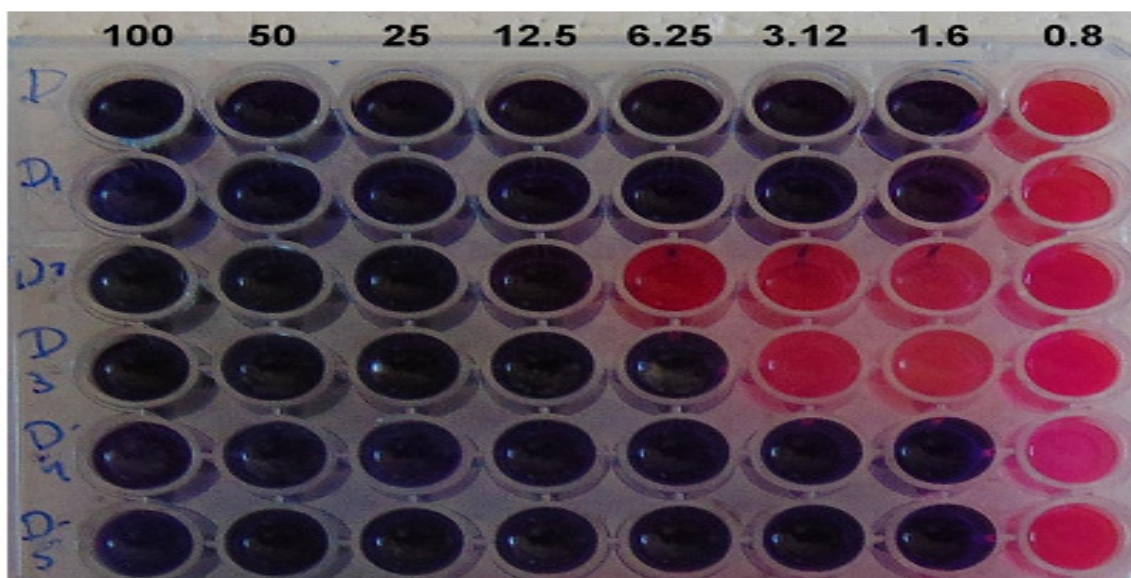


Figure-31: Anti-Tuberculosis MIC inhibition zones ($\mu\text{g/ml}$) of complex D, D1-D5.

Anti TB activity of compound **D** was found to be significantly high as compare to **B** and **C** (MIC, 1.6µg/ml). In compound **D**, methoxy group present at 5th position of indole ring has increased the lipophilicity of this compound and contributed toward enhanced activity. Compound **D1**, **D4** and **D5** showed similar anti TB activity as that of **D**, however a decrease in the activity has been observed in **D2** and **D3** (Table 44, Figure 31).

Table-44: Anti-tuberculosis activity of synthesised compounds (D, D1-D5)

S. No	Compound	Mycobacterium tuberculosis H37RV strain							
		MIC (µg /mL)							
		100	50	25	12.5	6.25	3.12	1.6	0.8
1.	D	S	S	S	S	S	S	S	R
2.	D1	S	S	S	S	S	S	S	R
3.	D2	S	S	S	S	R	R	R	R
4.	D3	S	S	S	S	S	R	R	R
5.	D4	S	S	S	S	S	S	S	R
6.	D5	S	S	S	S	S	S	S	R
7.	Pyrazinamide*	S	S	S	S	S	S	R	R
8.	Ciprofloxacin*	S	S	S	S	S	S	R	R
9.	Streptomycin*	S	S	S	S	S	R	R	R

* = Control

S= Sensitive, R = Resistant

7.3.4 Anti-Tuberculosis activity of 5-methoxy indole-N¹-methyl-3-thiosemicarbazone (A) and its complexes (A1-A5):

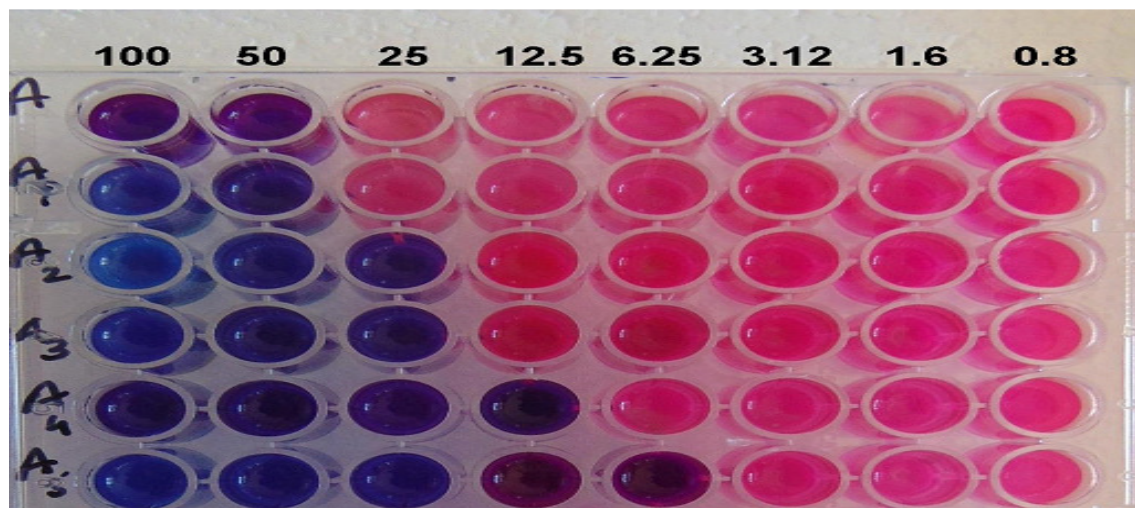


Figure-32: Anti-Tuberculosis MIC inhibition zones (µg/ml) of complex A, A1-A5.

An exceptional trend was obtained in the anti TB activity of compounds **A** and **A1-A5** (Table 44, Figure 32). The anti TB activity of **A** (MIC, 50 μ g/ml) was found to be much less than **B**, **C** and **D** in spite of the presence of indole ring in its structure. Probably the methoxy group at indole ring in **A** has an important role in decreasing its Anti TB activity. However, complexation of **A** with copper (I) (**A1-A3**) (MIC, 50-25 μ g/ml) and silver (I) (**A4** (MIC, and **A5**) (MIC, has enhanced its anti TB activity probably due to presence of phenyl rings of triphenylphosphine molecules. The enhancement in activity was found to be more in silver(I) complexes. (Table 45, Figure 32).

Table-45: Anti-tuberculosis activity of synthesised compounds (A, A1-A5)

S. No	Compound	Mycobacterium tuberculosis H37RV strain							
		MIC (μ g /mL)							
		100	50	25	12.5	6.25	3.12	1.6	0.8
1.	A	S	S	R	R	R	R	R	R
2.	A1	S	S	R	R	R	R	R	R
3.	A2	S	S	S	R	R	R	R	R
4.	A3	S	S	S	R	R	R	R	R
5.	A4	S	S	S	S	R	R	R	R
6.	A5	S	S	S	S	S	R	R	R
7.	Pyrazinamide*	S	S	S	S	S	S	R	R
8.	Ciprofloxacin*	S	S	S	S	S	S	R	R
9.	Streptomycin*	S	S	S	S	S	R	R	R

* = Control

S= Sensitive, R = Resistant

7.3.5 Anti-Tuberculosis activity of 9-anthraldehyde thiosemicarbazones (E) and its complexes (E1-E5):

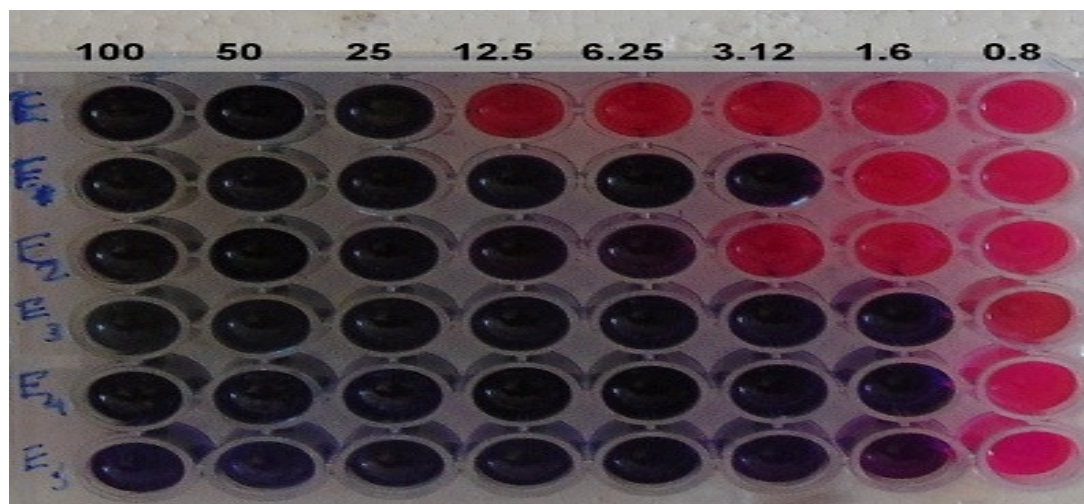


Figure-33: Anti-Tuberculosis MIC inhibition zones (μ g/ml) of complex E, E1-E5.

Anti TB activity of compound **E** (MIC, 50 μ g/ml) was found significantly active than than **A**. There is unusual enhancement in anti-tuberculosis activity in all the complexes of **E** (**E1-E5**) (Table 46, Figure 33). Compound **E3-E5** show a similar and effective trend as in **C1-C5** with MIC inhibition zones at (1.6 MIC μ g/ml). These significant results can be probably assigned to presence of phenyl ring of anthraldehyde and triphenylphosphine rings which results in increased delocalisation and electron density. Further, the assumed antimicrobial activity of thiosemicarbazones[89] and presence of sulfur enhances the lipophilicity and mycobacterial permeability of these complexes.

Table-46: Anti-tuberculosis activity of synthesised compounds (E, E1-E5)

S. No	Compound	Mycobacterium tuberculosis H37RV strain							
		MIC (μ g /mL)							
		100	50	25	12.5	6.25	3.12	1.6	0.8
1.	E	S	S	S	R	R	R	R	R
2.	E1	S	S	S	S	S	S	R	R
3.	E2	S	S	S	S	S	R	R	R
4.	E3	S	S	S	S	S	S	S	R
5.	E4	S	S	S	S	S	S	S	R
6.	E5	S	S	S	S	S	S	S	R
7.	Pyrazinamide*	S	S	S	S	S	S	R	R
8.	Ciprofloxacin*	S	S	S	S	S	S	R	R
9.	Streptomycin*	S	S	S	S	S	R	R	R

* = Control

S= Sensitive, R = Resistant

7.3.6 Anti-Tuberculosis activity of 9-anthraldehyde-N¹-methyl-3-thiosemicarbazone (F) and its complexes (F1-F5):

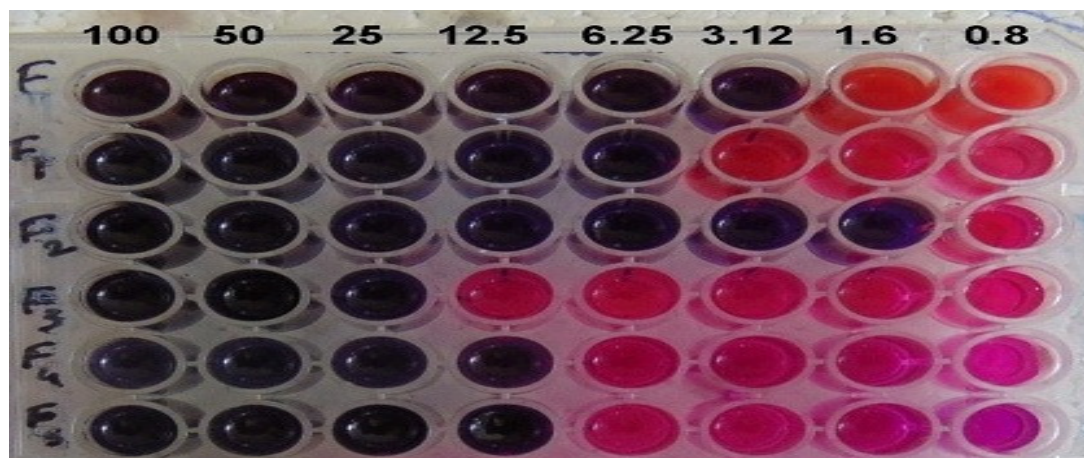


Figure-34: Anti-Tuberculosis MIC inhibition zones (μ g/ml) of complex F, F1-F5.

Compound **F** has shown interesting anti-*Tuberculosis* compared to activity shown by **A**. Observed MIC values for **C** is 3.12MIC $\mu\text{g/ml}$. There is unusual decrease in anti-tuberculosis activity in all the complexes of **E** (**E1-E5**) (Table 47, Figure 34) except in case of **E2** (1.6MIC $\mu\text{g/ml}$). Substitution of methyl group at N¹ atom in **E** vis-à-vis **F**, lowered the activity in complexes. Probably the dimeric structure of silver complexes with S-bridging hinders the interaction with the supposed mycobacterial receptor.

Table-47: Anti-tuberculosis activity of synthesised compounds (F, F1-F5)

S. No	Compound	Mycobacterium tuberculosis H37RV strain							
		MIC ($\mu\text{g/mL}$)							
		100	50	25	12.5	6.25	3.12	1.6	0.8
1.	F	S	S	S	S	S	S	R	R
2.	F1	S	S	S	S	S	R	R	R
3.	F2	S	S	S	S	S	S	S	R
4.	F3	S	S	S	R	R	R	R	R
5.	F4	S	S	S	S	R	R	R	R
6.	F5	S	S	S	S	R	R	R	R
7.	Pyrazinamide*	S	S	S	S	S	S	R	R
8.	Ciprofloxacin*	S	S	S	S	S	S	R	R
9.	Streptomycin*	S	S	S	S	S	R	R	R

* = Control

S= Sensitive, R = Resistant

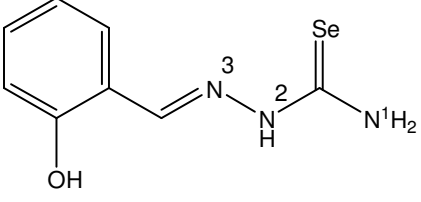
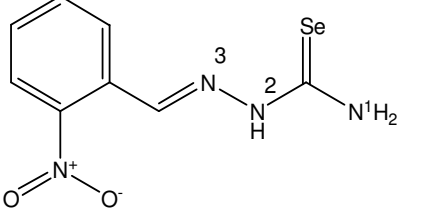
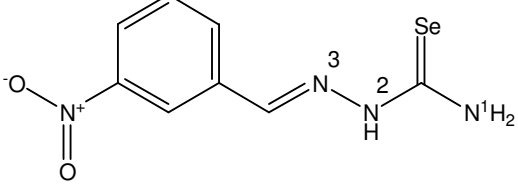
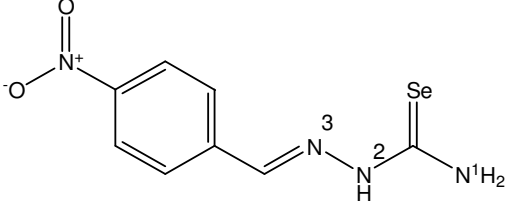
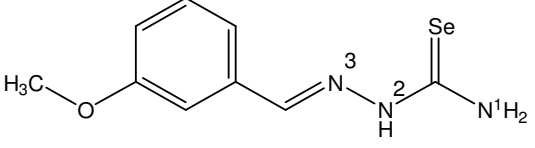
CHAPTER 8

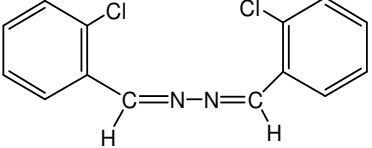
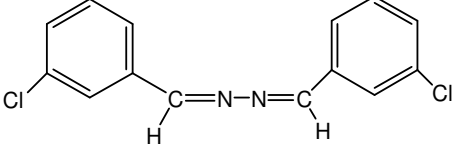
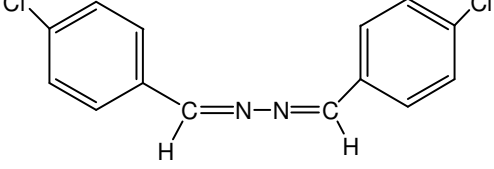
SELENOSEMICARBAZONES

8.1. Selenosemicarbazones:

A series of selenosemicarbazones H^7L - $H^{11}L$ were prepared by the reaction of various aldehydes with cyclohexanone selenosemicarbazone while similar reaction in $H^{12}L$ - $H^{14}L$ lead to dimerization resulting in the formation of azo compound.

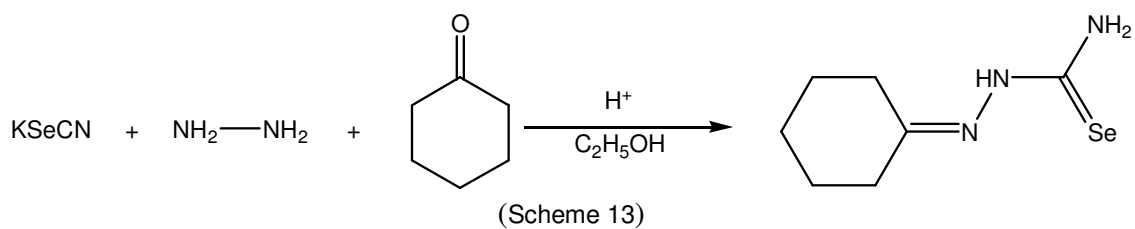
Table-48: List of ligands of Selenosemicarbazones prepared H^7L - $H^{11}L$ and dimerized azo compounds $H^{12}L$ - $H^{14}L$

{3-OH-Hbsesc (H^7L)}	
{2-NO ₂ -Hbsesc (H^8L)}	
{3-NO ₂ -Hbsesc (H^9L)}	
{4-NO ₂ -Hbsesc ($H^{10}L$)}	
{3-MeO-Hbsesc ($H^{11}L$)}	

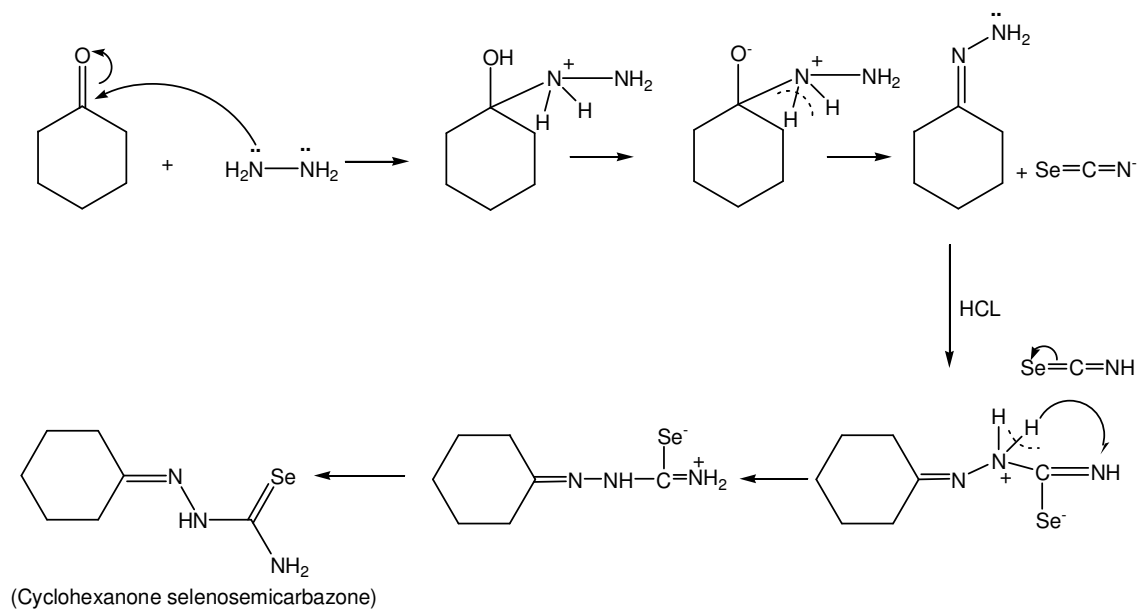
<p>{1,2-bis(2-chlorobenzylidene)hydrazine (H¹²L)}</p>	
<p>{1,2-bis(3-chlorobenzylidene)hydrazine (H¹³L)}</p>	
<p>{1,2-bis(4-chlorobenzylidene)hydrazine (H¹⁴L)}</p>	

8.2 Result and discussion:

Reaction of KSeCN, hydrazine hydrate and cyclohexanone in ethanol resulted in the formation of cyclohexanone selenosemicarbazone (Scheme 13). Acidic conditions are required for the formation of this ligand.

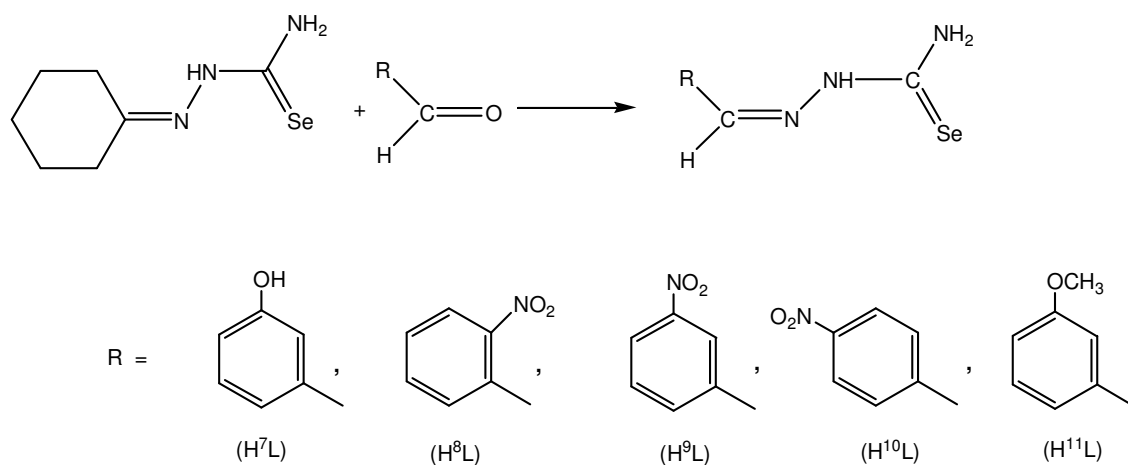


Proposed mechanism for this synthesis is given in Scheme 14.



(Scheme 14)

When cyclohexanone selenosemicarbazone was reacted with m-hydroxy benzaldehyde, o-nitro benzaldehyde, m-nitrobenzaldehyde, anisaldehyde in 1:1 ratio in methanol respective selenosemicarbazone were obtained. (Scheme 15)



(Scheme 15)

8.3 Discussion on IR spectroscopy:

$\nu(\text{NH}_2)$ band of cyclohexanone selenosemicarbazone appears in the range of 3362 - 3252 cm^{-1} in IR spectra (Table-49). This band shows high energy shift in ligands $\text{H}^7\text{L} - \text{H}^{11}\text{L}$ (3226-3428 cm^{-1}) vis-a-vis cyclohexanone selenosemicarbazone. The $\nu(-\text{NH}-)$ obtained in ligands 3043-3138 cm^{-1} which is at lower wave number vis-a-vis cyclohexanone selenosemicarbazone (3159 cm^{-1}).

The characteristic $\nu(\text{C}=\text{Se})$ band of cyclohexanone selenosemicarbazone appeared at 856 cm^{-1} this band shows high energy shift in ligands $\text{H}^7\text{L} - \text{H}^{11}\text{L}$ {835(H^7L), 848(H^8L), 835(H^9L), 855(H^{10}L), 868(H^{11}L)}. The shift in $\nu(\text{C}=\text{Se})$ band indicates formation of the ligand $\text{H}^7\text{L} - \text{H}^{11}\text{L}$.

Table-49: Important peaks in IR spectrum for cyclohexanone selenosemicarbazone and ligands $\text{H}^7\text{L} - \text{H}^{11}\text{L}$.

Compound	$\nu(\text{NH}_2)$	$\nu(-\text{NH}-)$	$\nu(\text{C}=\text{N}) + \nu(\text{C}=\text{C}) + \delta$ (NH_2)	$\nu(\text{C}=\text{Se})$
Cyclohexanone selenosemicarbazone	3362s 3252s	3159s	1639m, 1597s, 1491s	856s
H^7L	3423w 3226w	3043w	1645w, 1564w	835s
H^8L	3406s 3250s	3109s	1602s, 1566s, 1477s	848s
H^9L	3408m 3232m	3128m	1614s, 1597s, 1479s	835s
H^{10}L	3428m 3252m	3138m	1674sh, 1587s, 1497s	855s
H^{11}L	3383s 3246s	3047s	1600s, 1541s, 1464s	868s

8.4 Discussion on NMR spectroscopy:

Formation of cyclohexanone selenosemicarbazone was confirmed by NMR spectroscopy. In ^1H NMR, N^2H proton of this ligand appeared at $\delta 6.976$ ppm. Two broad singlets appeared at $\delta 7.664$ ppm and $\delta 6.976$ ppm due to non equivalent N^1H_2 proton. Proton of cyclic ring appeared in the range $\delta 2.96$ ppm- $\delta 1.6$ ppm.

The N^2H proton in selenosemicarbazone ligands (H^7L - H^{11}L) appeared in the range $\delta 10.30$ ppm- $\delta 11.94$ ppm. Signal due to $^1\text{NH}^2$ proton gets obscured by the signal of phenyl ring of seleno- ligand. Appearance of these signals ensure the presence of amino and amido group. The signal due to C^2H proton appeared in the range $\delta 8.55$ ppm- $\delta 8.89$ ppm in these ligands indicated the replacement of cyclic ring by aromatic ring. Presence of aromatic ring was also confirmed by the appearance of multiplet in the range of $\delta 6.93$ ppm - $\delta 8.48$ ppm. Additional singlet at $\delta 2.5$ ppm in ligand H^5L indicated the presence of methoxy group.

In ^{13}C NMR spectrum of selenosemicarbazone, C^1 and C^2 carbon appeared at $\delta 175.1$ ppm and $\delta 158.7$ ppm respectively. Other ring carbon appeared within $\delta 34.4$ ppm- $\delta 25.40$ ppm (Table-51).

Table-50: ^1H NMR signals for H^7L - H^{11}L (δ , ppm).

Complexes	(1H, N^2H)	(1H, C^2H)	(1H, N^1H_2)	(Ring protons),
H^7L [3-OH-Hbsesc]	11.36	8.89	obscured by ring proton	7.55-6.93
H^8L [2- NO_2 -bsesc]	11.94	8.62	obscured by ring proton	8.38-7.48
H^9L [3- NO_2 -bsesc]	11.79	8.63	obscured by ring proton	8.48-7.54
H^{10}L [4- NO_2 -bsesc]	10.30	8.54	obscured by ring proton	8.34-7.24
H^{11}L [3-MeO-Hbsesc]	-	8.55	obscured by ring proton	C^8 , 7.39(1H); $\text{C}^{4,6}$, 7.29; C^5 , 6.96, 3.79(s); O- CH_3 , 2.5

Table-51: ^{13}C NMR signals for H^7L - H^{11}L (δ , ppm).

Complexes	(C^1)	(C^2)	(Ring case),
H^7L [3-OH-Hbsesc]	164.93	160.04	C^4 , 133.66; C^3 , 132.78; C^5 , 119 ; C^8 , 117.5; C^6 , 117.3
H^8L [2- NO_2 -bsesc]	174.88	157.88	C^4 , 147.9; C^3 , 139.31; C^5 , 133.3 ; C^8 , 129.11; C^6 , 127.8;
H^9L [3- NO_2 -bsesc]	174.44	160.00	C^4 , 148.24; C^3 , 141.31; C^5 , 135.8; C^8 , 130.1; C^6 , 125.3
H^{10}L [4- NO_2 -bsesc]	190.43	151.19	123.61-151.19
H^{11}L [3-MeO-Hbsesc]	166.95	161.14	111.7-134.79 - OCH_3 , 54.88

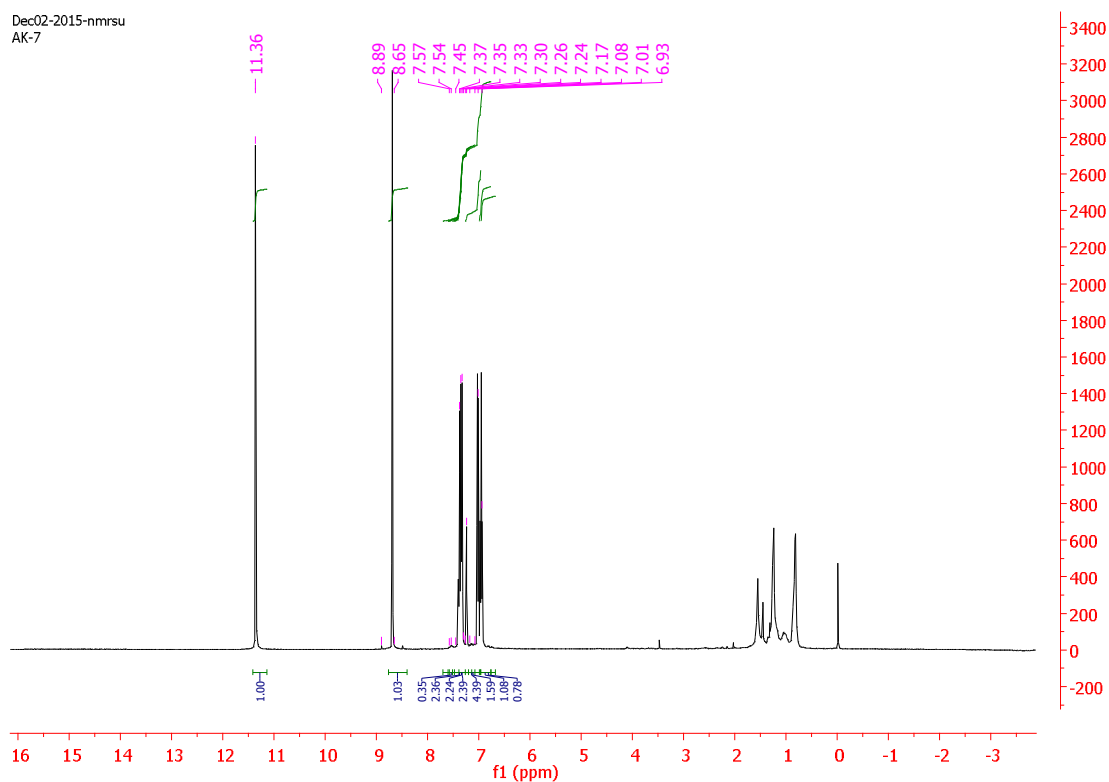


Figure 35a. ^1H NMR signals for 3-hydroxybenzaldehyde H^7L (δ , ppm).

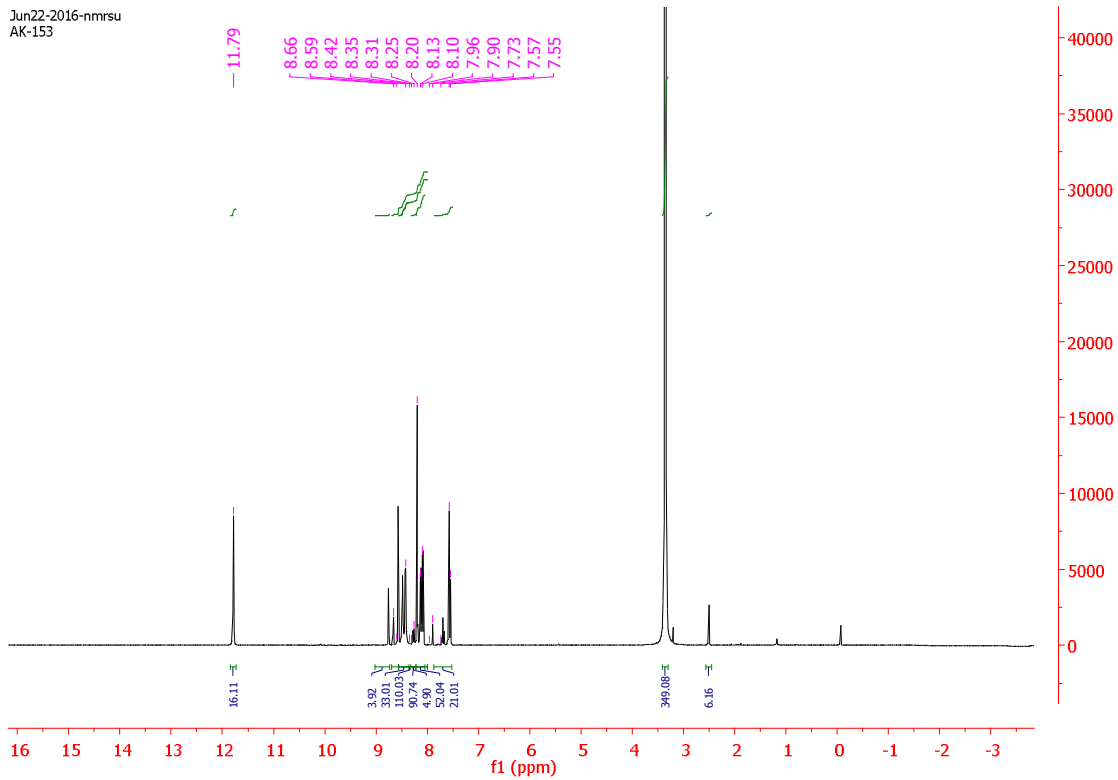


Figure-35b: ^1H NMR signals for (3-nitrobenzaldehyde) H^9L (δ , ppm).

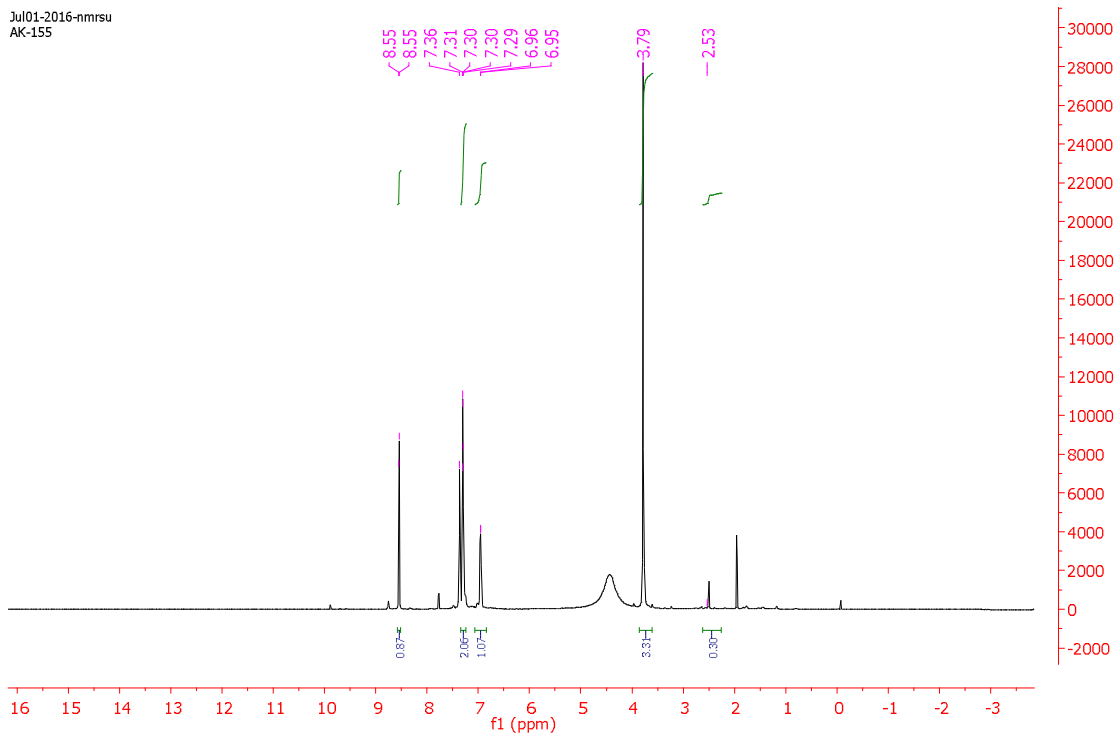


Figure-35c: ^1H NMR signals for (3-methoxybenzaldehyde) H^{11}L (δ , ppm).

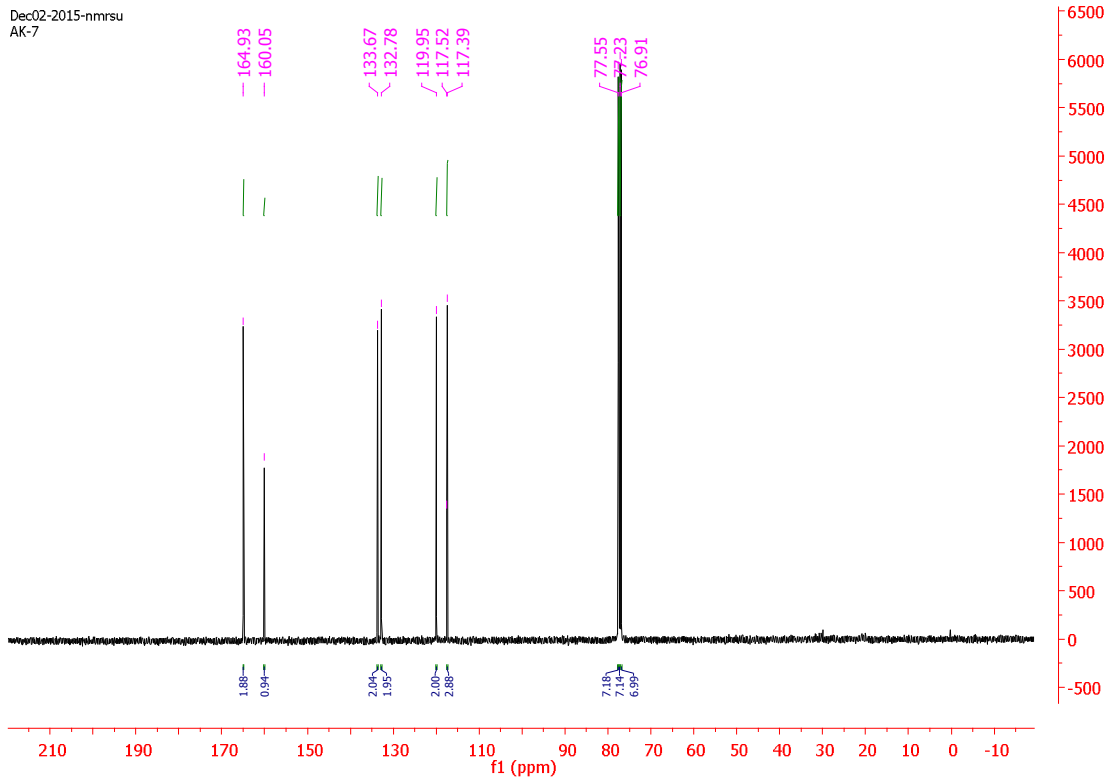


Figure-35d: ^{13}C NMR signals for 3-hydroxybenzaldehyde H^7L (δ , ppm).

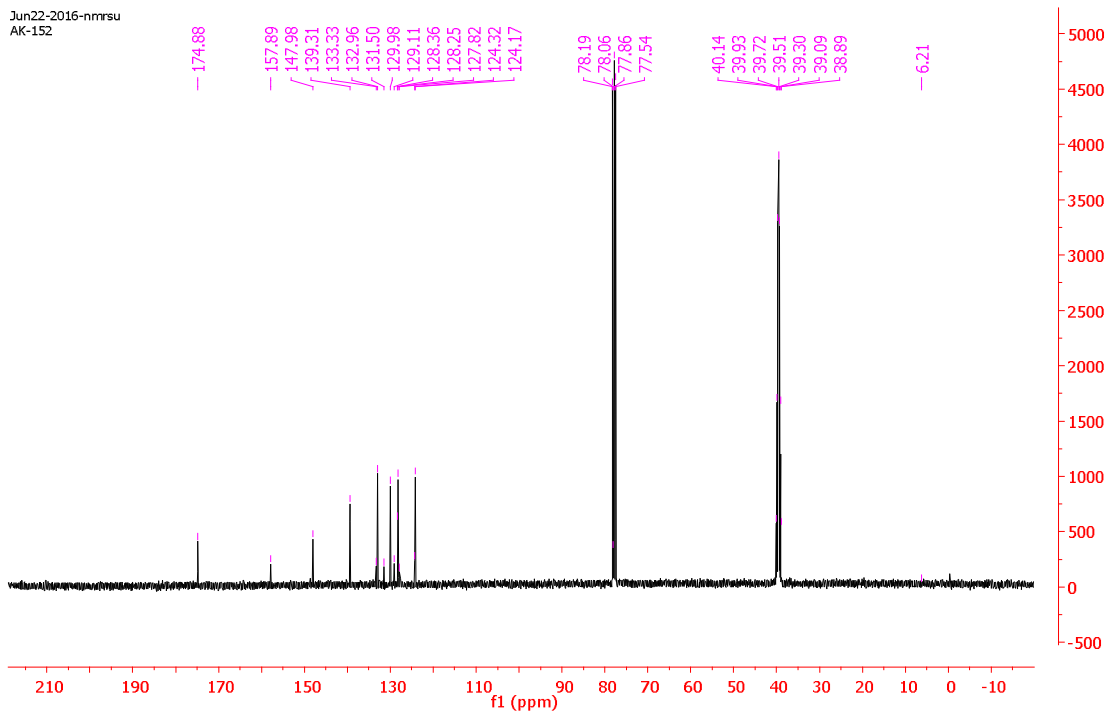


Figure-35e: ^{13}C NMR signals for (2-nitrobenzaldehyde) H^8L (δ , ppm)

Jun22-2016-nmrsu
AK-153

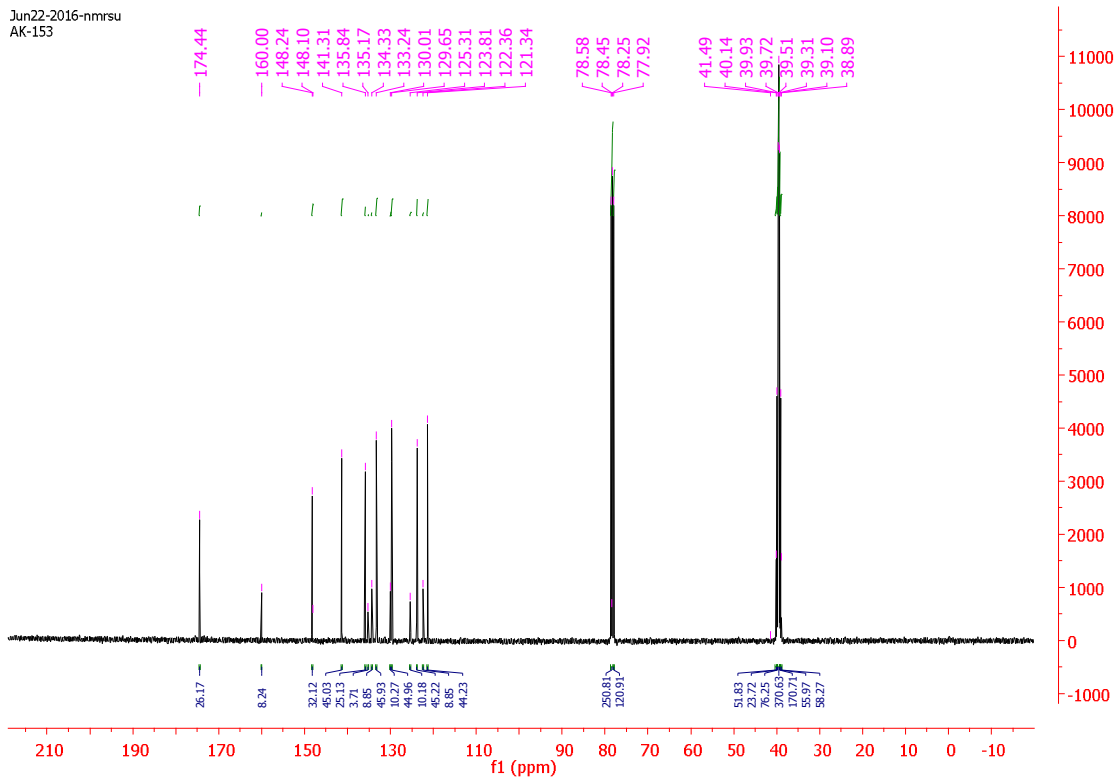


Figure-35f: ^{13}C NMR signals for (3-nitrobenzaldehyde) H^9L (δ , ppm).

Jul01-2016-nmrsu
AK-155

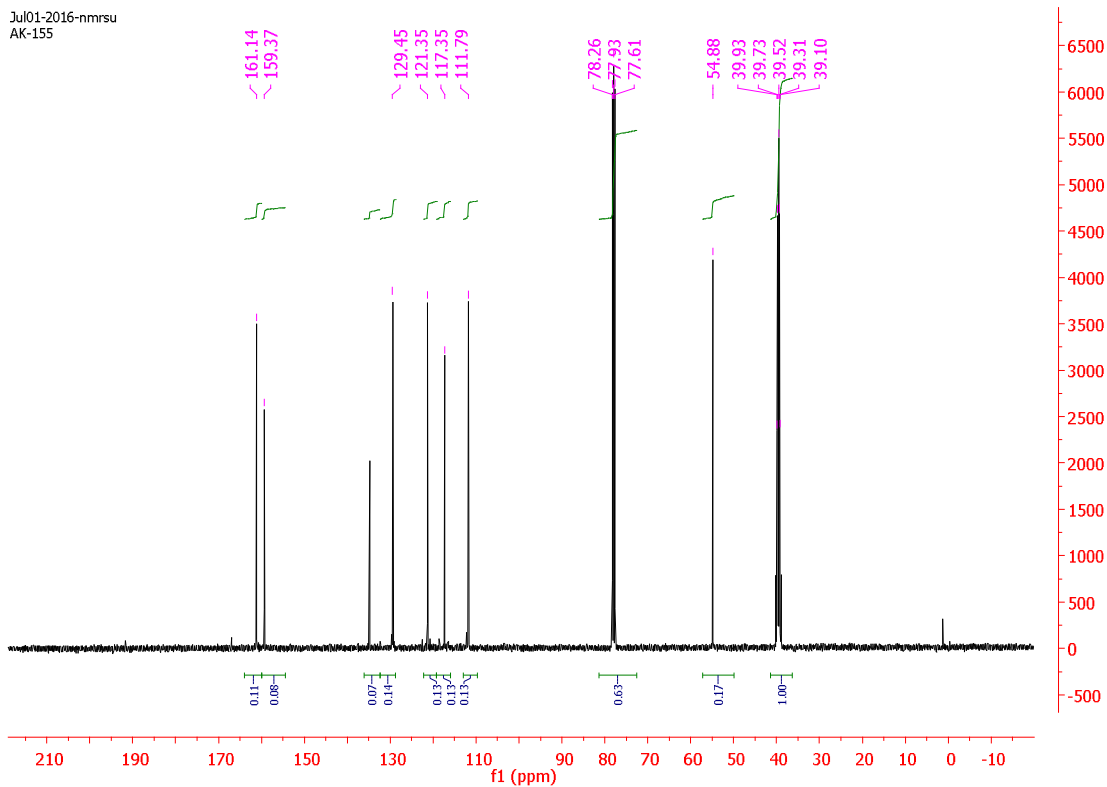


Figure-35g: ^{13}C NMR signals for (3-methoxybenzaldehyde) H^{11}L (δ , ppm).

In ^{13}C NMR of ligand C^1 and C^2 appeared in the range $\delta 164.93$ - $\delta 190.43$ ppm and $\delta 151.19$ - $\delta 161.14$ ppm respectively. Appearance of these two carbons ensures presence of selenosemicarbazones group. The ring carbon of phenyl ring in the ligands appeared in the range $\delta 117.3$ - 151.19 ppm. An additional peak at $\delta 54.58$ ppm in ligand H^5L appeared due to methoxy carbon.

The similar reaction of cyclohexanone selenosemicarbazone with o-, m-, p-chlorobenzaldehyde didn't yield respective selenosemicarbazones. The schiffs base dissociated and undergo dimerization to form azo compound. The formation of these azo compounds was established by ^1H and ^{13}C NMR. X-ray structure of azo compounds of m-chlorobenzaldehyde(H^{13}L) and p-chlorobenzaldehyde(H^{14}L) (Scheme 16) has been established.

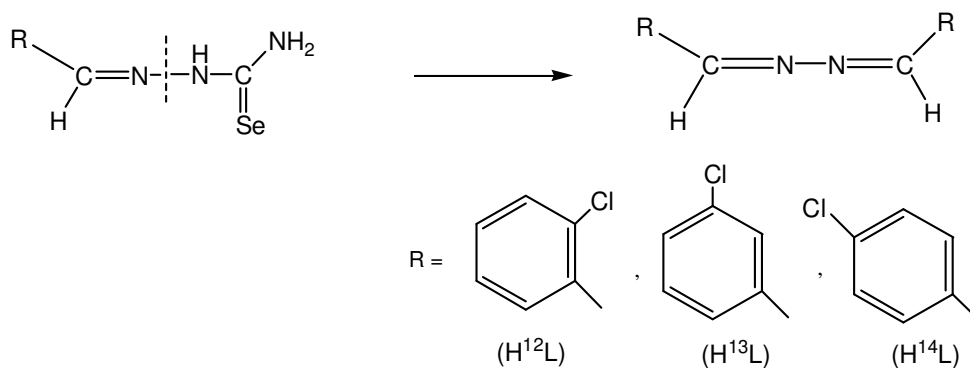
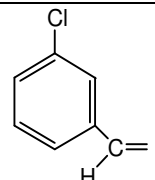
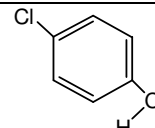


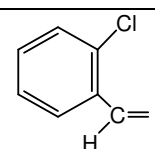
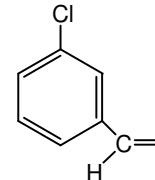
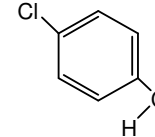
Table-52: ^1H NMR signals for H^{12}L - H^{14}L (δ , ppm).

Complexes	(CH)	Ring of protons	
{1,2-bis(2-chlorobenzylidene)hydrazine} H^{12}L	9.067	$\text{C}^3, \text{H d}$ 8.20; $\text{C}^{4,5,6}$ m 7.53-7.20ppm	

{1,2-bis(3-chlorobenzylidene)hydrazine} H ¹³ L	8.57	C ² ,H s 7.85; C ⁶ ,H m 7.71; C ^{4,5} H m,7.57-7.35ppm	
{1,2-bis(4-chlorobenzylidene)hydrazine} H ¹⁴ L	8.58	C ^{3,5} ,H s 7.76; C ^{2,6} H m 7.49ppm;	

In ¹H NMR spectra of H¹²L, H¹³L, H¹⁴L the azomethine proton of H¹²L appeared at low field, δ 9.067 ppm as compared to H¹³L and H¹⁴L. In H¹²L, C³H proton appeared as doublet at δ 8.20 ppm, whereas C^{4,5,6}H appeared as multiplet in the range of δ 7.20-7.53 ppm. In p-chlorobenzylidene selenosemicarbazone two singlets of C²H and C⁶H appeared at δ 7.85 and δ 7.71 ppm respectively. The C^{4,5}H protons appeared as multiplet in the range, δ 7.35-7.57 ppm. In case of H¹⁴L, C^{3,5}H and C^{2,6}H protons appeared at δ 7.76 and δ 7.49 ppm respectively (Table-52). In ¹³C NMR spectrum of C¹ carbon appeared at δ 159.26-161.26 ppm. Other ring carbon appeared within δ 137.56 ppm- δ 127.22 ppm (Table-53).

Table-53: ¹³C NMR signals for H¹²L - H¹⁴L (δ , ppm).

Complexes	(C ¹)	Ring of protons	
{1,2-bis(2-chlorobenzylidene)hydrazine} H ¹² L	159.26	C ³ , 136.07; C ² 132.40; C ⁵ 131.68; C ⁷ , 130.29; C ⁴ , 128.54; C ⁶ , 127.28	
{1,2-bis(3-chlorobenzylidene)hydrazine} H ¹³ L	161.09	C ⁴ , 135.95; C ² 135.21; C ⁵ , 131.51; C ⁶ 130.28; C ³ , 128.36; C ⁷ , 127.22	
{1,2-bis(4-chlorobenzylidene)hydrazine} H ¹⁴ L	161.26	C ⁵ , 137.56; C ² 132.71; C ^{3,7} 129.96; C ^{4,6} , 129.37	

Jun23-2016-nmrsu
AK-154

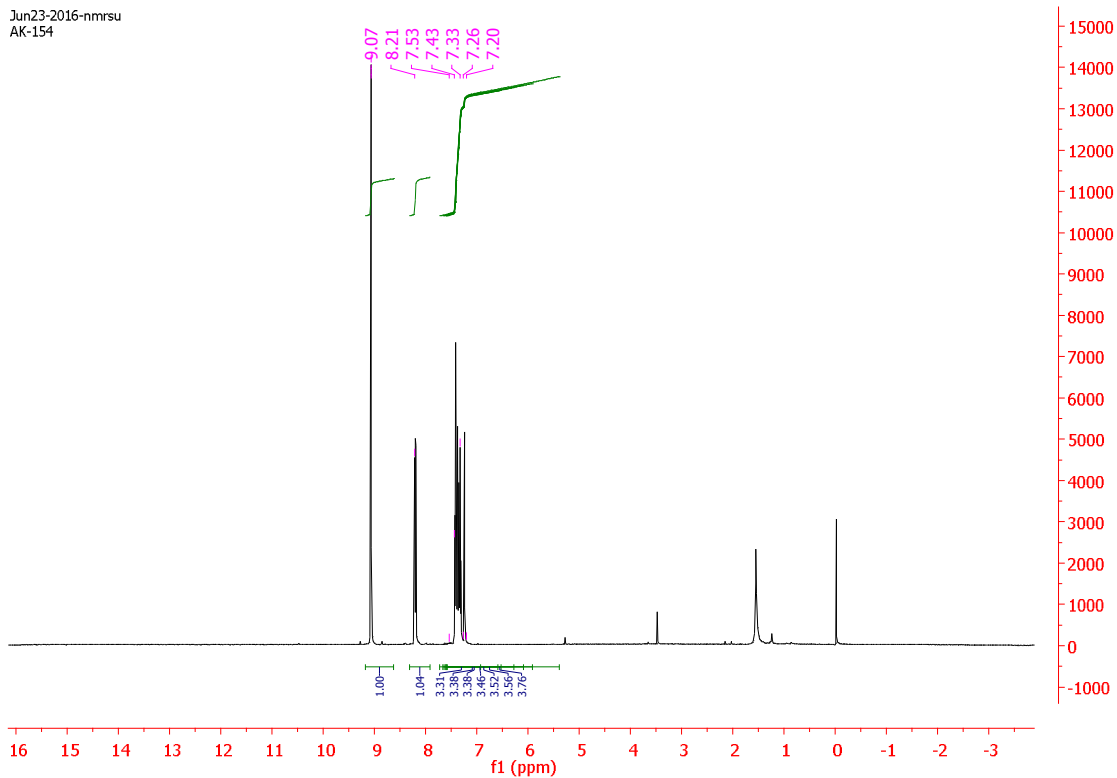


Figure-35h: ¹H NMR signals for {1,2-bis(2-chlorobenzylidene)hydrazine} H¹²L (δ, ppm).

Jun21-2016-nmrsu
AK-151

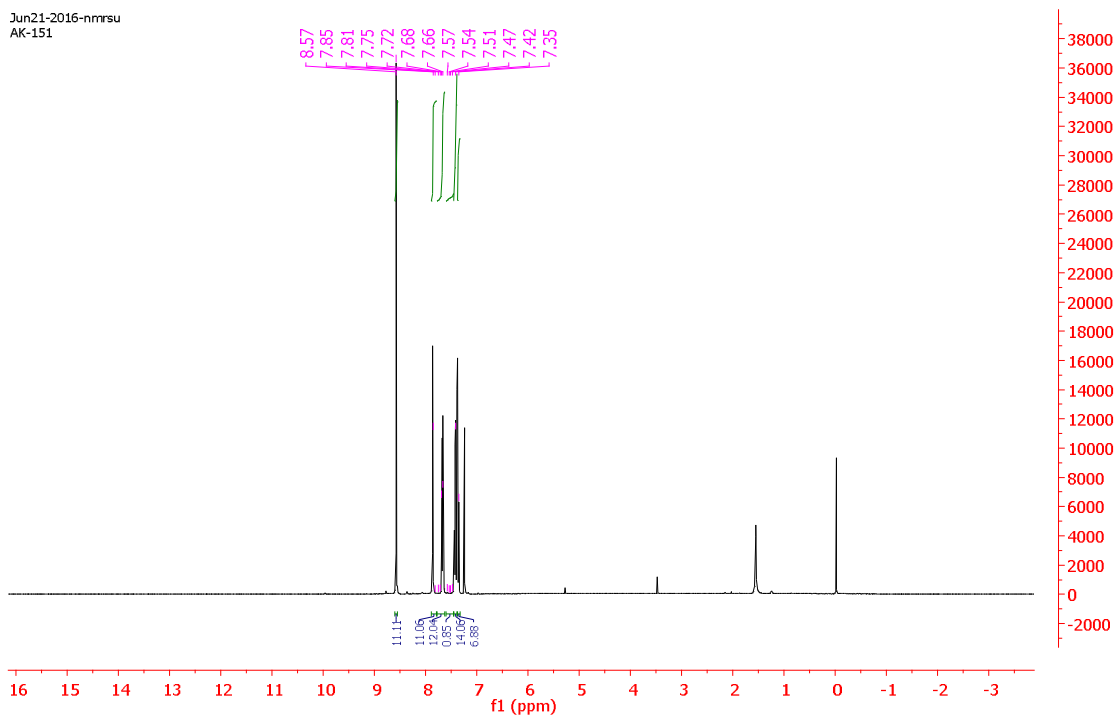


Figure-35i: ¹H NMR signals for {1,2-bis(3-chlorobenzylidene)hydrazine} H¹³L (δ, pm).

Jun23-2016-nmrsu
AK-160

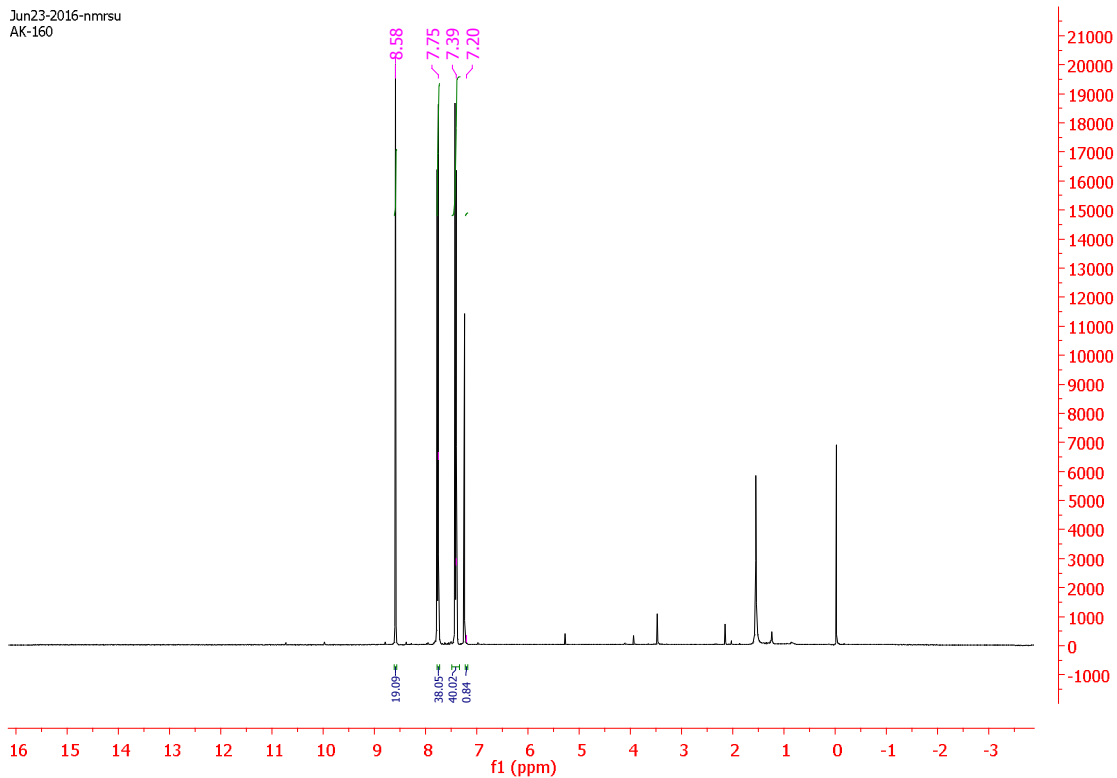


Figure-35j: ^1H NMR signals for {1,2-bis(4-chlorobenzylidene)hydrazine} H^{12}L (δ , ppm).

Jun23-2016-nmrsu
AK-154

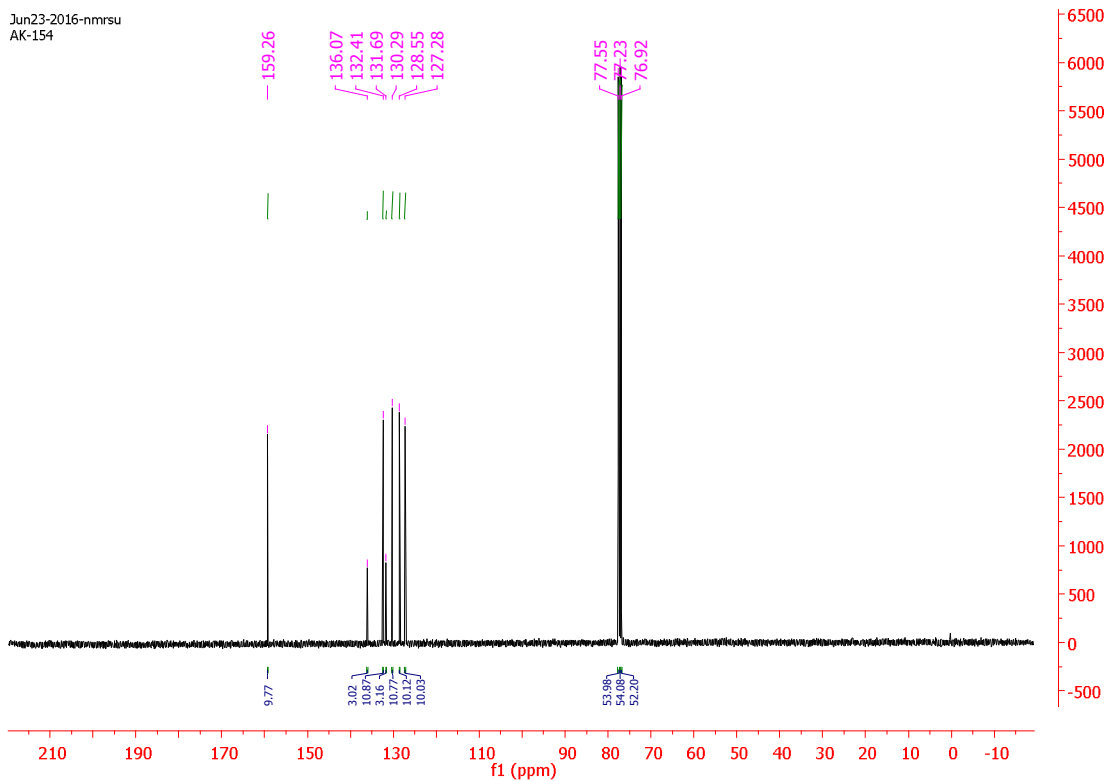


Figure-35k: ^{13}C NMR signals for {1,2-bis(2-chlorobenzylidene)hydrazine} H^{12}L (δ , ppm).

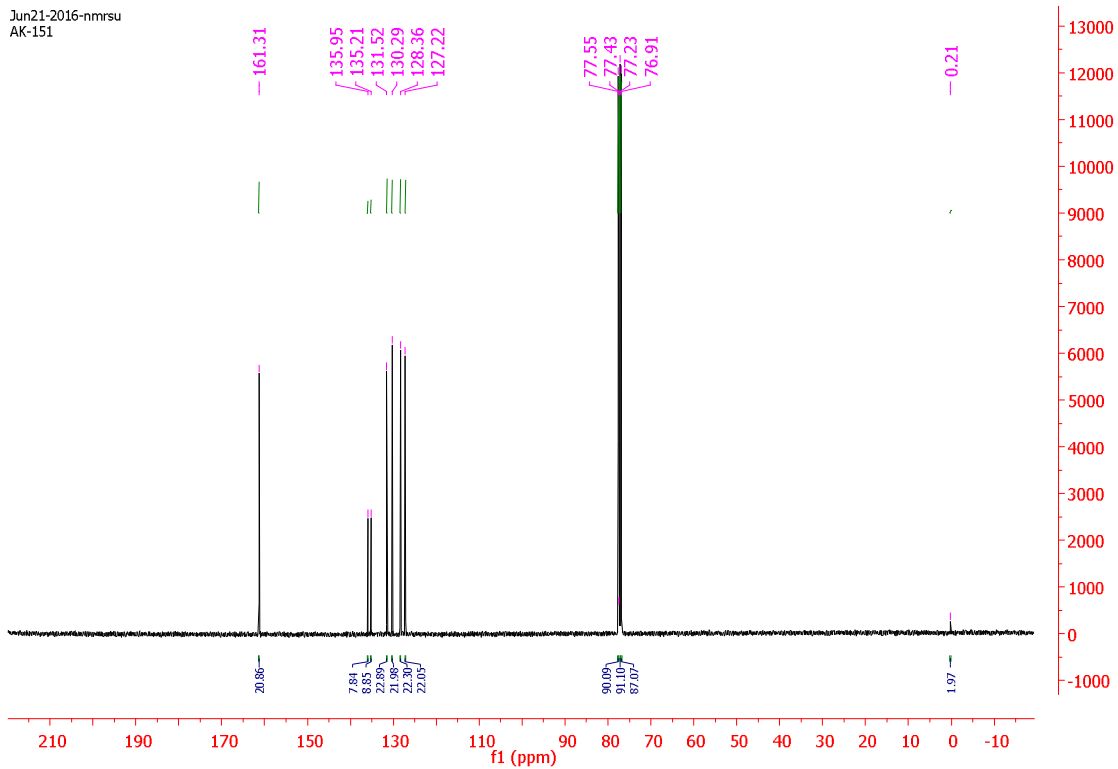


Figure-35(l): ^{13}C NMR signals for {1,2-bis(3-chlorobenzylidene)hydrazine} H^{13}L (δ , ppm).

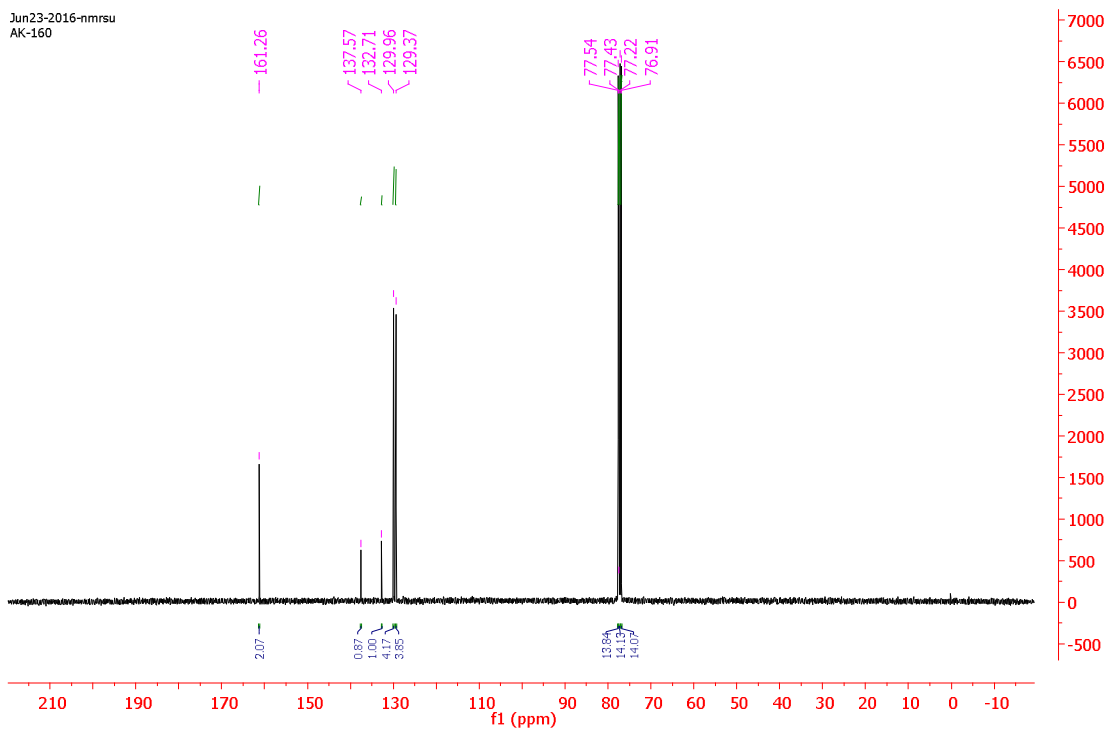


Figure-35(m): ^{13}C NMR signals for {1,2-bis(4-chlorobenzylidene)hydrazine} H^{14}L (δ , ppm).

8.5 Structure of 1,2-bis(3-chlorobenzylidene)hydrazine H¹³L and 1,2-bis(4-chlorobenzylidene)hydrazine H¹⁴L.

1,2-bis(3-chlorobenzylidene)hydrazine H¹³L and 1,2-bis(4-chlorobenzylidene)hydrazine H¹⁴L crystallizes in monoclinic crystal system with space group P2₁/c. Molecular structure are given in Figure-36(H¹³L), 37 (H¹⁴L), packing diagrams of these molecules are given in Figures-36a(H¹³L), 37a(H¹⁴L), crystallographic data and important bond parameters are given in Tables 54(H¹³L), 55(H¹⁴L) and Tables 56(H¹³L), 57(H¹⁴L) respectively.

The molecule 1,2-bis(3-chlorobenzylidene)hydrazine and 1,2-bis(4-chlorobenzylidene)hydrazine H¹⁴L is centrosymmetric with the midpoint of the N—N bond located on the inversion centre. C=N bond distance of 1.277 (2) Å(H¹³L), 1.278(3)Å(H¹⁴L) is longer than the C=N bond distance 120.88(2) Å in (*E*)Benzaldehyde(2, 4, 6-trichlorophenyl)hydrazone[105] and 119.25(2) Å in 2 methoxybenzaldehyde 2, 4-dinitrophenylhydrazone[106] but shorter than found in other related hydrazone structures, *e.g.* 1.295 (2) Å in (*E*)-3-methoxyacetophenone 4-nitrophenylhydrazone (Fan *et al.*, 2008), 1.298 (2) Å in (*E*)-2-furylmethylketone 2,4-dinitrophenylhydrazone (Shan, Tian *et al.*, 2008) and 1.293 (2) Å in benzylideneacetone 2,4-dinitrophenylhydrazone (Shan *et al.*, 2004). Both (H¹³L) and (H¹⁴L) molecule display an approximately planar structure, with C=C=N-N torsional angle of 179.34(16)°(H¹³L) and 179.73(2)°(H¹⁴L) which is similar to 179.67(7)° C=C=N-N in 2 methoxybenzaldehyde 2, 4-dinitrophenylhydrazone but smaller when compared to 176.91°in (*E*)Benzaldehyde(2, 4, 6-trichlorophenyl)hydrazone. The C=N bond distance found are 1.277(3)Å in (H¹³L), 1.278(3) Å in (H¹⁴L) while N=N bond distance are 1.412(3) in (H¹³L) and 1.407(3) in Å(H¹⁴L). The C-Cl bond length 1.74(2) Å in (H¹³L) and (H¹⁴L) is close to C-Cl bond length 1.73(2) Å in(*E*)Benzaldehyde(2, 4, 6-trichlorophenyl)hydrazone. The molecule assumes an E configuration with two chlorobenzylidene hydrazine located on the opposite sides of the N=N bond. The C-C=N bond angle 121.96(19)°(H¹³L) and 121.24(19)°(H¹⁴L) are larger than120.88(2)° and119.25(2)° in (*E*)Benzaldehyde(2, 4, 6-trichlorophenyl)hydrazone and 2 methoxybenzaldehyde 2, 4-dinitrophenylhydrazone respectively.

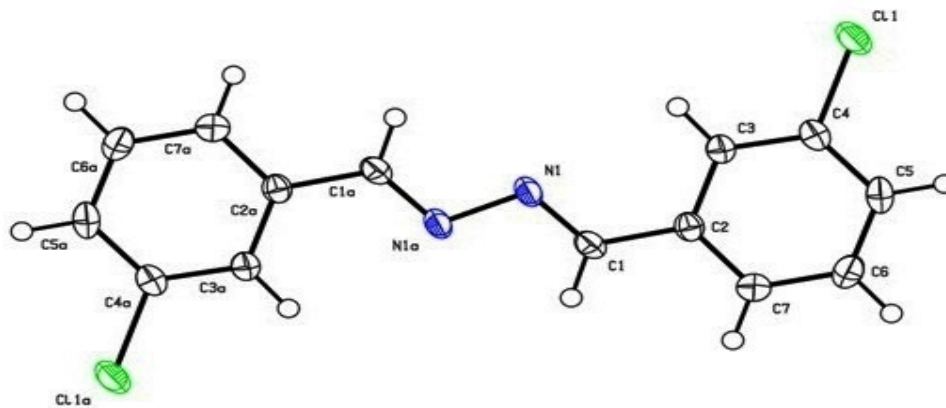


Figure-36: ORTEP view of 1,2-bis(3-chlorobenzylidene)hydrazine $H^{13}L$ with numbering scheme.

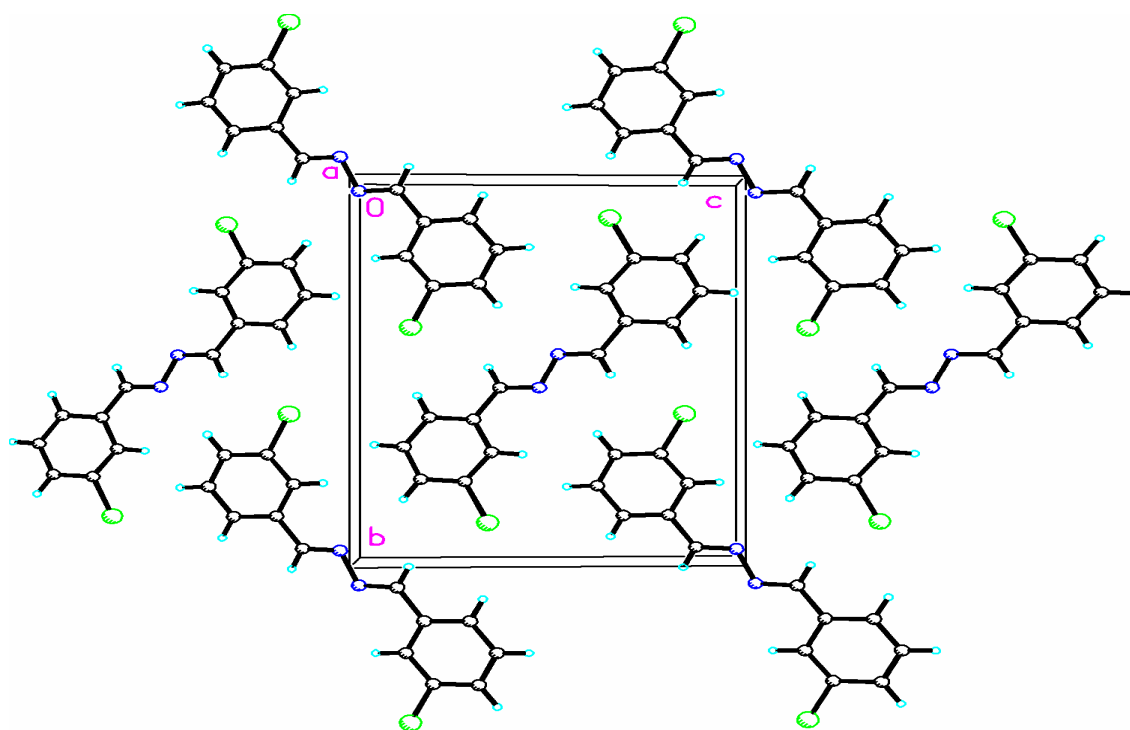


Figure-36a: Packing Diagram of 1,2-bis(3-chlorobenzyl)hydrazine $H^{13}L$.

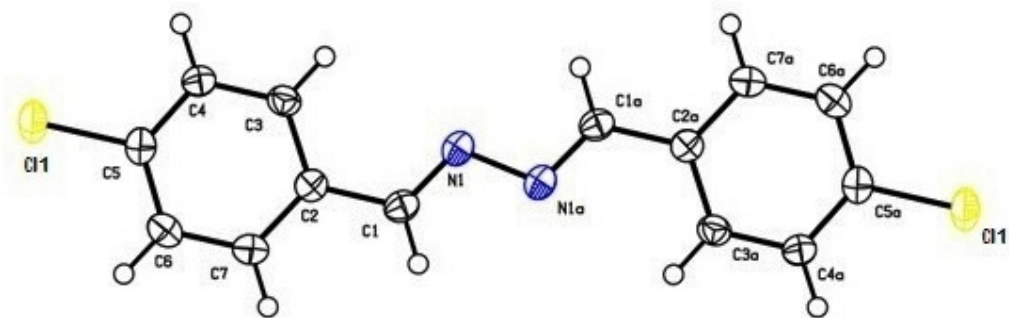


Figure-37: ORTEP view of 1,2-bis(4-chlorobenzylidene)hydrazine H¹⁴L with numbering scheme.

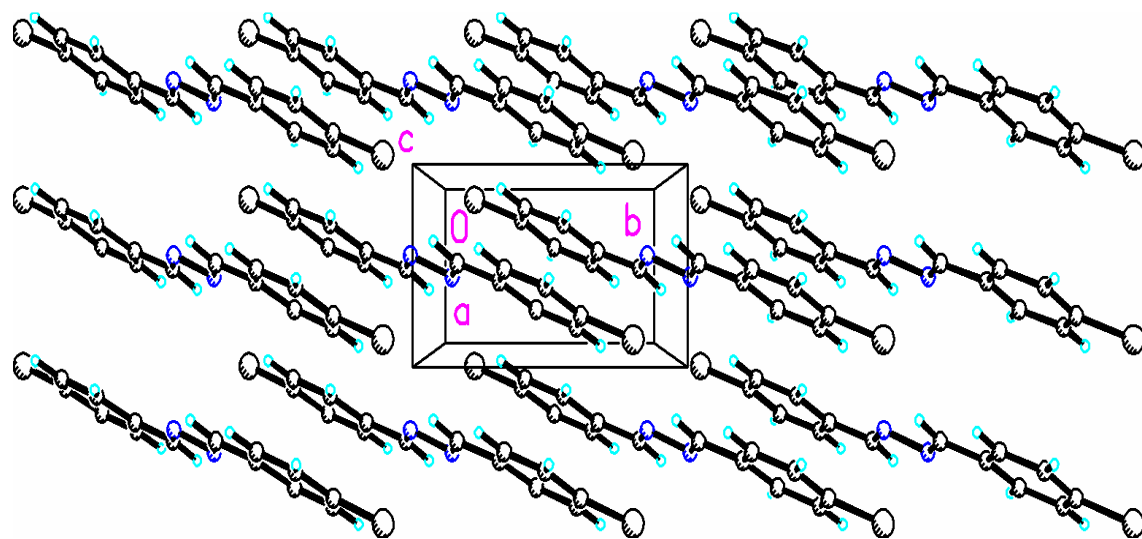


Figure-37a: Packing Diagram of 1,2-bis(4-chlorobenzyl)hydrazine H¹⁴L.

Table-54: Crystallographic data of 1,2-bis(3-chlorobenzyl)hydrazine H¹³L.

Empirical formula	C ₁₄ H ₁₀ Cl ₂ N ₂
Formula weight	277.14
Temperature/K	173(2)
Crystal system	Monoclinic
Space group	P2 ₁ /c
a/Å	3.8193(2)
b/Å	14.9615(9)
c/Å	11.1307(8)
α/°	90
β/°	93.341(6)
γ/°	90
Volume/Å ³	634.95(7)
Z	2
ρ _{calc} /g/cm ³	1.450
μ/mm ⁻¹	4.438
F(000)	284.0
Crystal size/mm ³	0.48 × 0.18 × 0.12
Radiation	CuKα (λ = 1.54184)
2θ range for data collection/°	9.916 to 143.034
Index ranges	-4 ≤ h ≤ 3, -11 ≤ k ≤ 18, -9 ≤ l ≤ 13
Reflections collected	2070
Independent reflections	1197 [R _{int} = 0.0171, R _{sigma} = 0.0247]
Data/restraints/parameters	1197/0/82
Goodness-of-fit on F ²	1.062
Final R indexes [I > 2σ (I)]	R ₁ = 0.0339, wR ₂ = 0.0961
Final R indexes [all data]	R ₁ = 0.0370, wR ₂ = 0.0995
Largest diff. peak/hole / e Å ⁻³	0.33/-0.27

Table-55: Crystallographic data of 1,2-bis(4-chlorobenzyl)hydrazine H¹⁴L.

Empirical formula	C ₁₄ H ₁₀ Cl ₂ N ₂
Formula weight	270.36
Temperature/K	173(2)
Crystal system	Monoclinic
Space group	P2 ₁ /c
a/Å	3.8897(2)
b/Å	6.9913(4)
c/Å	23.0085(14)
α/°	90
β/°	90.788(5)
γ/°	90
Volume/Å ³	625.63(6)
Z	2
ρ _{calc} /cm ³	1.435
μ/mm ⁻¹	3.693
F(000)	280.0
Crystal size/mm ³	0.38 × 0.12 × 0.06
Radiation	CuKα (λ = 1.54184)
2θ range for data collection/°	13.236 to 142.436
Index ranges	-4 ≤ h ≤ 3, -7 ≤ k ≤ 8, -21 ≤ l ≤ 28
Reflections collected	1923
Independent reflections	1191 [R _{int} = 0.0326, R _{sigma} = 0.0444]
Data/restraints/parameters	1191/0/83
Goodness-of-fit on F ²	1.068
Final R indexes [I > 2σ (I)]	R ₁ = 0.0466, wR ₂ = 0.1264
Final R indexes [all data]	R ₁ = 0.0509, wR ₂ = 0.1321
Largest diff. peak/hole / e Å ⁻³	0.43/-0.32

Table -56: Bond distance (Å) and bond angles (°) for 1,2-bis(3-chlorobenzyl)hydrazine H¹³L.

Bond Distance (Å) H ¹³ L	
Cl(1) – C(4)	1.7472(17)
N(1) – N(1)	1.412(3) 3_766
N(1) – C(1)	1.277(2)
C(1) – H(1)	0.9500
C(1) – C(2)	1.459(2)
C(2) – C(3)	1.403(2)
C(2) – C(7)	1.395(2)
C(3) – H(3)	0.9500
C(3) – C(4)	1.378(2)
C(4) – C(5)	1.390(2)
C(5) – H(5)	0.9500
C(5) – C(6)	1.386(3)
C(6) – H(6)	0.9500
C(6) – C(7)	1.387(2)
C(7) – H(7)	0.9500
Bond Angle (°)H ¹³ L	
C(1) – N(1) – N(1)	111.44(16) – 3.766
N(1) – C(1) – H(1)	119.0
N(1) – C(1) – C(2)	121.97(14)
C(2) – C(1) – H(1)	119.0
C(3) – C(2) – C(1)	121.11(14)
C(7) – C(2) – C(1)	119.50(14)
C(7) – C(2) – C(3)	119.39(14)
C(2) – C(3) – H(3)	120.6
C(4) – C(3) – C(2)	118.85(15)
C(4) – C(3) – H(3)	120.6
C(3) – C(4) – Cl(1)	118.63(13)
C(3) – C(4) – C(5)	122.37(15)
C(5) – C(4) – Cl(1)	119.00(13)

C(4) – C(5) – H(5)	120.8
C(6) – C(5) – C(4)	118.36(15)
C(6) – C(5) – H(5)	120.8
C(5) – C(6) – H(6)	119.7
C(5) – C(6) – C(7)	120.61(16)
C(7) – C(6) – H(6)	119.7
C(2) – C(7) – H(7)	119.8
C(6) – C(7) – C(2)	120.42(15)
C(6) – C(7) – H(7)	119.8

Table-57: Bond distance (Å) and bond angles (°) for 1, 2-bis(4-chlorobenzyl)hydrazine H¹⁴L.

Bond Distance (Å) for H ¹⁴ L			
Cl(1) – C(5)	1.743(2)	C(2) – C(7)	1.398(3)
N(1) – N(1) ¹	1.407(3)	C(3) – C(4)	1.380(3)
N(1) – C(1)	1.278(3)	C(4) – C(5)	1.383(3)
C(1) – C(2)	1.464(3)	C(5) – C(6)	1.384(3)
C(2) – C(3)	1.404(3)	C(6) – C(7)	1.385(3)
Bond Angle for (°)H ¹⁴ L			
C(1) – N(1) – N(1) ¹	112.0(2)	C(3) – C(4) – C(5)	118.81(19)
N(1) – C(1) – C(2)	121.25(19)	C(4) – C(5) – Cl(1)	119.05(17)
C(3) – C(2) – C(1)	120.94(18)	C(4) – C(5) – C(6)	121.97(19)
C(7) – C(2) – C(1)	120.35(19)	C(6) – C(5) – Cl(1)	118.97(17)
C(7) – C(2) – C(3)	118.70(19)	C(5) – C(6) – C(7)	118.83(19)
C(4) – C(3) – C(2)	120.91(18)	C(6) – C(7) – C(2)	120.79(19)

8.6 Complexes of copper(I) and silver(I) halides with selenosemicarbazones:

Complexes of copper(I) with 2-nitrobenzaldehyde selenosemicarbazones[2-NO₂-Hbsesc], 3-nitrobenzaldehyde selenosemicarbazones[3-NO₂-Hbsesc] and silver(I) halides with 4-nitrobenzaldehyde selenosemicarbazones[4-NO₂-Hbsesc] are listed in Table-58.

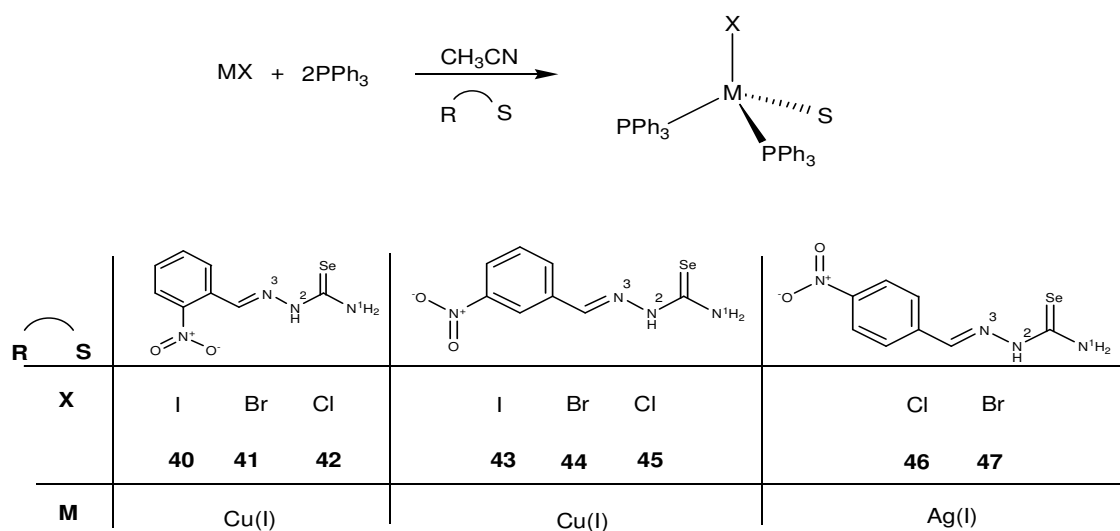
Table-58: List of complexes of selenosemicarbazones.

Complex	Structure of Ligand used
[CuI(η ¹ -Se- 2-NO ₂ -Hbsesc)(Ph ₃ P) ₂] (40)	
[CuBr(η ¹ -Se- 2-NO ₂ -Hbsesc)(Ph ₃ P) ₂] (41)	
[CuCl(η ¹ -Se- 2-NO ₂ -Hbsesc)(Ph ₃ P) ₂] (42)	
[CuI(η ¹ -Se- 3-NO ₂ -Hbsesc)(Ph ₃ P) ₂] (43)	
[CuBr(η ¹ -Se- 3-NO ₂ -Hbsesc)(Ph ₃ P) ₂] (44)	
[CuCl(η ¹ -Se- 3-NO ₂ -Hbsesc)(Ph ₃ P) ₂] (45)	

<p>[AgCl(η^1-Se- 4-NO₂-Hbsesc)(Ph₃P)₂] (46)</p>	
<p>[AgBr(η^1-Se- 3-NO₂-Hbsesc)(Ph₃P)₂] (47)</p>	

8.7 Synthesis

Reaction of copper(I) halides (X= I, Br, Cl) with 2-nitrobenzaldehyde selenosemicarbazones (2-NO₂-Hbsesc, H¹³L) or 3-nitrobenzaldehyde selenosemicarbazones (3-NO₂-Hbsesc, H¹⁴L) and triphenylphosphine in 1 : 1 : 1 (M : L : Ph₃P) molar ratio in acetonitrile formed highly insoluble compounds. To solubilise it, one mole of triphenylphosphine has been added. The clear solution thus formed gave complexes of stoichiometry [CuX(HL)(Ph₃P)₂] (H¹³L, X = I (40), Br (41), Cl (42), H¹⁴L, X = I (43), Br (44), Cl (45). The similar reaction of silver(I) halides (X= Br, Cl) with 4-nitrobenzaldehyde selenosemicarbazones (4-NO₂-Hbsesc, HL⁹) and triphenylphosphine in 1 : 1 : 2 molar ratio yielded complexes having formula, [AgX(HL)(Ph₃P)₂] (HL⁹, X = Cl (46), Br (47) (Scheme 17).



(Scheme 17)

8.8 Discussion on IR spectroscopy

$\nu(\text{NH}_2)$ band of ligands $\text{H}^8\text{L} - \text{H}^{10}\text{L}$ appears in the range of $(3232\text{-}3406 \text{ cm}^{-1}) \text{ cm}^{-1}$ in IR spectra (Table-59). This band shows high energy shift in complexes **40-47** $(3251\text{-}3450 \text{ cm}^{-1})$ vis-a-vis ligands. The $\nu(-\text{NH}-)$ obtained in ligands range from $3109\text{-}3171 \text{ cm}^{-1}$ which is at lower wave number $(3110\text{-}3181 \text{ cm}^{-1})$ in complexes **40-47**.

The characteristic $\nu(\text{C}=\text{Se})$ band of ligands $\text{H}^8\text{L} - \text{H}^{10}\text{L}$ appeared in the range of $(835\text{-}855 \text{ cm}^{-1})$ $\{848(\text{H}^8\text{L}), 835 (\text{H}^9\text{L}), 855(\text{H}^{10}\text{L})\}$ this band shows high energy shift in $(838\text{-}874 \text{ cm}^{-1})$. The shift in $\nu(\text{C}=\text{Se})$ band indicates binding of metal center by selenium of seleno-ligands.

Table-59: Important peaks in IR spectrum for complexes **40-47** cyclohexanone selenosemicarbazone and ligands $\text{H}^8\text{L} - \text{H}^{10}\text{L}$.

Compound	$\nu(\text{NH}_2)$	$\nu(-\text{NH}-)$	$\nu(\text{C}=\text{N}) + \nu(\text{C}=\text{C}) + \delta$ (NH_2)	$\nu(\text{C}=\text{Se})$
H^8L	3406s 3250s	3109s	1602s, 1566s, 1477s	848s
40	3450m 3260m	3110s	1631s, 1591s, 1475s	844s
41	3437m 3265m	3113s	1626s, 1568s, 1473s	844s
42	3445m 3265	3139	1651s, 1583s, 1432s	850s
H^9L	3408m 3232m	3128m	1614s, 1597s, 1479s	835s
43	3439m 3271m	3174s	1620m, 1599m, 1473s	838s
44	3443m 3261m	3179s	1614m, 1567m, 1433s	841s
45	3431m 3251m	3181s	1633m, 1589m, 1463s	851s
H^{10}L	3428m 3252m	3171s	1654m, 1587s, 1497s	855s

46	3417m 3275m	3119s	1681w, 1587w, 1476s	874s
47	3421m 3258m	3123s	1651w, 1569w, 1477s	852s

8.9 Discussion on NMR spectroscopy:

The N²H proton in selenosemicarbazone ligands (H⁸L - H¹⁰L) appeared in the range δ 10.30 ppm- δ 11.98 ppm which showed a downfield shift (in range δ 9.07- δ 9.13ppm) in complexes (40-42), were as in complexes 43-45 showed upfield shift in the range of (δ 11.92- δ 1.98ppm) vis-a-vis free ligand. Signal due to ¹NH² proton gets obscured by the signal of phenyl ring of seleno- ligand. Appearance of these signals ensure the presence of amino and amido group. The signal due to C²H proton appeared in the range δ 8.54 ppm- δ 8.63 ppm in these ligands and showed downfield shift in the range δ 8.82 ppm- δ 8.87 ppm in complexes 40,43-45 except in (δ 8.26- δ 8.27 ppm ppm)41, 42 (δ 8.16- δ 8.18 ppm), 46,47. Presence of aromatic ring was also confirmed by the appearance of multiplet in the range of δ 7.03 ppm - δ 8.70 ppm. The presence of all these protons indicate that no deprotonation take place during complexation and all the ligands coordinate to the metal center in neutral form. (Table 60)

Table-60: ¹H NMR signals for H⁸L -H¹⁰L (δ , ppm).

Complexes	(1H, N ² H)	(1H, C ² H)	(1H, N ¹ H ₂)	(Ring protons),
H ⁸ L	11.94	8.62	obscured by ring proton	8.38-7.48
40	9.13	8.84	obscured by ring proton	8.32-7.24
41	9.09	8.27	obscured by ring proton	8.08-7.24
42	9.07	8.26	obscured by ring proton	8.09-7.26
H ⁹ L	11.79	8.63	obscured by ring proton	8.48-7.54

43	11.98	8.82	obscured by ring proton	8.69-7.26
44	11.96	8.84	obscured by ring proton	8.70-7.26
45	11.92	8.87	obscured by ring proton	7.63-7-7.03
H ¹⁰ L	10.30	8.54	obscured by ring proton	8.34-7.24
46	-	8.16	obscured by ring proton	7.75-7.24
47	-	8.18	obscured by ring proton	7.72-7.25

Due to the poor yield of synthesized selenosemicarbazones and their complexes, biological activities could not be obtained.

CHAPTER 9

SUMMARY AND CONCLUSION

Synthesis of various ligands viz. Isatin-N¹-methyl-thiosemicarbazone (H₂itsc-N¹-Me), isatin-N¹-ethyl-thiosemicarbazone (H₂itsc-N¹-Et), indole-3-thiosemicarbazone (HIntsc, H¹L), indole-N¹-methyl-3-thiosemicarbazone (HIntsc-N¹-Me, H⁴L), 5-methoxy indole-3-thiosemicarbazone (5-MeOHIntsc, H²L) and 5-methoxy indole-N¹-methyl-3-thiosemicarbazone (5-MeOHIntsc-N¹-Me, H³L), 9-anthraldehyde-3-thiosemicarbazone (9-Hantsc, H⁵L) and 9-anthraldehyde-N¹-methyl-3-thiosemicarbazones (9-Hanttsc-N¹-Me, H⁶L) has been carried out and the effect of substituents (at N¹ atom of isatin-3-thiosemicarbazones) on nuclearity of copper(I) and silver(I) halide complexes has been investigated. All these complexes have been characterized using analytical and spectroscopic data (IR, ¹H, ¹³C NMR). The single crystal structure has been solved for H₂L¹, H²L and **2**, **12**, **19**, **20**, **13**, **14**, **22** **31**, **35** and **38**. The complex **2** has distorted tetrahedral geometry around copper(I) and isatin-N¹-methyl-thiosemicarbazone coordinated to metal center as neutral, bidentate, N³, S-chelating ligand. The complex **12**, **19**, **20** have distorted tetrahedral geometry around copper(I) and H¹L (**12**), H³L (**19**, **20**) coordinated to metal center as neutral, monodentate, ligand while the complex **13**, **14** form halogen bridged dimers with each Cu atom bonded to one atom of thiosemicarbazones, one terminal P atom from triphenylphosphine, and two halogen atoms in central kernel. The complex **35** has distorted tetrahedral geometry around copper(I) and 9-anthraldehyde-N¹-methyl-3-thiosemicarbazone coordinated to metal centre as neutral, monodentate, ligand while the complex **31** form halogen bridged dimers around copper(I) and 9-anthraldehyde-3-thiosemicarbazones with each Cu atom bonded to one atom of thiosemicarbazones, one terminal P atom from triphenylphosphine, and two halogen atoms in central kernel. Complex **38** form a dimer where Ag atom is bonded to one halogen atom, one P atom and two S atoms from two different thiosemicarbazone ligands bridging two Ag centres, with central kernel, Ag₂(μ₂-S)₂Ag and two tetrahedral share a sulphur-sulfur edge, Ph₃P and halogen ligands occupy trans orientation across the central kernel.

It has been observed that substituent at N¹ atom of fused ring thiosemicarbazones influenced the nuclearity of their copper(I) and silver(I) complexes. The ligands and their complexes have shown low to moderate antifungal and antibacterial studies. Interestingly, all the thio-ligands exhibit significant anti-TB activity and this activity gets enhanced on

complexation. Most of the complexes showed anti-TB activity even more than the standard drugs. These complexes can be studied for in vivo anti-TB activity for getting good drugs.

A series of selenosemicarbazones H^7L - $H^{11}L$, (with various aldehydes viz. m-hydroxy benzaldehyde, o-nitrobenzaldehyde, m-nitrobenzaldehyde, p-nitrobenzaldehyde and 3-methoxybenzaldehyde have been prepared however $H^{12}L$ - $H^{14}L$ (with o-, m-, p-chlorobenzaldehyde) lead to dimerization resulting in the formation of azo compound. Only few complexes of silver(I) and copper(I) halides could be obtained, which were characterized by IR, NMR (1H and ^{13}C). Although stabilization of selenosemicarbazone and their binding with copper(I) and silver(I) is a challenge, it provides a large scope to the researcher in this field.

CHAPTER 10

REFERENCES

1. T. S. Lobana, Rekha, R. J. Butcher, *Transition Met. Chem.* **2004**, 29, 291.
2. T. S. Lobana, Rekha, R. J. Butcher, A. Castineiras, E. Bermejo, P. V. Bharatam, *Inorg. Chem.* **2006**, 45, 1535.
3. T. S. Lobana, S. Khanna, R. J. Butcher, A. D. Hunter, M. Zeller, *Inorg. Chem.* **2007**, 46, 5826.
4. T. S. Lobana, S. Khanna, R. J. Butcher, *Z. Anorg. Allg. Chem* **2007**, 633, 1820.
5. T. S. Lobana, P. Kumari, R. J. Butcher, *Inorg. Chem. Commun.* **2008**, 11, 11.
6. E. M. Jouad, A. Riou, M. Allain, M. A. Khan, G. M. Bouet, *Polyhedron*, **2001**, 20, 67.
7. S. Lhuachan, S. Siripaisarnpipat, N. Chaichit, *Eur.J.Inorg.Chem.* **2003**, 263.
8. E. Bermejo, R. Carballo, A. Castineiras, R. Dominguez, C. Maichle-Mossmer, J. Strahle, D. X. West, *Polyhedron* **1999**, 18, 3695.
9. P. Gomez-Saiz, J. Garcia-Tojal, M. A. Maestro, J. Mahia, F. J. Arniaz, L. Lezama, T. Rojo, *Eur. J. Inorg. Chem.* **2003**, 2639
10. E. Labisbal, K. D. Haslow, A. Sousa-Pedrares, J. Valdes-Martinez, S. Harnandez-Ortega, D. X. West, *Polyhedron* **2003**, 22, 2831.
11. L. J. Ashfield, A. R. Cowley, J. R. Dilworth, P. S. Donnelly, *Inorg. Chem.* **2004**, 43, 4121.
12. I. Pal, F. Basuli, T. C. W. Mak, S. Bhattacharya, *Angew. Chem. Int. Ed.* **2001**, 40, 2923.
13. H. G. Raubenheimer, G. J. Kruger, L. Linford, C. F. Marais, R. Otte, J. T. Z. Hattingh, A. Lombard *J.Chem.Soc. Dalton Trans.* **1989**, 1565.
14. S. Fuchs, K. Angermaier, A. Bauer, H. Schmidbaur, *Chem. Ber.* **1997**, 130, 105.
15. C. O. Kienitz, C. Thone, P. G. Jones, *Inorg. Chem.* **1996**, 35, 3990.
16. Y. Cheng, T. J. Emge, J. G. Brennan, *Inorg. Chem.* **1996**, 35, 342.
17. Y. Cheng, T. J. Emge, J. G. Brennan, *Inorg. Chem.* **1996**, 35, 7339.
18. D. X. West, J. S. Ives, J. Krejci, M. M. Salberg, T. L. Zumbahlen, G. A. Bain, A. E. Liberta, J. Valdes-Martinez, S. Harnandez-Ortiz, R. A. Toscano, *Polyhedron*

- 1995, 14, 2189.
19. M. B. Ferrari, F. Bisceglie, G. G. Fava, G. Pelosi, P. Tarasconi, R. Albertini, S. Pinelli, *J. Inorg. Biochem.* **2002**, 89, 36.
 20. J. S. Casas, E. E. Catellano, M. D. Couce, J. Ellena, A. Sanchez, J. Sordo, C. Taboada, *J. Inorg. Biochem.* **2006**, 100, 1858.
 21. T. S. Lobana, Rekha, R. J. Butcher, A. Castineiras, E. Bermejo, P. V. Bharatam, *Inorg. Chem.* **2006**, 45, 1535.
 22. D. X. West, A. E. Liberta, S. B. Padhye, R. C. Chikate, P. B. Sonawane, A. S. Kumbhar, R. G. Yerande, *Coord. Chem. Rev.* **1993**, 123 49.
 23. D. X. West, S. B. Padhye, P. B. Sonawane, *Struct. Bond.* **1991**, 76, 1.
 24. G. Pelosi, *Open Crystallogr. J.* **2010**, 3, 16.
 25. D. Dekanski, T. Todorovic, D. Mitic, N. Filipovic, N. Polovic, K. Anelkovic, *J. Serb. Chem. Soc.* **2013**, 78 1503.
 26. T. S. Rajic, M. Zec, T. Todorovic, K. Anelkovic, S. Radulovic, *Eur. J. Of Medicinal Chem.* **2011**, 46, 3734.
 27. C. R. Kowol, R. Eichinger, M. A. Jakupec, M. Galanski, V. B. Arion, B. K. Keppler, *J. Inorg. Biochem.* **2007**, 101, 1946.
 28. A. Molter, J. Rust, C. W. Lehmann, G. Deepa, P. Chiba, Fabian Mohr. *Dalton Trans.* **2011**, 40 9810.
 29. P. Bippus, A. Molter, D. Müller, F. Mohr, *J. of Organometallic Chemistry*, **2010** 695, 1657.
 30. V.M Leovac. B.Ribar, Gy Argay, A Kalman, I.Brceski, *J. Coord. Chem.* **1996**, 39, 11.
 31. Gy Argay, A Kalman, L Parkanyi, V. M Leovac, I. D Brceski, P. N. Radivojsa, *J Cord. Chem.* **2000**, 51, 9.
 32. K. C. Agarwal, B. A Booth, R. L. Michaud, E, C, Moore, A. C. Sartorelli, *Biochem Pharmacol.* **1974**, 23, 2421.
 33. T. R. Todorovic, A Bacchi, N.O. Juranic, D. M Sladic, G. Plezzi, T.T. Bozic, N. R. Filipovic, K.K Anelkovic, *Polyhedron*, **2007**, 26, 3428.
 34. R. T. Steven, Jr. C. Shipman, C. D. John, *J. Gen Virol.* **1986**, 67, 1625.
 35. E. Labisbal, A. Sousa, A. Castineiras, A. Garcia-Vazquez, J. Romero, D. X. West, *Polyhedron*, **2000**, 19, 1255.

36. J. S. Casas, E. E. Castellano, M. S. Garcia-Tasende, A. Sanchez, J. Sordo, *Inorg. Chim. Acta*, **2000**, 304, 283.
37. M. B. Ferrari, C. Pelizzi, G. Pelosi, M. C. Rodriguez-Arguelles, *Polyhedron*, **2002**, 21, 2593.
38. T. S. Lobana, Rekha, A. P. S. Pannu, G. Hundal, R. J. Butcher, A. Castineiras, *Polyhedron*, **2007**, 26, 2621.
39. T. S. Lobana, Rekha, B. S. Sidhu, A. Castineiras, E. Bermejo, T. Nishioka, *J. Coord. Chem.* **2005**, 58, 803.
40. J. S. Casas, A. Castineiras, M. C. Rodriguez-Arguelles, A. Sanchez, J. Sordo, A. Vazquez-Lopez, *J. Chem. Soc. Dalton Trans.* **2000**, 4056.
41. D. Wang, M. Ebel, C. Schulzke, C. Gruning, S. K. S. Hazari, D. Rehder, *Eur. J. Inorg. Chem.* **2001**, 935.
42. V. M. Leovac, B. Ribar, G. Argay, A. Kalman, I. Brceski, *J. Coord. Chem.* **1996**, 39, 11.
43. L. Ze-Hua, D. Chun-ying, L. Ji-hui, L. Yong-jiang, M. Yu-Hua, Y. Xiao-Zeng, *New J. Chem*, **2000**, 24 1057.
44. Z. Afrasiabi, E. Sinn, S. Padhye, S. Dutta, S. Padhye, C. Newton, C. E. Anson, A. K. Powell, *J. Inorg. Biochem.* **2003**, 95, 306.
45. J. S. Casas, E. E. Catellano, M. D. Couce, J. Ellena, A. Sanchez, J. Sordo, C. Taboada, *J. Inorg. Biochem.* **2006**, 100 1858.
46. T. S. Lobana, Rekha. S. Bhavdeep, Sidhu, A. Castineiras, T. Bermejo, Nishioka, *Journal of Coordination Chemistry*, **2005**, 58, 803.
47. M. B. Ferrari, C. Pelizzi, G. Pelosi, C. Maria, R. Arguelles, *Polyhedron*, **2002**, 21, 2593.
48. J. S. Casas, E. E. Castellano, Garcia, M. S. Tasende, A. Sanchez, Sordo, *Inorganica Chimica Acta.* **2000**, 304, 283.
49. E. Labisbal, A. Sousa, A. Castineiras, J. Gracia-Vazquez, J. A. Romero, D. X. West, *Polyhedron*, **2000**, 19, 1255.
50. J. S. Casas, A. Castineiras, C. Maria, Rodriguez-Arguelles, A. Sanchez, J. Sordo, V-L. Antonia, M. V-L. Ezequiel, *J. Chem. Soc. Dalton Trans.* 2000, 4056.
51. E. Cristurean, C. Parnau, M. Badea, R. Olar, *Analele Universităţii din Bucuresti* **2004**, I-II, 155.
52. F. A. Beckford, G. Leblanc, J. Thessing, M. Shaloski Jr., B. J. Frost, L. Li, N. P.

- Seeram, *Inorganic Chemistry Communications*, **2009**, 12, 1094–1098.
53. A. A. Ibrahim, H. Khaledi, P. Hassandarvish, H. M. Ali, H. Karimian, *Dalton Trans.* **2014**, 43, 3850.
 54. R. Sharma, T.S. Lobana, M. Kaur, N. Thathai, G. Hundal, J. P. Jasinski, R. J. Butcher, *Indian Academy of Sciences.* **2016**, DOI 10.1007/s12039-016-1097.
 55. T.S. Lobana, R. Sultana, R. J. Butcher, J. P. Jasinski, T. Akitsu, *Zeitschrift für anorganische Chemie* DOI: 10.1002/zaac. **2014**, 00064.
 56. K. Onodera, N. C. Kasuga, T. Takashima, A. Hara, A. Amano, H. Murakami, K. Nomiya, *J. Chem. Soc. Dalton Trans.* **2007**, 3646.
 57. T. R. Todorovic, A. Bacchi, G. Pelizzi, N. O. Juranic, D. M. Sladic, I. D. Brceski, K. K. Anđelkovic, *Inorg. Chem. Commun.* **2006**, 9, 862.
 58. N. Gligorijević, T. Todorović, S. Radulović, D. Sladić, N. Filipović, D. Godevac, D. Jeremić, K. Anđelković, *Eur. J. Med. Chem.* **2008**, 44, 1623.
 59. A. Molter, F. Mohr, *Dalton Trans.* **2011**, 40, 3754.
 60. P. Bippus, A. Molter, D. Müller, F. Mohr, *Journal of Organometallic Chemistry*, **2010**, 695, 1657-1662.
 61. S. Bjelogrić, T. Todorović, A. Bacchi, M. Zec, D. Sladić, T. S. Rajić, D. Radanović, S. Radulović, G. Pelizzi, K. Anđelković, *Journal of Inorganic Biochemistry* **2010**, 104, 673–682.
 62. N. R. Filipović, S. Bjelogrić, G. Portalone, S. Pelliccia, R. Silvestri, O. Klisurić, M. Senćanski, D. Stanković, T. R. Todorović, C. D. Mulleri, *MedChemComm.* DOI: 10.1039/C6MD00199H.
 63. T.R. Todorović, A. Bacchi, G. Pelizzi, N. O. Juranić, D. M. Sladić, I. D. Brćeski, K. K. Anđelković, *Inorganic Chemistry Communications*, **2006**, 9, 862–865.
 64. T.R. Todorović, A. Bacchi, N.O. Juranić, D.M. Sladić, G. Pelizzi, T.T. Božić, N.R. Filipović, K.K. Anđelković, *Polyhedron* **2007**, 26, 3428.
 65. T. R. Todorović, A. Bacch, D.M. Sladić, N. M. Todorović, T. T. Božić, D. D. Radanović, N. R. Filipović, G. Pelizzi, K. K. Anđelković, *Inorg. Chim. Acta* **2009**, 362, 3813.
 66. I. D. Brceski, V. M. Leovac, G. A. Bogdanovi, S. P. Sovilj, M. Revenco, *Inor. Chem. commun.* **2004**, 7, 253.

67. A. Molter, F. Mohr, *Dalton Trans.* **2011**, 40, 3754.
68. A. Molter, J. Rust, C. W. Lehmann, G. Deepa, P. Chiba, F. Mohr, *Dalton Trans.* **2011**, 40, 9810.
69. A. Molter, E. Bill, F. Mohr, *Inorg. Chem. Commun.* **2012**, 17, 124.
70. A. Molter, G. N. Kaluderovic, H. Kommera, R. Paschke, T. Langer, R. Pottgen, F. Mohr, *J. Org. Met. Chem.* **2012**, 701, 80.
71. P. Bippus, A. Molter, D. Müller, F. Mohr. *J of Organometallic Chem.* **2010**, 695, 1657-1662.
72. T. S. Lobana, Rekha, A.P.S. Pannu, G. Hundal, R. J. Butcher, A.Castineiras, *Polyhedron*, **2007**, 26, 2621.
73. T. S. Lobana, Rekha, B. S. Sidhu, A. Castineiras, E. Bermejo, T. Nishioka, *J. Coord. Chem.* **2005**, 58, 803.
74. J. R. Dilworth, R. Huetting, *Inorg. Chim. Acta*, **2012**, 389.
75. G. A. Bain, D. X. West, J. Krejci, J. S. Hernández –Ortega, R. A. Toscanob, *Polyhedron*, **1997**, 16, 855.
76. J. E. Huheey, E. A. Keiter, R. L. Keiter *Inorganic Chemistry: Principals of Structure and Reactivity*, 1993, 4th ed.; Harper Collins College Publishers: New York.
77. M. Hakimi, H. Vahedi, M. Rezvaninezhad, E. Schuh, F. Mohr, *J. Sulf. Chem.* **2011**, 32, 55.
78. S. Lhuachan, S. Siripaisarnpipat, N. Chaichit, *Eur. J. Inorg. Chem.* **2003**, 263.
79. R. D. Pike, A. B. Wiles, T. A. Tronic, *Acta Cryst.* **2006**, E62, m347.
80. B-K. Teo, J.C. Calabrese, *Inorg. Chem.* **1976**, 15, 2467.
81. S. Zartilas, S. K. Hadjikakou, N. Hadjiliadis, N. Kourkoumelis, L. Kyros, M. Kubicki, M. Baril, Ian S. Butler, S. Karkabounas, J. Balzarini, *Inorganica Chimica Acta*, **2009**, 362, 1003–1010.
82. T. S. Lobana, P. Kumari, R. J. Butcher, *Inorg. Chem. Commun.* **2008**, 11, 11.
83. K. M. Kim, C. F. McDonagh, L. Westendorf, L. L. Brown, D. Sussman, T. Feist, R. Lyon, S. C. Alley, N. M. Okeley, X. Zhang, M. C. Thompson, I. Stone, H. P. Gerber, P. J. Carter, *Mol Cancer Ther.* **2008**, 7, 2486.
84. Compounds were constructed and docked with builder tool kit of software package ArgusLab 4.0.1.23 (www.arguslab.com).

85. T. S. Lobana, R. Sharma, G. Hundal, A. Castineiras, R. J. Butcher *Polyhedron*, **2012**, 47, 134–142.
86. T. S. Lobana, R. Sharma, , R. J. Butcher *Polyhedron*, **2009**, 28, 1103–1110.
87. T. S. Lobana, Rekha, R. J. Butcher, T. W. Failes and P. Turner, *J. Coord. Chem.* **2005**, 58, 1369–1375.
88. a) T. S. Lobana, A. Castineiras, *Polyhedron*, 21 (**2002**) 1603
 b) T. S. Lobana, G. Hundal, *I J. Chem. Soc. Dalton Trans.* (**2002**) 2203
 c) T. S. Lobana, R. Mahajan, Castineiras, *Trans. Met. Chem.* (**2001**, 26, 440.
89. a) T. S. Lobana, R. Sharma, G. Hundal, A. Castineiras, R. J. Butcher, *Polyhedron*, **2012**, 47, 134–142
 b) T. S. Lobana, and Rekha, *Transition Metal Chemistry*, **2004**, 29, 291–295
90. T. S. Lobana, P. Kumari, R. J. Butcher, *Inorg. Chem. Commun.* **2008**, 11, 11.
91. L. J. Ashfield, A. R. Cowey, J. R. Dilworth, P. S. Donnelly, *Inorg. Chem.* **2004**, 43, 4121.
92. T. S. Lobana, S. Khanna, R. Sharma, G. Hundal, R. Sultana, M. Chaudhary, R. J. Butcher, and A. Castineiras, *Crystal Growth and Design*, **2004**, 8, 1202-1212.
93. Q. P. Qin, Y.C. Liu, H. L. Wang, J. L. Qin, F. J. C. S. F. Tang H. Liang *Royal Society of Chemistry*, **2015**, DOI: 10.1039/c5mt00027k
94. L. Pauling, *The Nature of the Chemical Bond*, Ithaca, Cornell University, 3rd edn
95. J. E. Huheey, E. A. Keiter, R. L. Keiter, *Inorganic Chemistry: Principal of Structure and Reactivity*, 4th edit. Harker Colin College Publishers, New York, **1993**
96. P. Karagiannidis, P. Aslanidis, S. Kokkou, C. Cheer, *J. Inog. Chimica Acta*, **1990**, 172, 247.
97. V. Sharma, P. Kumar, and D. Pathak *J. Heterocyclic Chem.* **2010**, 47, 491-502.
98. S. Lhuachan, S. Siripaisarnpipat, N. Chaichit, *Eur. J. Inorg. Chem.* **2003**, 263-267.
99. T. S. Lobana, A. Sanchez, J. S Casas. A. Castineiras, J. Sordo, M. S. Garcia-Tasende, E. M. Vazquez-Lopez, *J. Chem. Soc. Dalton Trans.* **1997**, 4289.
100. F. H. Allen, O. Kennard, R. Taylor, *Acc. Chem. Res.* **1983**, 16, 146
101. R. Sharma, T. S. Lobana, M. Kaur, N, Thathai, G. Hundal, J. P. Jaisinski, R. J.

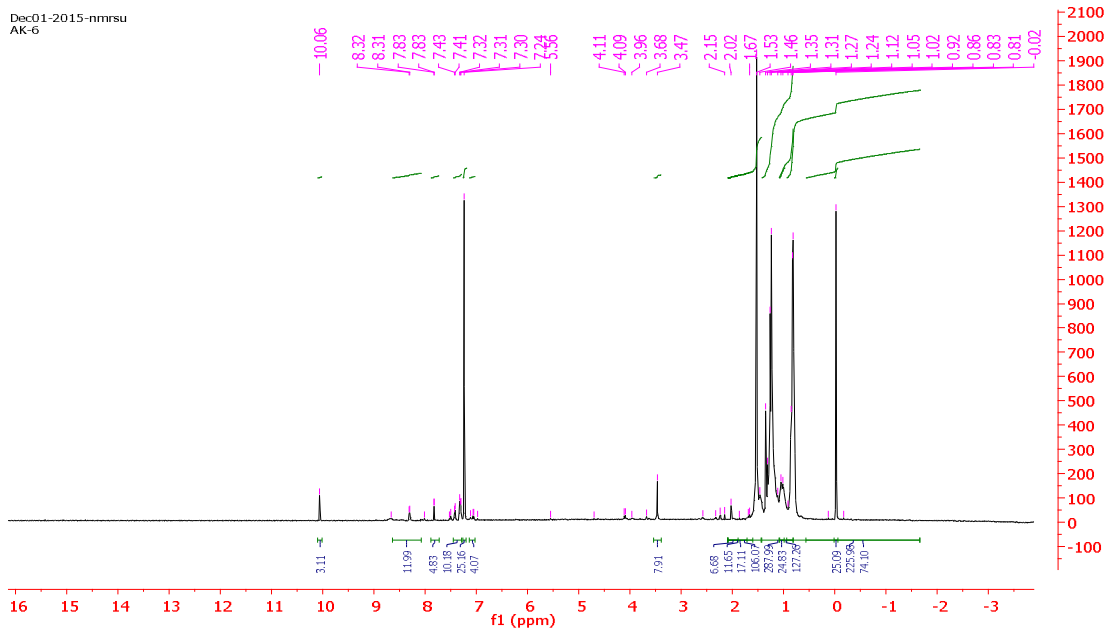
- Butcher, *J. Chem. Sci.* **2016** DOI 10.1007/s12039-016-1097.
102. N. K. Jain, M. K. Chourasia, S. Jain, S. K. Jain, *Indian J Pharm Sci.* (**2003**) 65, 113–121.
103. M. C. S. Lourenco, Ma. V. N deSouza, A. C. Pinheiro, M.de L. Ferreira, R. B. Goncalves, T. Cristina, M. Nogueira, M. A. Peralta, *ARKIVOC* xv **2007**, 181-191.
104. F. R. Pavan, P. I. da S. Maia, S. R. A. Leite, V. M. Deflon, A. A. Batista, D. N. Sato, S. G. Franzblau, C. Q. F. Leite, *European Journal of Medicinal Chemistry* **2010**, 45, 1898–1905.
105. Y. L. Huang, D.Fengli, J.Sun, J. H. Gao, S. Shan, *Acta Crystallographica* **2011**, 67, 528.
106. H. K. Fun, R. Kia, H. Kargar *Acta Crystallographica* **2009**, 65, 246-247.

LIST OF PUBLICATIONS

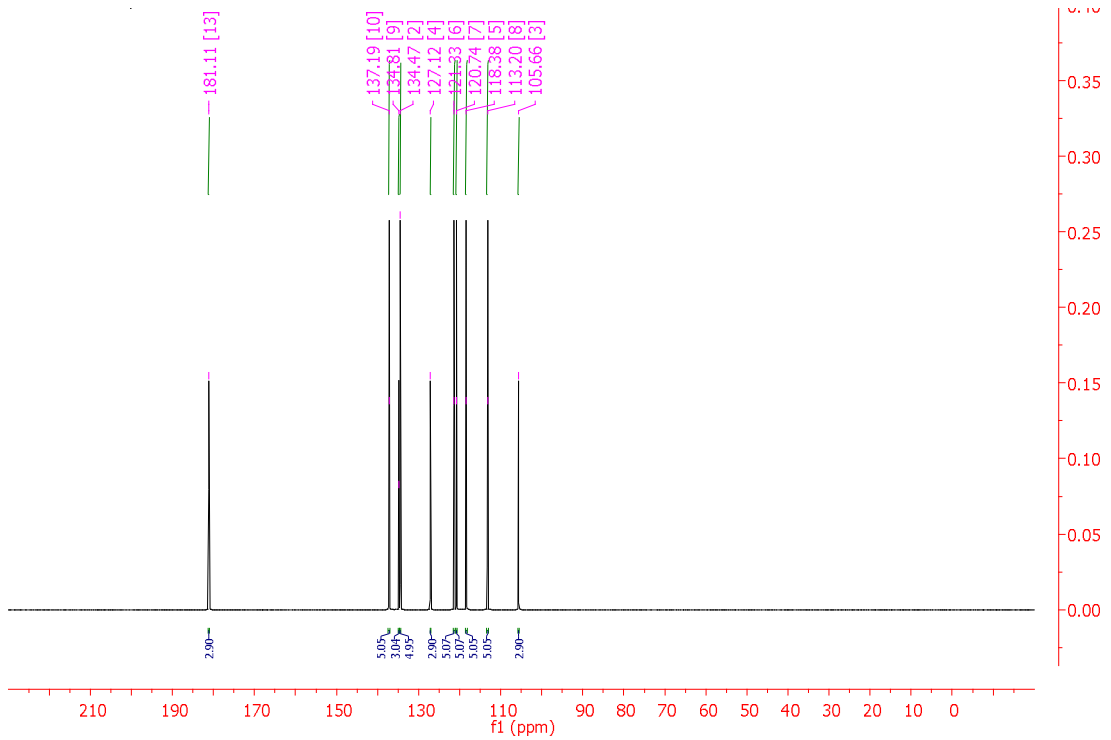
1.	<p>Synthesis, structure and cytotoxicity evaluation of complexes of N1-substituted-isatin-3-thiosemicarbazone with copper(I) halides.</p> <p>Ashiq Khan, Jerry P. Jasinski, Victoria A. Smoleaski, Kamaldeep Paul, Gurpinder Singh, Rekha Sharma <i>Inorganica Chimica Acta</i> 449 (2016) 119–126.</p>
2.	<p>Synthesis and crystal structure of [chlorobis(triphenylphospino)(p-chlorobenzaldehyde thiosemicarbazone)] copper(I) complex.</p> <p>Ashiq Khan, Poonam Sharma, Rajnikant, Vivek K Gupta, Naresh Padha and Rekha Sharma <i>J. Chem. Sci.</i> Vol. 128, No. 2, February 2016, pp. 185–191.</p>
3.	<p>Unusual enhancement in the anti-tuberculosis activity of Indole based thiosemicarbazones on complexation with Cu(I) halides.</p> <p>Ashiq Khan, Jerry P. Jasinski, V. A. Smolenski, Rekha Sharma <i>Inorganica Chimica Acta</i> (Submitted).</p>
4.	<p>Thiosemicarbazone complexes of silver(I): Synthesis and structure of fused ring thiosemicarbazones complexes of silver(I).</p> <p>Ashiq Khan, Jerry P. Jasinski, V. A. Smolenski, Rekha Sharma <i>Journal of Molecular Structure</i> (Under preparation).</p>

ANNEXURE
NMR (¹H AND ¹³C) SPECTRA

Dec01-2015-nmrstu
AK-6

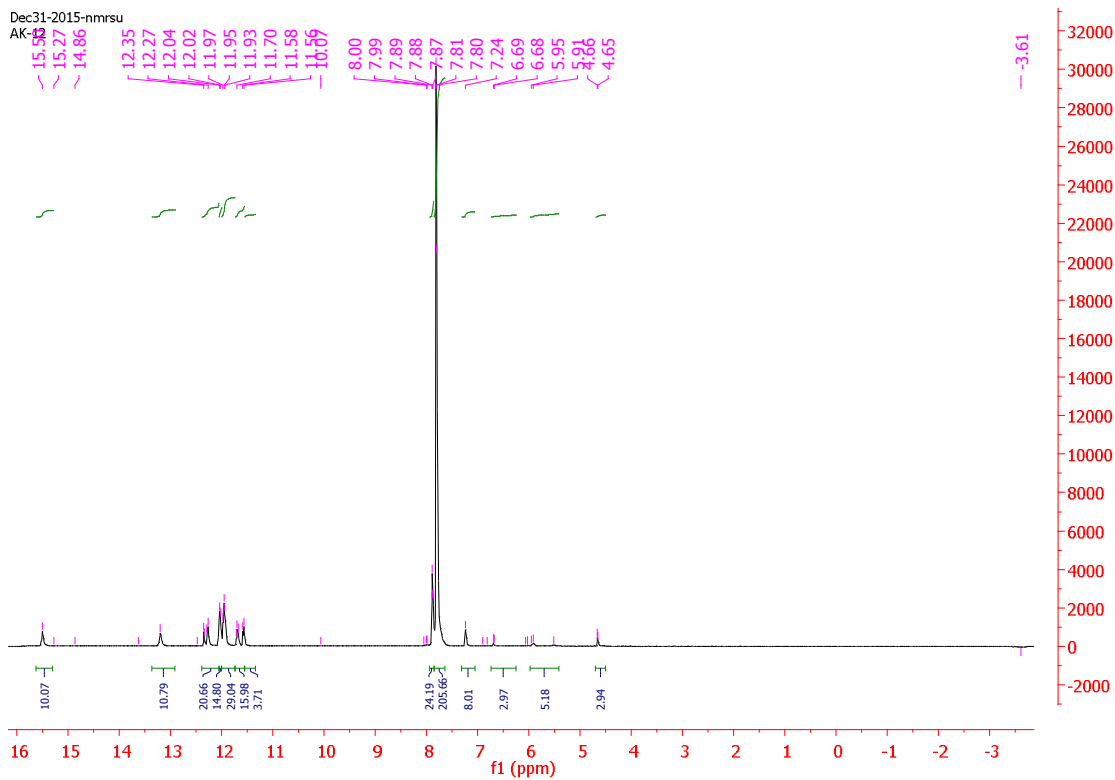


(a)

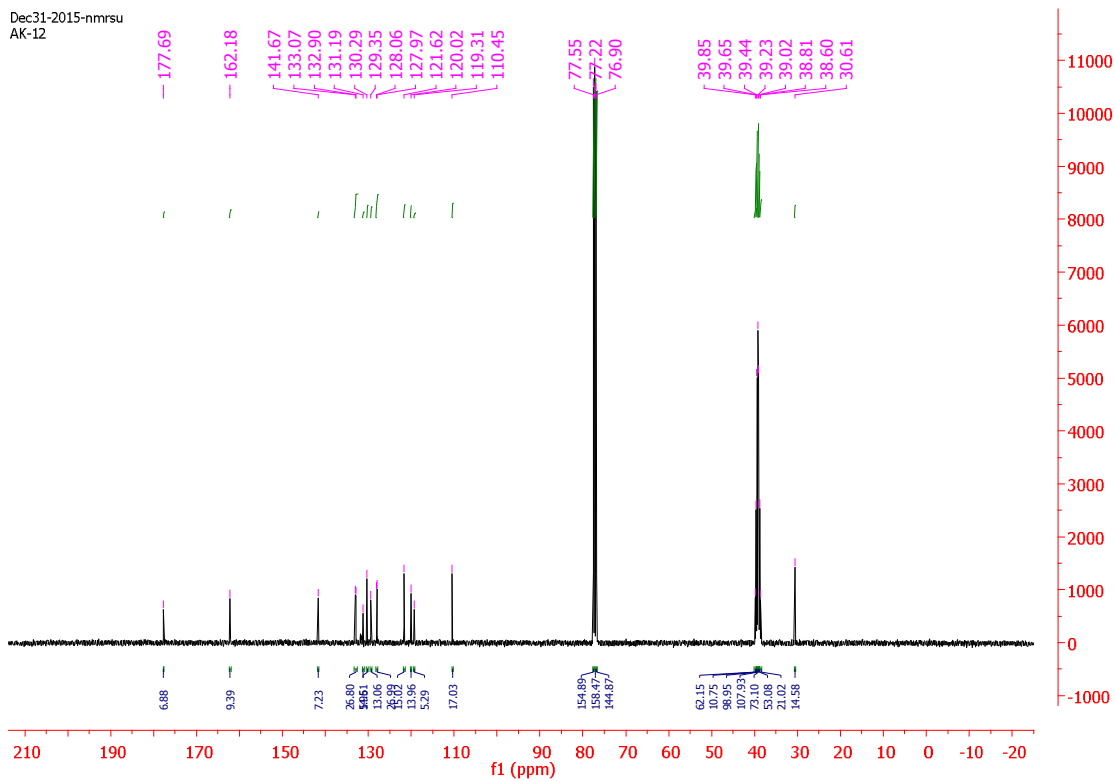


(b)

Figures-38: ¹H NMR(a) and ¹³C NMR(b) spectra of Indole-3-thiosemicarbazone (HIntsc)

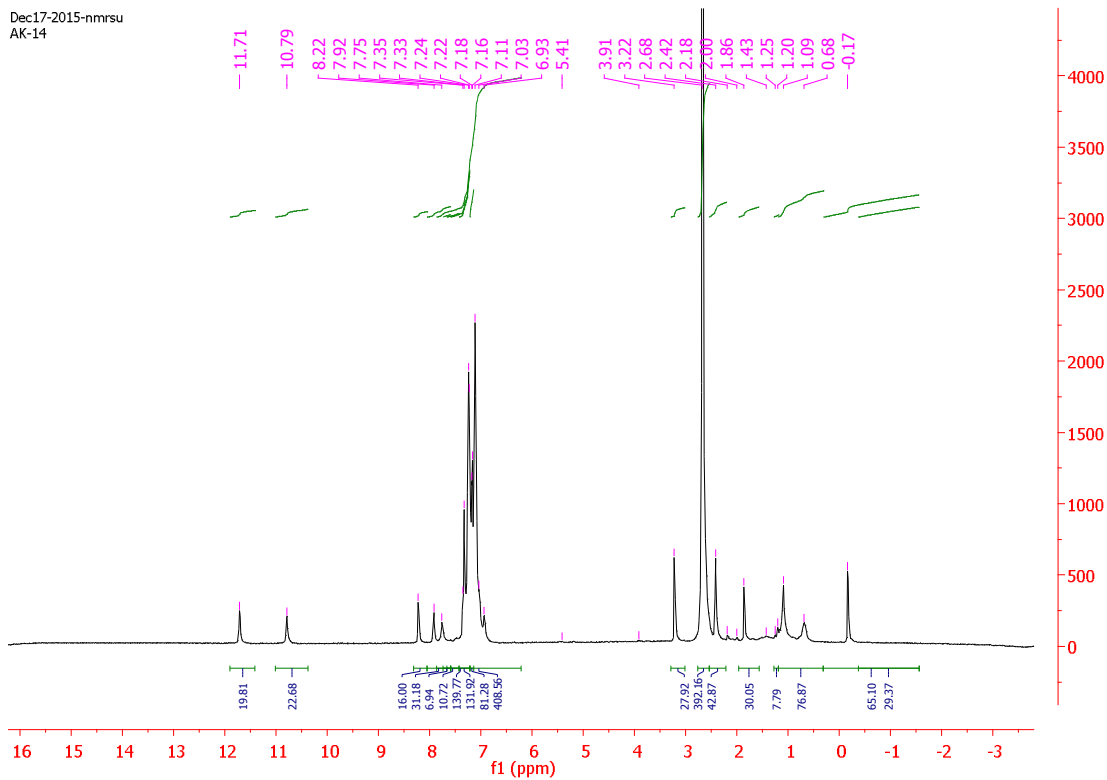


(a)

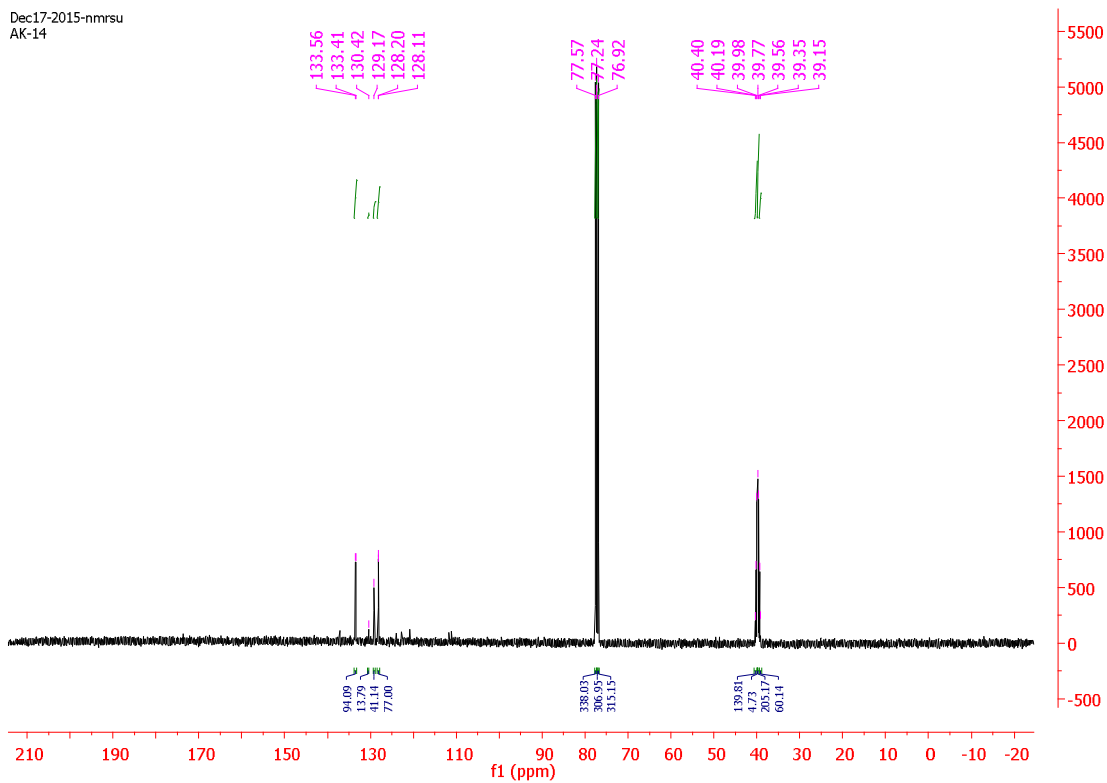


(b)

Figures-39: ^1H NMR(a) and C^{13} NMR(b) spectra of $[\text{CuBr}(\eta^1\text{-S-Hintsc})(\text{Ph}_3\text{P})_2]$

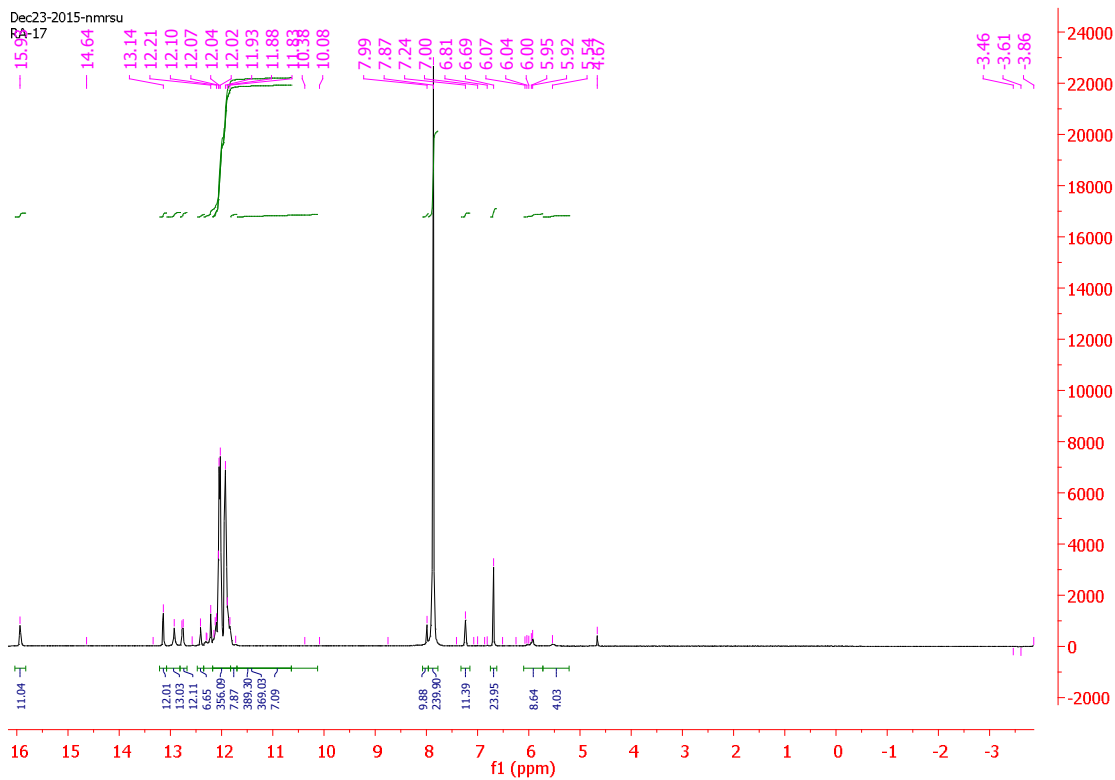


(a)

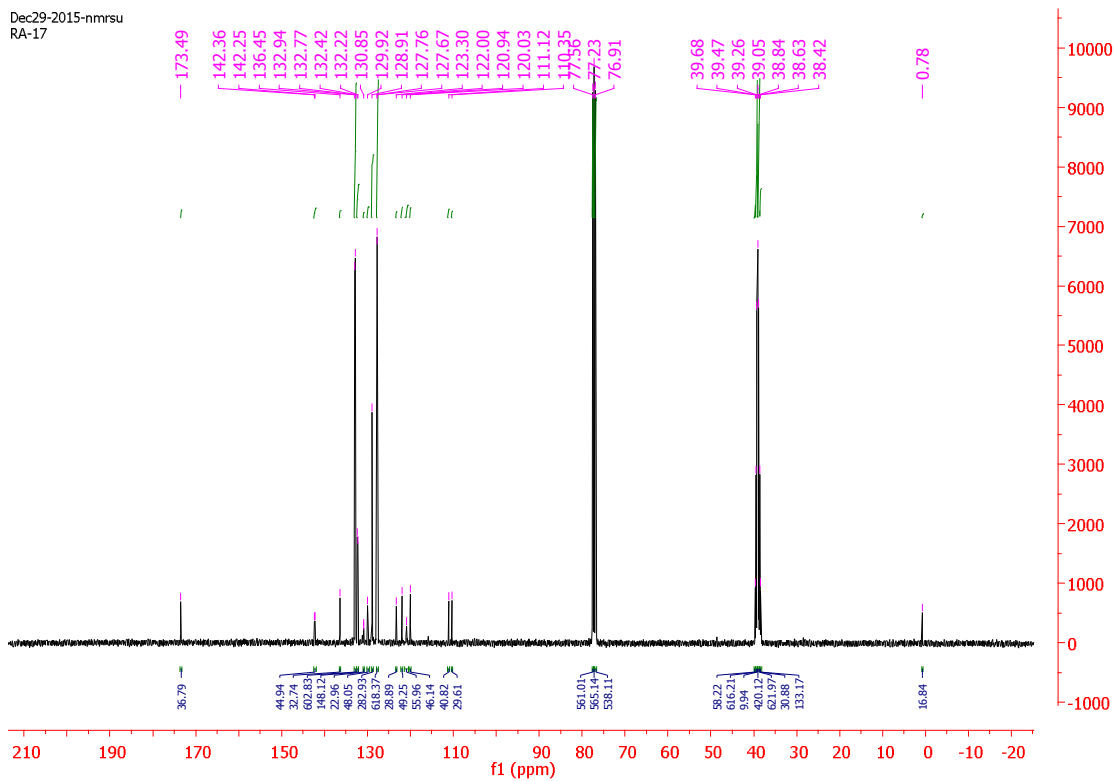


(b)

Figures-40: ^1H NMR(a) and C^{13} NMR(b) spectra of $[\text{CuCl}(\eta^1\text{-S-Hintsc})(\text{Ph}_3\text{P})_2]$.

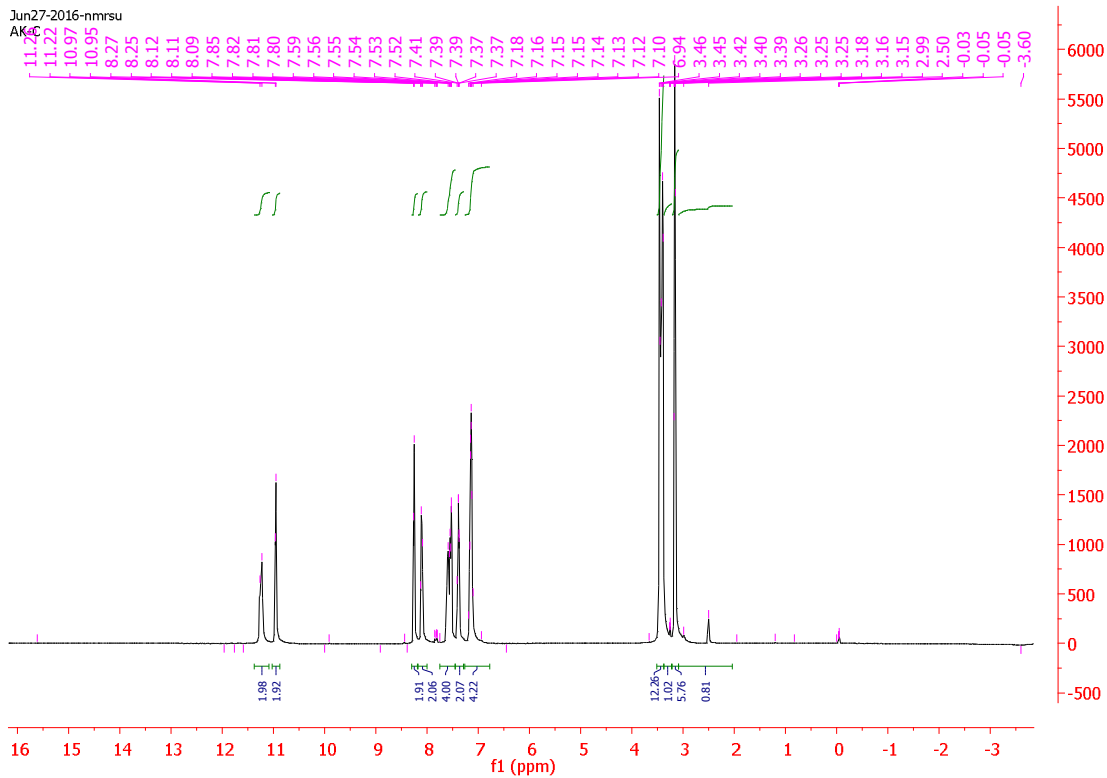


(a)

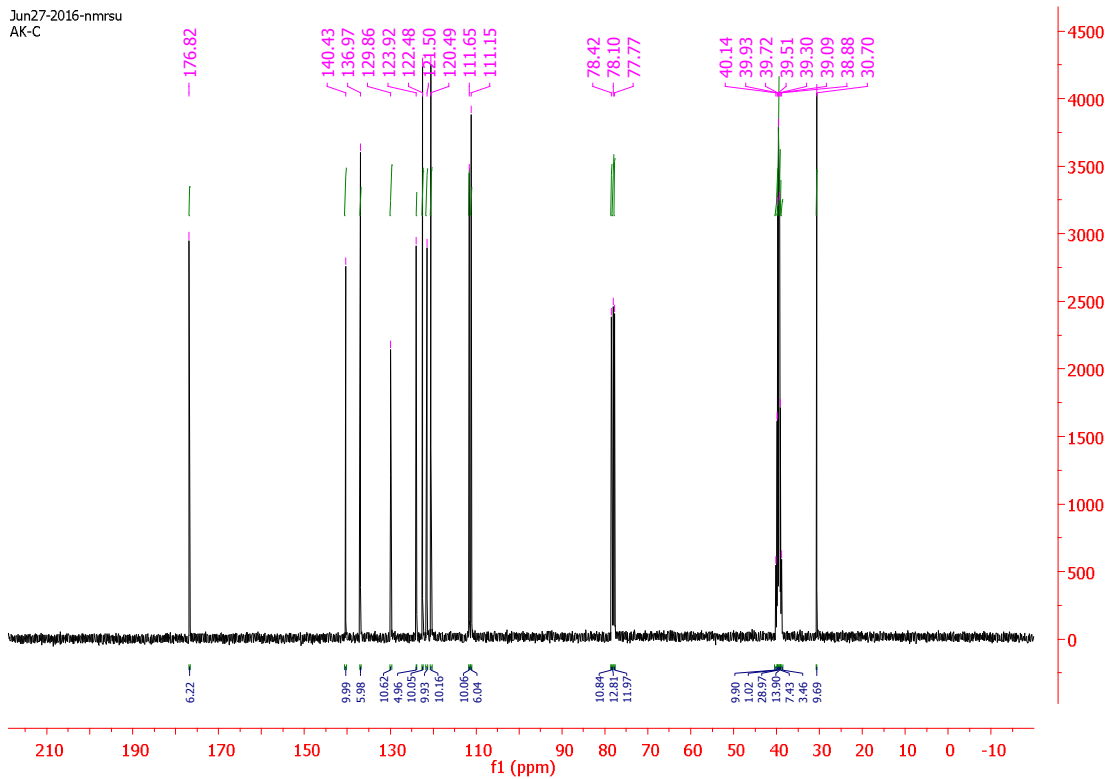


(b)

Figures-41: ^1H NMR(a) and C^{13} NMR(b) spectra of $[\text{AgCl}(\eta^1\text{-S-HIntsc})(\text{Ph}_3\text{P})_2]$

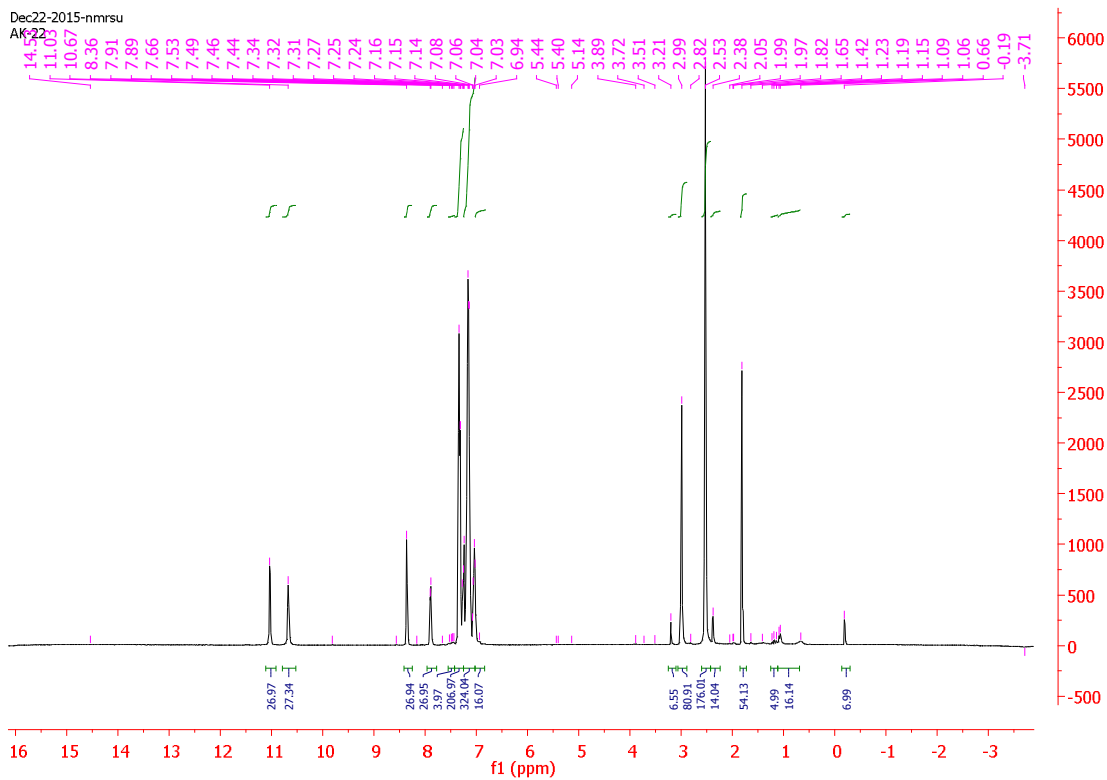


(a)

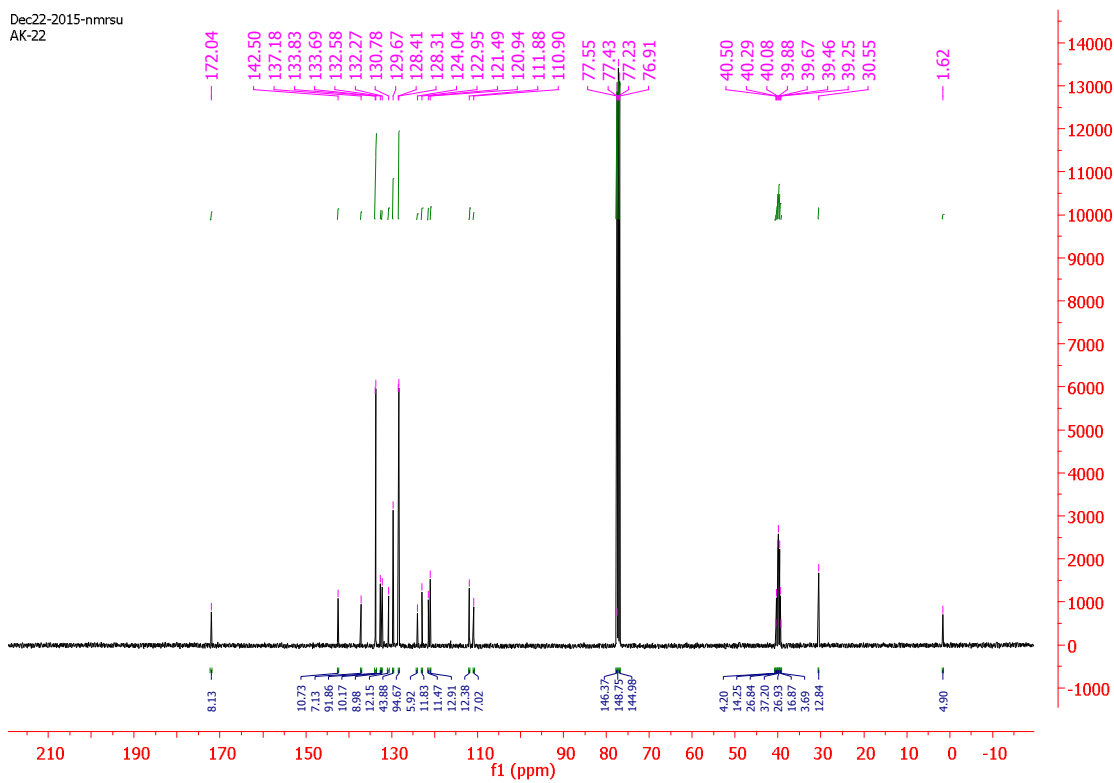


(b)

Figures-42: ^1H NMR(a) and ^{13}C NMR(b) spectra of Indole- N^1 -methyl-3-thiosemicarbazone (HIntsc- N^1 -Me).

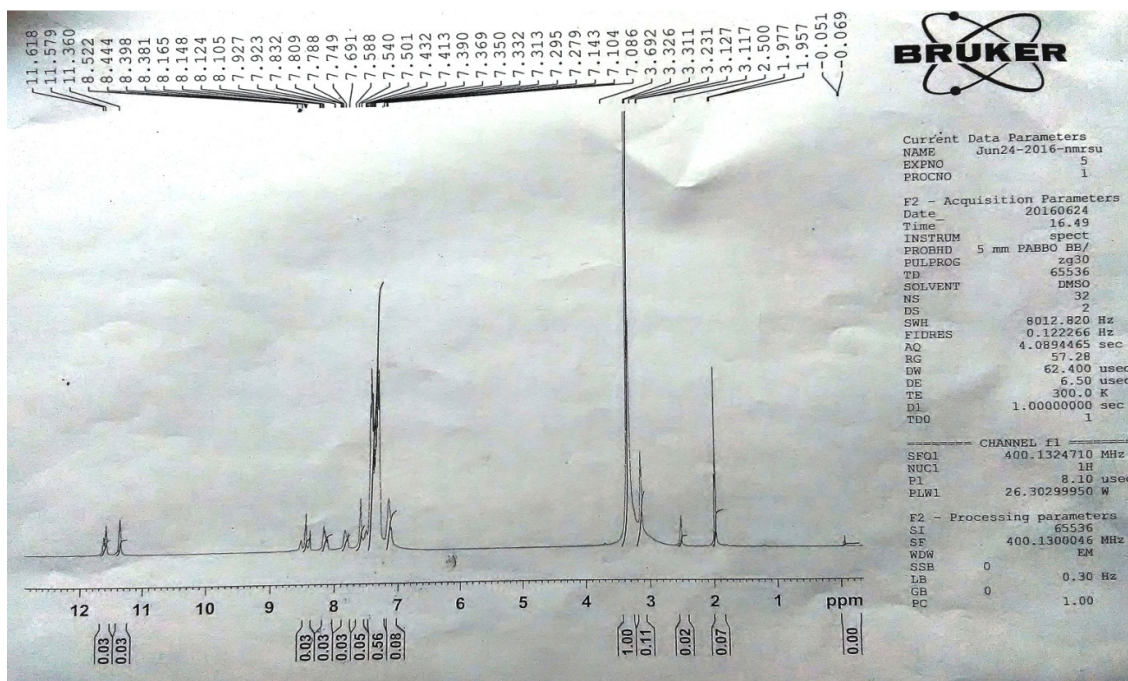


(a)

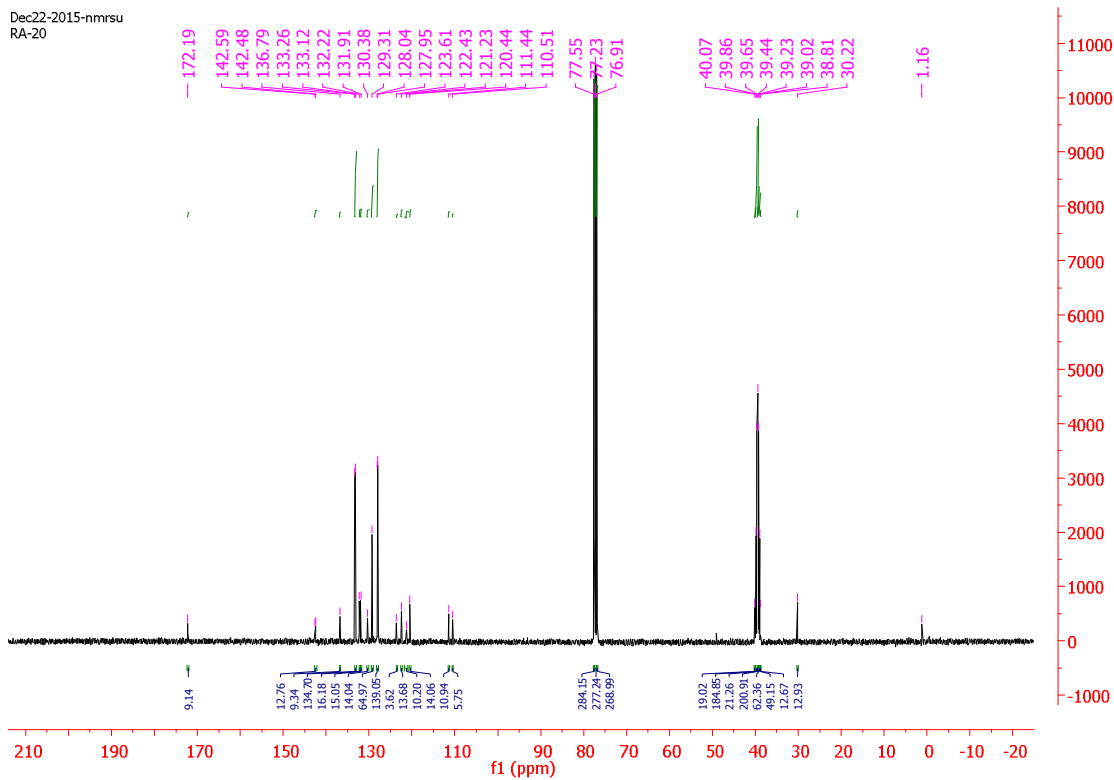


(b)

Figures-43: ¹H NMR(a) and ¹³C NMR(b) spectra of [Cu₂(μ₂-I)₂(HIntsc-N¹-Me)₂(Ph₃P)₂]

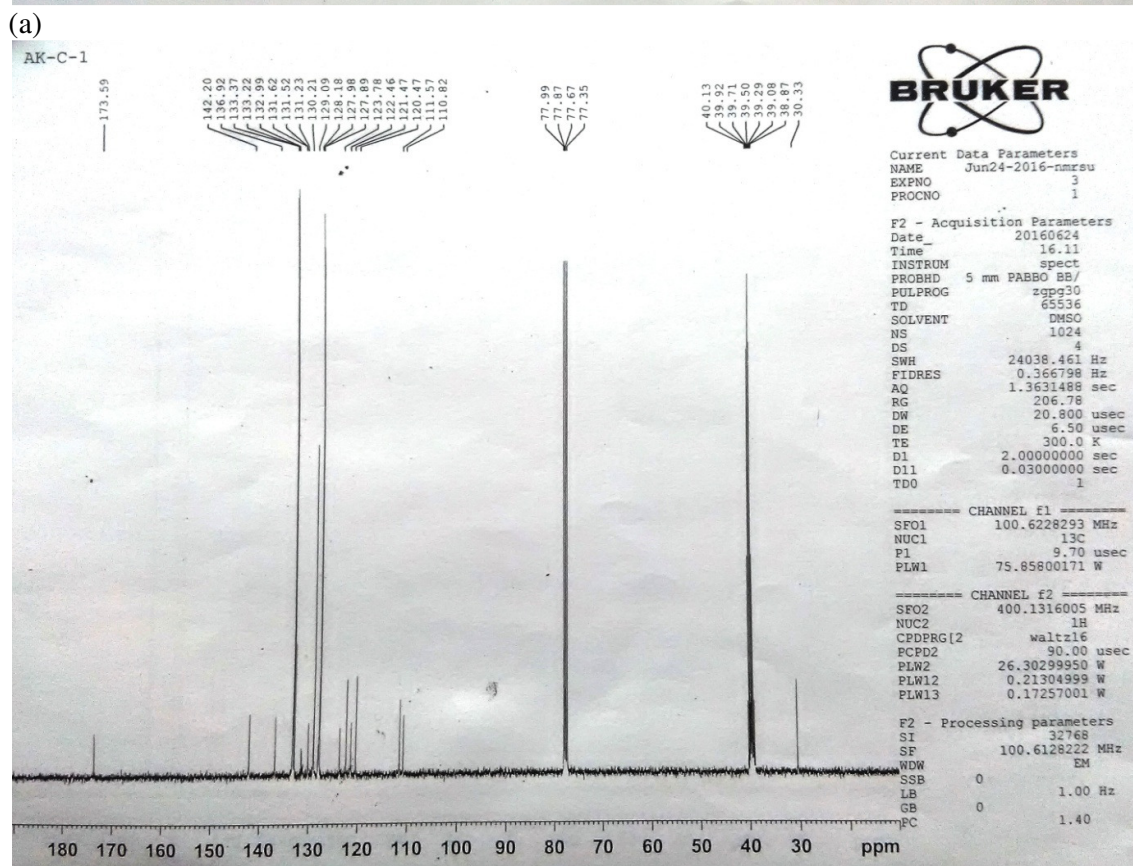
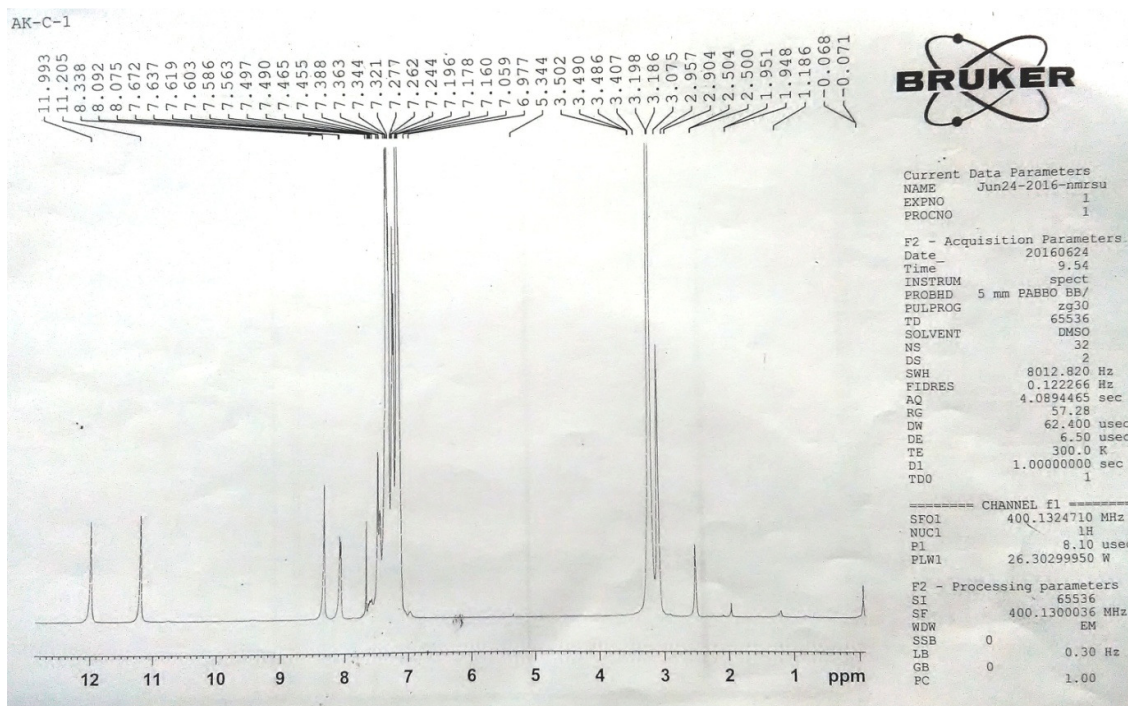


(a)

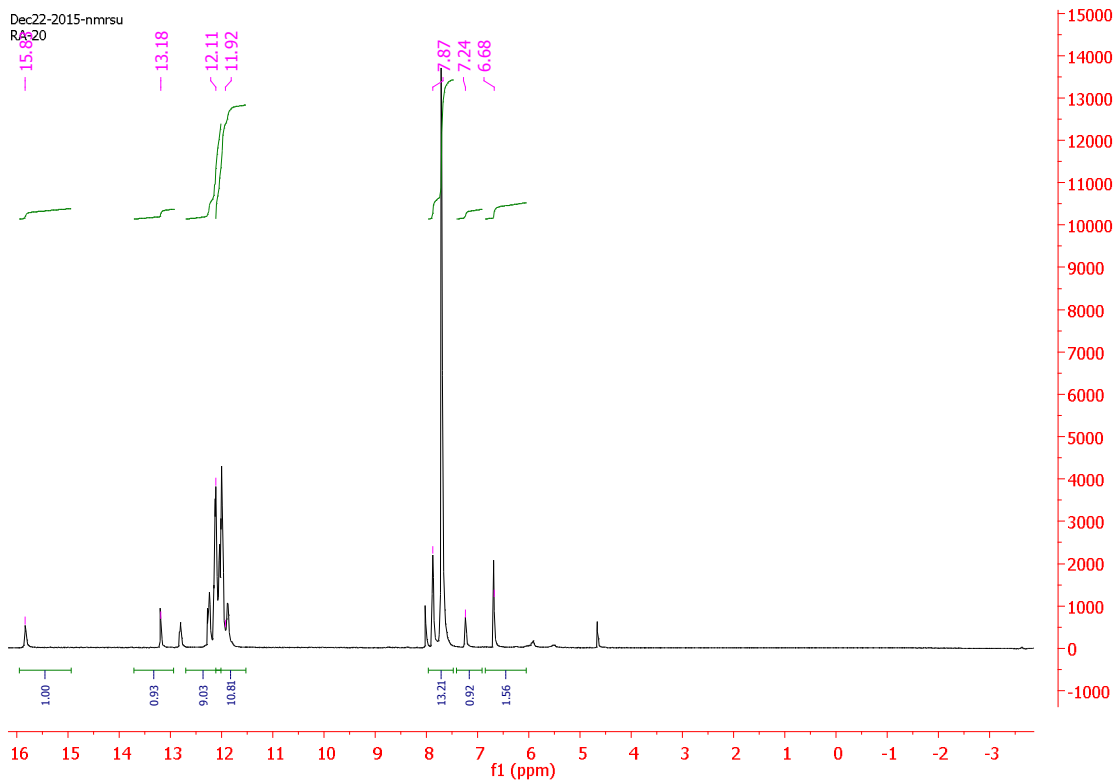


(b)

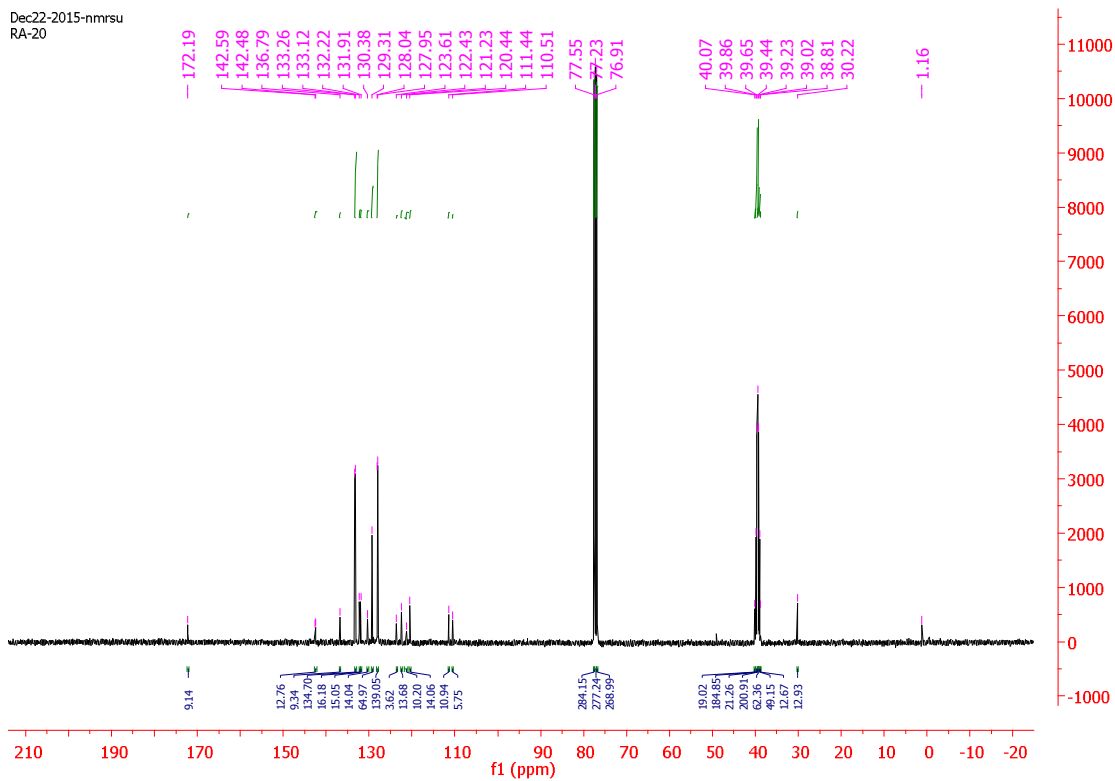
Figures-44 : ^1H NMR(a) and ^{13}C NMR(b) spectra of $[\text{Cu}_2(\mu_2\text{-Br})_2(\text{HIntsc-N}^1\text{-Me})_2(\text{Ph}_3\text{P})_2]$.



(b)
 Figures-45 : ^1H NMR(a) and C^{13} NMR(b) spectra of $[\text{Cu}_2(\mu_2\text{-Cl})_2(\text{HIntsc-N}^1\text{-Me})_2(\text{Ph}_3\text{P})_2]$.



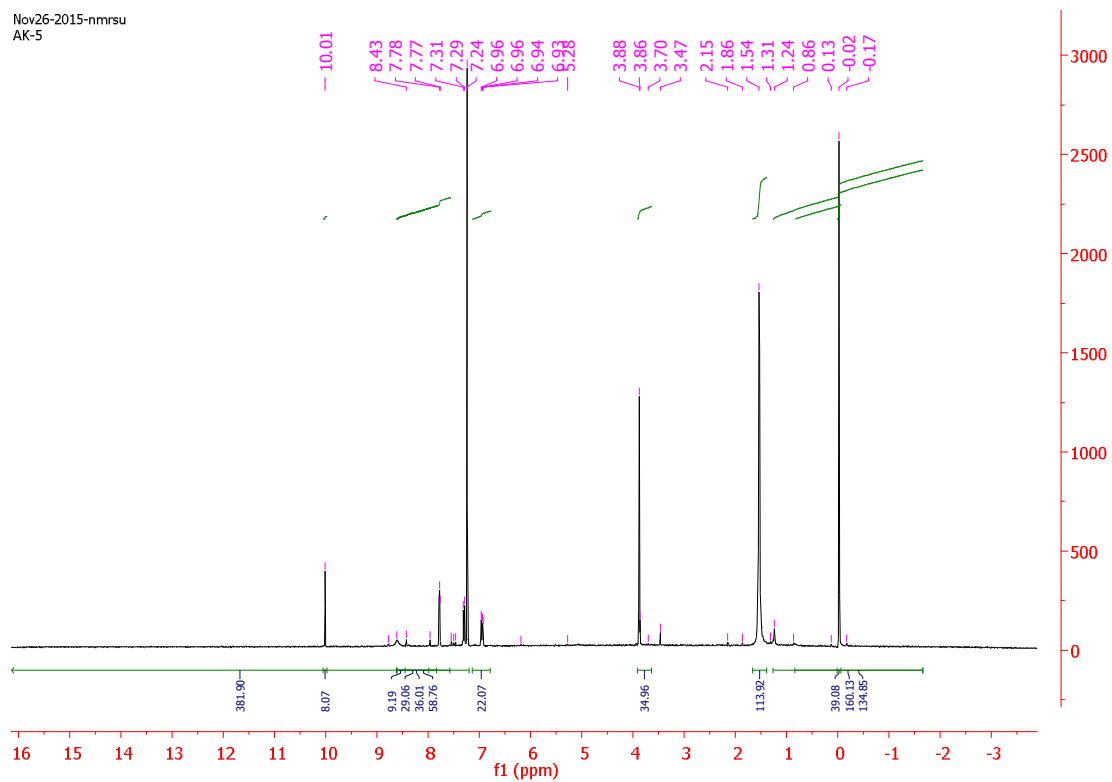
(a)



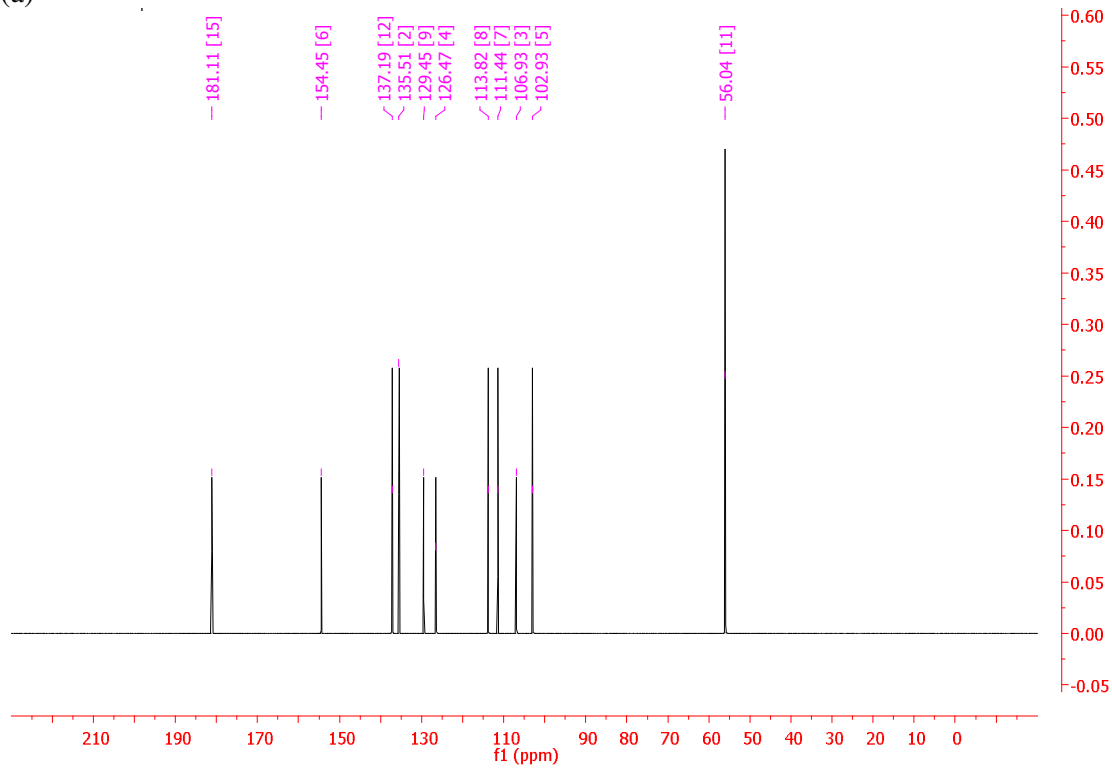
(b)

Figures-46 : ^1H NMR(a) and ^{13}C NMR(b) spectra of $[\text{AgBr}(\eta^1\text{-S-HIntsc})(\text{Ph}_3\text{P})_2]$.

Nov26-2015-nmrsu
AK-5

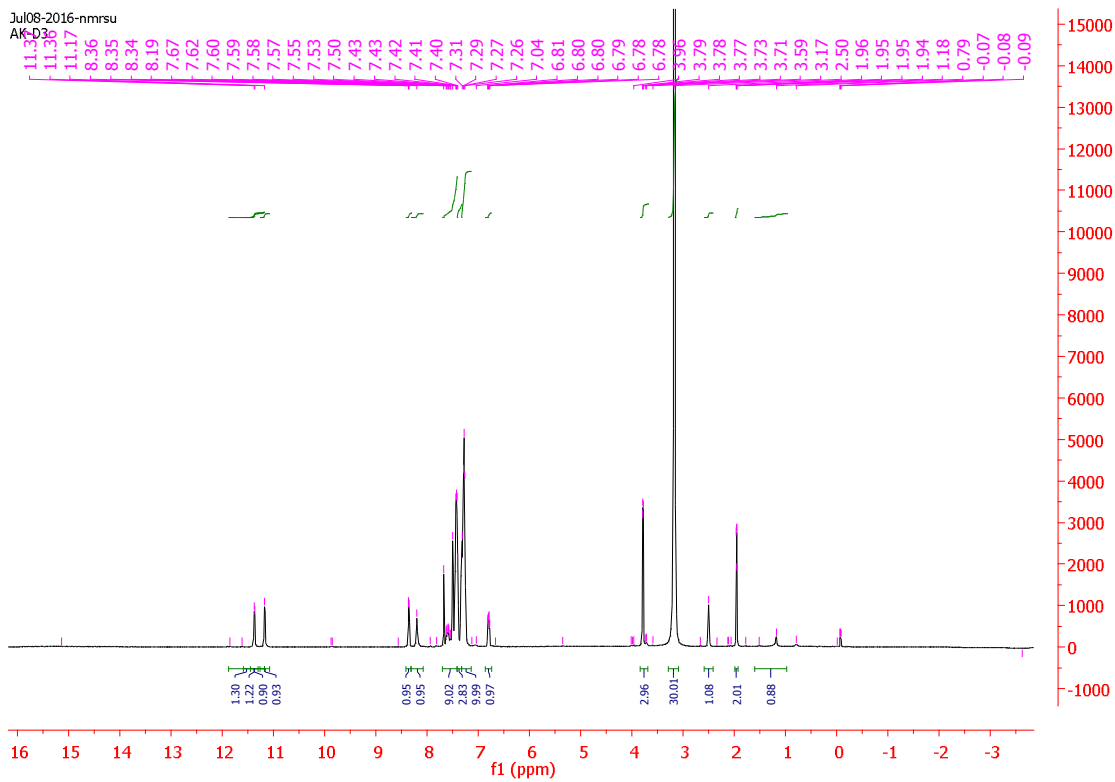


(a)

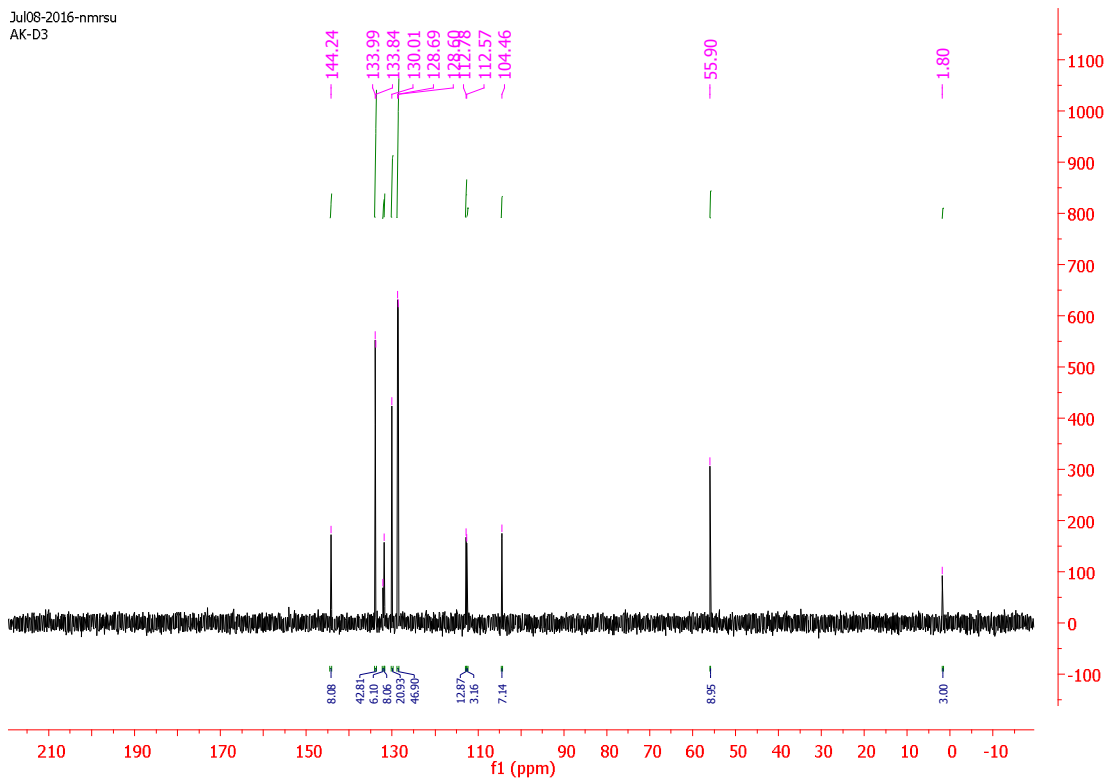


(b)

Figures-47: ^1H NMR(a) and ^{13}C NMR(b) spectra of 5-methoxy indole-3-thiosemicarbazone (5-MeOHIntsc).

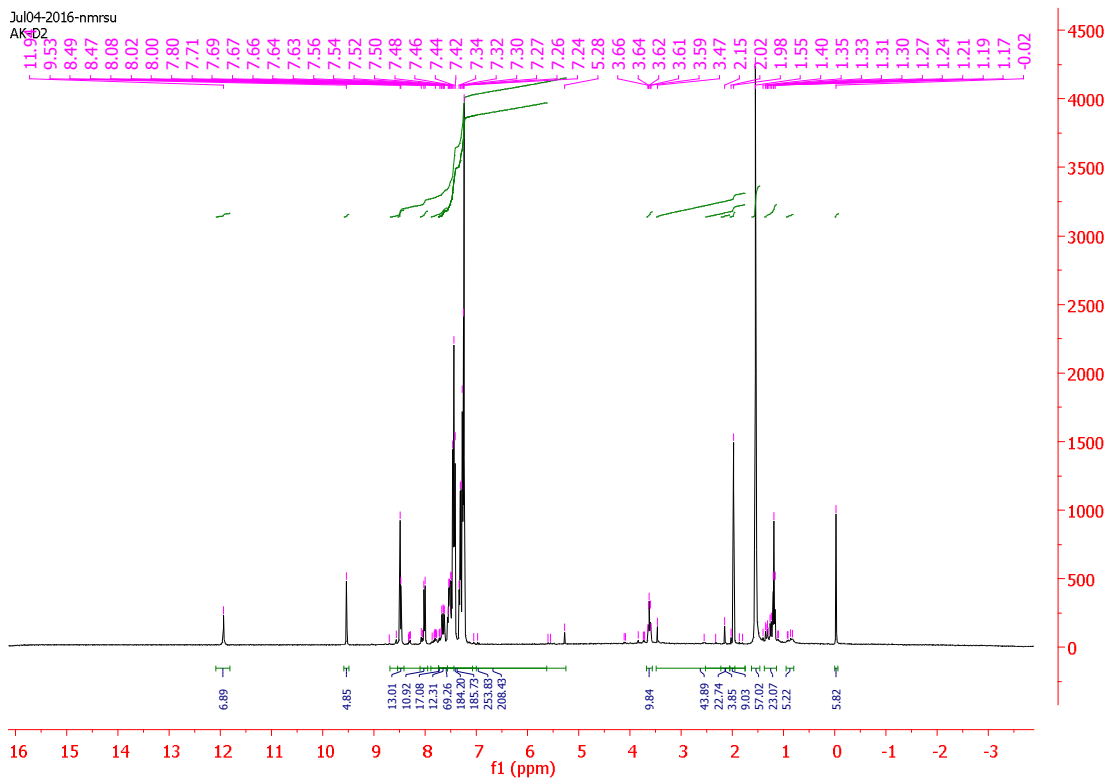


(a)

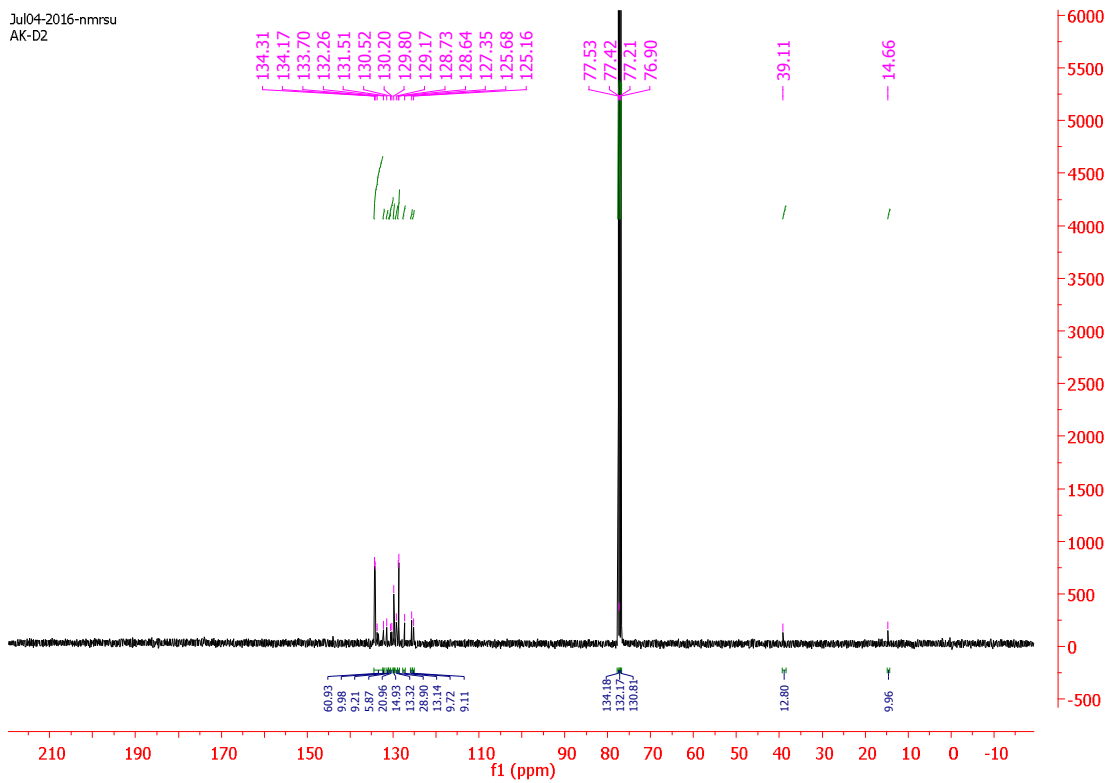


(b)

Figures-48: ^1H NMR(a) and C^{13} NMR(b) spectra of $[\text{CuI}(\eta^1\text{-S-5-MeOHIntsc})(\text{Ph}_3\text{P})_2]$

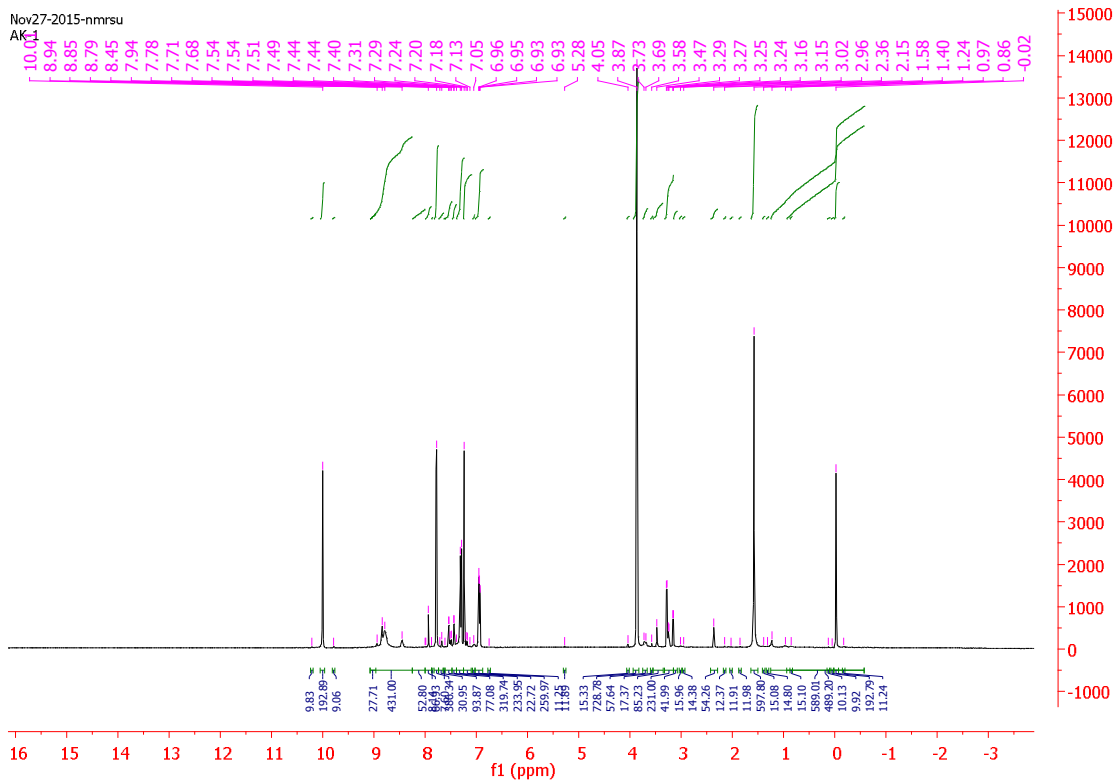


(a)

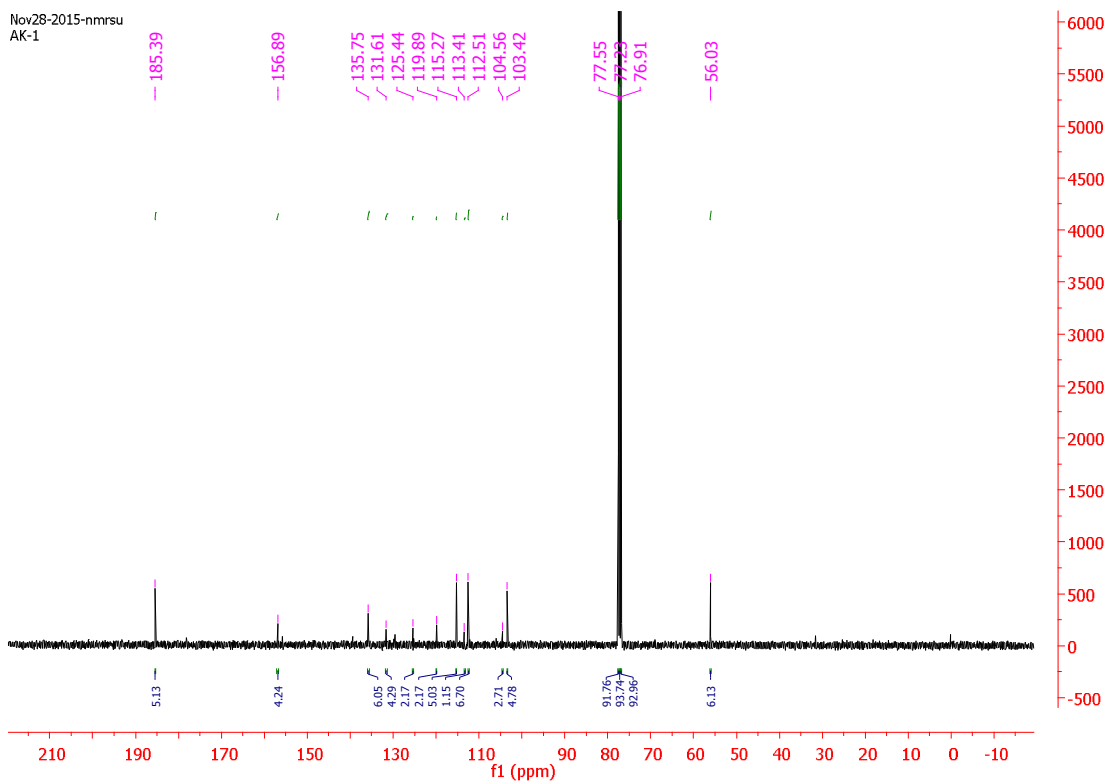


(b)

Figures-49: ^1H NMR(a) and ^{13}C NMR(b) spectra of $[\text{CuBr}(\eta^1\text{-S-5-MeOHIntsc})(\text{Ph}_3\text{P})_2]$

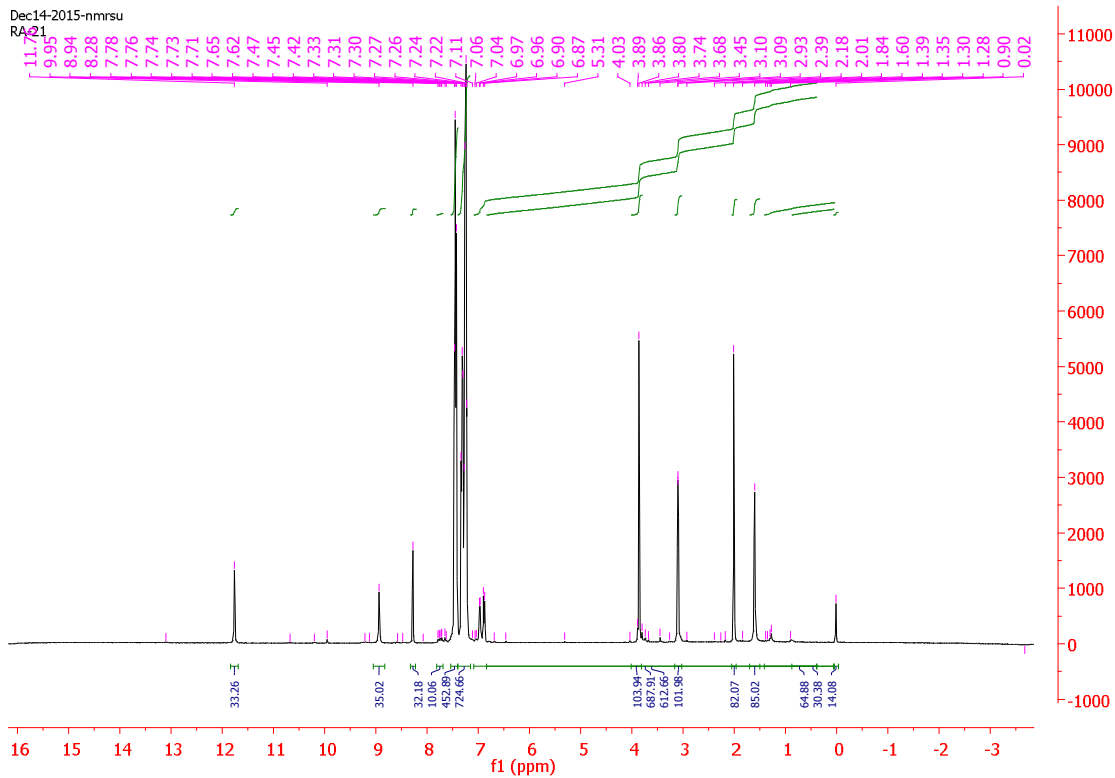


(a)

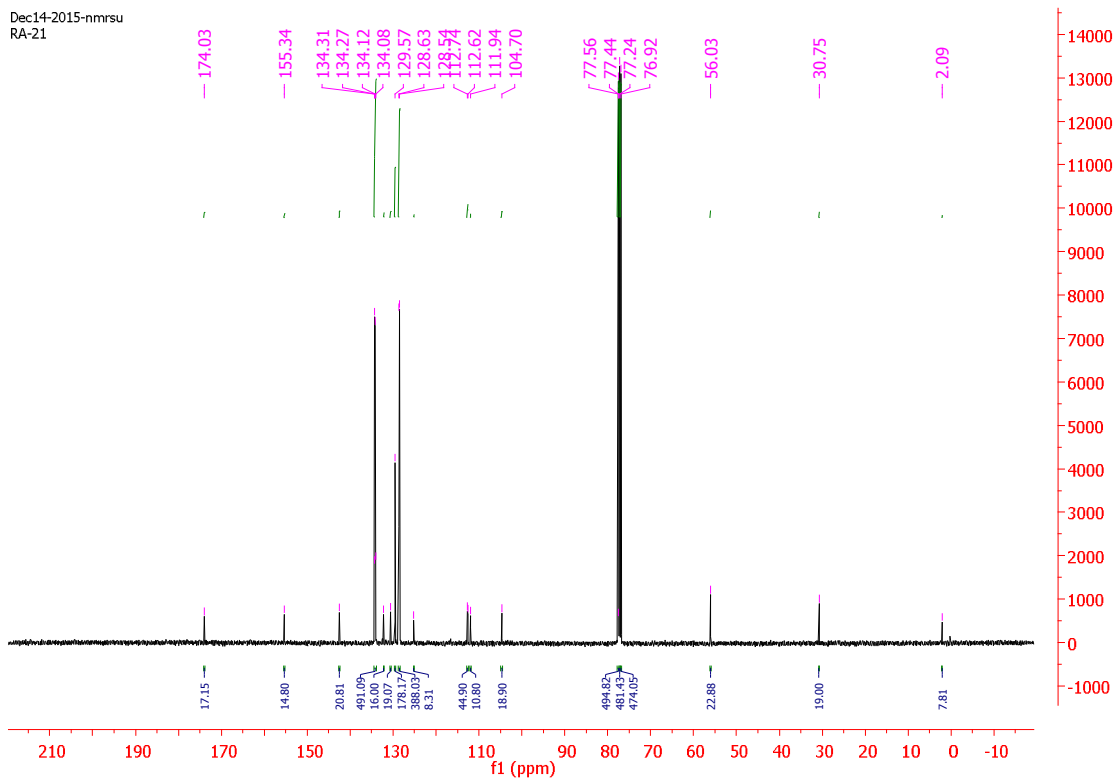


(b)

Figures-50: ^1H NMR(a) and C^{13} NMR(b) spectra of 5-methoxy indole- N^1 -methyl-3-thiosemicarbazone (5-MeOHIntsc- N^1 -Me).

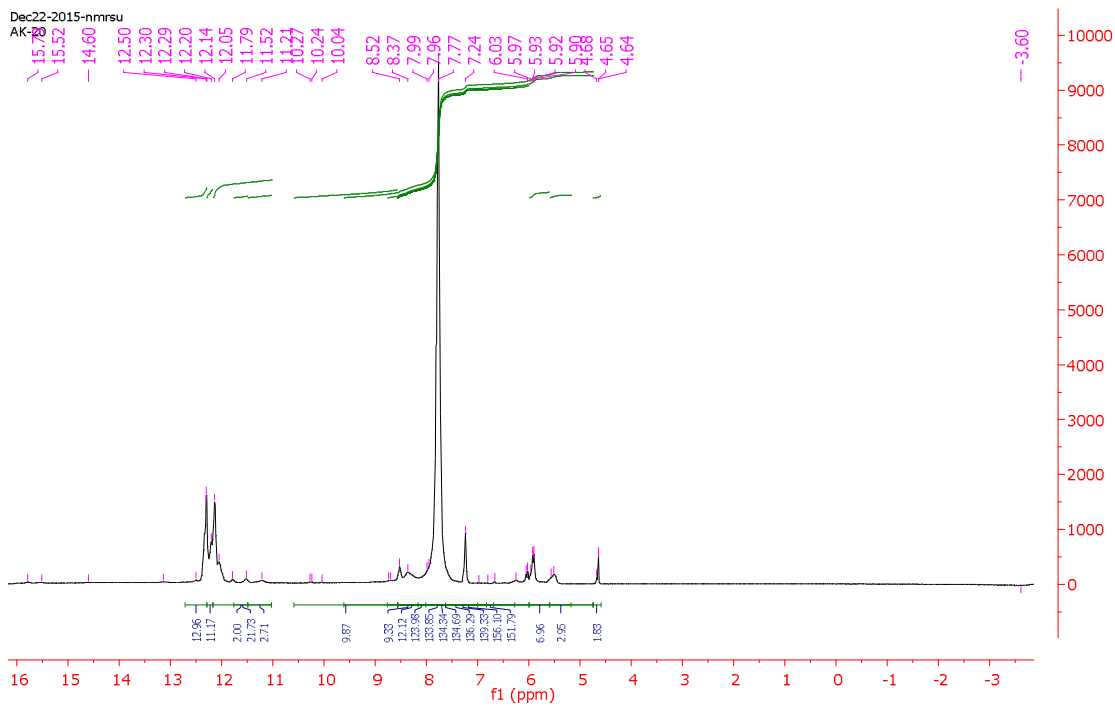


(a)

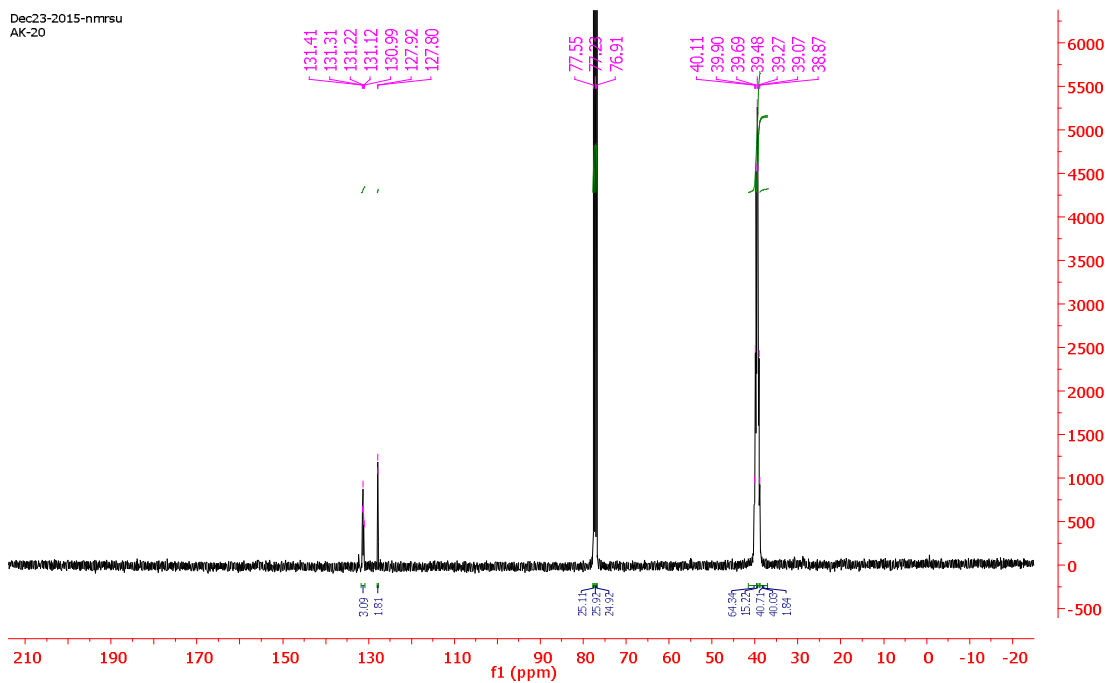


(b)

Figures-51: ^1H NMR(a) and ^{13}C NMR(b) spectra of $[\text{CuBr}(\eta^1\text{-S-5-MeOHIntsc-N}^1\text{-Me})(\text{Ph}_3\text{P})_2]\cdot\text{CH}_3\text{CN}$



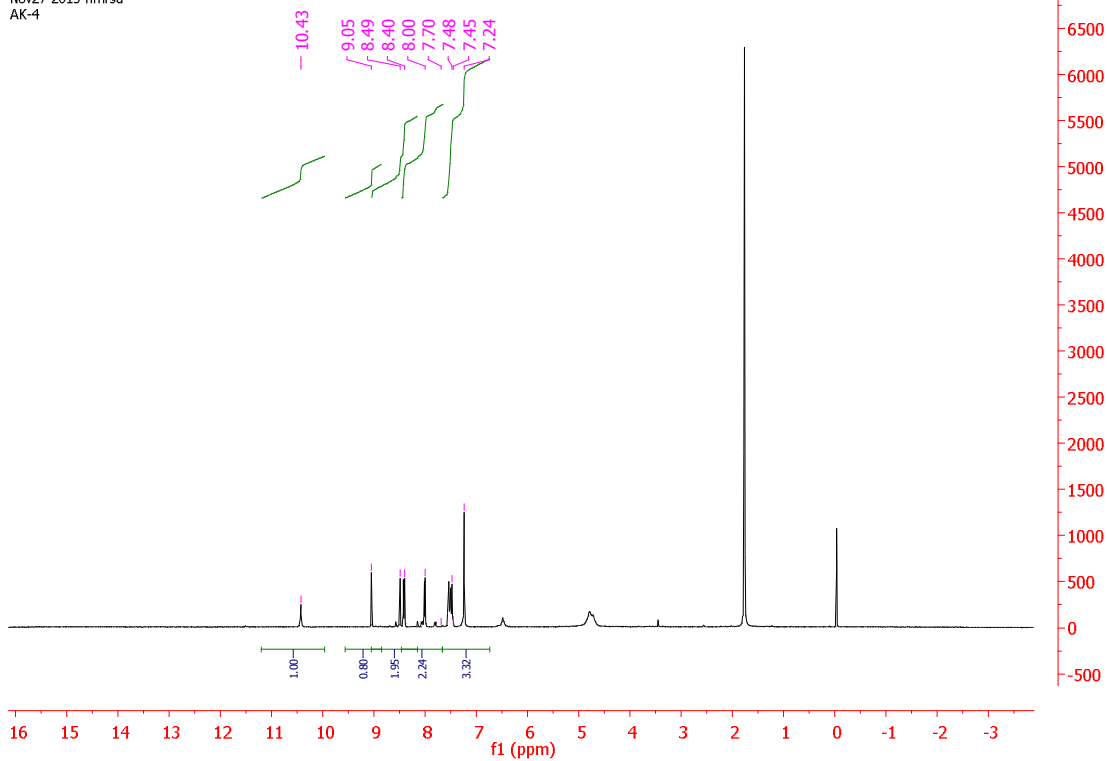
(a)



(b)

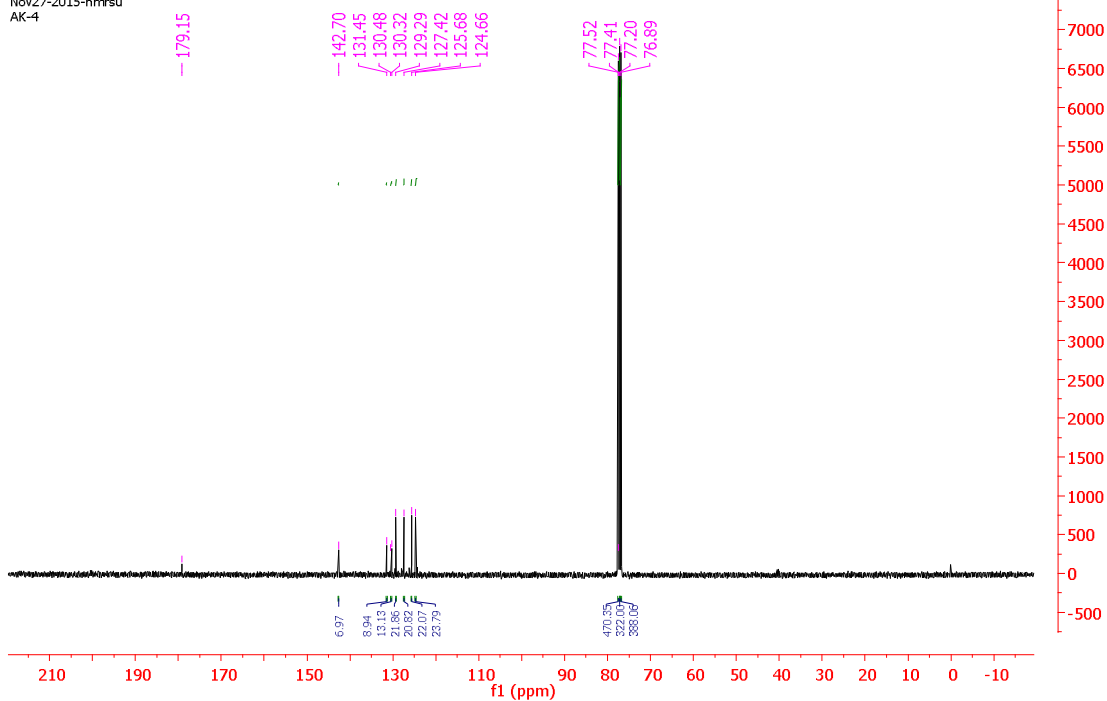
Figures-52: ^1H NMR(a) and C^{13} NMR(b) spectra of $[\text{CuCl}(\eta^1\text{-S-5-MeOHIntsc-N}^1\text{-Me})(\text{Ph}_3\text{P})_2]$.

Nov27-2015-nmrsu
AK-4



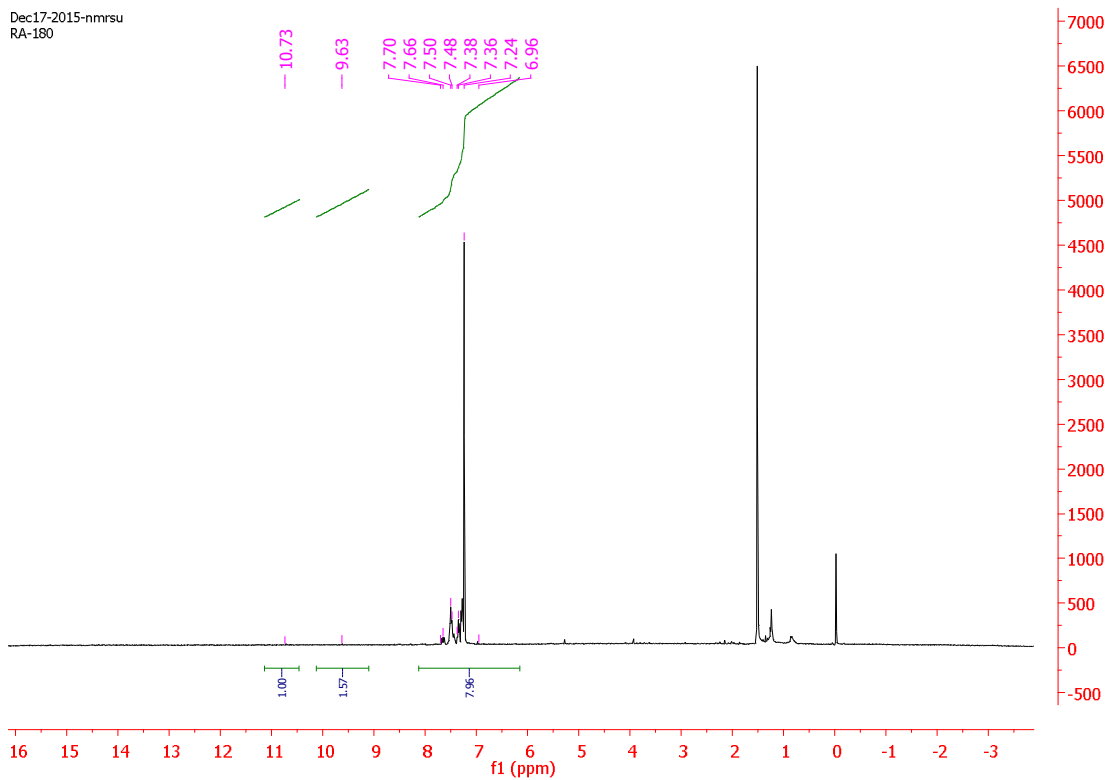
(a)

Nov27-2015-nmrsu
AK-4

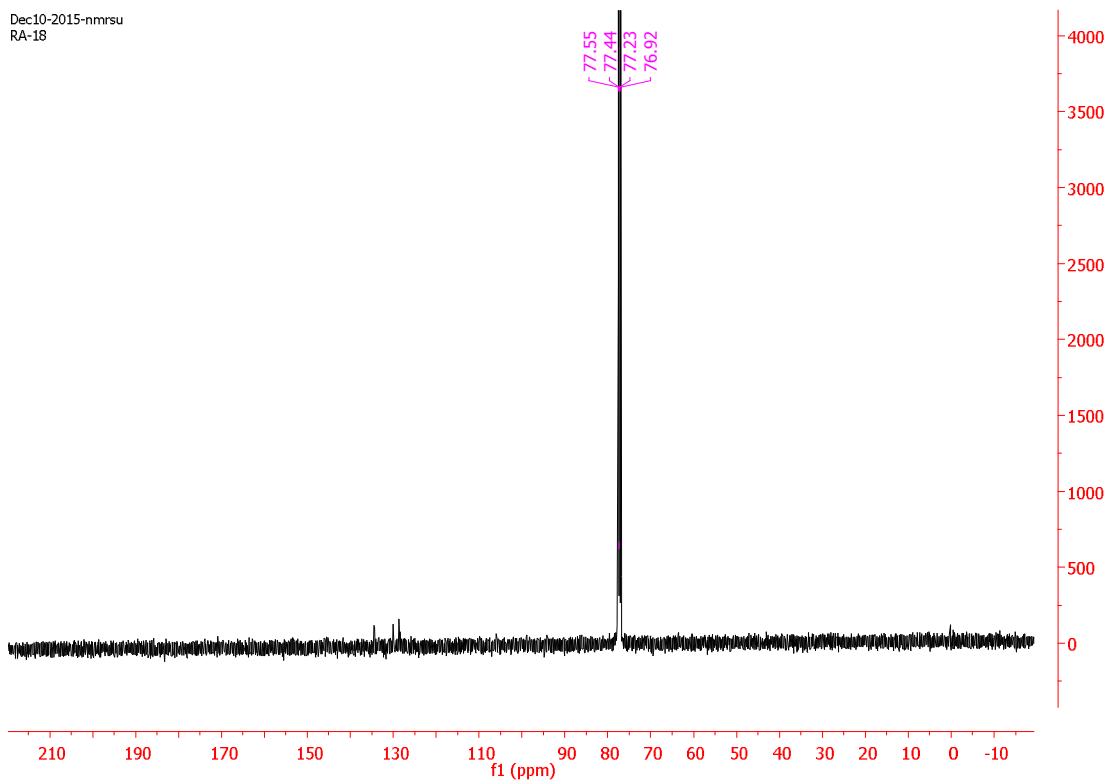


(b)

Figures-53: ^1H NMR(a) and C^{13} NMR(b) spectra of 9-anthraldehyde thiosemicarbazones (9-Hantsc).

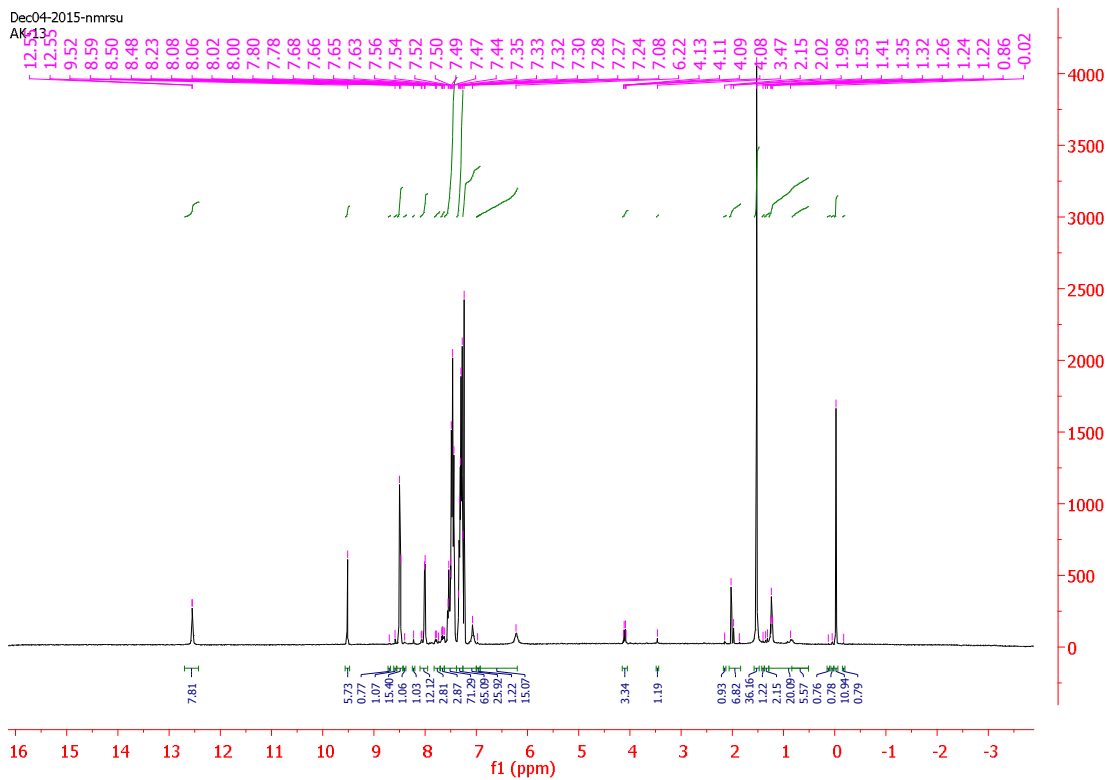


(a)

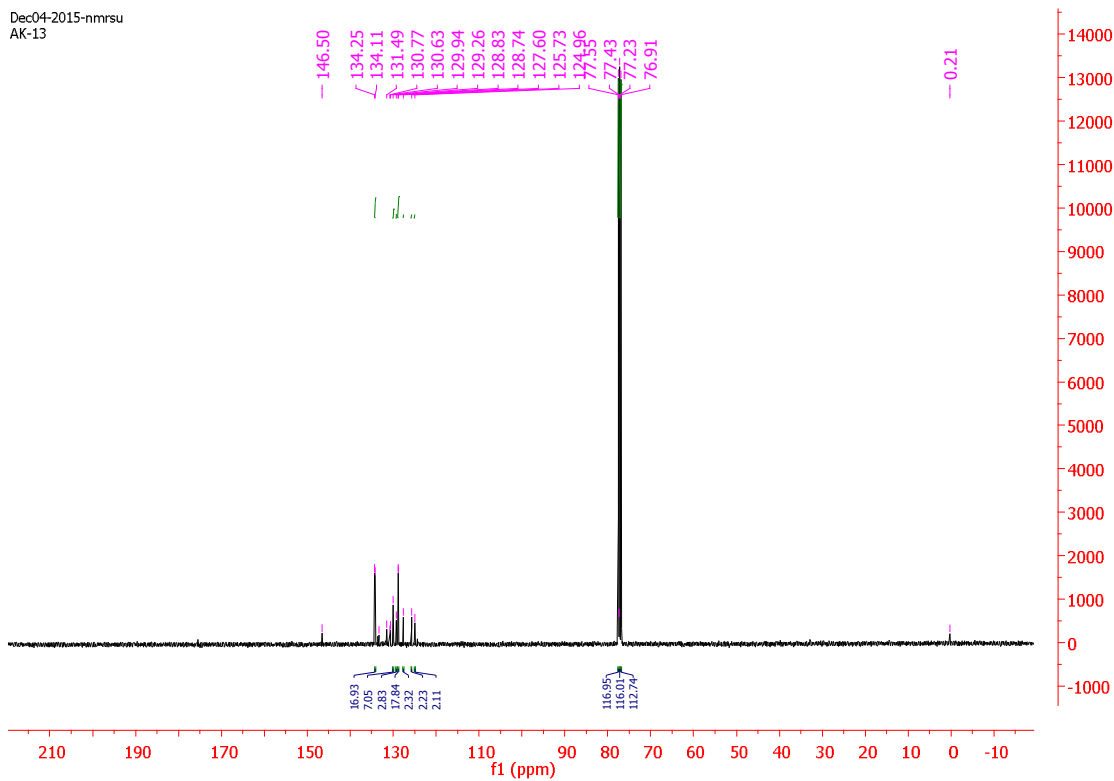


(b)

Figures-54: ^1H NMR(a) and ^{13}C NMR(b) spectra of $[\text{Cu}_2(\mu_2\text{-I})_2(\eta^1\text{-S-9-Hanttsc})(\text{Ph}_3\text{P})_2]$.

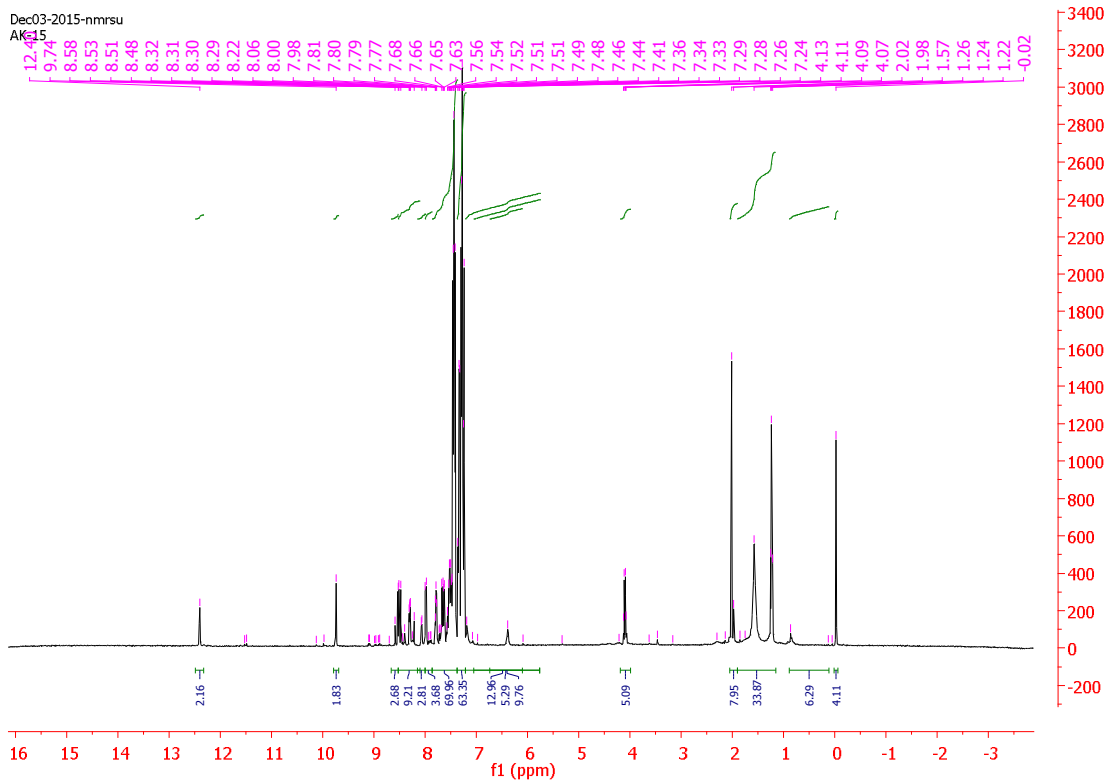


(a)

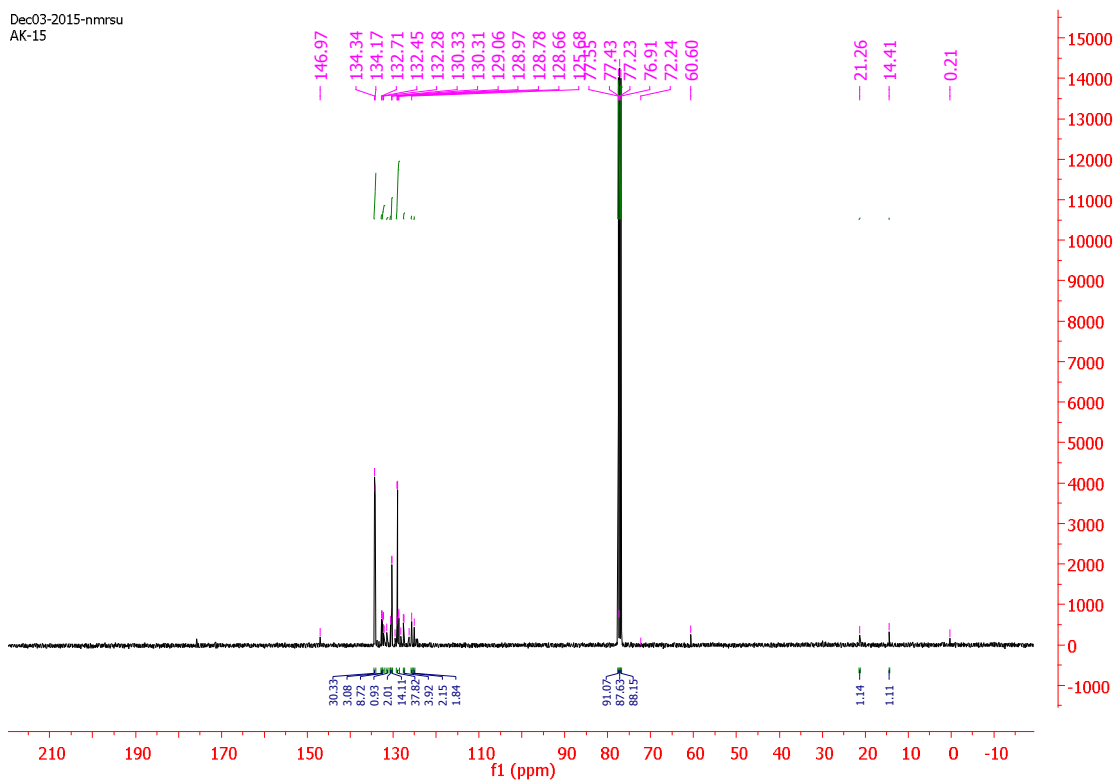


(b)

Figures-55: ^1H NMR(a) and ^{13}C NMR(b) spectra of $[\text{Cu}_2(\mu_2\text{-Br})_2(\eta^1\text{-S-9-Hanttsc})(\text{Ph}_3\text{P})_2]$.

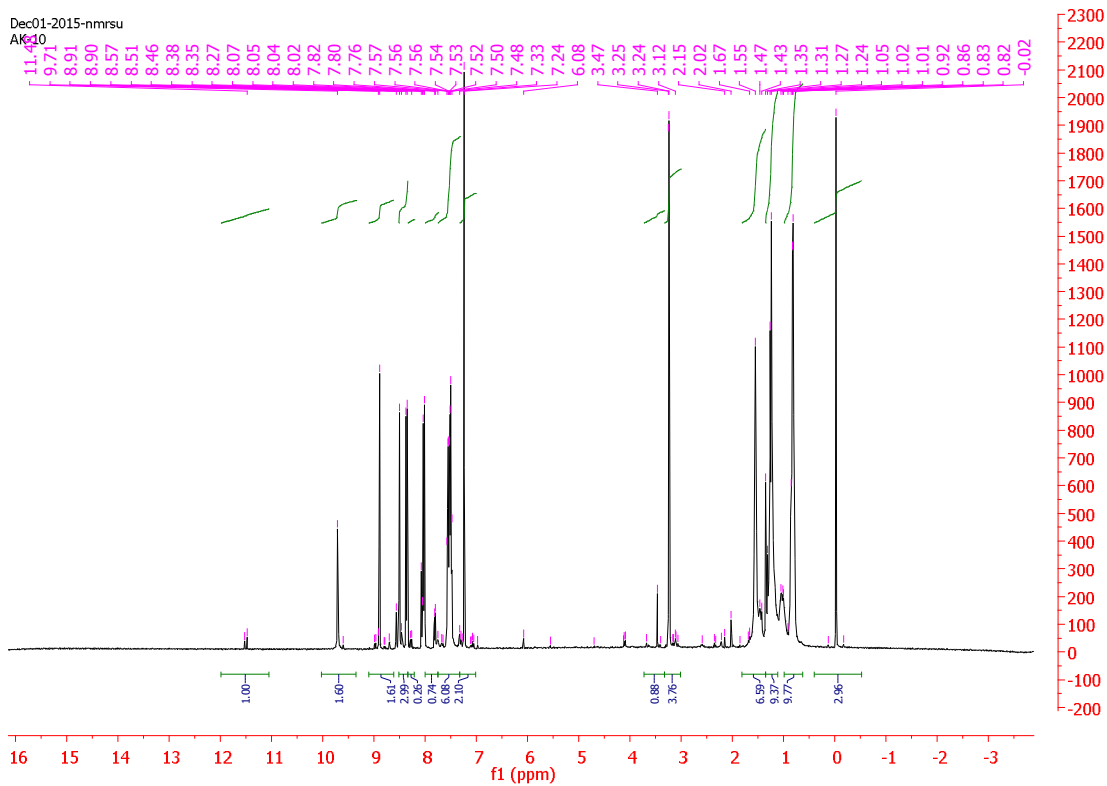


(a)

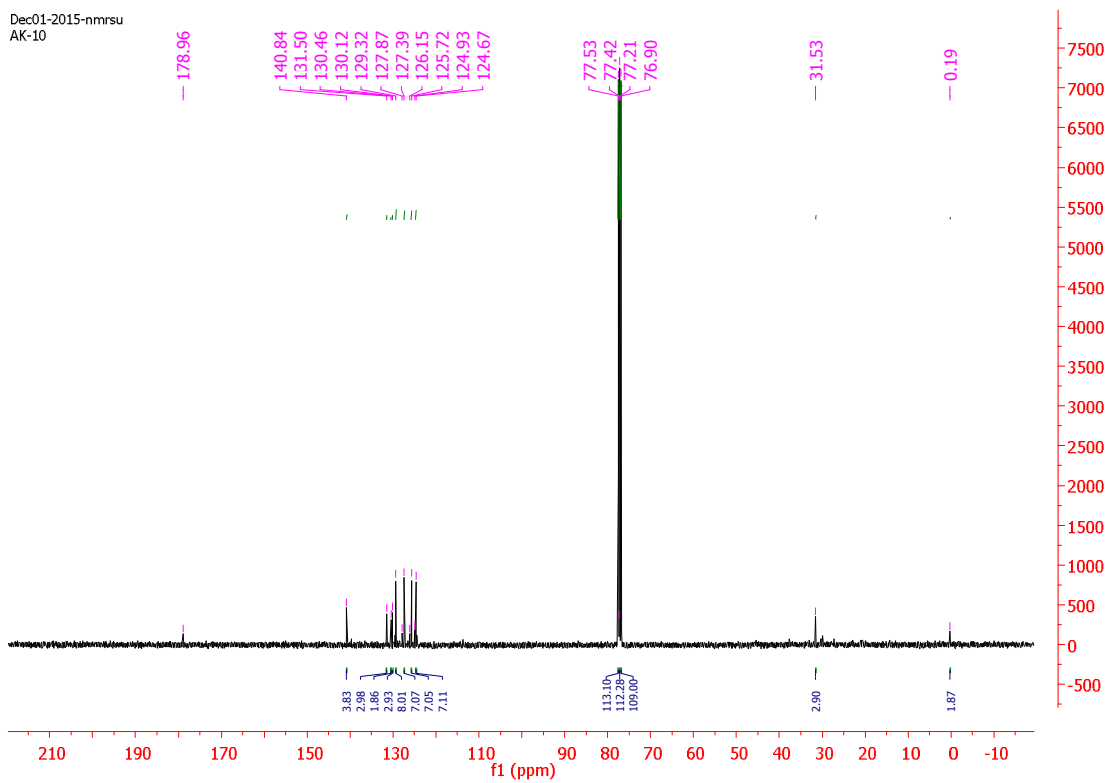


(b)

Figures-56: ^1H NMR(a) and C^{13} NMR(b) spectra of $[\text{AgBr}(\eta^1\text{-S-9-Hanttsc})(\text{Ph}_3\text{P})_2]$.

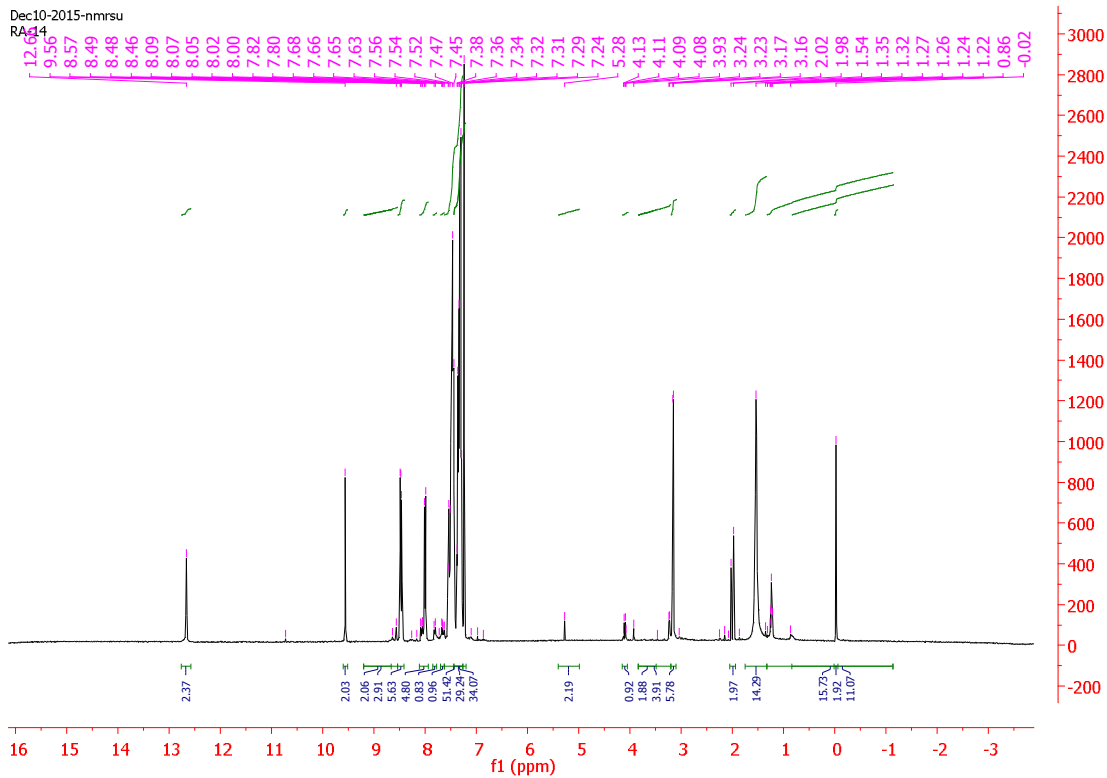


(a)

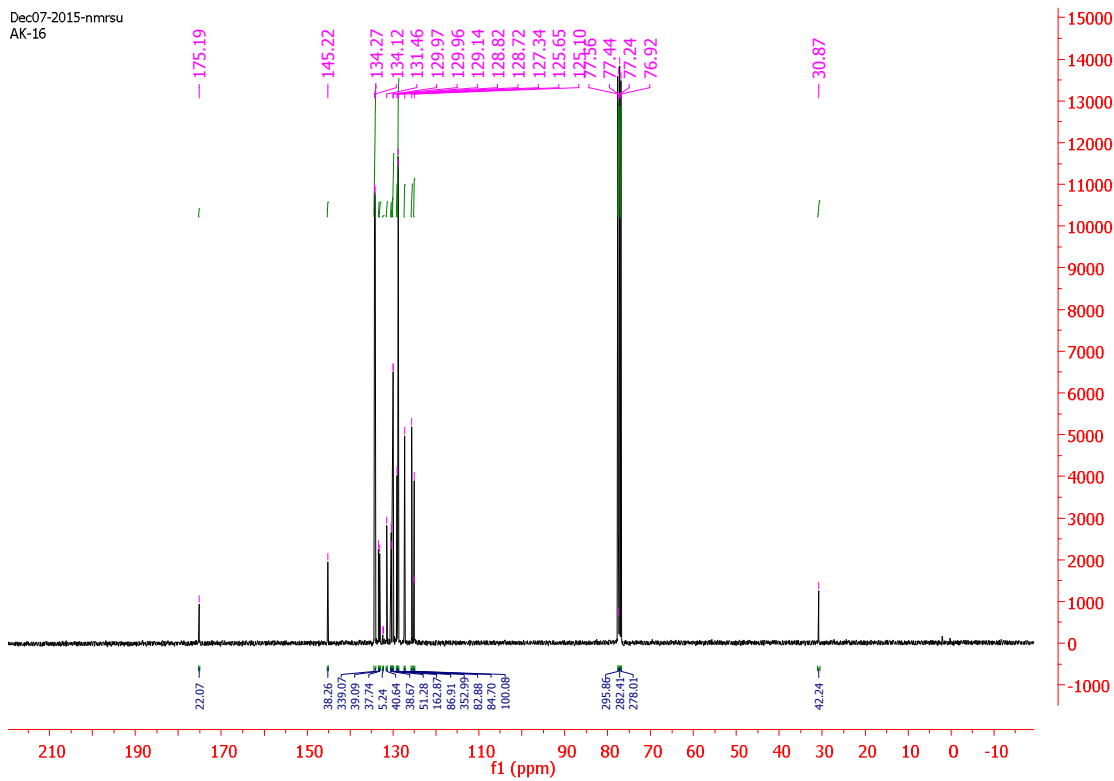


(b)

Figures-57: ^1H NMR(a) and ^{13}C NMR(b) spectra of 9-anthraldehyde thiosemicarbazones (9-Hanttsc- N^1 -Me).

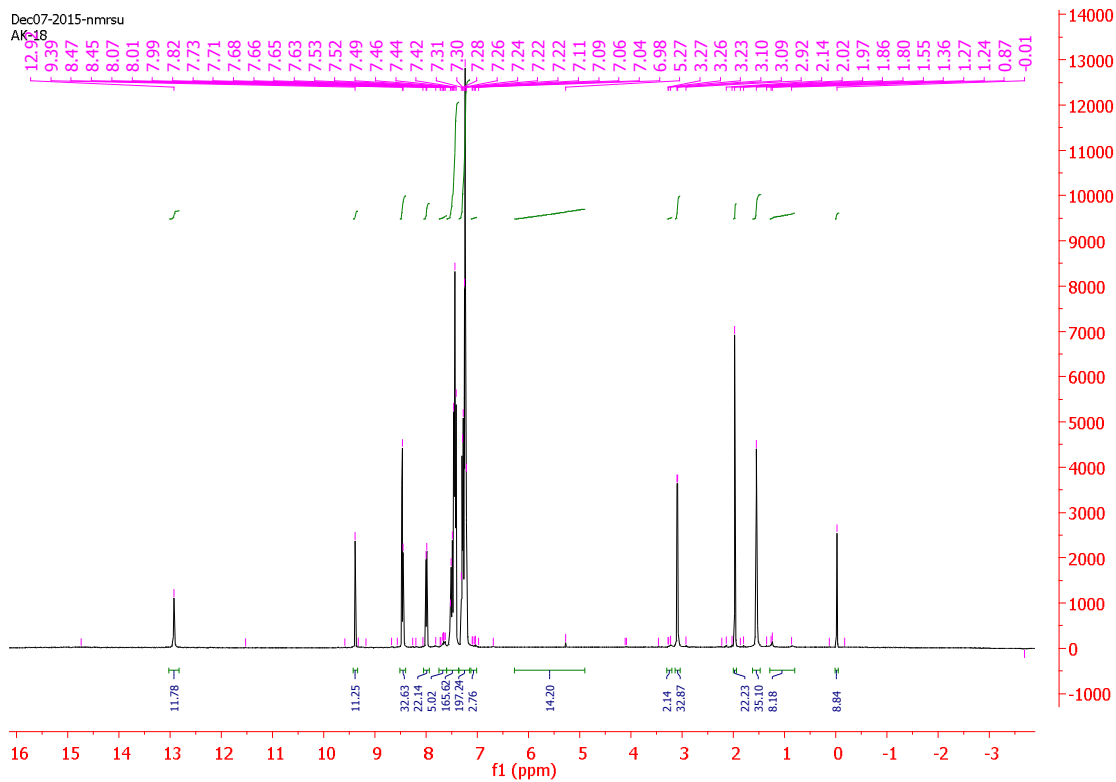


(a)



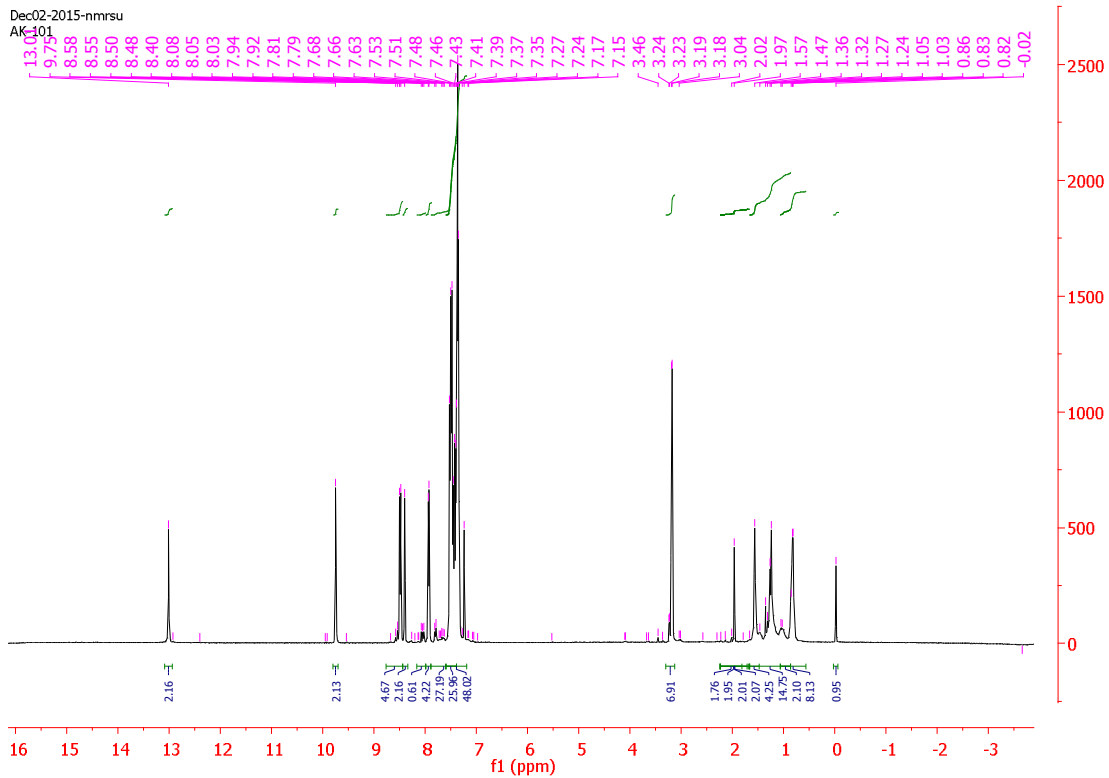
(b)

Figures-57: ^1H NMR(a) and ^{13}C NMR(b) spectra of $[\text{CuBr}(\eta^1\text{-S-9-Hanttsc-N}^1\text{-Me})(\text{Ph}_3\text{P})_2]$.

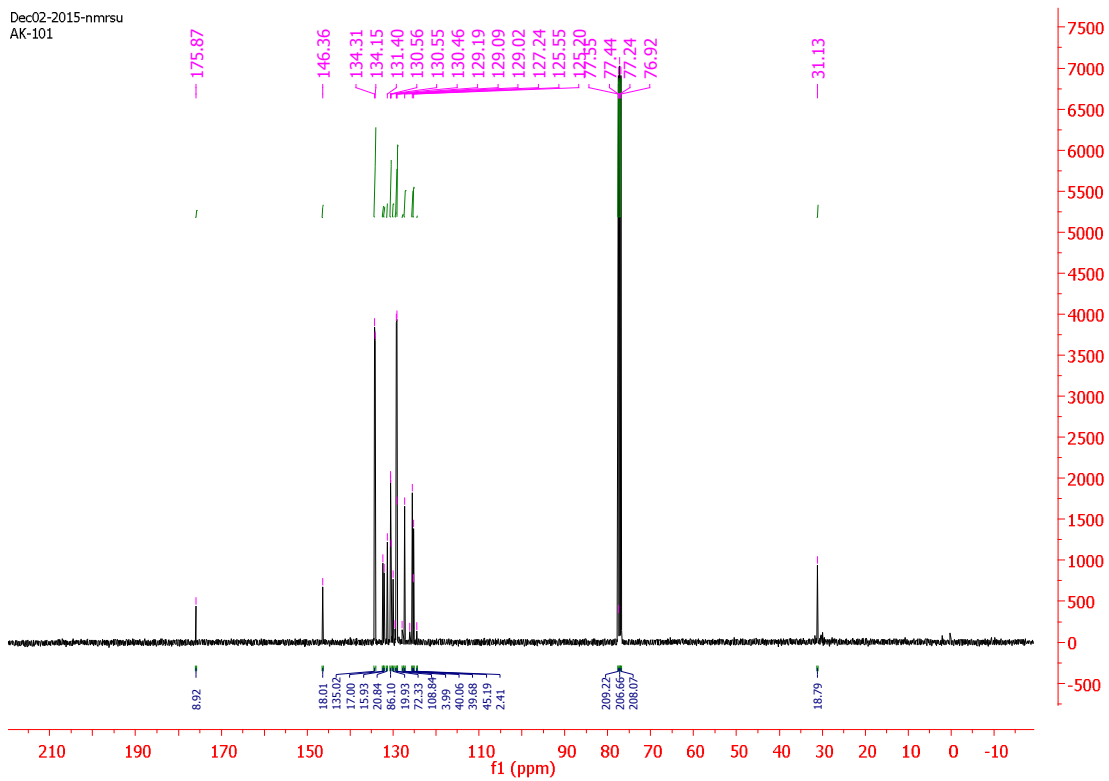


(a)

Figures-58: ^1H NMR(a) spectra of $[\text{CuCl}(\eta^1\text{-S-9-Hanttsc-N}^1\text{-Me})(\text{Ph}_3\text{P})_2]$.

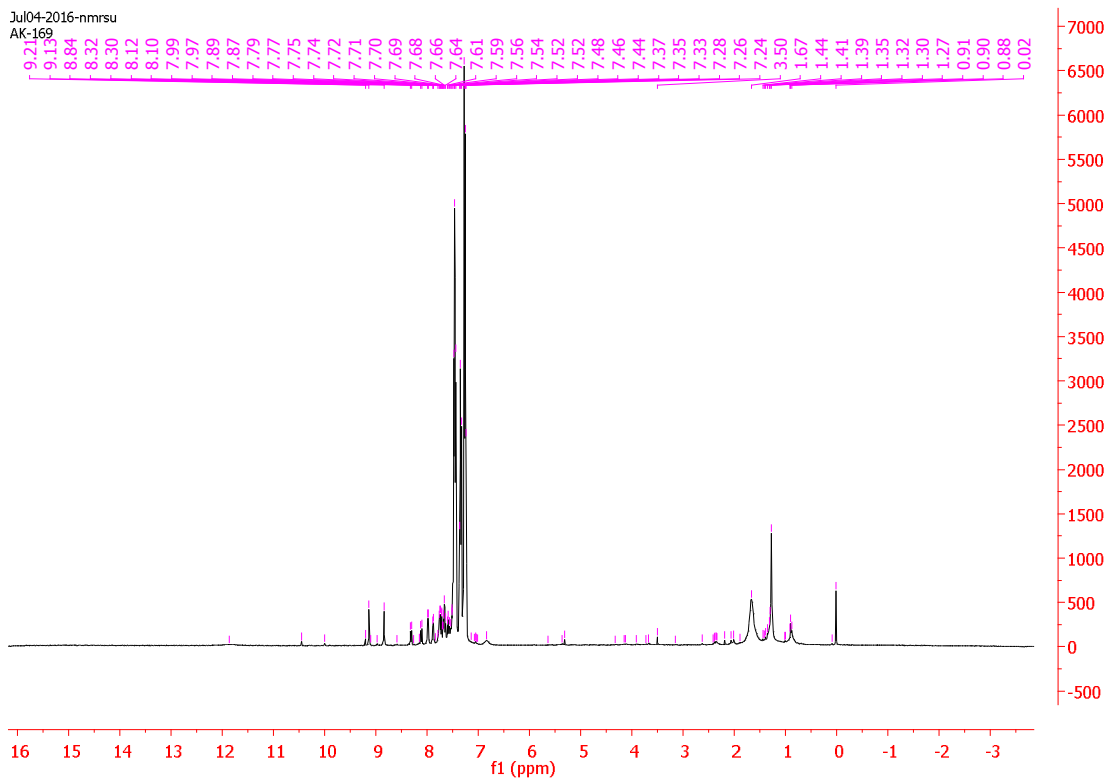


(a)

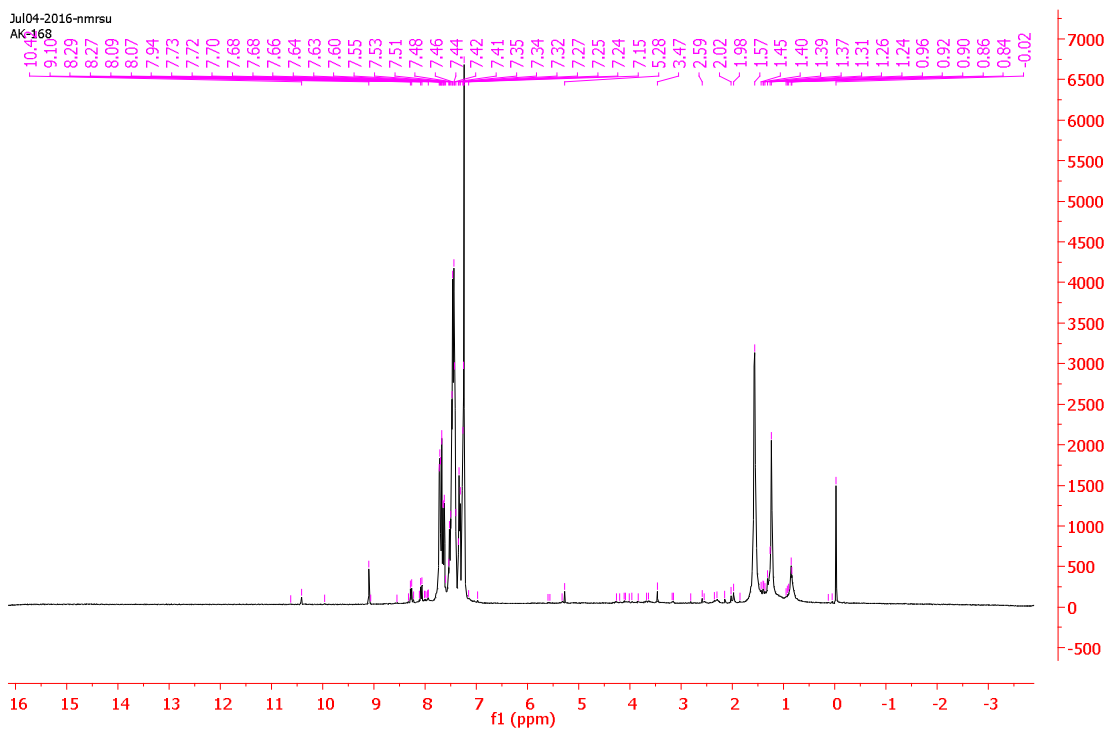


(b)

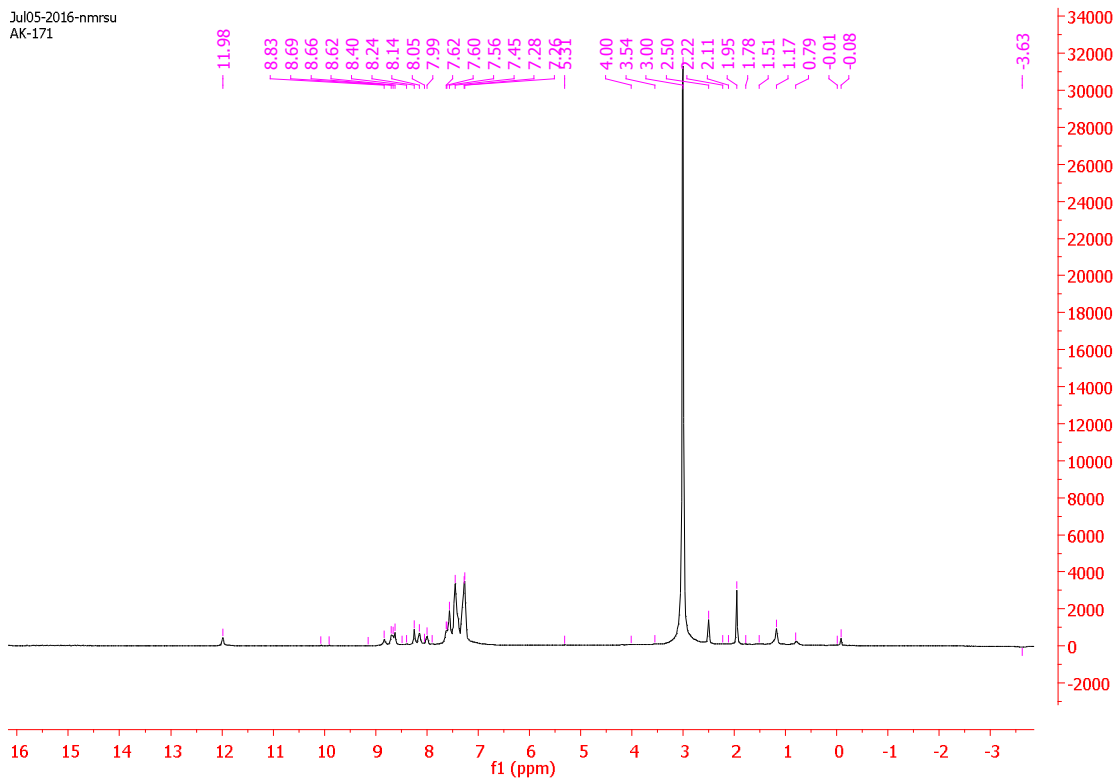
Figures-59: ^1H NMR(a) and ^{13}C NMR(b) spectra of $[\text{Ag}_2\text{Cl}_2(\mu_2\text{-S-9-Hantsc-N}^1\text{-Me})(\text{Ph}_3\text{P})_2]$.



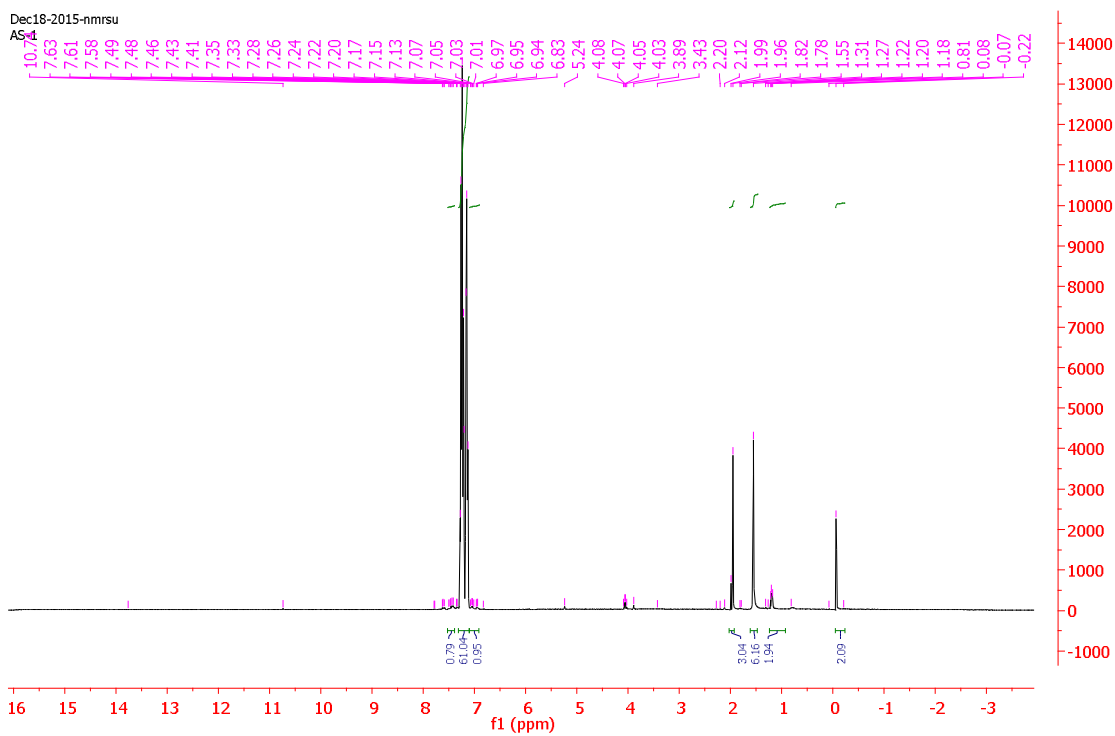
Figures-60: ^1H NMR spectra of $[\text{CuI}(\eta^1\text{-Se-2-NO}_2\text{-Hbsesc})(\text{Ph}_3\text{P})_2]$.



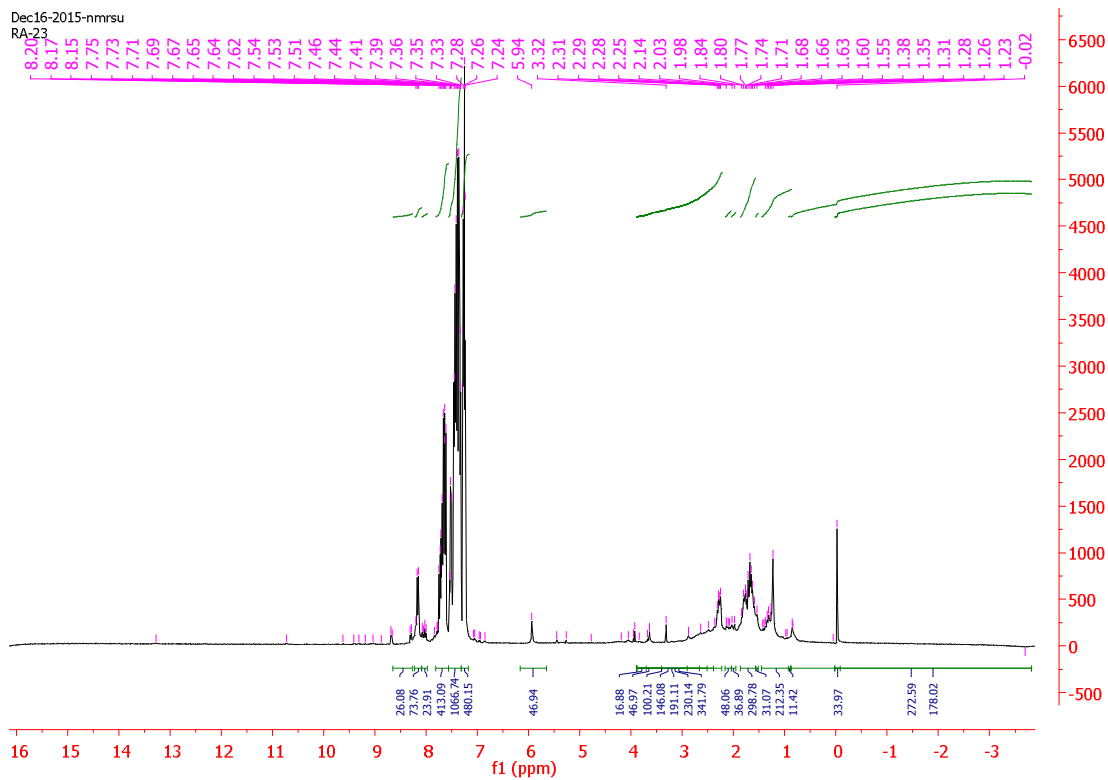
Figures-61: ^1H NMR spectra of $[\text{CuBr}(\eta^1\text{-Se-2-NO}_2\text{-Hbsesc})(\text{Ph}_3\text{P})_2]$.



Figures-62: ^1H NMR spectra of $[\text{CuI}(\eta^1\text{-Se-3-NO}_2\text{-Hbsesc})(\text{Ph}_3\text{P})_2]$.



Figures-63: ^1H NMR spectra of $[\text{CuCl}(\eta^1\text{-Se-3-NO}_2\text{-Hbsesc})(\text{Ph}_3\text{P})_2]$.



Figures-64: ^1H NMR spectra of $[\text{AgCl}(\eta^1\text{-Se-4-NO}_2\text{-Hbsesc})(\text{Ph}_3\text{P})_2]$.